



UNIVERSITY OF
BIRMINGHAM

**SOURCE IDENTIFICATION AND REACTIVITY
STUDY ON ATMOSPHERIC POLYCYCLIC
AROMATIC HYDROCARBONS**

by

EUNHWA JANG

A thesis submitted to the University of Birmingham

for the degree of

DOCTOR OF PHILOSOPHY

Division of Environmental Health and Risk Management

School of Geography, Earth and Environmental Sciences

University of Birmingham

November 2014

UNIVERSITY OF
BIRMINGHAM

University of Birmingham Research Archive

e-theses repository

This unpublished thesis/dissertation is copyright of the author and/or third parties. The intellectual property rights of the author or third parties in respect of this work are as defined by The Copyright Designs and Patents Act 1988 or as modified by any successor legislation.

Any use made of information contained in this thesis/dissertation must be in accordance with that legislation and must be properly acknowledged. Further distribution or reproduction in any format is prohibited without the permission of the copyright holder.

Abstract

Polycyclic aromatic hydrocarbons (PAH) are ubiquitous compounds produced through incomplete combustion processes from various sources in different proportions. They are of concern because of their recognized mutagenic and carcinogenic properties. There are a number of receptor modelling (RM) studies that identify sources of urban atmospheric PAH, despite concerns over the application of RM to the relatively reactive PAH. This thesis utilizes Positive Matrix Factorization (PMF) with extensive PAH datasets, and compares the results with local and national emission inventories. An atmospheric chemical reactivity study for PAH is also investigated; highlighting the importance of taking reactivity into consideration when applying source apportionment models.

The results demonstrate that traffic sources are significantly responsible for the PAH mass (Σ PAH) at UK urban sites throughout the year. A substantial fraction of benzo[*a*]pyrene emissions was apportioned to solid fossil fuel combustion sources, showing significant seasonal variations.

A conceptual simulation of PAH ratios has been investigated using urban and rural data. Results were in good agreement between simulated ratios and empirically obtained values. The results provide a better understanding of PAH reactivity and their atmospheric fate, indicating the potential for long-range transport of high molecular weight PAH.

Dedication

To my angel, Sua Yoon

With eternal love

Acknowledgements

Firstly, I would like to thank my supervisor, **Professor Roy Harrison**, for his invaluable guidance and encouragement over the last three years. I really appreciate the discerning advice he gave to me. Discussions with him on the various aspects of my study greatly enriched it. My thanks also go to **Dr Salim Alam**, who provided me with useful material and academic assistance.

I appreciate the financial support given me by many institutes. Joint funding by the **UK government** (UK CHEVENING scholarship) and the **Ministry of Science, ICT and Future Planning** (Republic of Korea) and aid from both **Busan Metropolitan City** and the **University of Birmingham** allowed me to focus on my studies.

I would like to thank **Forough, Suad and Margherita** who have provided mental support. **Dr Taesuk Kang, Dr Seongwon Lee and Father Jacob** have given me encouragement. **Pallavi, Lami, Adobi, Barbara, Ian, Massimiliano, Paul and Tuan** accompanied me during the PhD journey. **Sohyun Park, Minkyung Kim and Mikyung Seo** gave me their friendship. **Pyungjong Yu and Gigon Kim** provided royal patronage. I would like to express my gratitude to **Helen Hancock** for her editorial help.

I shall not forget the very special support given me by my **parents-in-law**. My special thanks go to my **mother** for her endless love; and my love goes to my daughter, my angel, **Sua Yoon**. Most importantly, my gratitude goes to my husband, **Seonghwan Yoon** for providing inspiration, encouragement, patience and steadfast support. Without him, I would not have been able to reach the finishing line in this PhD marathon.

Table of Contents

Chapter 1. Introduction	1
1.1 Background	1
1.2 Urbanization	2
1.3 Atmospheric pollutants and health effects	3
1.4 The chemistry of ambient polycyclic aromatic hydrocarbons (PAH).....	9
1.4.1 Generation of PAH	9
1.4.2 PAH reactivity	13
1.4.3 Phase distribution of PAH (partitioning)	18
1.4.4 Long-range transport of PAH	21
1.5 Seasonal variation of PAH	22
1.6 Toxicity and regulations of PAH.....	24
1.7 Source identification of PAH	27
1.7.1 Diagnostic ratio (DR)	30
1.7.2 Principal components analysis (PCA)	31
1.7.3 Positive matrix factorization (PMF)	32
1.8 Thesis objective and overview	36
 Chapter 2. Methodology	 39
2.1 Positive matrix factorization (PMF)	39
2.2 Source apportionment of total PAH.....	43

2.3	Local source profiles (spatial analysis)	48
2.4	UK national source profiles (emission estimates)	52
2.5	Overview of the possibility of obtaining meaningful source profiles	53

Chapter 3. Source apportionment for total PAH57

3.1	Background	57
3.2	Results.....	59
3.2.1	Jeddah, Saudi Arabia	59
3.2.2	UK urban sites	65
3.2.3	UK industrial urban sites	72
3.2.4	UK site-specific PAH contributions	77
3.3	Conclusion and discussion	80

Chapter 4. Comparison with spatial analysis84

4.1	Background	84
4.2	Results.....	86
4.2.1	Source profiles of urban sites	86
4.2.2	Source profiles of industrial sites	89
4.2.3	Comparison between PMF source profiles and net concentration profiles	91
4.3	Conclusion	94

Chapter 5. Comparison with UK Emissions Inventory	96
5.1 Background	96
5.2 Results.....	98
5.2.1 Source profiles for industrial activities.....	98
5.2.2 Source profiles for domestic combustion	99
5.2.3 Source profiles relating to vehicular emissions.....	101
5.2.4 Comparison between PMF source profiles and UK emission estimate source profiles	103
5.3 Conclusion	108
 Chapter 6. Overview of possibility of meaningful source profiles.....	 109
6.1 Introduction	109
6.2 Source profiles of particle-bound PAH.....	111
6.2.1 Domestic combustion sites	111
6.2.2 Industrial urban sites.....	116
6.2.3 Urban sites	122
6.3 Source profiles of high molecular weight PAH	129
6.3.1 Background.....	129
6.3.2 Results	130
6.4 Sensitivity of chemical reactivity	135
6.4.1 Background.....	135
6.4.2 Results	139
6.5 Summary and discussion	141

Chapter 7. Simulation of PAH reactivity	142
7.1 Background	142
7.2 Methodology	145
7.2.1 Sampling and air mass trajectory analysis.....	145
7.2.2 OH estimation.....	146
7.2.3 Particle fractions	148
7.2.3.1 Theoretical particle fractions	148
7.2.3.2 Measured particle fractions.....	151
7.2.4 Simulation description.....	152
7.3 Results.....	154
7.3.1 Data selection	154
7.3.2 OH estimation.....	161
7.3.3 Phase distribution of PAH between gaseous and particulate phases	163
7.3.3.1 Theoretical particle fractions	163
7.3.3.2 Field measurements of particle fractions	168
7.3.3.3 Comparison of phase distribution for three PAH congeners between theoretical estimation and empirical measurement	169
7.3.4 Simulations	172
7.3.5 Sensitivity	177
7.3.5.1 Sensitivity of simulated ratios to variations in parameters	177
7.3.5.2 Simulations for individual air masses for winter	180
7.4 Discussion	185
 Chapter 8. Conclusions	 189
8.1 Summary	189

8.2	Implications.....	192
8.3	Future work.....	195
Appendix A:	Source emission contributions of air pollutants ranked by sector.....	197
Appendix B:	PAH emissions in the UK, 2002 – 2006.....	200
Appendix C:	UK energy consumption	204
References	205

List of Figures

Chapter 1

- Figure 1.1:** Environmental disease burden by WHO subregion. The disease burden is measured in deaths per 100,000 population for the year 2002. 3
- Figure 1.2:** Annual emissions of SO₂ in the European countries 1980-2000 (Gun Lövblad, 2004). 5
- Figure 1.3:** A rough picture of soot formation in homogeneous mixtures (premixed flames) from Ravindra et al. (2008a)..... 11
- Figure 1.4:** A schematic diagram of multi-ring PAH formation (Violi et al., 1999). 12
- Figure 1.5:** Global change of sulphur levels of diesel fuels (UNEP, 2006-2014)..... 27
- Figure 1.6:** A schematic diagram of source identification (Belis et al., 2014)..... 29

Chapter 2

- Figure 2.1:** Sampling locations in Jeddah in Saudi Arabia. 44
- Figure 2.2:** Pictures of samplers used at UK PAH monitoring sites (Brown et al., 2011)..... 49
- Figure 2.3:** Locations for local source profile analysis. 51

Chapter 3

- Figure 3.1:** PAH factor profile for total PAH and temporal variation for Jeddah (F1). . 60
- Figure 3.2:** PAH factor profile for total PAH and temporal variation for Jeddah (F2). . 61

Figure 3.3:	PAH factor profile for total PAH and temporal variation for Jeddah (F3)..	63
Figure 3.4:	Source specific contributions to Sites A, B and C in Jeddah (TE: traffic emissions; IE: industrial emissions; D/O: diesel and oil combustion)...	64
Figure 3.5:	PMF factor profile for total PAH and temporal variation at urban sites in the UK (Factor 1).....	67
Figure 3.6:	PMF factor profile for total PAH and temporal variation at urban sites in the UK (Factor 2).....	69
Figure 3.7:	PMF factor profile for total PAH and temporal variation at urban sites in the UK (Factor 3).....	70
Figure 3.8:	PMF factor profile for total PAH and temporal variation at urban sites in the UK (Factor 4).....	72
Figure 3.9:	PMF factor profile for total PAH and temporal variation at industrial urban sites in the UK (Factor 1).	74
Figure 3.10:	PMF factor profile for total PAH and temporal variation at industrial urban sites in the UK (Factor 2).	75
Figure 3.11:	PMF factor profile for total PAH and temporal variation at industrial urban sites in the UK (Factor 3).	76
Figure 3.12:	Source specific PAH mass contributions in the UK (DE: diesel emissions; UP: unburned petroleum; CC: coal combustion; WC: wood combustion).	78

Chapter 4

Figure 4.1:	Source profile of urban PAH from cross sectional analysis.	87
Figure 4.2:	Source profiles of industrial urban PAH from cross sectional analysis..	90

Figure 4.3:	Comparison between PMF source profiles and net contribution profiles	92
--------------------	---	----

Chapter 5

Figure 5.1:	PAH source profiles of industry extracted from UK emission estimates.	99
Figure 5.2:	PAH source profiles of domestic combustion extracted from UK emission estimates.	101
Figure 5.3:	PAH source profiles of traffic emissions extracted from UK emission estimates.	103
Figure 5.4:	Comparison of source profiles obtained with different approaches.	107

Chapter 6

Figure 6.1:	PMF factor profile for PM ₁₀ -bound PAH and source-specific seasonal variation (Northern Ireland – Factor 1).	113
Figure 6.2:	PMF factor profile for PM ₁₀ -bound PAH and source-specific seasonal variation (Northern Ireland – Factor 2).	114
Figure 6.3:	PMF factor profile for PM ₁₀ -bound PAH and source-specific seasonal variation (Northern Ireland – Factor 3).	115
Figure 6.4:	Site-specific source contributions (DO: domestic oil combustion; TE: traffic emissions; DC: domestic coal combustion).....	116
Figure 6.5:	PMF factor profile for PM ₁₀ -bound PAH and source-specific seasonal variation (Industrial urban – Factor 1).....	118

Figure 6.6:	PMF factor profile for PM ₁₀ -bound PAH and source-specific seasonal variation (Industrial urban – Factor 2).....	119
Figure 6.7:	PMF factor profile for PM ₁₀ -bound PAH and source-specific seasonal variation (Industrial urban – Factor 3).....	120
Figure 6.8:	PMF factor profile for PM ₁₀ -bound PAH and source-specific seasonal variation (Industrial urban – Factor 4).....	120
Figure 6.9:	Site-specific source contributions (DO: domestic oil combustion; TE: traffic emissions; DC: domestic coal combustion; MI: metallurgical industry).....	121
Figure 6.10:	PMF factor profile for PM ₁₀ -bound PAH and source-specific seasonal variation at urban sites (Factor 1).....	123
Figure 6.11:	PMF factor profile for PM ₁₀ -bound PAH and source-specific seasonal variation at urban sites (Factor 2).....	124
Figure 6.12:	PMF factor profile for PM ₁₀ -bound PAH and source-specific seasonal variation at urban sites (Factor 3).....	125
Figure 6.13:	PMF factor profile for PM ₁₀ -bound PAH and source-specific seasonal variation at urban sites (Factor 4).....	125
Figure 6.14:	Site-specific seasonal source variations for particle-bound PAH, sampled by Digitel sampler (DO: domestic oil combustion; TE: traffic emissions; DC: domestic coal combustion; MI: metallurgical industry).....	127
Figure 6.15:	UK PAH monitoring sites (light blue circle: urban background sites; dark blue circle: urban traffic sites; yellow circle: Northern Ireland sites; red circle: industrial urban sites) and the metallurgical industrial sites (black star).....	128

Figure 6.16:	Comparison between Andersen high molecular PAH dataset and Digitel particulate PAH dataset.....	131
Figure 6.17:	Site-specific seasonal source variations based on the PMF results in dataset for HMW, sampled by Andersen sampler (DE: diesel vehicular emissions; TE: traffic emissions; DC: domestic coal combustion; MI: metallurgical industry).....	134
Figure 6.18:	PMF sensitivity analysis for uncertainty of variables.	140

Chapter 7

Figure 7.1:	Backward trajectory of clustered airmass, at Weybourne transported from UK mainland during winter campaign (each point; three hours).	159
Figure 7.2:	Measured particle fractions (P(%)) at EROS (1.2 °C) and at Weybourne transported from the UK mainland (2.9 °C), EU mainland (2.6 °C) and North Sea (2.0 °C).	168
Figure 7.3:	Normalised concentrations over reaction time.	174
Figure 7.4:	Simulated ratios during transport.	176
Figure 7.5:	Sensitivity of PAH-PAH ratios to variations in parameters.....	179
Figure 7.6:	Comparison between simulated ratios and measured ratios as a function of back trajectory.	181
Figure 7.7:	Simulated ratios with increased OH radical concentration of 2.0×10^6 molecules/cm ³ with transport time of 15 hours.....	184
Figure 7.8:	Simulated ratios with increased transport time of 20 hours at the estimated OH concentrations of 1.45 and 1.47×10^6 molecules/cm ³ sampled on 17 th and 18 th February 2010, respectively.	184

List of Tables

Chapter 1

Table 1.1:	Rate coefficients of key reactions of aromatic hydrocarbon formations (Violi et al., 1999).....	10
Table 1.2:	Physicochemical information on 16 USEPA priority PAH.	13
Table 1.3:	Experimental rate coefficients of gaseous LMW PAH with oxidants (Keyte et al., 2013).	16
Table 1.4:	Laboratory rate coefficients for heterogeneous reaction of HMW PAH with oxidants (Keyte et al., 2013).....	17
Table 1.5:	Target PAH and their risk.	24
Table 1.6:	Statistics of diagnostic ratios (Galarneau, 2008).	30
Table 1.7:	Formulas for PMF uncertainty (S_{ij}) (Reff et al., 2007).....	33
Table 1.8:	Measurement detection limits (MDL), estimated measurement error (α) and detection limit uncertainty (β) (Hemann et al., 2008).	34

Chapter 2

Table 2.1:	PAH congeners for PMF analysis of Jeddah.	44
Table 2.2:	Geographical information on sites.....	46
Table 2.3:	PAH congeners for PMF analysis.....	47
Table 2.4:	Digitel PAH congeners for local source profiles.	50
Table 2.5:	Pairs for local source profiles.	51
Table 2.6:	Geographical information on Digitel sampling sites.	54

Table 2.7:	Geographical information for two datasets.	55
-------------------	---	----

Chapter 3

Table 3.1:	Annual trend in average sulphur content in gasoline and diesel fuels, ppm (AEA, 2009)..	66
-------------------	--	----

Chapter 6

Table 6.1:	Details of industrial sites.	117
Table 6.2:	A calculated extra uncertainty based on the reactions of PAH with the OH radical.....	136

Chapter 7





















Table 7.1:	Physicochemical properties of gaseous PAH congeners.	155
Table 7.2:	Concentrations and ratios at a source site (EROS) and three aged air masses (at Weybourne) during winter campaign.....	156
Table 7.3:	Concentrations and ratios at a source site (BROS) and three aged air masses (at Weybourne) during summer campaign.	156
Table 7.4:	Selected samples for a simulation of PAH transport for winter.....	160
Table 7.5:	Selected samples for a simulation of PAH transport for summer.....	160
Table 7.6:	Estimated concentrations of hydroxyl radicals (OH) for winter (2.9 °C).	162
Table 7.7:	Estimated concentrations of hydroxyl radicals (OH) for summer (18 °C).	162












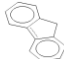
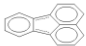




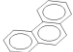


Table 7.8:	Variation of OM/OC ratios depending on sources and seasons.....	164
Table 7.9:	Different ratio of OC/EC depending on airborne particle size fraction and location (Laongsri, 2012).	164
Table 7.10:	Carbon fractions in PM ₁₀ used in this study both at the EROS site and at the Weybourne site.	165
Table 7.11:	Regression parameters for Equation 7.7 and calculated K _{OA}	166
Table 7.12:	Regression equations for Henry's law constant and calculated K _{SA}	167
Table 7.13:	Estimated C _{TSP} and theoretical particle fractions for PAH (P(%)) at an urban site (EROS, 274.2K) and at a rural site (Webourne, 275.9K). ...	167
Table 7.14:	Generalised concentrations over reaction time ($e^{-k(g)OH*[OH]^*t}$, denotes K).	173
Table 7.15:	Comparison of ratios between simulation and real measurement for winter.	176
Table 7.16:	Simulated ratios at t = t (at Weybourne).	178
Table 7.17:	Estimated OH concentrations using individual samples at Weybourne site.	181
Table 7.18:	Daily air pollution concentrations at rural background site (Harwell).	187

List of Abbreviations

DEFRA	Department of Environment, Food and Rural Affairs
DPF	Diesel particulate filters
DR	Diagnostic ratio
EPA	Environmental Protection Agency
HACA	H-atom abstraction and acetylene additions
HMW	High molecular weight
IU	Industrial urban
LMW	Low molecular weight
NAEI	National Atmospheric Emissions Inventory
PAH	Polycyclic aromatic hydrocarbons
PCA	Principal components analysis
PM	Particulate matter
PMF	Positive matrix factorization
RB	Rural background
RM	Receptor model
SA	Source apportionment
SVCs	Semi-volatile compounds
SVOCs	Semi-volatile organic compounds
UB	Urban background
UT	Urban traffic
WHO	World Health Organization

PAH congeners

1MA		1-Methyl anthracene
1MPhe		1-Methyl phenanthrene
2MA		2-Methyl anthracene
2MPhe		2-Methyl phenanthrene
4,5MPhe		4,5-Methylene phenanthrene
5MChr		5-Methyl chrysene
9MA		9-Methyl anthracene
Ace		Acenaphthene
Acy		Acenaphthylene
Ant		Anthracene
Anth		Anthanthrene
BaA		Benzo[<i>a</i>]anthracene
BaP		Benzo[<i>a</i>]pyrene
BbF		Benzo[<i>b</i>]fluoranthene
BjF		Benzo[<i>j</i>]fluoranthene
BcPhe		Benzo[<i>c</i>]phenanthrene
BeP		Benzo[<i>e</i>]pyrene
BghiPe		Benzo[<i>ghi</i>]perylene
BkF		Benzo[<i>k</i>]fluoranthene
BN21T		Benzo[<i>b</i>]naph[2,1- <i>d</i>]thiophene

CcdP		Cyclopenta[<i>c,d</i>]pyrene
Chr		Chrysene
Cor		Coronene
DacA		Dibenzo[<i>a,c</i>]anthracene
DaeF		Dibenzo[<i>a,e</i>]fluoranthene
DaeP		Dibenzo[<i>a,e</i>]pyrene
DacA		Dibenzo[<i>a,c</i>]anthracene
DahA		Dibenz[<i>a,h</i>]anthracene
DahP		Dibenzo[<i>a,h</i>]pyrene
DaiP		Dibenzo[<i>a,i</i>]pyrene
DalP		Dibenzo[<i>a,l</i>]pyrene
Flu		Fluorene
FluA		Fluoranthene
IcdP		Indeno[<i>1,2,3-cd</i>]pyrene
IcdF		Indeno[<i>1,2,3-cd</i>]fluoranthene
Nap		Naphthalene
Per		Perylene
Phe		Phenanthrene
Pyr		Pyrene
Ret		Retene

CHAPTER 1: INTRODUCTION

The introductory chapter of this thesis provides a general overview of urban atmospheric pollution with a particular focus on polycyclic aromatic hydrocarbons (PAH). The objectives of this research are to identify source contributions and assess the reactivity of PAH congeners in both vapour and particulate phases.

1.1 Background

Polycyclic aromatic hydrocarbons (PAH) are of concern in urban areas because of their recognized mutagenic and carcinogenic properties. They are a group of semi-volatile compounds which exist in both gaseous and particulate phases, depending on their vapour pressures. PAH are ubiquitous compounds which are emitted from various sources. The complexity of their sources sometimes makes it difficult to separate out these in an urban atmosphere. Additionally, individual atmospheric PAH have different physicochemical properties influenced by meteorological conditions such as temperature and solar intensity, which make it more difficult to quantify source-specific contributions.

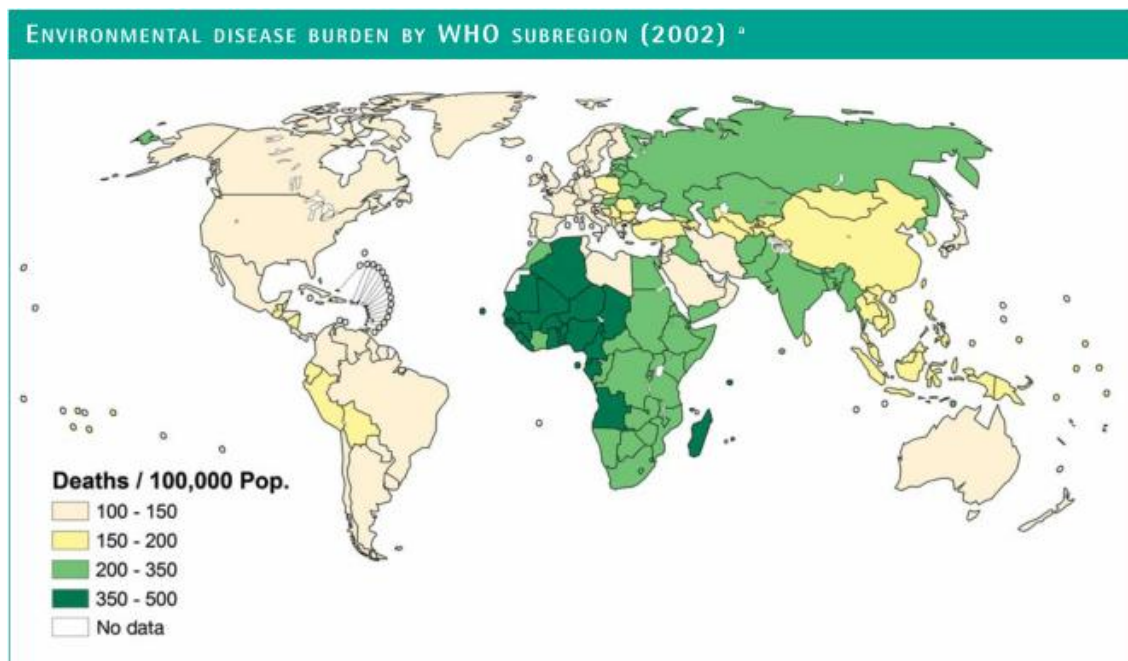
It will be possible to devise an efficient abatement strategy for PAH when their sources and atmospheric fates are comprehensively understood. The understanding of source identification of PAH and of local emission characteristics from geographically different regions, is paramount in order to prepare detailed strategies for policy makers.

This chapter provides the broad characteristics of urban pollutants, focusing particularly on PAH; covering their chemistry, their associated regulations, and the tools used for the identification of their sources.

1.2 Urbanization

Populations are becoming increasingly concentrated in cities globally. According to a report of the World Health Organization (WHO), over 50% of people were living in urban areas in 2010, which was up by around 10% from 20 years ago, and this percentage is expected to rise to 70% by 2050 (WHO, 2010).

In centralized areas, there is a potential for high levels of pollution originating from various kinds of anthropogenic activities. These elevated concentrations of pollutants are responsible not only for acute effects on health but also for chronic diseases resulting from long term exposure. It has been suggested that particulate matter (PM) increases mortality from cardiopulmonary disease by 3% throughout the world (Cohen et al., 2005). An estimation of daily deaths related to respiratory problems caused by pollution levels in 10 US cities showed that atmospheric environment affects health not only immediately but also slowly, in a lagged response (Luís Ferreira Braga et al., 2001). It was established that 23% of deaths were caused by environmental factors and this percentage might be increased if unknown diseases or chronic injuries that might be attributable to environmental causes were taken into consideration (Corvalán, 2006). The WHO has estimated the environmental disease burden (see Figure 1.1), and it is estimated that 800,000 people die prematurely every year owing to urban air pollution.



^a The disease burden is measured in deaths per 100 000 population for the year 2002. See Annex 1 for a list of the countries in each WHO subregion.

Figure 1.1. *Environmental disease burden by WHO subregion. The disease burden is measured in deaths per 100,000 population for the year 2002.*

1.3 Atmospheric pollutants and health effects

Various organic and inorganic compounds have been studied as tracers of urban atmospheric pollution on a regional scale. A summary of the source emission contributions in the UK, obtained from the UK National Atmospheric Emissions Inventory (NAEI), is provided for each air quality pollutant (Table A1, Appendix A) and USEPA's 16 priority PAH including BaP (Table A2, Appendix A). This section provides the general characteristics of atmospheric pollutants, including their formation processes, main sources and health impacts.

Oxides of nitrogen (NO_x)

Oxides of nitrogen (NO_x) are chemical combinations of nitrogen with oxygen, such as nitric oxide (NO) and nitrogen dioxide (NO₂), produced under very high temperature conditions. Primarily emitted NO oxidizes to NO₂ by photochemical reactions in the presence of ozone (O₃). NO₂ concentrations can therefore be considered as secondary emissions. Road vehicles have been recognised as a main anthropogenic contributor to the atmospheric NO_x level in urban areas. NO₂ concentrations have been widely studied as an indicator of exposure to traffic related emissions, and many epidemiological studies have shown the link between both short-term or long-term exposure to NO₂ and health problems such as lung malfunction and respiratory diseases (Pekkanen et al., 2000, WHO, 2003, WHO, 2006, Gillespie-Bennett et al., 2011, Parenteau and Sawada, 2011).

Sulphur dioxide (SO₂)

A main production process for atmospheric sulphur dioxide (SO₂) is the oxidation of sulphur (S) contained in fossil fuels through combustion. Industrial combustion and coal-fired power plants have been recognised as the most significant anthropogenic source of SO₂ (Gaffney and Marley, 2009). Non-industrial activities such as domestic heating or vehicles with internal combustion engines have been found to be another significant source of SO₂ in urban air (Gaffney and Marley, 2009). It was found that anthropogenic sulphur emissions could be decreased substantially over decades in Europe and the United States by improving control facilities and reducing the sulphur content in fuels (Jones and Harrison, 2011). Vestreng et al. (2007) explained that SO₂ emissions were reduced by 27% in Europe between 1980 and 2004. This was due to a

high reduction in SO_2 emissions from the industrial sector resulting from various regulations. The EMEP (European Monitoring and Evaluation Programme) projections for a steep reduction of annual SO_2 emissions over 20 years in Europe are shown in Figure 1.2 (Gun Lövblad, 2004). However, various epidemiological studies, including studies of pulmonary malfunction and bronchoconstriction symptoms may reflect the necessity for continuous monitoring of SO_2 in terms of its health impact (Schouten et al., 1996, Peters et al., 1997, Aekplakorn, 2003, Neuberger et al., 2007).

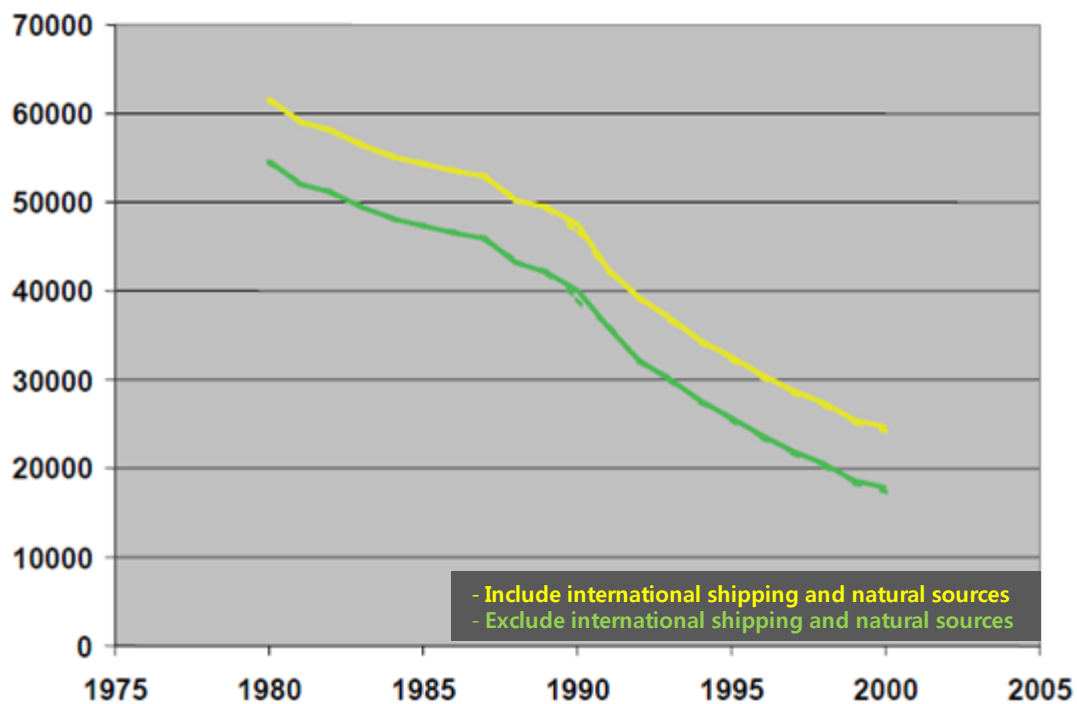


Figure 1.2. Annual emissions of SO_2 in the European countries 1980-2000 (Gun Lövblad, 2004).

Ozone (O_3)

The level of atmospheric ozone (O_3) consists of tropospheric and stratospheric O_3 . The former is responsible for about 10% and the latter for 90% of O_3 in the atmosphere. Ground level O_3 in the troposphere results from the combination of natural productions

and secondary emissions formed through complicated photochemical reactions involving precursor pollutants such as nitrogen oxides (NO_x) and volatile organic compounds (VOCs) (WHO, 2003, Ebi and McGregor, 2008). A relatively stronger sunlight is responsible for a high O_3 concentration in the summer (Ebi and McGregor, 2008) and a diurnal pattern showing higher concentrations during the daytime (WHO, 2003). Additionally, O_3 is considered as a main source of the hydroxyl radical (OH), which plays a significant part in the atmospheric oxidization of other pollutants (Monks et al., 2009). It was estimated that a daily increase in the O_3 level of 10 ppb_v in summer contributes to a mortality increment of 0.41% (WHO, 2003). O_3 has been investigated in relation to mortality, cardiopulmonary diseases and lung problems (Fattore et al., 2011).

Particulate matter (PM)

A large portion of airborne particulate matter (PM) is produced through incomplete combustion processes (Ito et al., 2005), and exists as a condensed phase of both solids and liquids. Atmospheric PM consists of the primary particles emitted directly from sources and the secondary aerosols formed from gas phase reactions. Gas phase precursors such as NO_x , SO_2 and NH_3 can contribute to the PM mass concentration significantly by forming secondary inorganic matter such as ammonium sulphate $(\text{NH}_4)_2\text{SO}_4$ and ammonium nitrate (NH_4NO_3) . Recently, many studies have focused on the size distribution and number concentration of atmospheric particles (Kavouras and Stephanou, 2002, Harrison and Jones, 2005, Dall'Osto et al., 2008). The different combustion processes generate different ranges of PM, providing additional information for source identification. Common size classifications of PM are coarse mode (2.5-10

µm), accumulation mode (0.18-2.5 µm), and ultrafine mode (< 0.10 µm). Different formation processes subdivide the ultrafine mode into the larger soot mode (0.04-0.10 µm) and the smaller nucleation mode (< 0.03 µm) (Kuhn et al., 2005). The former mode is predominantly produced from an internal combustion engine, and the latter mode is a condensed fraction of the gaseous phase, forming within 0.5s through dilution and cooling after emission from tail pipes (Virtanen et al., 2006). A dominant PM number concentration on-road is seen in the nucleation mode, with an average diameter of 0.02 µm (Virtanen et al., 2006). Nanoparticles (< 0.05 µm) are generally explained as secondary particles, agglomerating together or coated by semi-volatile organic pollutants through an incomplete combustion process of fossil fuels. It is still being debated whether particles themselves have a direct health impact or whether it is the chemical composition of particles that is more linked to health problems (Sofowote et al., 2010b). Extensive health effect studies of PM have been conducted from the aspect of particle size (Curtis et al., 2006). The significance of understanding the nano-structural heterogeneity of PM was introduced to explain the health mechanism of source-specific particles (Hays and Vander Wal, 2007). To conclude, integrated studies considering the composition, mass/number concentration, structure of PM and size segregation that combine source apportionment may improve understanding of the source-specific formation process of particle-bound pollutants and the health influence mechanism both quantitatively and qualitatively.

Polycyclic aromatic hydrocarbons (PAH)

Polycyclic aromatic hydrocarbons (PAH) are an organic compound group consisting of two or more fused benzene rings produced mostly from various incomplete combustion

processes. PAH are ubiquitous compounds, having various sources. They can be produced from both natural sources and anthropogenic sources. Volcanic eruptions and forest fires are examples of natural sources of atmospheric PAH. The combustion processes of mobile vehicles, and of industries and domestic activities such as burning of coal, oil and wood, are recognised as main anthropogenic sources. In the air, they can be present in both the gaseous and particulate phases. Most low molecular weight (LMW) PAH having two or three rings are emitted predominantly in the gas phase, through combustion processes, and quickly react with atmospheric oxidants (OH, NO₃ and O₃) (Gutiérrez-Dabán et al., 2005). High molecular weight (HMW) PAH consisting of five or more rings have a relatively low flux of volatilization and tend to remain in the particle phase. It is known that they are strongly attracted by carbon rich particles such as soot and black carbon (Lammel et al., 2009). They resist oxidation from radicals by adsorbing onto the airborne particles and absorbing into organic matter. Moreover, shielding gases surrounding airborne particles make it more difficult for radicals to reach the inner particle-associated PAH. There is a relatively flexible compound group in terms of phase distribution of PAH. The phase partitioning for three to four ring PAH is very sensitive to the ambient temperature (Yamasaki et al., 1982). PAH have been getting attention because of their recognised carcinogenic and mutagenic properties, which have an influence on human health (Vinggaard et al., 2000, Farmer et al., 2003).

Many efforts have been made over several decades to identify the sources of PAH in urban areas. It has been globally recognised that traffic exhaust fumes are a significant source of atmospheric PAH (Guo, 2003, Motelay-Massei et al., 2007, Sharma et al., 2007, Vardoulakis et al., 2008, Miller et al., 2010). Similarities between diurnal

variations in PAH and gaseous traffic markers such as CO and NO_x, which both peak in the rush hour (Nielsen, 1996), may reflect this traffic source. Inefficient coal combustion during domestic heating, leading to significant PAH emissions, has been commonly recognised as a global concern (Chen et al., 2005, Fu et al., 2010, Shen et al., 2010). A significant contribution to PAH levels from coal combustion activity in industrial sectors such as aluminum and steel production activities has also been recognised as a significant source of atmospheric PAH (Ciaparra et al., 2009, Baraniecka et al., 2010, Sofowote et al., 2010a, Ooi and Lu, 2011, Dall'Osto et al., 2012, Menezes and Cardeal, 2012). The physicochemical properties of PAH are discussed in subsequent sections.

1.4 The chemistry of ambient polycyclic aromatic hydrocarbons (PAH)

1.4.1 Generation of PAH

As previously mentioned, polycyclic aromatic hydrocarbons (PAH) are emitted predominantly through incomplete combustion processes, influenced by combustion conditions and fuel types; so it may be useful to understand the general PAH formation process from the point of view of sources. This chapter considers several thermal PAH generation processes, leading to soot formation.

The first aromatic ring can be produced through an early pyrolysis of fuels at a temperature of 700 °C and an oxidation in the fuel-rich core (Violi et al., 1999, Hays and Vander Wal, 2007, Rajput and Lakhani, 2010). The rate coefficients of key reactions in the formation of aromatic hydrocarbons are reported in Table 1.1.

Table 1.1. Rate coefficients of key reactions of aromatic hydrocarbon formations (Violi et al., 1999).

Reactions	Rate coefficient (cm ³ molecules ⁻¹ s ⁻¹)
<i>Benzene formation</i>	
$C_3H_3 + C_3H_3 = C_6H_5 + H$	3.0E + 12
$nC_4H_5 + C_2H_2 = C_6H_6 + H$	1.0E + 16
$nC_4H_3 + C_2H_2 = C_6H_5$	2.8E + 03
$C_3H_3 + H_3CCHCCH = C_6H_5CH_2 + H$	3.0E + 12
<i>Larger aromatic formation</i>	
$C_6H_5CH_2 + C_3H_3 = C_{10}H_8 + H + H$	3.0E + 12
$C_6H_5 + C_3H_3 = C_6H_5C_3H_2 + H$	3.0E + 12
$C_6H_5C_3H_2 + C_3H_3 = C_6H_5C_6H_4 + H$	3.0E + 12
$C_6H_5C_6H_4 + C_2H_2 = C_{14}H_{10} + H$	6.6E + 33
$C_5H_5 + C_5H_5 = C_{10}H_8 + H + H$	3.8E + 12
$C_9H_7 + C_5H_5 = C_{14}H_{10} + H + H$	3.8E + 12
$C_6H_5 + C_2H_2 = C_6H_5C_2H + H$	5.1E + 38
$C_6H_5C_2H + H = C_6H_4C_2H + H_2$	2.5E + 14
$C_6H_4C_2H + C_2H_2 = C_{10}H_7$	1.4E + 51

Near the flame front, at a temperature of 1300 °C, acetylene (C₂H₂) is produced through the breakdown of PAH and fuel components (Hays and Vander Wal, 2007). Undetected C₂H₂ among compounds evaporated from soot samples in fuel rich C₂H₂ flames reflects the possibility of reactions between C₂H₂ and carbon atoms (Homann and Wagner, 1967). It has been recognised that sequential reactions of H-atom abstraction and acetylene additions (HACA) are responsible for PAH growth. This is the most broadly used mechanism of PAH growth that is modelled in studies, and it also contributes to

the formation of primary solid particles as seen in Figure 1.3 (Ravindra et al., 2008a). Additionally, it has been shown that the nanostructures of particles can be varied through the PAH growth process, depending on combustion temperatures and fuel types (Hays and Vander Wal, 2007).

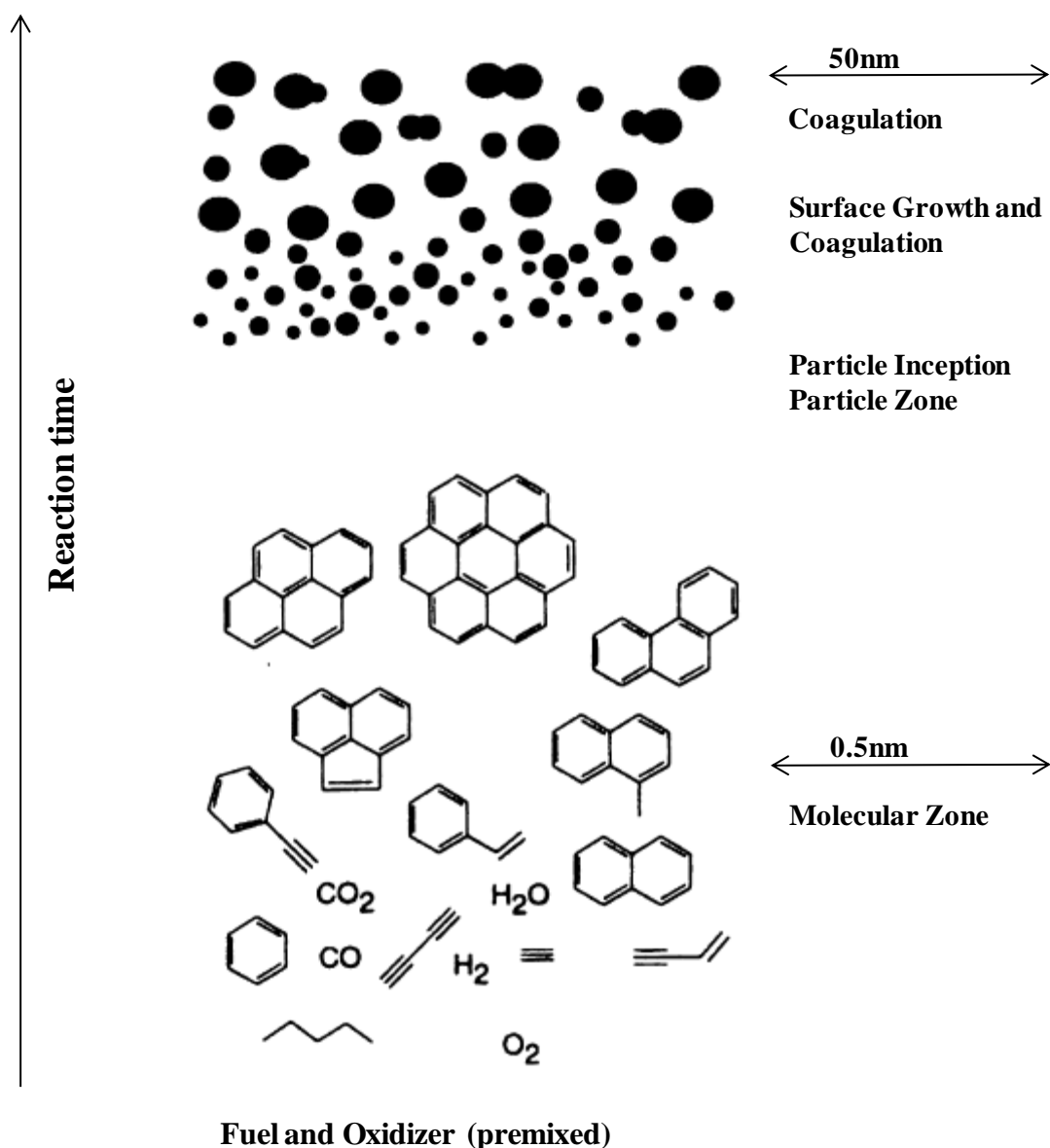


Figure 1.3. A rough picture of soot formation in homogeneous mixtures (premixed flames) from Ravindra et al. (2008a).

Not only progressive processes (HACA) but also other mechanisms, such as the combination of two neutral PAH (PAH-PAH) or of neutral and ionic PAH (PAH-PAH⁺), can contribute to PAH growth (Weilmünster et al., 1999). It has been suggested that a polymerization of small PAH is a significant growth process leading to a high molecular mass compound (Violi et al., 1999). The role of radicals in PAH growth has been recognised. For example, the addition of phenyl radicals and benzene to existing PAH can contribute to the formation of larger ring PAH (Comandini et al., 2012). It is possible that combinations of resonantly stabilized free radicals such as benzylpropargyl (Figure 1.4a), cyclopentadienyl-cyclopentadienyl (Figure 1.4b) and indenyl-cyclopentadienyl (Figure 1.4c) can produce significant numbers of larger aromatic compounds, because a single HACA model was insufficient to explain the total yield of multi-ring aromatic formation (Violi et al., 1999).

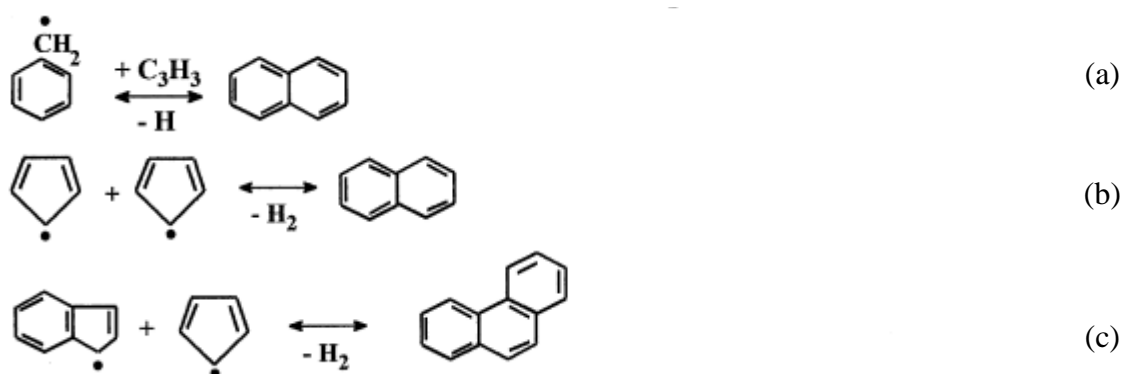


Figure 1.4. A schematic diagram of multi-ring PAH formation (Violi et al., 1999).

It has been shown that fuel types can influence the rate of PAH formation. Aromatic fuel flames (benzene) have shown a higher rate of PAH formation and produced 100 times more PAH than aliphatic fuel flames (acetylene) under the same C/O ratio (Homann and Wagner, 1967). Fuel types also vary the association of PAH with different airborne

particle sizes (Tiwari et al., 2013). Other factors such as C/O ratios, concentrations of oxygen (O₂) and temperatures at which combustion takes place are responsible for the yield of PAH formation (Violi et al., 1999), leading to a heterogeneity of nano-particle structures (Hays and Vander Wal, 2007) and a size-segregation of particle-associated PAH (Allen et al., 1996, Kaupp and Michael, 1998, Zhu et al., 2014).

1.4.2 PAH reactivity

It is important to study not only the formation processes of PAH but also their atmospheric reactivity after emission from sources.

PAH are semi-volatile compounds that exist both in the gaseous phase and particulate phases corresponding to their vapour pressure, and they are sensitive to ambient temperatures (Yamasaki et al., 1982). Physicochemical information of the US Environmental Protection Agency's (EPA's) 16 priority PAH are shown in Table 1.2.

Table 1.2. *Physicochemical information on 16 USEPA priority PAH.*


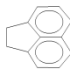


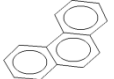
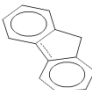
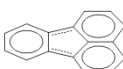
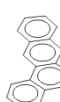
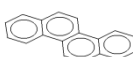


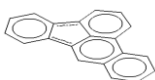
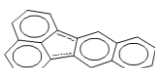



	Compounds (Abbreviation)	Structures	Molecular weight ^a (g mol ⁻¹)	Vapour pressure ^b (mmHg at 20°C)
1	naphthalene (Nap)		128.17	8.89E-02
2	acenaphthene (Ace)		154.21	3.75 E-03
3	acenaphthylene (Acy)		152.20	2.90 E-02

Table 1.2. (Continued).

	Compounds (Abbreviation)	Structures	Molecular weight ^a (g mol ⁻¹)	Vapour pressure ^b (mmHg at 20°C)
4	anthracene (Ant)		178.23	2.55 E-05
5	phenanthrene (Phe)		178.23	6.80 E-04
6	fluorene (Flu)		166.22	3.24 E-03
7	fluoranthene (FluA)		202.26	8.13 E-06
8	Benzo[<i>a</i>]anthracene (BaA)		228.29	1.54 E-07
9	chrysene (Chr)		228.29	7.80 E-09
10	pyrene (Pyr)		202.26	4.25 E-06
11	Benzo[<i>a</i>]pyrene (BaP)		252.32	4.89 E-09
12	Benzo[<i>b</i>]fluoranthene (BbF)		252.32	8.06 E-08
13	Benzo[<i>k</i>]fluoranthene (BkF)		252.32	9.59 E-11
14	Dibenz[<i>a,h</i>]anthracene (DahA)		278.35	2.10 E-11
15	Benzo[<i>ghi</i>]perylene (BgHiPe)		276.34	1.00 E-10
16	indeno[1,2,3- <i>cd</i>]pyrene (IcdP)		276.34	1.40 E-10

^a Sander and Wise, 1997; ^b Bojes and Pope, 2007

Most low molecular weight (LMW) PAH, having 2-3 rings and relatively high volatilization flux, are initially emitted in the gas phase not only through incomplete combustion processes (pyrogenic) but also through volatilisation processes, being usually emitted from ‘unburned petroleum sources’ (petrogenic) (Rogge et al., 1993, Gogou et al., 1996, Kavouras et al., 2001, Zuo et al., 2007) or ‘re-volatilised source’ from ground surface (Lammel et al., 2009, Cabrerizo et al., 2011). They are predominantly distributed in the vapour phase in the air. It has generally been recognised that PAH vapour is oxidized by oxidants such as hydroxyl (OH), ozone (O₃) and nitrate (NO₃), which determines the atmospheric fate of LMW PAH. Sometimes, the oxidations of PAH lead to the formation of nitro-PAH and oxy-PAH, which are reported in being mutagenic and carcinogenic (Atkinson and Arey, 1994).

The significance of OH radical reaction with PAH vapour phase is shown in Table 1.3. Many experimental studies have focused on quantifying the OH reaction rate coefficients of individual PAH congeners (Atkinson and Aschmann, 1988, Brubaker and Hites, 1998, Reisen and Arey, 2002). Concurrently, air plume studies have been conducted to get a realistic estimation of atmospheric OH concentrations (Blake et al., 1993, Dillon et al., 2002). Photochemical modelling studies have compared OH concentration between predicted values and field measurements (Emmerson et al., 2005, Harrison et al., 2006).

Table 1.3. Experimental rate coefficients of gaseous LMW PAH with oxidants (Keyte et al., 2013).

	OH reactions k_{OH} ($\text{cm}^3 \text{ molecules}^{-1} \text{ s}^{-1}$)	NO_3 reactions $k_{\text{NO}_3}^a$ (s^{-1})	O_3 reactions k_{O_3} ($\text{cm}^3 \text{ molecules}^{-1} \text{ s}^{-1}$)
Acy	$1.1\text{-}1.3 \times 10^{-10}$ (295-296K)	$5.5 \times 10^{-12}^b$ ($296 \pm 2\text{K}$)	$1.6\text{-}5.5 \times 10^{-16}$ ($296 \pm 2\text{K}$)
Ant	$1.3 \times 10^{-11} \text{-} 2.0 \times 10^{-10}$ (296-298K)		
Phe	$1.3\text{-}3.4 \times 10^{-11}$ (296-299K)	$1.2 \times 10^{-13}^d$ ($296 \pm 2\text{K}$)	4.0×10^{-19} ($296 \pm 2\text{K}$)
Flu	$1.3\text{-}1.6 \times 10^{-11}$ (297-300K)	$3.5 \times 10^{-14}^c$ ($297 \pm 2\text{K}$)	
FluA	1.1×10^{-11} (298K)	6.6×10^{-17} ($296 \pm 2\text{K}$)	
Pyr	5.0×10^{-11} ($296 \pm 2\text{K}$)	2.1×10^{-16} ($296 \pm 2\text{K}$)	

^a $k_{\text{NO}_3} (\text{s}^{-1}) = k_{\text{NO}_3} (\text{cm}^3 \text{ molecules}^{-1} \text{ s}^{-1}) \times [\text{NO}_2]$; ^b $[\text{NO}_2] = < 1.2 \times 10^{15} \text{ molecules cm}^{-3}$; ^c $[\text{NO}_2] = (7.2\text{-}2.4) \times 10^{13} \text{ molecules cm}^{-3}$; ^d $[\text{NO}_2] = (4.8\text{-}24) \times 10^{13} \text{ molecules cm}^{-3}$

High molecular weight (HMW) PAH, having five or more rings and relatively lower vapour pressure, are usually associated with airborne particles. They can be absorbed into organic particles or adsorbed onto the surface of particles. It has reported that the dominant loss mechanism for airborne particulate PAH is a wet deposition (Ravindra et al., 2008a). However, as they are predominantly distributed to fine particles and have a relatively high potential for long-range transport (Baek et al., 1991), it is important to take into account any oxidation reaction in understanding the atmospheric fate of HMW PAH. Extensive laboratory studies of heterogeneous degradation of PAH have also been conducted and shown in Table 1.4.

Table 1.4. Laboratory rate coefficients for heterogeneous reaction of HMW PAH with oxidants (Keyte et al., 2013).

	OH reactions k_{OH} (cm ³ molecules ⁻¹ s ⁻¹)	NO ₂ reactions k_{NO_2} (cm ³ molecules ⁻¹ s ⁻¹)	O ₃ reactions k_{O_3} (cm ³ molecules ⁻¹ s ⁻¹)
FluA	1.4×10^{-14} (K) - 3.2×10^{-12} (G)	3.2×10^{-21} (S) - 2.9×10^{-17} (G)	1.5×10^{-17} (S) - 1.9×10^{-17} (G)
Pyr	1.6×10^{-14} (K) - 3.2×10^{-12} (G)	1.0×10^{-19} (K) - 3.2×10^{-16} (S)	2.5×10^{-17} (G) - 9.3×10^{-17} (S)
BaA	9.2×10^{-15} (K) - 5.6×10^{-13} (G)	1.0×10^{-19} (K) - 3.3×10^{-17} (G)	2.8×10^{-17} (G) - 8.7×10^{-17} (S)
BaP	1.1×10^{-14} (K) - 4.1×10^{-12} (G)	1.0×10^{-19} (K) - 9.3×10^{-16} (S)	5.3×10^{-17} (G) - 1.4×10^{-16} (S)
BkF	1.0×10^{-14} (K) - 3.5×10^{-12} (G)	1.0×10^{-19} (K) - 2.5×10^{-17} (G)	5.3×10^{-17} (G) - 1.4×10^{-16} (S)
IcdP	3.5×10^{-13} (D)	1.0×10^{-19} (K) - 7.5×10^{-18} (D)	1.9×10^{-17} (G) - 3.8×10^{-17} (S)
BghiPe	5.9×10^{-12} (G)	1.0×10^{-19} (K) - 4.7×10^{-17} (S)	
DahA	1.6×10^{-14} (K)	1.0×10^{-19} (K)	

K: Kerosene flame soot; G: Graphite particles; S: Silica particles; D: Diesel exhaust particles SRM 1650a

Dependent upon the different types of substrates, such as graphite, silica and diesel, in which PAH are distributed, the rate coefficients of individual PAH can vary with respect to atmospheric oxidants (OH, O₃ and NO₃) (Esteve et al., 2004, Perraudin et al., 2005, Esteve et al., 2006, Perraudin et al., 2007). However there is still some doubt as to whether or not these experimental rate constants, obtained from laboratory simulations, are consistent with real atmospheric values. In practice, a limitation of the accessibility of radicals to particle-bound PAH has been mentioned, and shielded secondary gases surrounding the particles additionally increase resistance to the oxidation of PAH (Marr et al., 2006).

1.4.3 Phase distribution of PAH (partitioning)

As mentioned in the previous section, ambient PAH, are semi-volatile organic compounds (SVOC), which can exist in the gaseous phase and is associated with airborne particulates. The LMW PAH consisting of 2-3 benzene rings are predominantly distributed in the gas phase, and the HMW PAH having more than 5 rings usually remain in the particle phase. The phase distributions (G/P partitioning) of PAH in the atmosphere are important in determining their fate because the two phases have different rates of chemical reactions and transport. G/P partitioning of individual PAH is determined by their vapour pressure corresponding to ambient temperature. This can be constantly rearranged after being emitted from sources, due to the physicochemical reactions they undergo in the air. Various meteorological conditions and types of airborne particles can also have an influence on G/P partitioning (Ravindra et al., 2008a).

There has been considerable progress in our understanding of G/P partitioning. Generally, two main mechanisms are presented in a PAH partitioning model: one is a process whereby PAH are adsorbed onto the surface of soot aerosol particles; and the other is a process whereby PAH are absorbed into aerosol organic matter. However, which mechanism dominates this process is still unclear.

Until 1994, the Langmuirian adsorption theory, developed by Pankow, was considered the main mechanism for G/P partitioning of SVOCs (see Equation 1.1) (Lohmann and Lammel, 2004, Vardar et al., 2004).

Particle-gas partition coefficient (K_p) defined by Pankow is

$$K_p \text{ (m}^3 \mu\text{g}^{-1}\text{)} = (F/A)/\text{TSP} \quad \text{Equation 1.1.}$$

where K_p is the particle-gas partition coefficient, F is a particulate concentration onto a filter, A is a gaseous concentration from an adsorbent, and TSP is the total suspended particulate phase.

Based on Equation 1.1, a predicted particulate fraction (Φ) is obtained in Equation 1.2.

$$\Phi = K_p \text{TSP}/(K_p \text{TSP} + 1) \quad \text{Equation 1.2.}$$

Alternatively, for the adsorption, Pankow derived K_p can be expressed as (Lohmann and Lammel, 2004)

$$K_p \text{ (m}^3 \mu\text{g}^{-1}\text{)} = \frac{N_s A_{\text{TSP}} T_e^{(Q_L - Q_V)/RT}}{16P_L^\circ} \quad \text{Equation 1.3.}$$

where N_s is the surface concentration of sorption sites (mol cm^{-2}), A_{TSP} is the specific surface area of the TSP ($\text{cm}^2 \mu\text{g}^{-1}$), T_e is the ambient temperature (K), Q_L is the enthalpy of the desorption from the surface, Q_V is the enthalpy of vaporization of the subcooled liquid (kg mol^{-1}), R is the ideal gas constant ($8.3 \text{ J mol}^{-1} \text{ K}^{-1}$) and P_L° is the vapor pressure of the subcooled liquid (torr).

On the other hand, phase partitioning of SVOCs, including PAH, can also appear through absorption into the primary or secondary aerosol organic matter. For the

predominant absorption mechanism, octanol-air partitioning coefficient (K_{OA}) is recommended as an alternative to vapour pressure (P_L^0). These are expressed in Equations 1.4 and 1.5.

The partitioning coefficient (K_p) expressed as K_{OA} is,

$$K_p = f_{OM} \frac{MW_{oct} \gamma_{oct}}{MW_{OM} \gamma_{OM} 10^{12} \rho_{oct}} K_{OA} \quad \text{Equation 1.4.}$$

where f_{OM} is the organic matter phase fraction for total suspended particles (TSP), MW_{oct} and MW_{OM} are the mean molecular weights for octanol and the organic matter phase, γ_{oct} and γ_{OM} are activity coefficients of SVOCs in the octanol and organic matter phase, respectively, and ρ_{oct} is the density of octanol.

Equation 1.4 can be simplified with an assumption that $MW_{oct}/MW_{OM} = 1$ and $\gamma_{oct}/\gamma_{OM} = 1$ (Harner and Bidleman, 1998b).

$$\log K_p = \log K_{OA} + \log f_{OM} - 11.91 \quad \text{Equation 1.5.}$$

Recently, several modelling studies have considered both the adsorption and absorption mechanisms for PAH partitioning. It has been mentioned that adsorption is the dominant PAH G/P partitioning mechanism, as absorbed PAH are responsible for the minor (<10%) fraction of total particle-bound PAH (Dachs and Eisenreich, 2000). However, an initial dominance of the adsorption mechanism onto the surface of particles can shift to an absorption into the organic material mechanism when PAH concentration is increased and adsorption-available surface is limited (Lohmann and Lammel, 2004). A nonlinear equation considering both absorption and adsorption mechanisms can be expressed as,

$$K_p = 10^{-12} \left(f_{OM} \frac{MW_{oct} \gamma_{oct}}{MW_{OM} \gamma_{OM} \rho_{oct}} K_{OA} + f_{BC} \frac{\sigma_{atm-BC}}{\sigma_{soot} \rho_{BC}} K_{soot-air} \right) \quad \text{Equation 1.6.}$$

where ρ_{BC} is the density of BC, $K_{soot-air}$ is the partitioning coefficient between diesel soot and air, and σ_{atm-BC} and σ_{soot} are the available surfaces of the atmospheric BC and diesel soot, respectively.

It has been widely recognised that the fate of atmospheric PAH is significantly determined by phase distribution during transport, depending on the meteorological conditions. This may be responsible for a significant mechanism in PAH transport at a regional and global scale in modelling studies.

1.4.4 Long-range transport of PAH

The significance of the long-range transport of fine particles, which have a relatively long life time in the air, has been discussed (Colvile et al., 2001). And the very high particulate matter concentrations at the Arctic during the cold season have been explained by the long-range transport of anthropogenic pollution (Sofowote et al., 2010c). The fact that particulate PAH are dominantly distributed as fine particles has made it necessary to consider the long-range transport of PAH. Size segregation of PAH has shown that most particulate PAH congeners have unimodal distribution from 0.4 μm to 1.1 μm , which means they are able to escape dry/wet deposition, and they are potentially able to travel long distances depending on urban atmospheric conditions (Nielsen et al., 1995, Zhu et al., 2014). Moreover, underestimation of particle-bound PAH in modelling studies comparing these to actual atmospheric particle fraction

(Halsall et al., 2001) may account for the resistance to degradation of airborne particle-bound PAH during transport (Zelenyuk et al., 2012, Friedman et al., 2014). In practice, PAH concentrations have been found in the atmosphere in remote areas that have few emission sources, or at unpolluted sites such as the Antarctic, which supports the possibility of influxes from the long-range transport of pollutants (Lohmann and Lammel, 2004, Read et al., 2007, Sofowote et al., 2011, Alam et al., 2014).

During long-range transport, PAH experience physicochemical reactions. They can be removed through wet/dry deposition; and they are also involved in reactions with radicals, accompanying a phase re-distribution between gaseous and particulate phases and producing PAH derivatives such as nitro-PAH and oxy-PAH.

1.5 Seasonal variation of PAH

There is general agreement on the seasonal variability of PAH measurements in urban air. Increased levels of low molecular weight (LMW) PAH are commonly seen in summer, explained by the relatively higher vapour pressures owing to the enhanced ambient temperature (Cincinelli et al., 2007). Significant summer concentrations of acenaphthene (Ace) and phenanthrene (Phe), predominantly responsible for total PAH concentrations, have been observed in London and Manchester during the summer (Tuominen et al., 1988, Coleman et al., 1997). In terms of sources, these enhanced LMW PAH contributions in summer are explained by ‘unburned petroleum sources’ which emit LMW PAH that have escaped from internal combustion engines (Harkov et al., 1984), burning fuels such as gasoline (Meijer et al., 2008) and diesel (Tuominen et

al., 1988, Coleman et al., 1997, Marr et al., 1999, Meijer et al., 2008, Park et al., 2011).

A significant winter level of particle-associated PAH is commonly seen in geographically different urban areas. This seasonality difference can be explained by several scenarios. Firstly, there are sources that have high emission intensity in winter. Domestic combustion activity for central heating is considered as one of the most significant sources of particle-bound PAH in the cold season. The possibility of contributions to the high level of PAH from vehicle exhausts has also been proposed due to inefficient combustion conditions at low temperatures (Westerholm and Egeback, 1994, Nielsen et al., 1995, Nielsen et al., 1999, Marchand et al., 2004). However it is not likely that only seasonal sources cause the seasonality of PAH levels, as little seasonal pattern in gaseous PAH, but an apparent seasonal variation in particulate PAH, has been observed in rural areas (Gustafson and Dickhut, 1996) where seasonal sources are rare and atmospheric PAH levels are determined by transported air masses from source regions. Meteorological conditions can also influence seasonal variations. Low mixing heights and low atmospheric temperatures that influence G/P partitioning of PAH are responsible for the high concentration of particulate PAH in winter (Nielsen et al., 1995, Tsapakis and Stephanou, 2005, Ravindra et al., 2008a, Delhomme and Millet, 2012). Furthermore, photochemical factors may also account for the seasonality of PAH concentrations. The high intensity of solar radiation in summer can produce more radicals, such as O_3 and OH, leading to active degradation of PAH, especially for PAH vapour. On the other hand, decreased photochemical reactions in the winter may be responsible for the increased particulate PAH levels found in the winter.

1.6 Toxicity and regulations of PAH

HMW PAH (> 5-ring), the group to which the inhalable size particles in an atmospheric environment are predominantly attributed, have a relatively high level of toxicity, and have the potential to pollute remote areas through long-range transport (Christensen and Arora, 2007). The toxicity of the LMW PAH is well known, but recent interest has been outlined on the toxicity of PAH derivatives such as nitro-PAH and oxygenated-PAH ('namely quinones'), which are produced primarily through incomplete combustion, by reactions with atmospheric oxidants (OH, NO₃ and O₃) (Atkinson and Arey, 2007, Tian et al., 2009). Due to the acknowledged mutagenic and carcinogenic properties of PAH, many human exposure studies have been conducted (Kameda et al., 2005, Orjuela et al., 2010, Ayi-Fanou et al., 2011). The toxicity information derived from the World Health Organization (WHO) and the International Agency for Research on Cancer (IARC) can be seen in Table 1.5. (Kameda et al., 2005, Delgado-Saborit et al., 2011).

Table 1.5. Target PAH and their risk.

Compounds	Abbreviation	Relative potency ^a to BaP	Classifications ^b
naphthalene	Nap	-	2B
acenaphthene	Ace	-	3
fluorene	Flu	-	3
phenanthrene	Phe	-	3
anthracene	Ant	-	3
fluoranthene	FluA	0.005	3
pyrene	Pyr	-	3
benz[a]anthracene	BaA	0.05	2B
chrysene	Chr	0.01	2B
benzo[e]pyrene	BeP	-	3
benzo[b]fluoranthene	BbF	0.12	2B

Table 1.5. (Continued).

Compounds	Abbreviation	Relative potency ^a to BaP	Classifications ^b
benzo[<i>k</i>]fluoranthene	BkF	0.03	2B
benzo[<i>a</i>]pyrene	BaP	1	1
dibenz[<i>a,h</i>]anthracene	DahA	2.1	2A
benzo[<i>ghi</i>]perylene	BghiPe	-	3
indeno[1,2,3- <i>cd</i>]pyrene	IcdP	0.13	2B
dibenzo[<i>a,e</i>]pyrene	DaeP	0.1	3
dibenzo[<i>a,c</i>]anthracene	DacA	0.1	-
dibenzo[<i>a,l</i>]pyrene	DalP	100	2A
dibenzo[<i>a,e</i>]fluoranthene	DaeF	1	3
dibenzo[<i>a,h</i>]pyrene	DahP	1.1	2B
dibenzo[<i>a,i</i>]pyrene	DaiP	0.1	2B

^a Risk values for lung cancer from WHO/IPCS (Kameda et al., 2005), ^b IARC (Delgado-Saborit et al., 2011), 1: Carcinogenic to humans; 2A: Probably carcinogenic to humans; 2B: Possibly carcinogenic to humans; 3: Not classifiable as to its carcinogenicity to humans

Due to the well-known mutagenic and carcinogenic properties of PAH, there has been a steady effort to regulate PAH worldwide. Benzo (a) pyrene (BaP), which is known as one of the most carcinogenic compounds amongst the PAH congeners (International Agency for Research on Cancer, 1987), is used as an alternative to the PAH mixtures for regulation. This is because the availability of BaP toxicological data (Collins et al., 1998), the stability of the concentration of individual PAH relative to BaP from mixture to mixture (Pufulete et al., 2004), and the accessibility of air-monitoring techniques for BaP (Collins et al., 1998). California's Toxic Air Contaminant program has included BaP as a reference for PAH mixtures in air monitoring (Collins et al., 1998). In 1989, the USA Environmental Protection Agency (EPA) listed 16 PAH as priority pollutants and categorized seven of them as carcinogenic ones (Wang et al., 2010). In 2005 the European Union set an annual target for BaP in ambient air of 1 ng m⁻³. The United Kingdom government adopted an air quality objective for PAH as a concentration of

BaP of 0.25 ng m^{-3} as an indicator of the PAH mixture (Delgado-Saborit et al., 2011). However, BaP is not always able to represent PAH mixtures, adequately. Therefore, toxic equivalent factors (TEF), namely those that have a BaP equivalent coefficient, are sometimes applied to individual PAH congeners to express the carcinogenicity level of a PAH mixture, Equation 1.7 (Callen et al., 2011).

$$(\text{BaP})_{eq} = \sum_{i=1}^N (\text{PAH})_i * \text{TEF}_i \quad \text{Equation 1.7.}$$

For decades, vehicles have been considered as a significant PAH contributor to urban air (Motelay-Massei et al., 2007). The diesel internal combustion engine has the advantage of lower emissions of carbon monoxide (CO) and oxides of nitrogen (NO_x); but not for PM and particulate PAH (Mi et al., 2000, Lim et al., 2005), as PAH are present in the crude oil and tend to end up in high concentrations in the diesel fuels, owing to the refining process. There is general agreement that gasoline combustion engines are significantly responsible for emissions of HMW PAH. Additionally, the significant amount of PAH emissions escaping from vehicle engines in the form of unburned PAH from fuels has been recognised (Mi et al., 2000, Lim et al., 2005). Thus, various abatement strategies have been applied to reduce vehicular emissions including installing a treatment device such as diesel particulate filters (DPF), improving the efficiency of the combustion engine, and moving to a cleaner fuel (Heeb et al., 2008). Reduction of sulphur content in diesel fuels is one of the efforts to reduce emissions originating from traffic. This reduction has contributed to an improvement of air quality throughout Europe (Jones et al., 2012). Figure 1.5 shows the global change of the sulphur content of diesel fuels from 2006 to 2014.

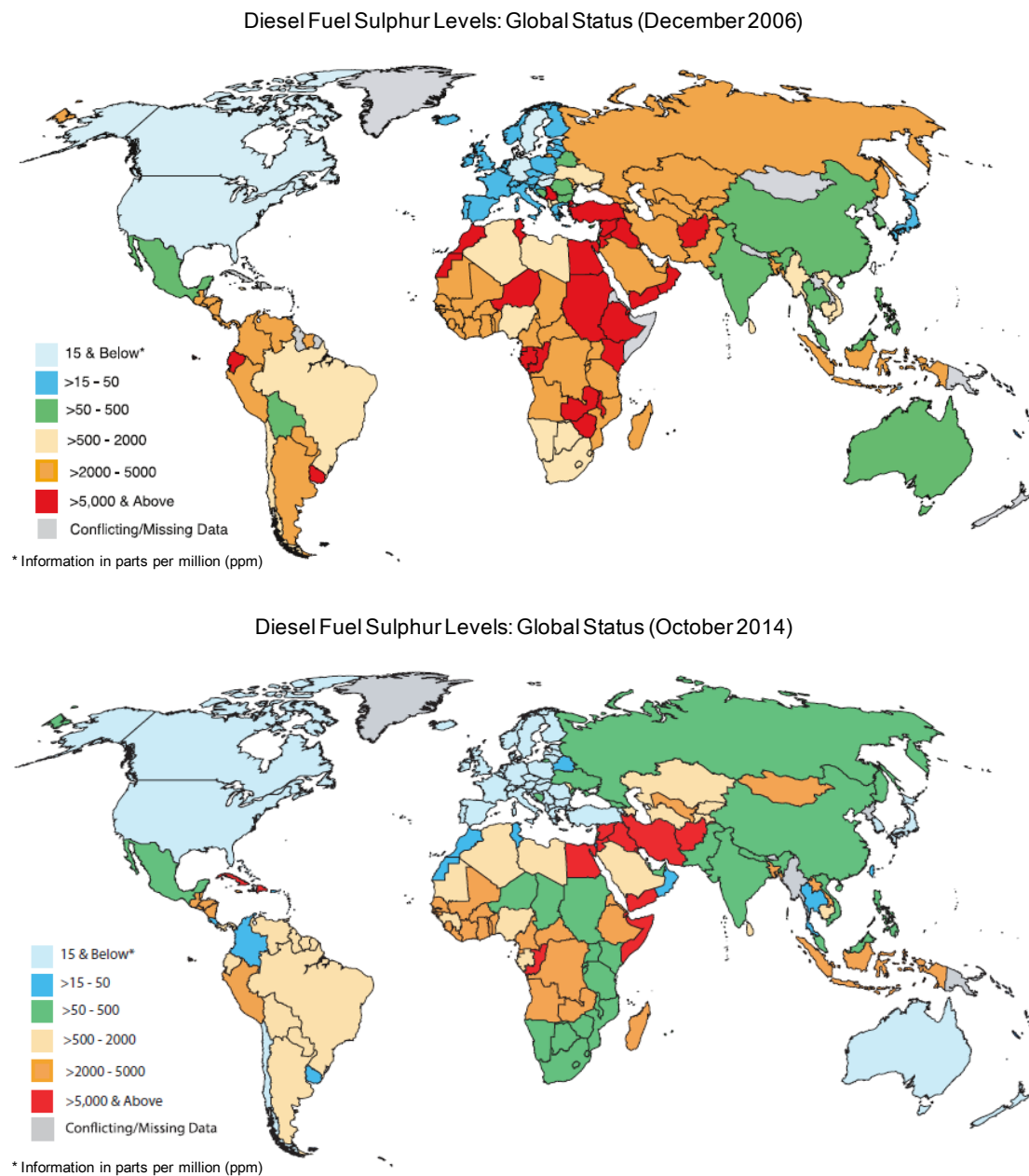


Figure 1.5. Global change of sulphur levels of diesel fuels (UNEP, 2006-2014).

1.7 Source identification of PAH

It is imperative to identify sources and quantify source-specific contributions to PAH, in order to design efficient strategies to reduce these compounds. Information on pollution

sources and their quantitative contributions to atmospheric pollution levels allows policy-makers to determine appropriate air quality plans to protect human health and to manage pollution levels in the environment on the local- and national-scale (Viana et al., 2008, Brown and Brown, 2012). In addition, source identification is useful to quantify transboundary pollution and to inform the public (Belis et al., 2014). Due to the direct implication of source identification for abatement strategies, it is important that the results should be reliable and reasonable (Galarneau, 2008).

Generally, there are two types of approaches for source apportionment (SA) (see Figure 1.6). One is a “bottom-up approach” that specifies source categories and figures for source-specific contributions through the combination of point source data, such as pollution inventory data for industrial emissions, and sub-national and local datasets such as statistics on energy use, major road traffic count and data for population and consumption (NAEI, 2012). The advantages of these emission estimations are: (a) information about pollution is easily accessible to the public, (b) long term emission trends can be read, (c) international comparison is possible, and (d) the compiled dataset is useful to plan integrated reduction policy in terms of efficiency (Tom Misselbrook et al., 2010). However, this approach needs comprehensive awareness of all possible sources (Sundqvist, 2009), otherwise these methods underestimate the real levels of pollution (Mooibroek et al., 2011). In addition, it may cause gaps between emission estimations and real measurements. Another technique is a statistical receptor model (RM) focused on observations (“top-down” approach). This method mathematically segregates and apportions measurements between sources under the assumption of mass conservation between emission sources and study sites, that is, ‘receptors’ (Lima et al.,

2002). This is less sensitive to missing or inaccurate emission data input than the emission estimates method, and is helpful to find sources that cannot be taken into consideration in the bottom-up approach (Dennis et al., 2010). Sometimes various sources make it difficult to interpret source-specific contributions to the observed pollution level. However, the little necessity for *a priori* knowledge has made it possible for these models to be used widely in source identification studies, as they do not involve consideration of the complex physicochemical processes of PAH such as oxidation, volatilization, deposition and G/P partitioning.

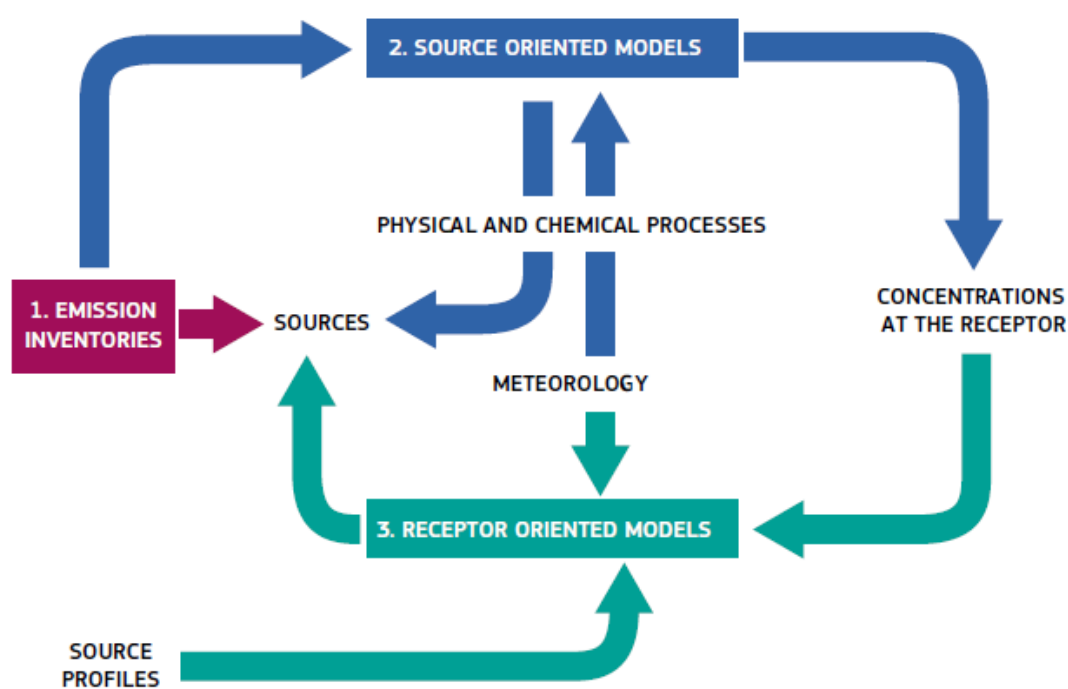


Figure 1.6. A schematic diagram of source identification (Belis et al., 2014).

In the following sections, three of the source identification methods most widely used for ambient pollutants are reviewed.

1.7.1 Diagnostic ratio (DR)

Diagnostic ratio (DR) analysis has been widely used to infer the sources of atmospheric PAH from those of petrogenic origin (originating from petroleum) to pyrogenic ones (derived from combustion), based on the assumptions that the relative proportions between PAH congeners are unique, depending on source types, and are preserved from each source to receptors (Ma et al., 2010, Dvorská et al., 2011, Tobiszewski and Namieśnik, 2012). To minimize the influence of variability between compounds in aspects such as volatility, solubility and ab/adsorption, a pair of PAH consisting of similar molecular mass is used to identify sources. Table 1.6 summarizes the statistical range of ratios for several sources of PAH.

Table 1.6. *Statistics of diagnostic ratios (Galarneau, 2008).*

Ratio	Source type						
	Coal combustion	Diesel vehicles	Gasoline vehicles	Natural gas combustion	Oil combustion	Vegetation combustion	Wood combustion
Phe/(Phe+Ant)	0.85±0.11 (n=12)	0.73±0.18 (n=2)	0.77±0.10 (n=7)	0.88±0.13 (n=12)	0.89±0.12 (n=10)	- (n=0)	0.84±0.16 (n=15)
FluA/(FluA+Pyr)	0.57±0.21 (n=14)	0.40±0.05 (n=2)	0.52±0.13 (n=7)	0.49±0.18 (n=20)	0.52±0.20 (n=12)	0.49±0.07 (n=5)	0.51±0.16 (n=24)
BaA/(BaA+Chr)	0.46±0.19 (n=14)	0.65±0.28 (n=2)	0.50±0.10 (n=6)	0.39±0.15 (n=12)	0.50±0.22 (n=15)	- (n=0)	0.59±0.25 (n=10)
IcdP/BghiPe	0.48±0.29 (n=11)	0.19±0.13 (n=2)	0.32±0.11 (n=5)	0.32±0.17 (n=8)	0.36±0.14 (n=6)	0.35±0.04 (n=3)	0.42±0.18 (n=9)

This approach is very useful when the distance between source and receptor site is small (Dvorská et al., 2011). However, overlapped values from different source types (intersource similarity) and the varying ratios in specific source category (intrasource

variability) contribute to uncertainty in examining source types clearly (Ravindra et al., 2006, Galarneau, 2008). This uncertainty has been explained either by mixed sources or by various types of atmospheric reactivity on the part of individual PAH congeners. For example, the partitioning of PAH between gaseous and particulate phases during sampling or transport may influence the transformation of ratios. Different aging rates through photodegradation and radical oxidation could also alter the PAH ratios (Esteve et al., 2004, Esteve et al., 2006, Perraudin et al., 2007, Kim et al., 2009). This may be an additional explanation for seasonal variability in the PAH ratios (Tobiszewski and Namieśnik, 2012). Furthermore, different combustion technologies are able to contribute to changes in the source-specific composition of PAH (Mari et al., 2010), and complex sources at a receptor site can lead to limited applicability of DR for source apportionment (Katsoyiannis et al., 2011). To conclude, many studies suggest that a DR should be applied cautiously in source identification (Manoli et al., 2004, Galarneau, 2008, Dvorská et al., 2011, Katsoyiannis et al., 2011, Alam et al., 2013).

1.7.2 Principal components analysis (PCA)

Principal Components Analysis (PCA) is one of the receptor models that have been most commonly used for environmental source apportionment (SA) studies (Hopke et al., 2005, Ravindra et al., 2006, Sofowote et al., 2008). This was used in a total of 30% of the SA studies reported in European publications up to 2005 (Viana et al., 2008). PCA is a useful mathematical tool consisting of (1) extraction of the principal components with fewer underlying dimensions (Hopke et al., 2005), (2) rotation for interpretation of potential sources (Paatero et al., 2005), and (3) identification of profiles

by comparison with literatures or source profiles (Hopke et al., 2005). Numerous studies have been conducted to identify the sources of atmospheric PAH (Harrison et al., 1996, Manoli et al., 2004, Brown and Brown, 2012).

This approach does not concern itself with source profiles. And it simplifies the understanding of complex sources by categorizing the original data set into smaller combinations (Ravindra et al., 2008a). PCA based on eigenvector analysis can be weighted by unrealistic errors that produce negative contributions of chemical compounds or factors, and make it impossible to establish the real observations (Hopke et al., 2005). Difficulties in the proper handling of missing data and values that are below the limit for detection are also recognised (Paatero et al., 2005). A recent study applied a novel combined diagnostic ratio - PCA approach for a SA of PAH to gain the benefits of both methods (Brown and Brown, 2012). However, PCA has limitations in terms of quantitative source apportionment analysis, due to the absence of non-negativity constraints.

1.7.3 Positive matrix factorization (PMF)

In 1993, the US EPA Positive Matrix Factorization (PMF) method was developed by Paatero and Tapper to solve the negative factor loading problem of PCA. The PMF model imposes non-negativity on source profiles and contributions to reduce the rotational problem, identify sources, and quantify source-specific contributions (Paatero et al., 2005, Sofowote et al., 2008). The PMF technique does not require source profiles as PCA does. This tool can also handle missing data and values below the detection

limit by substituting with geometric mean value and with one-half of the detection limit respectively. Non-negative chemical components and positive factor loadings are significant improvements in SA analysis. PMF is suitable for long-term data sets, producing more physically understandable results without a non-negative output (Dutton et al., 2010). Based on the advantages it offers, PMF has been widely used to interpret atmospheric pollution sources.

The input dataset for PMF consists of measurements (X) and their uncertainties (U). Uncertainty ($U = S_{ij}$) can be measured or estimated based on an equation. The equation consists of analytical uncertainty and the method detection limit, and is defined as follows (Reff et al., 2007).

$$S_{ij} = [(\alpha_j X_{ij})^2 + (\beta_j D_j)^2]^{1/2} \quad \text{Equation 1.8.}$$

where S_{ij} is the j_{th} measured species uncertainty in the i_{th} sample, α_j is the analytical uncertainty of j species, X_{ij} is the measurements, β_j is j_{th} species detection limit uncertainty, and D_j is the detection limit of j_{th} species. Several kinds of modified estimations of uncertainty for the PMF uncertainty matrix (S_{ij}) are set out in Table 1.7.

Table 1.7. Formulas for PMF uncertainty (S_{ij}) (Reff et al., 2007).

$C_3 \cdot X_{ij} + s_{ij}$	$0.3 + DL_{ij}$
$(0.05 \cdot X_{ij}) + DL_{ij}$	$K_j \cdot X_{ij} + DL_{ij} / 3$
$s_{ij} + DL_{ij}/3$	$(a_j s_{ij}^2 + b_j DL_{ij}^2)^{0.5}$
$S'_j + DL'_{ij}/3$	$[(rep)^2 + (0.05 \cdot X_{ij})^2]^{0.5}$
$s_{ij} + 0.2 \cdot DL_{ij}$	$[3 \cdot (s_{ij})^2 + DL_{ij}^2]^{0.5}$

Measurement detection limits (MDL), analytical errors for PM_{2.5} filter samples (α_j) and detection limit uncertainty (β_j) for several PAH in PM_{2.5} were reviewed in Table 1.8 (Hemann et al., 2008).

Table 1.8. Measurement detection limits (MDL), estimated measurement error (α) and detection limit uncertainty (β) (Hemann et al., 2008).

Species	MDL (ng m ⁻³)	α (%)	β (%)
Retene	0.079	12	316
Benzo[k]fluoranthene	0.0068	10	649
Benzo[b]fluoranthene	0.0068	10	649
Benzo[e]pyrene	0.0056	15	272
Indeno[1,2,3-cd]pyrene	0.017	13	1052
Indeno[1,2,3-cd]fluoranthene	0.021	13	1052
Benzo[ghi]perylene	0.023	10	169
Coronene	0.021	13	23

PMF decomposes receptors (X) by a three-matrix, factor contribution (G), factor profiles (F), and unexplained fraction (E). It is a well-known advantage of the receptor model that provides source profile matrices and contribution ones without *a priori* knowledge of pollutants (Ling et al., 2011).

$$X_{ij} = \sum G_{ik}F_{kj} + E_{ij} \quad \text{Equation 1.9.}$$

where X_{ij} is the j_{th} measured species concentration in the i_{th} sample, G_{ik} is the factor contribution of the k source to the i_{th} sample, F_{kj} is the fraction profile of the j species in the k source and E_{ij} is the matrix of residuals.

The solution of PMF is calculated through the weighted least square fit to search for the proper E_{ij} by minimizing the sum of the normalized Q value (Hopke, 2000, Larsen and Baker, 2003).

$$Q = \sum \sum (E_{ij}/S_{ij})^2 \quad \textbf{Equation 1.10.}$$

where E_{ij} is the residuals from PMF and S_{ij} is the estimation of uncertainty.

Extra uncertainty (0 - 25%) applied to all the species, and an intentional increase of uncertainty for individual species by categorizing to the ‘weak’, can be provided additionally by users for model fit (Norris et al., 2008). The robust mode is the default mode in PMF 3.0, which can lower the weight of the expected outliers, that have outlier distance greater than four ($(e_{ij}/\sigma_{ij})^2 > 4$ in Equation 1.10), in order to prevent outliers affecting the factorization (Reff et al., 2007, Sofowote et al., 2011).

Source identification using PMF implies a risk of misinterpretation through a combination of factors or a split into physically non-understandable factors. However the previously mentioned advantages have led to hundreds of published SA studies using PMF.

PMF modelling has been applied in this study to identify PAH source profiles and quantify source-specific contributions in urban air.

1.8 Thesis objective and overview

The objective of this thesis is to identify and quantify the major sources of polycyclic aromatic hydrocarbons (PAH) in pooled urban datasets using PMF. The possibility of extracting meaningful source profiles consisting of PAH congeners is extensively studied. Local source profiles derived from different concentrations spread between two sites are compared with PMF factor profiles. Concurrently, UK national emission estimates are reviewed to extract source signatures depending on emission activity categories.

The reactivity of PAH has been a matter of concern in the application of these compounds to the statistical modelling approach for SA. Therefore, this issue is extensively reviewed in this thesis. The thesis is subdivided into eight chapters and their contents are briefly discussed below.

In Chapter 2, the methodology for SA of PAH using PMF modelling is outlined. Detailed descriptions of PMF principles, dataset preparation and a review of possibilities for PMF factor profiles are included.

Chapter 3 includes source interpretations of PAH factor profiles obtained from PMF. Three datasets were prepared. One dataset consists of 54 measurements of 14 PAH congeners from three merged sites at an urban area of Jeddah in Saudi Arabia. The other two datasets were retrieved from the UK Department of Environment, Food and Rural Affairs (DEFRA) website, and consist of 29 PAH congeners, which includes urban (14

merged sites) and industrial urban (5 combined sites) datasets. Total PAH concentration (gaseous and particulate) is used to minimize the influence of G/P partitioning on the statistical analysis. Seasonal and geographical differences in source-specific contributions are outlined.

Chapter 4 deals with local source profiles, extracted from cross sectional spatial analysis of the UK urban sites. A net urban background profile is extracted using an urban background level (London Brent) and a rural level (Harwell). A net traffic profile is decided by the difference between a traffic site (London Crystal Palace) and an urban background (London Brent). A net industrial profile is obtained by using the difference in concentration between an industrial urban site (Port Talbot) and a nearby urban background site (Swansea). These three local source profiles are compared with the UK PMF factor profiles obtained in Chapter 3.

UK national emission estimates of PAH between 2002 and 2006 are reviewed to extract source-specific profiles in Chapter 5. These profiles are compared with the PMF factor profiles reviewed in Chapter 3.

Chapter 6 discusses the possibility of extracting meaningful PAH factor profiles using the PMF tool. Three 24-hour particle-associated PAH datasets containing information on known local emission sources (domestic, industrial and urban) and one 14-day HMW PAH dataset (urban) are subjected to PMF and there is a review of the reactivity issue, which is usually considered a matter of concern in the application of reactive compounds to PMF. Moreover, a sensitivity study of PMF is conducted by adding

additional uncertainty corresponding to the reactivity of individual PAH with the OH radical.

Chapter 7 includes a conceptual simulation of PAH ratios considering their various physicochemical reactivity properties such as radical oxidations and phase distributions between gaseous and particulate PAH during transport. This may provide better understanding of PAH reactivity in the air. This simulation is conducted based on the observations at an urban site (Birmingham) and at a rural site (Weybourne). Comparisons between kinetically obtained theoretical particle fractions and experimentally taken values are discussed.

A summary of the thesis is given in Chapter 8 including a discussion of possible future work.

CHAPTER 2: METHODOLOGY

This chapter describes a general technical processing of source apportionment using PMF, followed by a dataset selection procedure to obtain physically understandable source profiles. Comprehensive comparisons of PAH source profiles extracted from receptor modelling, local emissions and national emission estimates are described. Finally, a PMF sensitivity analysis is described to review the influence of the differing reactivity of individual PAH on source apportionment.

2.1 Positive matrix factorization (PMF)

Positive Matrix Factorization (PMF) is an advanced tool, developed in 1993, to identify sources without a negative contribution loading. All the processes including dataset preparation and PMF operation were conducted based on the EPA PMF 3.0 user guide. And interpretations of PMF source profiles were developed through the literature reviews.

PMF allows each sample and variable to be weighted individually, which is markedly different from PCA in which all are equally weighted (Park et al., 2011). The PMF input data files consist of two matrices: one is a concentration matrix (C), obtained from real measurements; and the other is an uncertainty matrix (U), containing sample-specific uncertainty or equation-derived uncertainty.

In this study, atmospheric PAH measurements in the UK were retrieved from the UK Department of Environment, Food and Rural Affairs (DEFRA) website for the C matrix of the PMF. Formula-based uncertainties (U) were used, owing to insufficient information on sample-specific uncertainty. Various experimental formulas for PMF uncertainty were described (Reff et al., 2007), and variable-specific uncertainty coefficients were introduced (Hemann et al., 2008). In this study, a 10% concentration was uniformly applied to analytical errors on individual PAH (Tauler et al., 2009, Kelishadi and Poursafa, 2010). Assumed uncertainty consisted of analytical errors and the detection limit (MLD), as revealed in Equation 2.1.

$$U = 0.1C + \text{MDL}/3 \quad \text{Equation 2.1.}$$

Generally, a missing value and its uncertainty are replaced by a geometric mean concentration (G_{mean}), and $4 \times G_{\text{mean}}$, respectively (Kim and Hopke, 2007). However, there were no missing concentrations in this study.

PMF decomposes input data (X) by a three-matrix: factor contribution (G), factor profiles (F), and unexplained fraction (E), without *a priori* knowledge of pollutants (Ling et al., 2011).

$$X_{ij} = \sum G_{ik} F_{kj} + E_{ij} \quad \text{Equation 2.2.}$$

where X_{ij} is the j_{th} measured species concentration in the i_{th} sample, G_{ik} is the factor contribution of the k source to the i_{th} sample, F_{kj} is the fraction profile of the j species in the k source, and E_{ij} is the matrix of residuals.

A solution in PMF is calculated through the weighted least square fit to search for a proper E_{ij} by minimizing the sum of the normalized Q value (Hopke, 2000, Larsen and Baker, 2003).

$$Q = \sum \sum (E_{ij}/S_{ij})^2 \quad \text{Equation 2.3.}$$

where E_{ij} is the residual from PMF and S_{ij} is the estimation of uncertainty.

Manual processes to optimize the PMF solution are given below.

- Appropriate extra modelling uncertainty (0 - 25%) applied to all variables was explored to cover additional uncertainties in PMF caused by a variation of source profiles and the chemical reactivity of variables.
- Categorization of variables makes it possible to handle the uncertainty of species individually. The default categorization of species is 'strong'. And if categorization of a species is selected as 'weak', PMF down weights those species by multiplying the stated uncertainty by three. When species are poorly modelled, they are categorized as 'bad' and excluded from the PMF analysis. This categorization is explored until the range of Q values of base runs ($n = 20$) is small.
- Where the temporal patterns of samples are extremely unusual, the EPA PMF 3.0 user guide recommends excluding these samples manually. However, this data pre-treatment has to be conducted with caution. As pooled datasets consisting of several sampling sites include heterogeneous emission characteristics, thus exclusion may lead to a distortion in comparison between site-to-site quantified concentration levels (Norris et al., 2008).

- The correlation coefficient (r^2) and slopes of individual PAH were reviewed to verify a good match between modeled values and measured concentrations.
- Scaled residuals (E/S) for individual PAH were checked to see whether they were within the range of -3 to 3.

$$Q = E/S \quad \text{Equation 2.4.}$$

where E is the difference between the measured concentration and the modelled concentration, and S is an estimated uncertainty.

- A robust mode is the default mode in PMF 3.0, which can down weight the expected outliers, that have outlier distance greater than four ($((e_{ij} / \sigma_{ij})^2 > 4$ in Equation 2.3), in order to prevent outliers affecting the factorization (Reff et al., 2007, Sofowote et al., 2011). And a true mode includes all measurements even though there are expected outliers. In this study, the stability of PMF driven Q (robust) and Q (true) were checked. Additionally Q (robust) was reviewed to see whether it was beyond the range -50% to +50%, compared to the theoretical Q value (Sofowote et al., 2011).

$$Q \text{ (theoretical)} = nm - p(n + m) \quad \text{Equation 2.5.}$$

where n is the number of species, m is the number of samples, and p is the number of expected factors.

- A least squares approach can produce multiple solutions – several pairs of F and G matrices with the same Q value, as a result of rotations driven by changing the initial starting point (Sofowote et al., 2011). In this study, Fpeak analysis was performed to find optimal solutions (Reff et al., 2007). For this the Fpeak

strength (rotational freedom parameter) was varied from -1.5 to 1 and an ultimate solution determined.

- Model random errors can be evaluated using a bootstrap technique. Bootstrapping was implemented to determine whether selected solutions were stable and whether they provided consistent results. This analysis selects samples randomly from among all the measurements. The default number of bootstrap replicate datasets is one hundred ($n = 100$) in PMF. This procedure may lead to a high standard deviation from the base run and bootstrap runs depending on the selected block by PMF (Kelishadi and Poursafa, 2010). However, this approach is useful to work out the stability of PMF solutions and for an optimization of modelling.

One of the advantages of PMF analysis is that factor solutions always exit without negative contributions. However, they may not be an appropriate solution and may be inconsistent with actual sources (Black and Black, 2009). To conclude, one should check whether factor solutions are physically interpretable or not, based on literature reviews and recognised local/national sources.

2.2 Source apportionment of total PAH

Source apportionment of PAH using PMF was applied in two different geographical locations: one in Saudi Arabia and one in the UK. In the work described in this chapter, total PAH concentration (vapour + particulate) was used to minimize the influence of the partitioning between the two phases on statistical modelling (Harrison et al., 1996).

Firstly, daily PAH measurements using a high volume air sampler were made from 23rd February 2013 to 23th April 2013 in Jeddah, the second largest city in Saudi Arabia which has grown rapidly over the last three decades. Sampling was conducted on three sites simultaneously, as shown in Figure 2.1. Site A was located to the east of Jeddah oil refinery. Site B was adjacent to a traffic site. Site C was considered to be an urban background site.

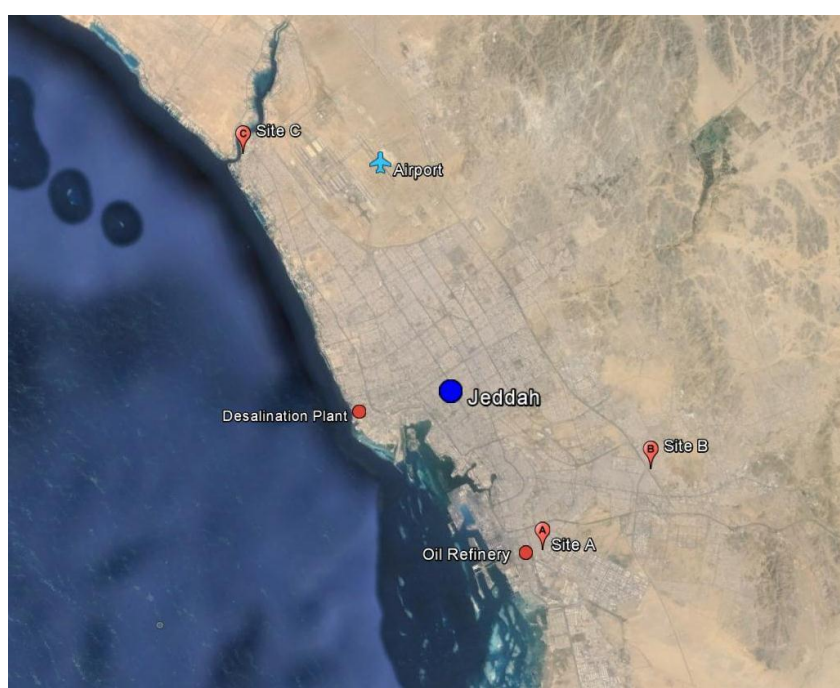


Figure 2.1. *Sampling locations in Jeddah in Saudi Arabia.*

One dataset consisting of 52 pooled samples, having 14 PAH congeners (Table 2.1), was subjected to PMF. The default weekend for PMF 3.0 is Saturday and Sunday. However, Thursday and Friday were the weekend in Saudi Arabia; so the sampling date needed to be processed to correspond to weekdays and weekends to see temporal variations in PMF.

Table 2.1. PAH congeners for PMF analysis of Jeddah.

	PAH variables	Abbreviation
1	Phenanthrene	Phe
2	Anthracene	Ant
3	Fluoranthene	FluA
4	Pyrene	Pyr
5	Benz[<i>a</i>]anthracene	BaA
6	Chrysene	Chr
7	Benzo[<i>b</i>]fluoranthene	BbF
8	Benzo[<i>k</i>]fluoranthene	BkF
9	Benzo[<i>a</i>]pyrene	BaP
10	Benzo[<i>e</i>]pyrene	BeP
11	Indeno[1,2,3- <i>cd</i>]pyrene	IcdP
12	Dibenzo[<i>a,h</i>]anthracene	DahA
13	Benzo[<i>ghi</i>]perylene	BghiPe
14	Coronene	Cor

Secondly, the quarterly total PAH measurements between 2002 and 2006, resulting from 14 days sampling time by GPS-1 sampler (Andersen), were retrieved from the UK Department of Environment, Food and Rural Affairs (DEFRA) for a source apportionment study. Two datasets covering a combination of 14 urban sites (256 samples) and 5 industry sites (80 samples) were prepared, under the assumption that the PAH source profiles would be different between the two categories. The sites were subjected to PMF analysis separately. The geographical information on each site can be seen in Table 2.2. In this study, twenty nine PAH congeners available out of the 39 congeners were included (see Table 2.3).

Table 2.2. *Geographical information on sites.*

Site name	Longitude	Latitude	Category	
			Urban (dataset 1)	Industry (dataset 2)
Birmingham	-1.83058	52.51172	o	
Cardiff Lakeside	-3.16934	51.51241	o	
Edinburgh St Leonards	-3.18219	55.94559	o	
Glasgow Centre	-4.25516	55.85773	o	
Hove	-0.18298	50.83659	o	
Kinlochleven	-4.96418	56.71445	o	
Leeds	-1.57862	53.76611	o	
Lisburn Dunmurry High School	-6.01402	54.53793	o	
Liverpool Speke	-2.84433	53.34633	o	
London Ashdown House	-0.13840	51.49680	o	
London Brent	-0.27622	51.58977	o	
Manchester Law Courts	-2.25198	53.48080	o	
Newcastle Centre	-1.61053	54.97825	o	
Newport	-2.97728	51.60120	o	
Bolsover	-1.29708	53.25637		o
Holyhead	-4.37590	53.18430		o
Middlesbrough	-1.22087	54.56930		o
Port Talbot Margam	-3.77082	51.58395		o
Scunthorpe Town	-0.63681	53.58634		o

Table 2.3. PAH congeners for PMF analysis.

	PAH variables	Abbreviation
1	Acenaphthylene	Acy
2	Acenaphthene	Ace
3	Fluorene	Flu
4	Phenanthrene	Phe
5	Anthracene	Ant
6	2-Methyl phenanthrene	2MPhe
7	2-Methyl anthracene	2MA
8	1-Methyl anthracene	1MA
9	1-Methyl phenanthrene	1MPhe
10	9-Methyl anthracene	9MA
11	4,5-Methylene phenanthrene	4,5MPhe
12	Fluoranthene	FluA
13	Pyrene	Pyr
14	Retene	Ret
15	Benzo[<i>c</i>]phenanthrene	BcPhe
16	Benz[<i>a</i>]anthracene	BaA
17	Chrysene	Chr
18	Cyclopenta[<i>c,d</i>]pyrene	CcdP
19	Benzo[<i>b</i>]naph[2,1- <i>d</i>]thiophene	BN21T
20	5-Methyl chrysene	5MChr
21	Benzo[<i>a</i>]pyrene	BaP
22	Benzo[<i>e</i>]pyrene	BeP
23	Indeno[1,2,3- <i>cd</i>]pyrene	IcdP
24	Benzo[<i>ghi</i>]perylene	BghiPe
25	Anthanthrene	Anth
26	Dibenzo[<i>a,l</i>]pyrene	DalP
27	Dibenzo[<i>a,e</i>]pyrene	DaeP
28	Dibenzo[<i>a,i</i>]pyrene	DaiP
29	Dibenzo[<i>a,h</i>]pyrene	DahP

PMF was applied to merged samples drawn from several sites with similar emission characteristic, as outlined above. In this study, source-specific contributions were quantified based on the assumptions that every factor has the same proportion of residuals (Jang et al., 2013).

$$X_{ij} = (G_{i1}F_{1j} + E_{ij}/n) + (G_{i2}F_{2j} + E_{ij}/n) + \dots + (G_{in}F_{nj} + E_{ij}/n) \quad \textbf{Equation 2.6.}$$

where X_{ij} is the j_{th} measured species concentration in the i_{th} sample, G_{in} is the factor contribution of the n_{th} source to the i_{th} sample, F_{nj} is the fraction profile of the j species in the n_{th} source, E_{ij} is the matrix of residuals, and n is the number of sources.

During the process of source apportionment by PMF, unusual extreme events in the time series and samples with extremely high scaled residuals were excluded as a precaution to minimize distortion in comparison between site-to-site contributions (Norris et al., 2008). The number of samples for each site was not exactly the same, thus averaged concentrations were compared.

2.3 Local source profiles (spatial analysis)

Different concentrations between two sites, having similar geographical locations, were investigated. The westerly wind is the main wind direction in the UK (Prevedouros, 2004), so an increased concentration at an eastern site may be the result of emissions in downwind areas and may provide information on local emission source signatures.

From March 2008, the UK PAH monitoring network replaced the original sampling method of the Andersen samplers with the Digitel samplers (see Figure 2.2), owing to concerns over the sampling ability of the PM₁₀ fraction in ambient air and the degradation of PAH during the long sampling time with the Andersen samplers of two weeks (Butterfield and Brown, 2012).

Andersen sampler



Digitel sampler



Figure 2.2. Pictures of samplers used at UK PAH monitoring sites (Brown et al., 2011).

A consistent sampling methodology is useful to compare PMF source profiles (2002 - 2006) with local source profiles. However, the fact that there were few Andersen PAH measurements for the rural sites made it necessary to use Digitel PAH measurements to understand local source profiles.

Twenty-four-hour daily measurements of particulate PAH using Ditigel samplers were included in this analysis. Data on twenty PAH congeners sampled between 2008 and 2009 were retrieved from the DEFRA website (see Table 2.4). Concurrently, calculations were conducted separately for summer (2Q and 3Q) and winter (1Q and 4Q) to analyse source profiles in terms of seasonal source and reactivity, as it is widely reported that PAH are fairly reactive compounds.

Table 2.4. *Ditigel PAH congeners for local source profiles.*

	PAH variables	Abbreviation
1	Benzo[<i>c</i>]phenanthrene	BcPhe
2	Benzo[<i>a</i>]anthracene	BaA
3	Chrysene	Chr
4	Cyclopenta[<i>c,d</i>]pyrene	CcdP
5	Benzo[<i>b</i>]naph[2,1- <i>d</i>]thiophene	BN21T
6	5-Methyl Chrysene	5MChr
7	Benzo[<i>b+j</i>]fluoranthene	Bb,jF
8	Benzo[<i>k</i>]fluoranthene	BkF
9	Benzo[<i>a</i>]pyrene	BaP
10	Benzo[<i>e</i>]pyrene	BeP
11	Perylene	Per
12	Indeno[1,2,3- <i>cd</i>]pyrene	IcdP
13	Dibenzo[<i>ah,ac</i>]anthracene	Dah,acA
14	Benzo[<i>ghi</i>]perylene	BghiPe
15	Anthanthrene	Anth
16	Dibenzo[<i>a,l</i>]pyrene	DalP
17	Dibenzo[<i>a,e</i>]pyrene	DaeP
18	Dibenzo[<i>a,i</i>]pyrene	DaiP
19	Dibenzo[<i>a,h</i>]pyrene	DahP
20	Coronene	Cor

Five sites were selected for this analysis and their locations can be seen in Figure 2.3.

Three site-pairs and their geographical information can be seen in Table 2.5.

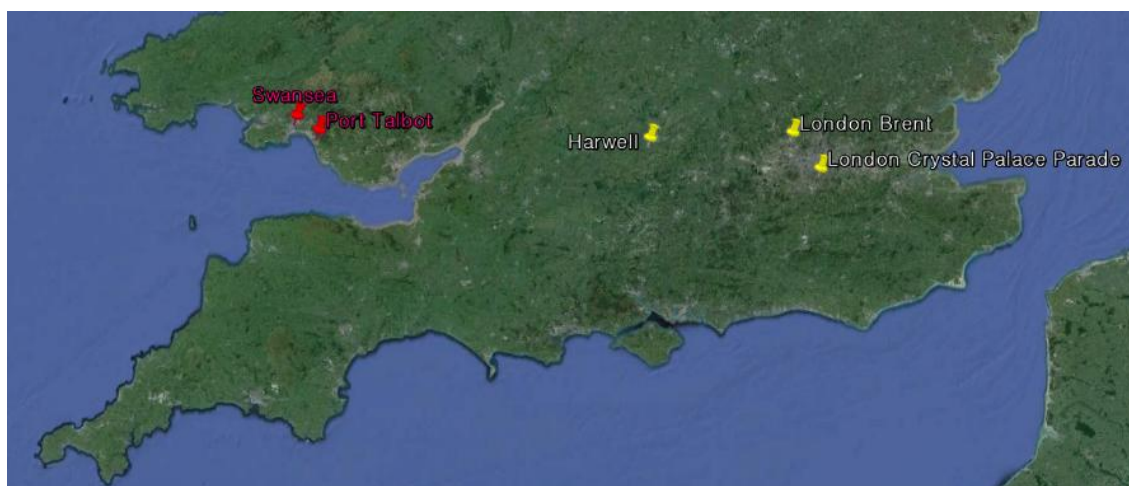


Figure 2.3. Locations for local source profile analysis.

Table 2.5. Pairs for local source profiles.

	Longitude	Latitude	Category		
			net traffic	net urban	net industry
Harwell	-1.32528	51.57108		o	
London Brent	-0.27622	51.58977	o	o	
London Crystal Palace Parade	-0.07553	51.42468	o		
Swansea Cwm Level Park	-3.93945	51.64584			o
Port Talbot Margam	-3.77082	51.58395			o

A different PAH level between an urban traffic site (UT: London Crystal Palace Parade) and an urban background site (UB: London Brent) is due to an increment from traffic (net traffic concentration). The contribution profile of traffic emissions is derived by dividing the net traffic concentration for individual PAH by the total concentration at the urban traffic site, i.e. $(UT - UB) / UT \times 100\%$.

Similarly, the concentration difference between an urban background site (UB: London Brent) and a rural site (RB: Harwell) reflects net urban emissions. And the difference between an industrial urban site (IU: Port Talbot) and a nearby urban background site (UB: Swansea) is related to a net industrial concentration. PAH congener contribution profiles of net urban and net industry emissions are expressed as a relative concentration, i.e. $(UB - RB) / UB \times 100\%$ and $(IU - UB) / IU \times 100\%$, respectively.

A comparison of these local emission source profiles with the PMF factor profiles is provided in Chapter 4.

2.4 UK national source profiles (emission estimates)

PMF is a method for receptor modelling that extracts source profiles from atmospheric measurements without *a priori* knowledge of source signatures. PMF factors do not always correspond to actual sources and they are not always unique (Black and Black, 2009) because complex physicochemical processes can influence source signatures after emission from sources. However, a source-oriented approach such as national emission estimates may provide strong support when one assigns sources at receptors to PMF factors.

In this study, source information on 16 USEPA's priority PAH was retrieved from the UK National Atmospheric Emissions Inventory (NAEI, <http://naei.defra.gov.uk/>). For comparison with the PMF factor profiles, estimated emissions for the same period, 2002 – 2006, were averaged. Minor emission sources were not included in this study. Source-

specific contributions were re-categorized based on the activity code, which contains detailed emission information, for example on fuel types and emission processes. Finally these inventory-driven source profiles were compared with the PMF source profiles with common PAH variables.

2.5 Overview of the possibility of obtaining meaningful source profiles

The reactivity of compounds is sometimes considered a concern when PMF is applied to PAH. However, it has been reported that specific PAH factor patterns are preserved under different oxidant levels (Dvorská et al., 2012). In the work discussed in Chapter 6, several methodologies were explored to review the possibility of extracting meaningful PAH source profiles by PMF. Additionally, PMF sensitivity analysis was conducted by adding additional uncertainty to individual PAH scaled according to their rate coefficient for reaction with OH.

The output of PMF, combined with detailed information on dominant sources, can be useful for obtaining physically understandable source profiles. In Section 6.2, PMF was applied to several large datasets of particle-associated PAH concentrations informed by knowledge of local emission characteristics in the UK. Three monthly datasets (domestic, industry and urban), consisting of particle-associated PAH sampled by the Digitel sampler between 2009 and 2010, were prepared. Geographical information on the sampling sites and grouping for three datasets are shown in Table 2.6.

Table 2.6. *Geographical information on Digitel sampling sites.*

	Longitude	Latitude	Category		
			Domestic (D1)	Industry (D2)	Urban (D3)
Ballymena Ballykeel	-6.25829	54.85862	o		
Birmingham	-1.83058	52.51172			o
Cardiff Lakeside	-3.16934	51.51241			o
Derry Brandywell	-7.33213	54.99234	o		
Edinburgh St Leonards	-3.18219	55.94559			o
Glasgow Centre	-4.25516	55.85773			o
Hove	-0.18298	50.83659			o
Kinlochleven	-4.96418	56.71445			o
Leeds	-1.57862	53.76611			o
Lisburn Dunmurry High School	-6.01402	54.53793	o		
Liverpool Speke	-2.84433	53.34633			o
London Brent	-0.27622	51.58977			o
London Crystal Palace Parade	-0.07553	51.42468			o
London Marylebone	-0.15461	51.52253			o
Newcastle Centre	-1.61053	54.97825			o
Newport	-2.97728	51.60120			o
Swansea Cwm Level Park	-3.93945	51.64584			o
Bolsover	-1.29708	53.25637		o	
Middlesbrough	-1.22087	54.56930		o	
Port Talbot Margam	-3.77082	51.58395		o	
Royston	-1.43945	53.60028		o	
Scunthorpe Low Santon	-0.59724	53.59583		o	
Scunthorpe Town	-0.63681	53.58634		o	
South Hiendley	-1.40084	53.61194		o	

The domestic combustion dataset (D1) was prepared by combining three Northern Ireland sites (Ballymena Ballykeel, Derry Brandywell and Lisburn Dunmurry) where there is only limited access to natural gas fuels, and coal and oil are widely used for domestic heating. The industry dataset (D2) consisted of seven sites that had strong

local industrial emissions. Lastly, 14 urban sites (D3) were pooled, including two traffic-heavy sites in London (Marylebone Road, Crystal Palace Parade). PMF was applied to the three datasets separately and the results compared with source profiles.

Secondly, Section 6.3 describes an approach to reviewing reactivity issues that applies PAH to PMF by preparing two datasets with obviously different sampling times (see Table 2.7).

Table 2.7. *Geographical information for two datasets.*

			Category	
			HMW PAH : Andersen (D4)	Particulate PAH : Digitel (D5)
	Longitude	Latitude		
Birmingham	-1.83058	52.51172	o	o
Cardiff Lakeside	-3.16934	51.51241	o	o
Edinburgh St Leonards	-3.18219	55.94559	o	o
Glasgow Centre	-4.25516	55.85773	o	o
Hove	-0.18298	50.83659	o	o
Kinlochleven	-4.96418	56.71445	o	o
Leeds	-1.57862	53.76611	o	o
Liverpool Speke	-2.84433	53.34633	o	o
London Ashdown House	-0.13840	51.49680	o	
London Brent	-0.27622	51.58977	o	o
London Crystal Palace Parade	-0.07553	51.42468	o	o
London Marylebone	-0.15461	51.52253		o
Manchester Law Courts	-2.25198	53.48080	o	
Newcastle Centre	-1.61053	54.97825	o	o
Newport	-2.97728	51.60120	o	o
Swansea Cwm Level Park	-3.93945	51.64584		o

One urban dataset (D4), consisting of HMW PAH (gaseous + particulate) sampled by Andersen sampler over 14-day sampling periods between 2002 and 2006, was prepared and subjected to PMF. The other dataset (D5), containing 24-hour Digital particulate PAH concentrations measured from December 2008 to November 2010, was subjected to PMF in work reported in Section 6.3, a comparison of source profiles between two sub-datasets. This comparison may elucidate the appropriateness of using reactive compounds in PMF, as HMW PAH are predominantly attributed to the particulate phase but sampling time was obviously different in the two datasets.

Lastly, a sensitivity analysis was applied to PMF in the work described in Section 6.4. PAH are reactive compounds in the atmosphere that can lead to a change in source signatures between the source emissions profile and the result of receptor modelling. In the previous PMF analysis, a 10% concentration was uniformly applied to PAH as an analytical uncertainty. Now, scaled uncertainty, corresponding to the reactivity of individual PAH was added to the previous uncertainty and PMF was conducted again.

CHAPTER 3: SOURCE APPORTIONMENT FOR TOTAL PAH

This chapter provides an extensive discussion of the identification of the main sources of PAH in urban areas. Positive matrix factorization (PMF) analysis was performed with three datasets. One consisted of 54 measurements of 14 PAH congeners for the three merged sites at the urban area of Jeddah in Saudi Arabia. The other two were retrieved from the UK DEFRA website, and consisted of 29 PAH congeners divided between an urban dataset (14 merged sites) and an industrial urban dataset (5 combined sites). The PMF method was applied to the sum of gaseous and particulate PAH concentrations (total PAH) to minimize the effect of G/P partitioning on the statistical factor analysis. Seasonal variations and geographical differences in the source-specific contributions were outlined.

3.1 Background

The fact that polycyclic aromatic hydrocarbons (PAH) comprise a large number of individual compounds, emitted from complex sources in different proportions, has required the application of an advanced tool to the identification of sources for these compounds. Historically, the diagnostic ratio (DR) method has generally been used for source identification of PAH; but more recently Galarneau (2008) has cast doubt on this approach, as an ambient PAH concentration is the output of a large number of sources,

and individual PAH have different chemical reactivity. However, the application of principal component analysis (PCA) has produced a valuable understanding of the major sources of atmospheric PAH at urban sites (Harrison et al., 1996, Mari et al., 2010), although PCA can produce negative values and the degree of quantitative interpretation is limited with this analysis.

PMF has been widely used as a tool for the quantitative source apportionment of PAH in recent years. It is generally recognised to be a more advanced tool than PCA, as there cannot be a negative value or percentage for a component in physical samples but it produces non-negative factor loadings (Paatero and Tapper, 1994). There have been some doubts over the application of PMF to PAH, owing to the latter's high and differing atmospheric reactivity for individual congeners and the G/P partitioning between gaseous and particulate phase. However, a recent study has shown that specific factor patterns for PAH congeners are preserved under the different oxidant levels (Dvorská et al., 2012). In this chapter, PMF was applied to several large databases of total PAH concentrations (gaseous and particulate) measured at urban sites, and the results will be discussed in detail in the following chapters.

3.2 Results

3.2.1 Jeddah, Saudi Arabia

From three to six factor solutions were examined by varying the model uncertainty (0 - 25%). PMF identified three factors, showing a good bootstrap result. Over 99 bootstrap runs were mapped to the selected one base run result for individual factors among one hundred bootstrapped datasets. Q (theoretical) and Q (robust) values for the selected one base run were 468 and 452, respectively. These values were stable among twenty base runs. Correlations between the observed concentrations and the modelled values were over 0.7 for individual PAH. Additionally, Fpeak analysis, which rotated the F or G matrix, was conducted by varying the rotational parameters between -1.0 and 0.5. An F matrix having a value of $F_{peak} = 0$ provided the most physically reasonable factor profiles.

The profile graph (see Figure 3.1a) consists of the concentration of each species apportioned to the factor (blue bars) and the percentage of each species apportioned to the factor (red diamonds). Factor 1 was identified with conventional traffic markers such as BaP, BghiPe and Cor (Harrison et al., 1996, Mastral et al., 2003, Ning et al., 2007 Callen et al., 2011). This factor accounted for 17% and 70% of the sum of PAH ($\sum_{14}PAH$) and BaP respectively. The difference between the average mass concentrations for weekdays and weekends was obvious, with the higher value occurring during weekdays (see Figure 3.1b). Figure 3.1c shows the contribution of

each factor to \sum PAH by samples. It is normalised so that the average of all contributions for each factor is 1 in y-axis. The x-axis displays the sampling date, however this information is not included in this study. As PMF identifies samples with sampling date thus date needs to be processed considering weekdays/weekends for three-pooled sites measured concurrently. A significant contribution from this factor to the \sum_{14} PAH at Sites A and B was observed (see Figure 3.1c). It appears that this factor is influenced by traffic emissions.

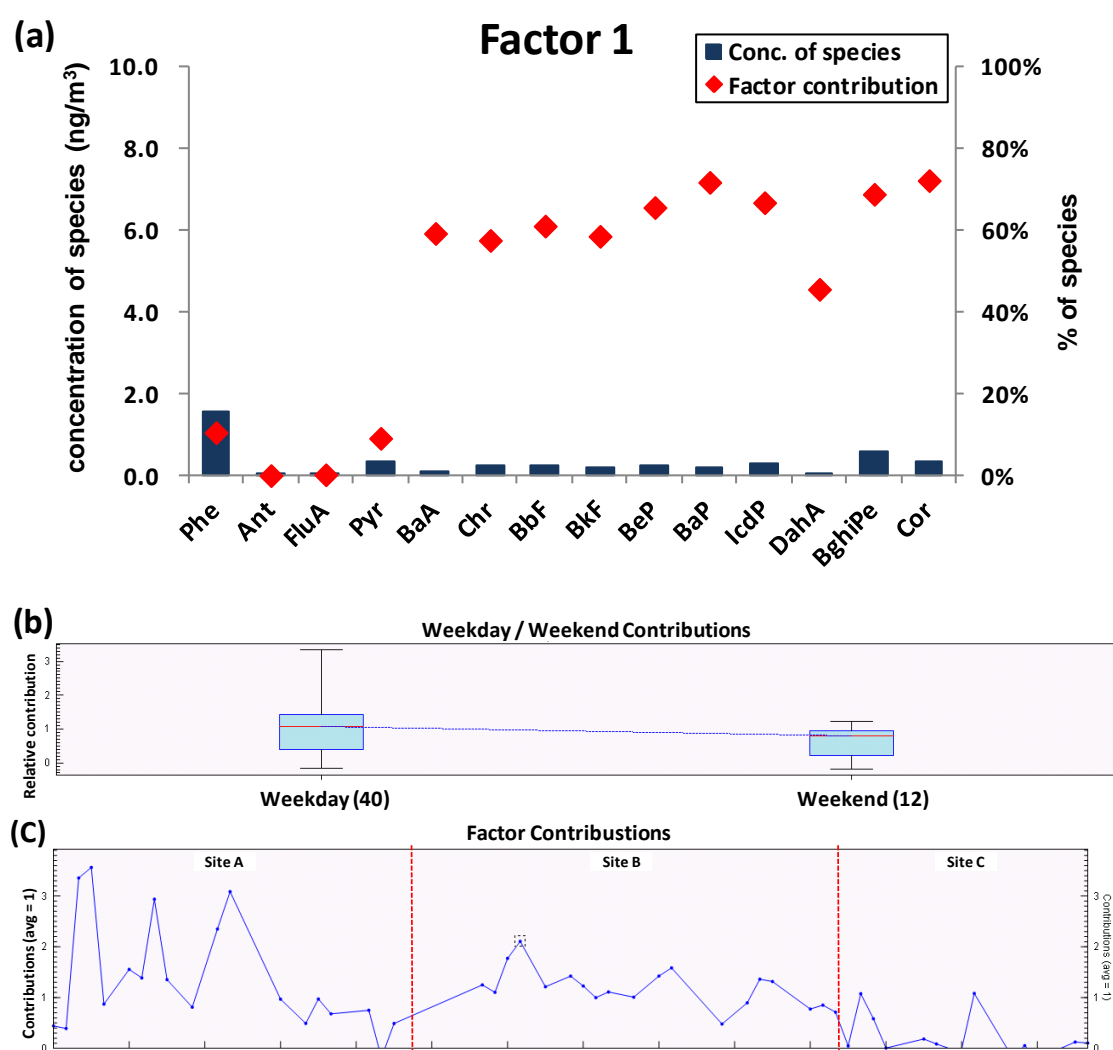


Figure 3.1. PAH factor profile for total PAH and temporal variation for Jeddah (Factor 1).

Factor 2 was assigned to an oil refinery industrial source. It was responsible for $\Sigma_{14}\text{PAH}$ and BaP of 33% and 7% respectively. This factor was distinguished by FluA, Pyr and DahA (see Figure 3.2a). In the UK, the PAH emissions (<http://naei.defra.gov.uk/>) recorded for the refinery combustion source (source code) using fuel oil (activity code) between 2002 and 2006 showed that FluA reached a relatively higher level, compared to the other PAH congeners. The significance of FluA, Pyr from oil combustion activity has been reported (Kulkarni and Venkataraman, 2000, Ravindra et al., 2006). The predominant emissions of Pyr, BaP and DahA have been observed when kerosene is used as a cooking fuel (Kulkarni and Venkataraman, 2000). The fact that the calculated contribution for DahA was small for the net traffic emissions (Jang et al., 2013) may reflect that this factor is related to a non-traffic source. The largest mass contribution ($\Sigma_{14}\text{PAH}$) was seen at Site A (see Figure 3.2c). The gradient of PAH contributions between sites is very obvious, going from Site A (near the oil refinery site) to Site B (near the traffic site) to Site C (urban background site).

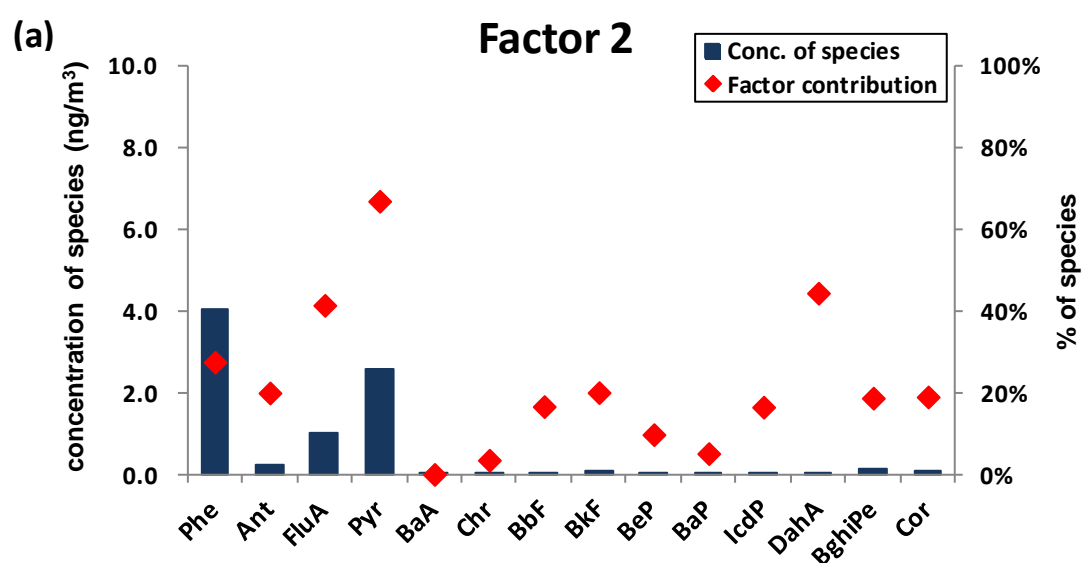


Figure 3.2. PAH factor profile for total PAH and temporal variation for Jeddah (Factor 2).

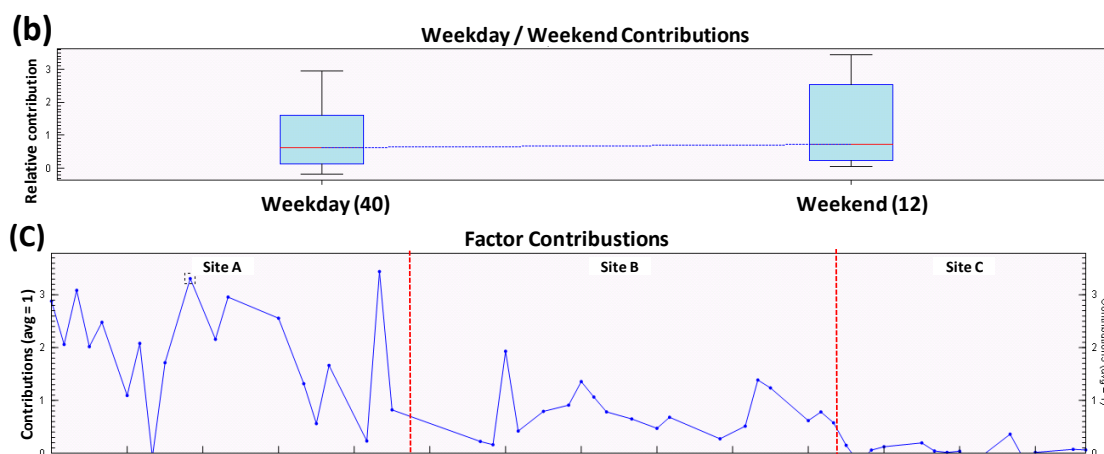


Figure 3.2. (Continued).

Factor 3 was responsible for 50% and 23% of the sum of PAH and BaP respectively. Figure 3.3a showed that the factor profile was dominated by LMW PAH (Phe, Ant, FluA, BaA and Chr). An enhanced level of volatile PAH can be associated either with oil combustion activity (Lee et al., 2004) or with diesel traffic emissions (Zielinska et al., 2004). The predominant concentration for Phe, along with FluA, Chr and Pyr, has been explained by the source signature for diesel exhaust emissions (Riddle et al., 2008, Rajput and Lakhani, 2010). It is likely that the increased significance of Ant, BaA and Chr seen in this source profile, compared to the UK inventory signature for diesel emissions (Jang et al., 2013), can be explained either by a different composition of diesel fuels or by the difference in meteorological conditions between the UK and Saudi Arabia. The larger emissions were shown during weekdays (see Figure 3.3b). This factor significantly influenced the PAH levels at all sites (see Figure 3.3c). To conclude, this factor was assigned to oil combustion sources, including diesel fuels from vehicles and oil fuels from nearby industries such as a desalination plant (see Figure 2.1).

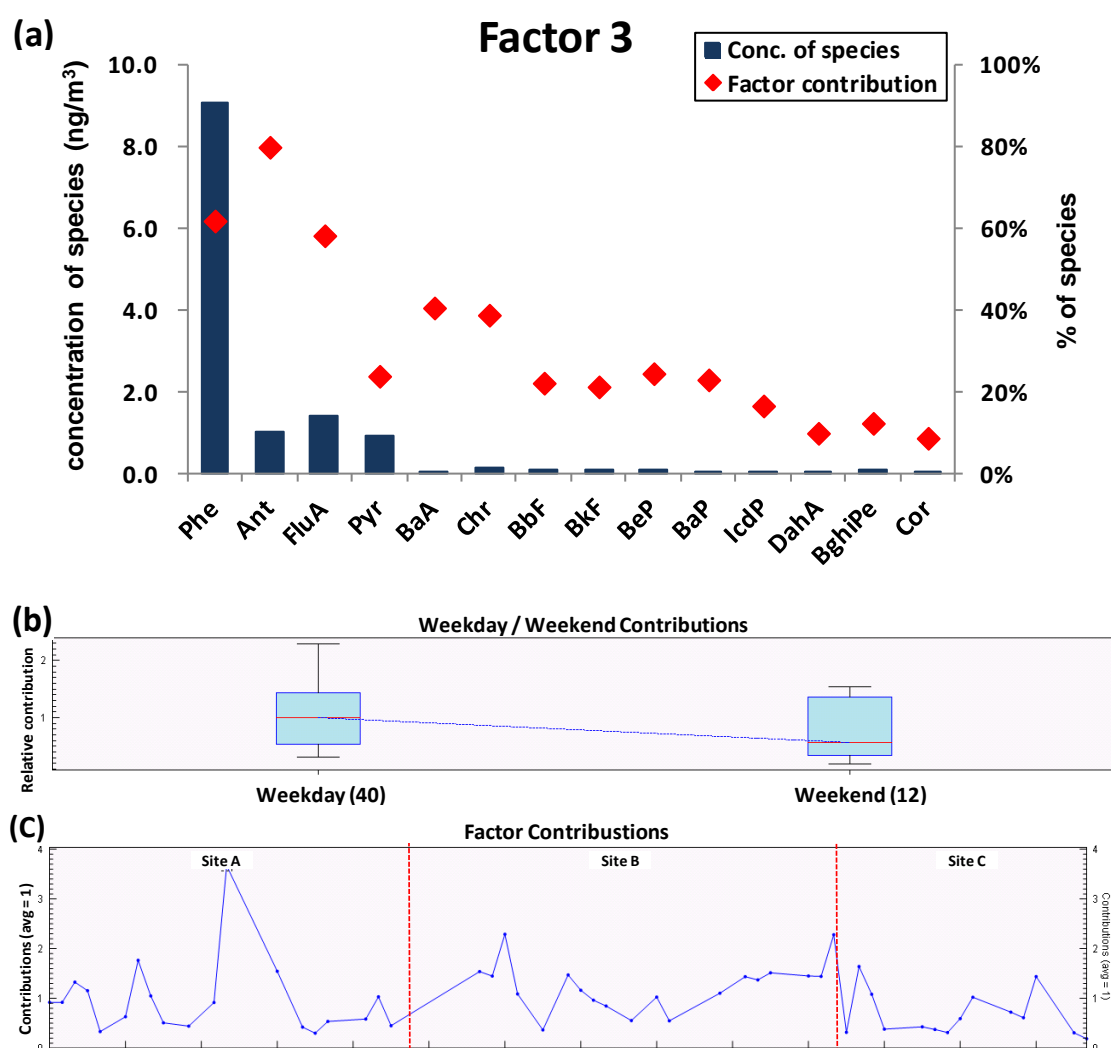


Figure 3.3. PAH factor profile for total PAH and temporal variation for Jeddah (Factor 3).

Figure 3.4 illustrates source-specific mass concentrations for weekdays and the weekend separately at each site. Mean concentrations were calculated because the number of samples for each site was not the same. Traffic PAH emissions (Factor 1) showed a distinctive weekdays/weekend pattern, and this difference was more obvious for BaP. The level of BaP at the three sites in Jeddah was significantly affected by vehicular sources. The difference in the industrial contributions (Factor 2) to the sum of PAH, was apparent between the sites, which may be related to the distance downwind from the oil refinery plant. Industrial emissions were responsible for the minor

concentration of BaP. Oil combustion sources (Factor 3), including diesel vehicle and industrial activity, were also a significant contributor to the level of PAH at all sites.

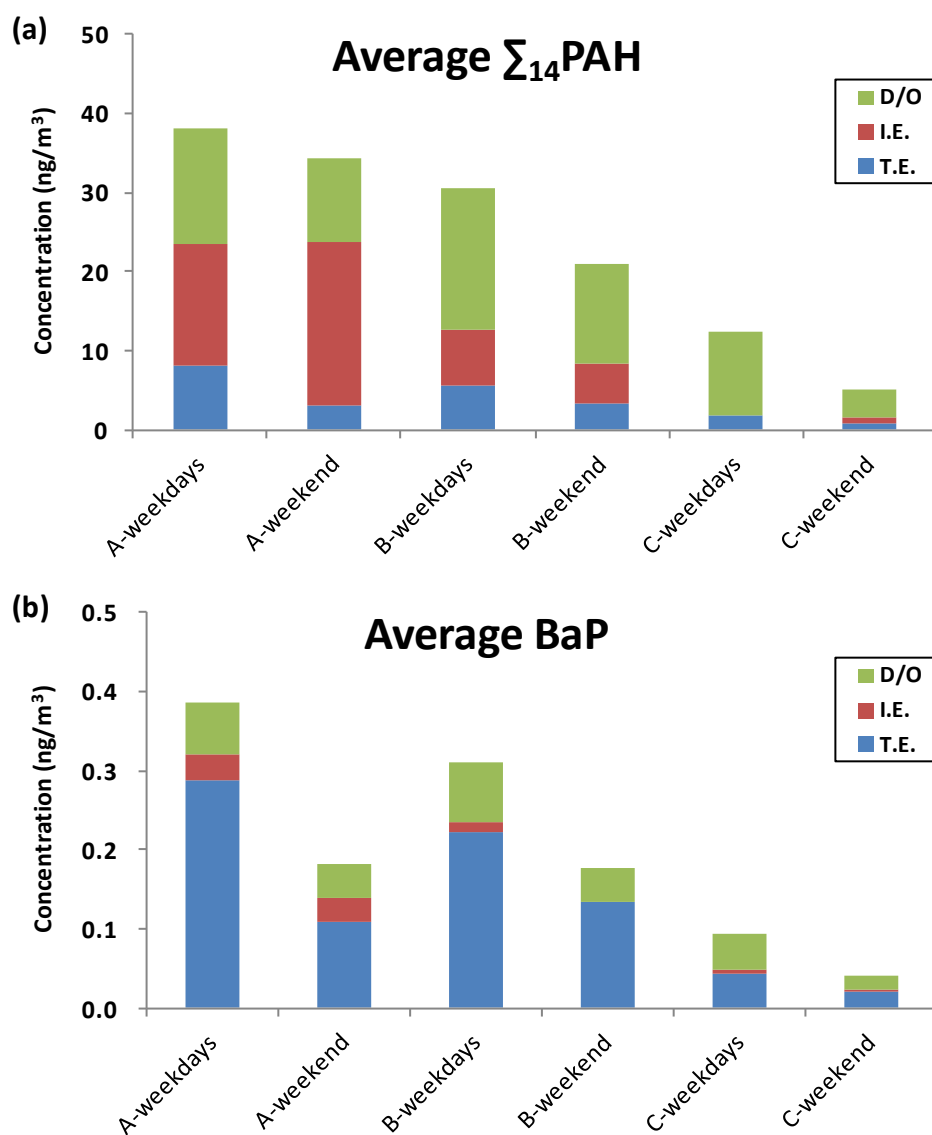


Figure 3.4. Source specific contributions to Sites A, B and C in Jeddah (TE: traffic emissions; IE: industrial emissions; D/O: diesel and oil combustion).

3.2.2 UK urban sites

Three-factor to eight-factor solutions were explored by varying an additional modelling uncertainty in PMF. A four-factor model gave the best fit in the PMF analysis, having a theoretical Q value of 3525 and a robust Q value of 2318. These values were stable during twenty base runs. The correlation coefficient (r^2) for individual PAH ranged between 0.53 and 0.97. Most correlation coefficients between modelled concentrations and measured concentrations were over 0.8 with lowest value for Ret of 0.53, but Ret was not excluded in this analysis, because it is a widely used source marker for wood combustion. A Fpeak parameter was changed from -1.4 to 0.2. Unmapped bootstrap runs, compared to the base runs, were not shown for all factors. Mass contributions ($\sum_{\text{total}} \text{PAH}$) were 21.4, 50.5, 15.0 and 13.1% for Factors 1, 2, 3 and 4 respectively.

Factor 1 (see Figure 3.5a) was explained by two distinctive PAH congeners, 2MA and BN21T, having 87.7 and 51.6% factor contributions respectively. Additionally, over 20% of Phe, FluA, Pyr and Ret were explained by this factor, followed by Flu, Ant, 5MChr, 1MPhe and BeP. Most source apportionment (SA) studies have focused on the USEPA's 16 priority congeners, and there are limited SA results with extensive PAH. However, Westerholm and Li (1994) reported that 2MA was one of the most abundant PAH congeners for emissions from diesel fuel vehicles. McCarry et al. (1996) conducted a SA study with parent PAH and the sulphur-containing PAH, 'thia-arenes'. They suggested that thia-arenes, including BN21T, were stable source markers for diesel traffic emissions, which showed a non-detectable level for gasoline emissions. Other studies have used BN21T and Pyr as indicators for diesel combustion to

differentiate between diesel and gasoline sources (Alsberg et al., 1989, Larsen and Baker, 2003). In a recent study, a factor extracted by PCA and PMF, having a significant contribution to dibenzothiophenes, was apportioned to diesel emissions (Sofowote et al., 2010a).

In Figure 3.5b, this factor showed a slightly increased concentration in the cold season; and a sudden decline in relative mass contribution was observed from 2005. It seems that this sudden disappearance is influenced by a change of diesel fuels, not a reduction in PAH emissions. As “sulphur free” (< 10ppm) fuels for use in highway vehicles started to be sold from 4 December 2007, with requirement that all highway vehicle fuels should be “sulphur free” by 1 January 2009 (Jones et al., 2012). The fact that lower sulphur content in fuels onward 2005 sampled from fuel leaving refineries and distribution terminal was reported (AEA, 2009), may relate to the sudden annual reduction for relative contribution (see Table 3.1). In a recent study, a reduction in PAH emissions was observed by lowering the fuel sulphur content of diesel vehicular emissions (Lim et al., 2005). However, there is still controversy about the factor’s influence on PAH emissions depending on the sulphur content.

Table 3.1. Annual trend in average sulphur content in gasoline and diesel fuels, ppm (AEA, 2009).

Fuel/Year	2001	2002	2003	2004	2005	2006	2007
							UK (EU)
Gasoline	49 (68)	41 (51)	37 (37)	37 (38)	33 (19)	34 (18)	34 (18)
Diesel	40 (223)	40 (169)	38 (125)	35 (113)	33 (25)	19 (22)	14 (23)

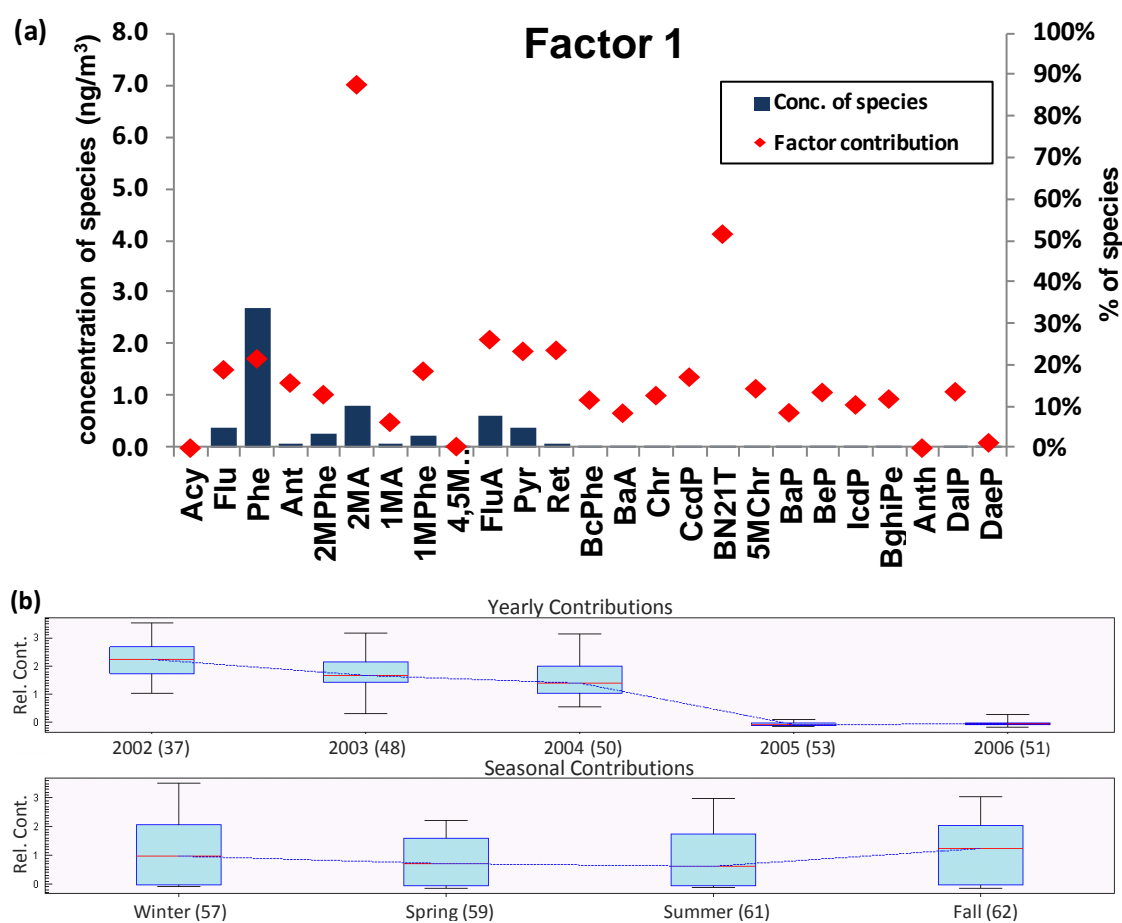


Figure 3.5. PMF factor profile for total PAH and temporal variation at urban sites in the UK (Factor 1).

Factor 2 (see Figure 3.6a) was identified with Phe and its methyl derivatives (MPhes). LMW PAH were predominantly responsible for this factor, providing 93.3% of 1MA, along with high loadings of 2MPhe, 1MPhe and 4,5MPhe that made over a 70% factor contribution. Additionally, 59.1% of the Phe concentration was attributed to this factor. Several studies have assigned high contributions of Phe and MPhes either to coal combustion sources or to unburned petroleum escaping from petroleum fuels through evaporation from vehicles (Rogge et al., 1993, Gogou et al., 1996, Kavouras et al., 2001, Zuo et al., 2007). However, the larger mass contribution in the warm season is not likely to be explained by coal combustion sources. A similar explanation can be applied to Ret, having 43.2% of factor contribution. This compound has been widely used as a source

indicator for wood combustion (Ramdahl, 1983, Benner et al., 1995,). However the fact that the mass contribution is larger in the summer than in the winter may suggest that this factor is not associated with solid fossil fuel combustion activity for domestic heating. Khalili et al. (1995) reported that Ret can also be emitted from internal combustion engines.

Other studies have attributed LMW PAH compounds either to gasoline emissions (Meijer et al., 2008, Park et al., 2011) or to emissions from diesel fuels (Marr et al., 2004). The ratios of MPhe to parent PAH are influenced by various factors such as fuel composition, the PAH content in the fuel and engine operating conditions (Nielsen, 1996). It has been reported that the values of MPhe/Phe for diesel vehicle emissions are relatively larger than those for gasoline emissions (Benner et al., 1989, Lim et al., 1999). To conclude, in the present study, this factor profile was attributed to unburned petroleum sources, which were related to the relatively volatile traffic emissions and commonly seen in congested cities (Harkov et al., 1984, Tuominen et al., 1988, Coleman et al., 1997, Meijer et al., 2008, Park et al., 2011).

The higher relative contribution observed in the warm weather (see Figure 3.6b) may be related to the volatility for LMW PAH depending on ambient temperature mentioned above. The trend in the annual mass from 2005 was distinguishable from that for the previous factor (diesel combustion). It seems that the increased emissions from 2005 for this factor are caused by a modelling bias, related to the reduced mass concentration in the factor for diesel fuel emissions. It appears that the mass increment from 2005 is responsible for a shift in the level of the diesel mass concentration.

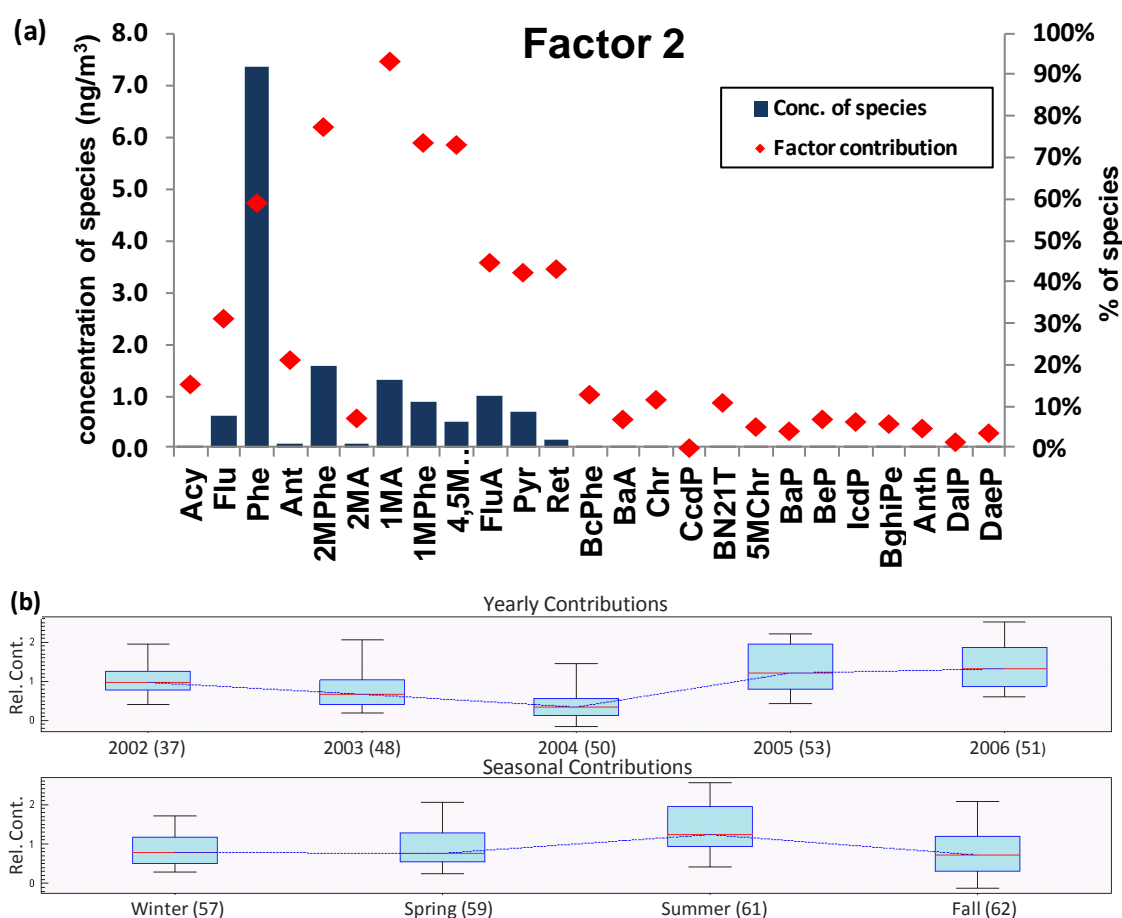


Figure 3.6. PMF factor profile for total PAH and temporal variation at urban sites in the UK (Factor 2).

Factor 3 was more influenced by HMW PAH (see Figure 3.7a). Over 80% of the contribution of DalP, DaeP and Anth was responsible for this factor. Four-ring PAH (BcPhe, BaA, 5MChr, Chr), five-ring PAH (BaP, BeP, CcdP) and six-ring PAH (BghiPe, IcdP) showed over 50% contribution. Some studies have indicated that HMW PAH are associated with industrial emissions (Sofowote et al., 2010a, Ling et al., 2011), for example from industries where coke ovens use coal fuels (Daisey et al., 1986, Yang et al., 2002). These compounds can also be produced from the steel and iron industries through coke manufacturing, sintering, iron and steel making, and the casting and cooling processes (Yang et al., 2002). In a recent study, Ciaparra et al. (2009) separated

out two kinds of source profiles from the steel making process using PCA: one is a coke-making profile consisting of LMW PAH (Flu, Phe, Ant, fluA and Pyr) and the other is a sintering profile comprised of HMW PAH (BaP, IcdP, Dah, acP and BghiPe). Slightly overlapped PCA clusters between urban and coal combustion related industry sites across the UK may partially reflect the effect of industrial emissions on nearby urban atmospheric PAH levels (Brown and Brown, 2012). As a result, Factor 3 was attributed to coal combustion sources.

There is little specific annual change in contribution between 2002 and 2006 (see Figure 3.7b). It seems that an obvious seasonal variation, showing a higher concentration in winter, is more related to seasonal sources, such as coal combustion for domestic heating. However, in this study, PMF could not separate out the two different source types of industrial coal combustion and domestic coal usage.

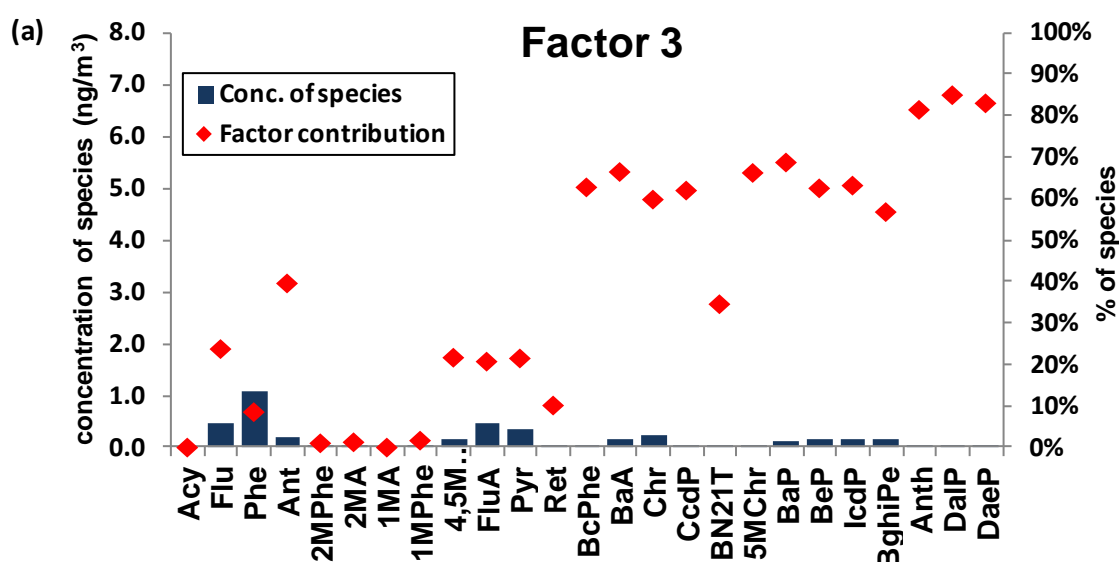


Figure 3.7. PMF factor profile for total PAH and temporal variation at urban sites in the UK (Factor 3).

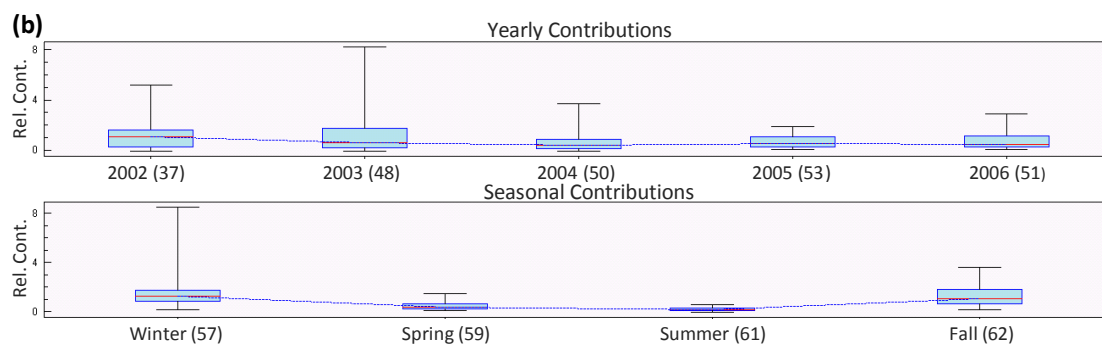


Figure 3.7. (Continued).

With Factor 4 (Figure 3.8a), it was indicated that Acy had a factor contribution of 84.6%, followed by BghiPe (25.6%), Ant (23.5%) and Ret (23.1%). McDonald et al. (2000) reported that significant amounts of PAH compounds such as Acy, Ant, BaP and BeP could be emitted from the wood combustion process. It was found that Ret (1-methyl-7-isopropylphenanthrene) could be produced through the thermal degradation process of the resin found in wood (Ramdahl, 1983), and therefore this compound has been widely used as a wood combustion indicator (Khalili et al., 1995, Wang et al., 2009, Dvorská et al., 2012).

There was a small change among the annual contribution; and an outstanding mass contribution in the cold season (see Figure 3.8b) may support this source as a seasonal one, since it is expected that the burning of wood for residential heating is more common in the winter.

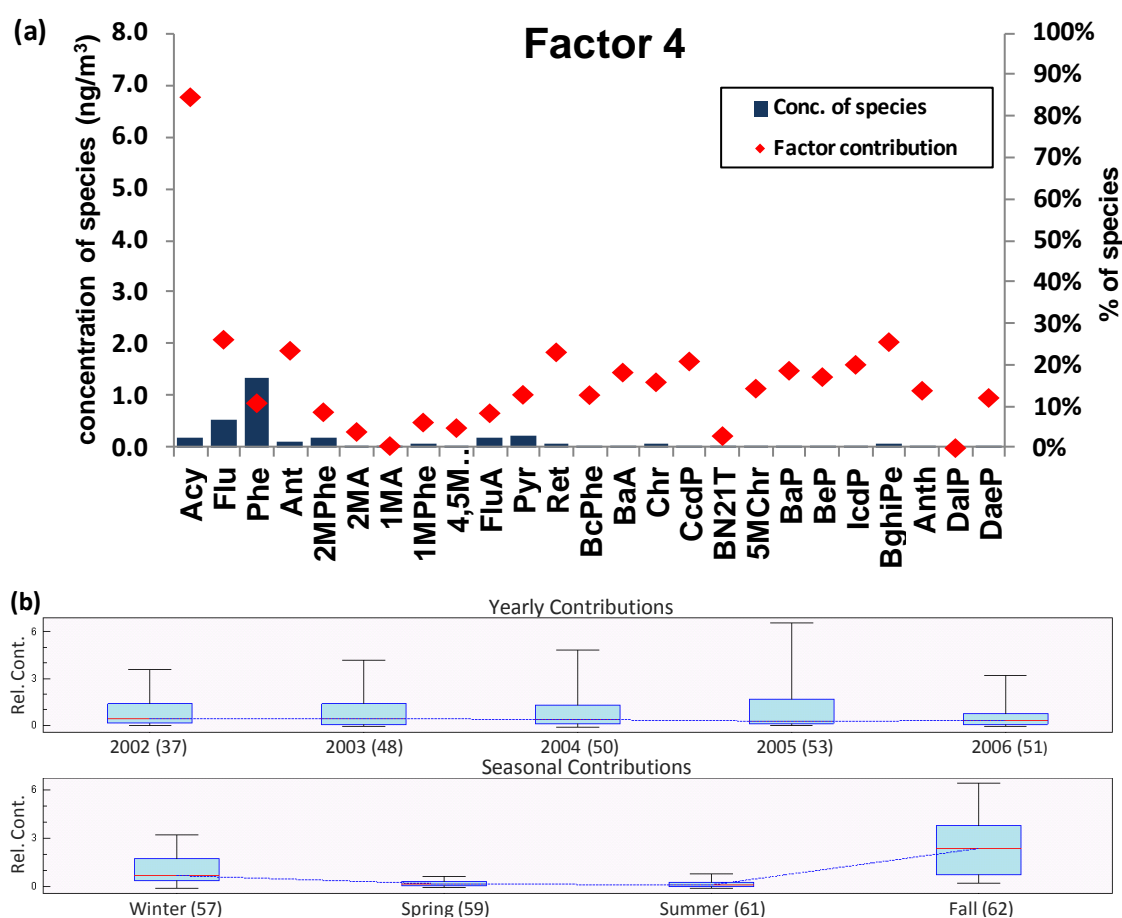


Figure 3.8. PMF factor profile for total PAH and temporal variation at urban sites in the UK (Factor 4).

3.2.3 UK industrial urban sites

PMF was applied to a merged dataset drawn from five urban sites that had local industrial emissions. The major source for PAH levels in Middlesbrough, Port Talbot and Scunthorpe was steelworks; Bolsover had a coalite works that converted coal to different types of solid fuel, although this was closed in 2004; and Holyhead had aluminum smelting plant until recently (Brown and Brown, 2012).

Three-factor to six-factor solutions were explored in PMF by varying the model uncertainty (u) and adjusting the uncertainty of variables through the categorization process until an optimized solution was obtained. A three-factor model showed the best fit solution in PMF, having stable Q values for twenty base runs. Selected theoretical and robust Q values were 969 and 733 respectively. The unmapped bootstrap runs, compared to the selected PMF base run, ranged from 1 to 4 for individual factors. An individual correlation coefficient (r^2) of PAH species was over 0.9 except for Flu (0.65) and 2MA (0.72). Mass contributions to the sum of PAH ($\sum_{\text{total}} \text{PAH}$) were 34.1, 48.4 and 17.5% for Factors 1, 2 and 3 respectively.

A PAH signature and seasonal trend for Factor 1 (see Figure 3.9) showed some similarity with the one for Factor 2 (Figure 3.6) obtained from the urban dataset in the UK. This factor was predominantly explained by 1MA (86.6%) and several methylated phenanthrenes (MPhes) including 1MPhe (71.7%) and 2MPhe (66.0%). As discussed in Section 3.2.2, the significance of Phe and MPhes was widely observed in the source signature for unburned fossil petroleum that evaporated from the vehicles in urban areas, having the larger mass contribution in the warm seasons (Rogge et al., 1993, Gogou et al., 1996, Mi et al., 2000, Kavouras et al., 2001, Zuo et al., 2007). Ret, commonly reported as a source indicator for wood burning (Ramdahl, 1983, Benner et al., 1995), showed a relatively significant contribution (53.6%) to this factor. However, other authors have reported that Ret can also be found in vehicular exhaust emissions (Khalili et al., 1995) and in coal combustion emissions from domestic heating (Shen et al., 2012). Based on the above reasons, this factor was assigned to unburned petroleum.

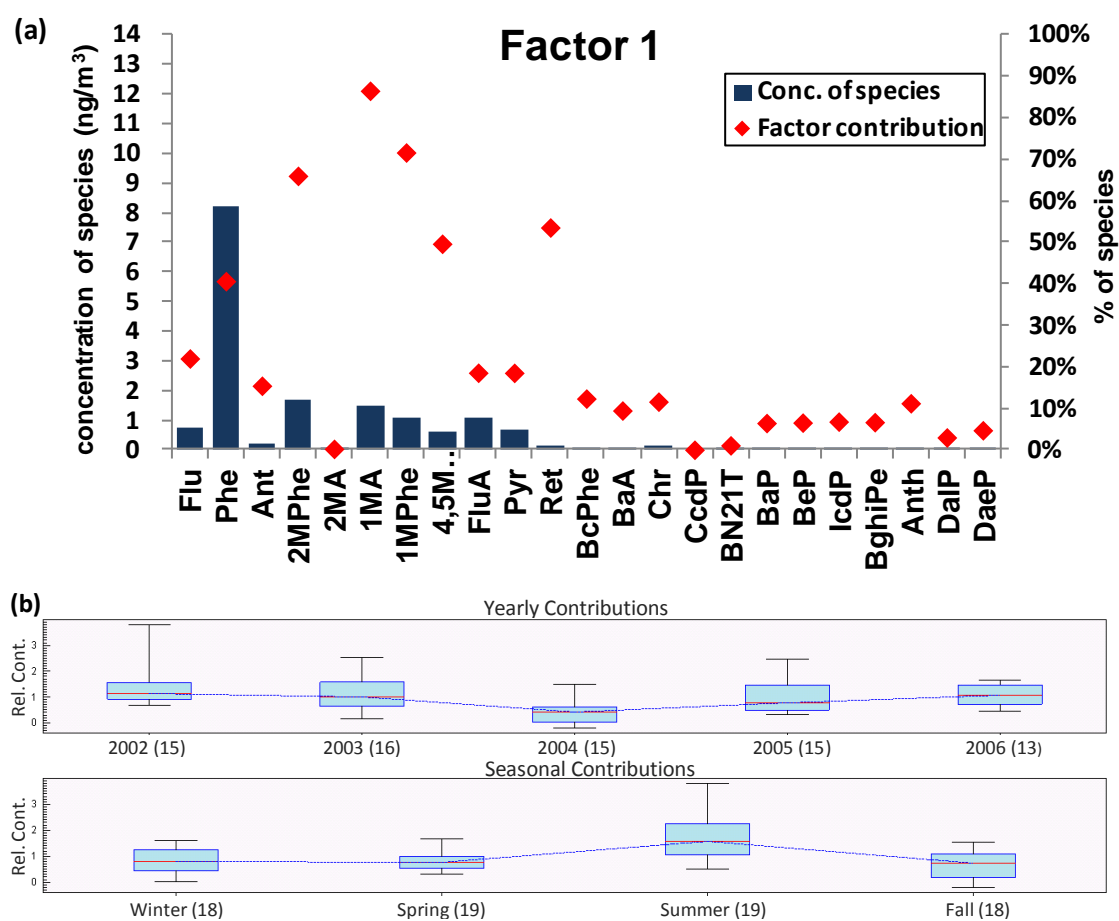


Figure 3.9. PMF factor profile for total PAH and temporal variation at industrial urban sites in the UK (Factor 1).

Factor 2 (see Figure 3.10) was responsible for 48.4% of the sum of PAH mass at the industrial urban sites. This factor was significantly associated with most of the PAH congeners except for methylated PAH. Anth had the highest factor contribution, at 83.8%, followed by BaA (73.0%) and derivatives of pyrene (BaP, IcdP, DalP and DaeP) (about 60%).

The significance of HMW PAH (see Figure 3.10) was comparable to the factor profile in Figure 3.7 that was attributed to coal combustion sources in the urban dataset. However, this source signature showed more enhanced contributions from the LMW

PAH, such as Flu, Phe and Ant. As outlined in Section 3.2.2, the steel industry includes coke-making and sintering processes, and these processes can produce both LMW and HMW PAH (Ciaparra et al., 2009). Physical distance from the industrial source may allow this factor to make a relatively high contribution to LMW PAH. On the other hand, it is expected that a reduced contribution to LMW PAH will be seen in remote areas, because these PAH are reactive compounds in the air. In addition, the seasonal trend having smaller seasonal variation, when compared to the one in Figure 3.7, reflects the different types of coal combustion source. To conclude, this factor profile seems to explain the metallurgical industry as a PAH source that includes coal combustion activities. With similarity to the previous results obtained in the urban dataset (Section 3.2.2), it was not possible with PMF to separate the two different types of coal combustion profiles into those resulting from domestic activities and those resulting from industrial activities in this industrial urban dataset.

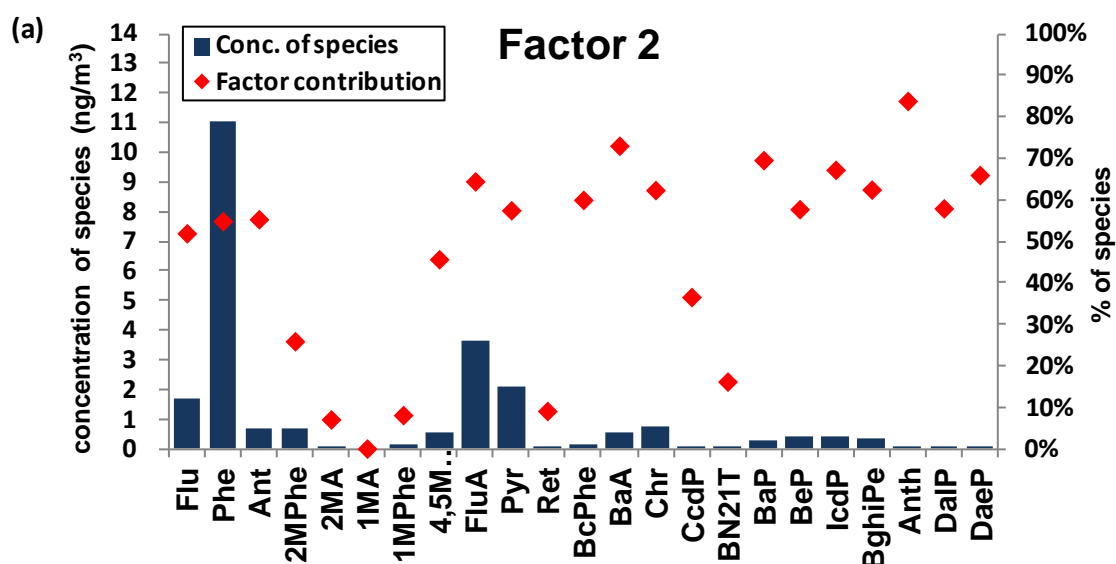


Figure 3.10. PMF factor profile for total PAH and temporal variation at industrial urban sites in the UK (Factor 2).

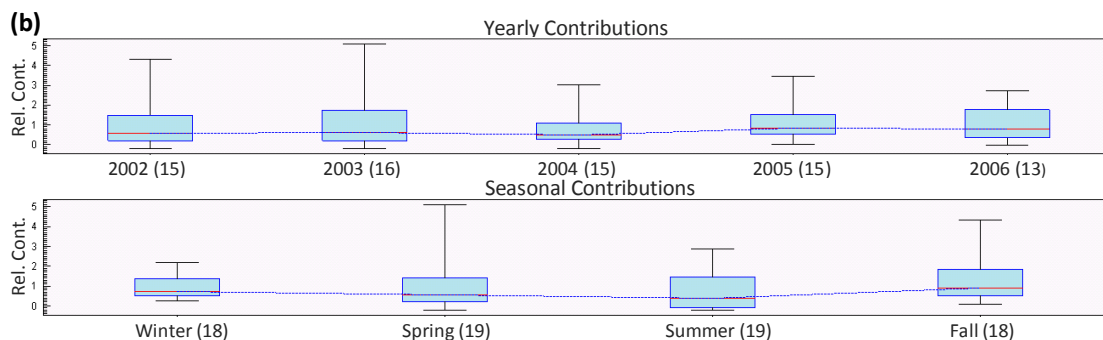


Figure 3.10. (Continued).

When the two were compared, Factor 3 (see Figure 3.11) showed considerable similarity to the diesel emissions factor profile (see Figure 3.5) that was extracted from the urban sites. A noticeable factor contribution from 2MA (92.8%) and BN21T (82.8%) was observed. These compounds have been reported as source markers for diesel emissions, as opposed to gasoline combustion (Alsberg et al., 1989, Westerholm and Li, 1994, Allen et al., 1996). There was no strong seasonal variation in the PAH mass. A significant decrease was shown from 2005, and a consistent result was also observed for the diesel emissions factor at the urban sites.

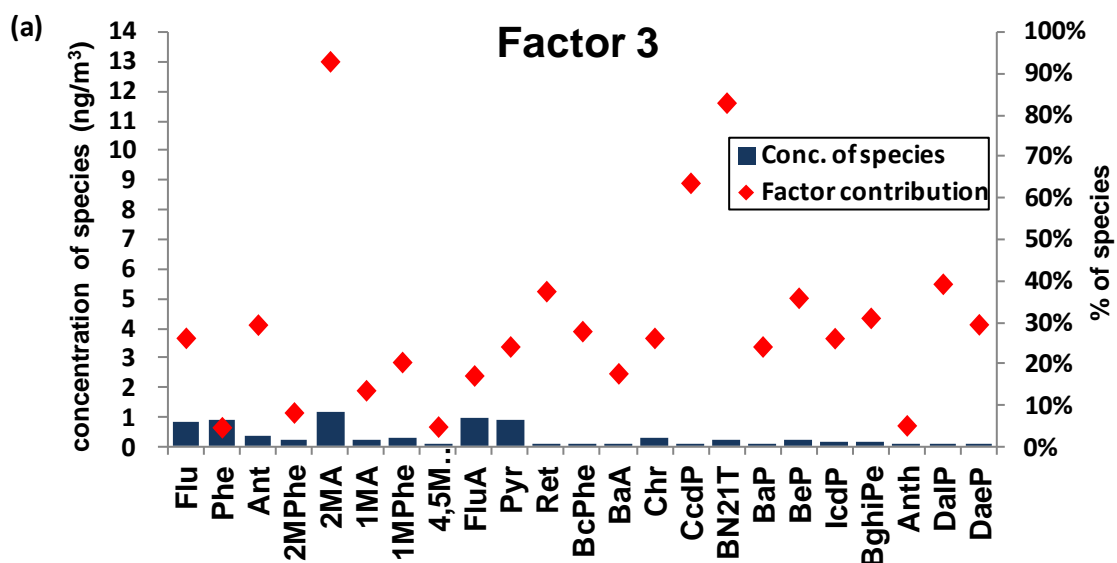


Figure 3.11. PMF factor profile for total PAH and temporal variation at industrial urban sites in the UK (Factor 3).

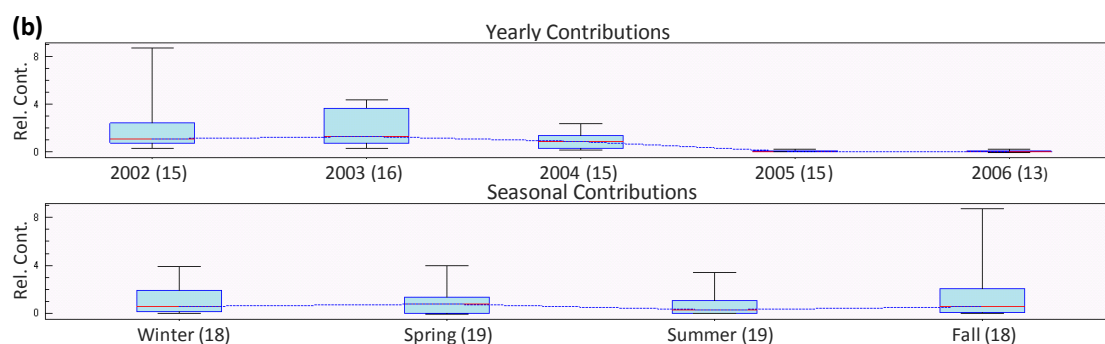


Figure 3.11. (Continued).

3.2.4 UK site-specific PAH contributions

Different local sources, with their different meteorological conditions and geographical locations, can cause variation in the compositions of PAH congeners and the mass contributions for individual PAH. When PMF is applied to a pooled dataset drawn from several sites with similar emission characteristic, it may be useful to calculate the source-specific contributions at each site. Figure 3.12 illustrates site-specific source contributions for PAH obtained from the UK urban dataset drawn from 14 sites and the industrial urban dataset drawn from 5 industrial sites.

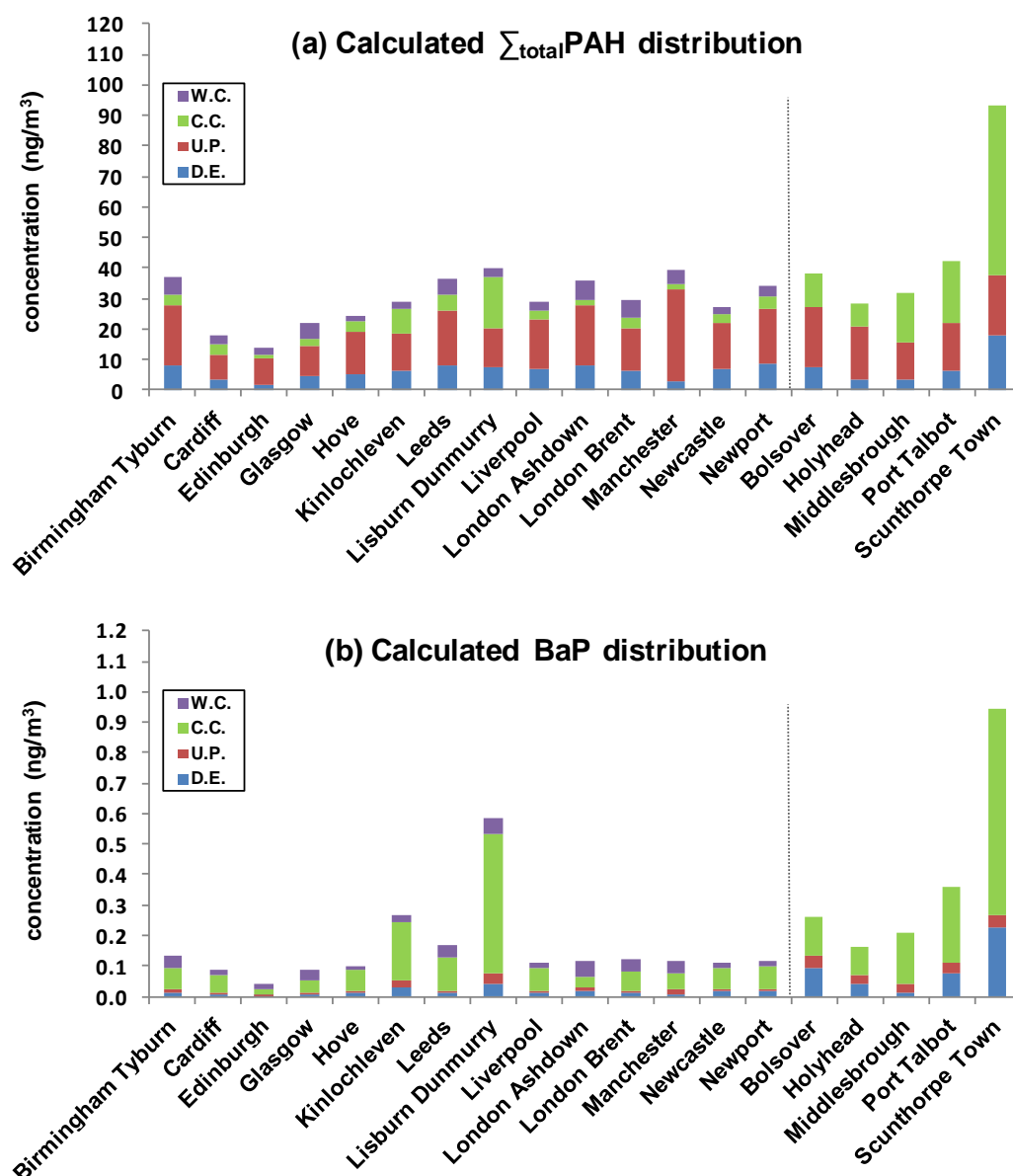


Figure 3.12. Source specific PAH mass contributions in the UK (DE: diesel emissions; UP: unburned petroleum; CC: coal combustion; WC: wood combustion).

PMF extracted four major factors for the total gaseous and particulate phase PAH from the urban dataset, and these were diesel emissions (DE), unburned petroleum (UP), coal combustion (CC) and wood combustion (WC). Three factors were responsible for the PAH mass at the industrial urban sites: diesel emissions (DE), unburned petroleum (UP) and coal combustion (CC). However, the wood combustion factor was not separated in

using this industry dataset. It seems that wood combustion emissions at industrial sites are a minor source, therefore they are ignored in PMF, which maybe the one of the limitations of factor analysis.

As regards the urban sites in the UK, the largest contribution to the sum of PAH mass ($\sum_{\text{total}} \text{PAH}$) was seen to come from the traffic-related sources such as diesel emissions and unburned petroleum. This may be caused by the abundant LMW PAH that usually exit in a high concentration in the air. Traffic related contributions were more obvious in the more populated cities. On the other hand, BaP concentrations were more associated with the combustion of solid fossil fuels such as coal and wood.

Interestingly, a notable PAH mass contribution from a coal combustion factor was seen at the Lisburn Dunmurry site, where fossil fuels such as coal and oil are widely used for residential heating because there is limited access to natural gas fuel in Northern Ireland. For BaP, relatively high contributions were seen at two urban sites: at the Kinlochleven site in Scotland, which until recently had a local aluminium smelting plant and is not connected to the UK natural gas network (Brown and Brown, 2012); and at Lisburn Dunmurry, which has widespread fossil fuel combustion activities as outlined above. Relatively high concentration for BaP from diesel emission and wood combustion sources at the Lisburn Dunmurry site, compared to other sites, may indicate high emissions produced through inefficient combustion conditions for the domestic heating.

For industrial urban sites, traffic sources were significantly responsible for the sum of PAH mass. Concurrently, an outstanding contribution to the PAH mass from coal

combustion sources was seen. As regards BaP, coal combustion emissions were the most significant contributor.

3.3 Conclusion and discussion

Extensive source apportionments for total PAH (the sum of the gaseous and particulate phases) were conducted. Three pooled datasets – the Jeddah urban dataset (3 sites), the UK urban dataset (14 sites), and the UK industrial urban dataset (5 sites) – were prepared and subjected to PMF. This study showed that PMF could quantitatively separate out the source-specific contributions to the sum of PAH concentrations, reflecting physically understandable local emissions.

Three factors were responsible for the PAH concentration at the Jeddah sites in Saudi Arabia, and these were traffic emissions, especially from gasoline vehicles (17%), industrial sources, particularly oil refinery process (33%), and diesel/oil combustion sources (50%). Traffic-related sources (gasoline and diesel) and oil combustion source were the predominant contributors to BaP at all the sites, and their weekday/weekend contributions were different. Industrial emissions seemed to be significantly responsible for the PAH levels in the Jeddah area, and these corresponded to the distance from the oil refinery plant, with Site A, followed by Site B and then Site C. However this source was not a significant contributor to the BaP concentration.

Application of PMF to the UK urban dataset revealed that four major sources contributed to the PAH concentration, and these were shown to be diesel emissions

(21.4%), unburned petroleum (50.5%), coal combustion (15.0%), and wood combustion (13.1%). The three combustion-related sources showed higher contributions in the cold season, whereas the unburned petroleum source was dominant in the warm season, which may be related to the high volatility of LMW PAH at high atmospheric temperatures. Although one factor identified with sulphur-containing PAH (BN21T) was assigned to diesel emission source, it seems that diesel emissions are also responsible for partial contribution of unburned petroleum source owing to the relatively enhanced significance of MPhe (Benner et al., 1989, Lim et al., 1999). A similar explanation can be applied to coal combustion factor distinguished with HMW PAH having significant winter contribution. In practice, other types of fuel combustion for space heating in urban areas could partially be associated with this factor contribution. These two cases may show the ambiguity and uncertainty in the identification of specific sources for receptor modelling, because minor factors are sometimes ignored and these can be combined into the major factors. Slightly different source-specific contribution was observed when two receptor modelling methods were applied to the same dataset (Cao et al., 2011). The possibility of combined factor contribution from several sources was reported (Lee et al., 2008). One factor did not consist of any particular source markers, was assigned to “other” source. (Larsen and Baker, 2003). The use of high quality datasets, sufficient understanding of local/national emissions and the development of source markers may overcome the problem which arises when apportioning sources to factors obtained from receptor modelling.

As regards BaP, the emissions were substantially determined by solid fossil fuel combustion sources such as coal combustion and wood combustion for residential

heating. Source-specific contributions varied among the different sites, and it is likely that they provide a reasonable explanation for local emissions. For example, a significant contribution of diesel exhaust emissions (DE) to the sum of PAH but little contribution of those to the BaP was observed at all the sites except at Kinlochleven and Lisburn Dunmurry. These two sites showed a relatively meaningful contribution from this factor to BaP, which may reflect that they were associated with different types of diesel combustion activity, such as oil combustion for domestic heating, although a factor characterised by BN21T was assigned to the DE in the pooled urban dataset.

PMF identified three major factors of PAH from industrial urban sites in the UK. Unburned petroleum, coal combustion and diesel emission sources accounted for the sum of total PAH, contributing 34.1%, 48.4% and 17.5% respectively. In terms of BaP, they contributed 7.8%, 67.8% and 24.4%. The contribution from coal use in the metallurgical industry to the sum of PAH was significant when looked at in the context of the urban dataset. Interestingly, coal combustion factor profiles were similar between the urban dataset and the industrial dataset, except in terms of LMW PAH. However, seasonal contributions were different. This may reflect the possibility of there being different types of coal combustion sources. By contrast with the urban dataset, PMF did not separate out a wood combustion factor from the industrial dataset. Acy, used as a source marker for wood combustion, was excluded from the analysis of input data with PMF. However, it is not likely that leaving out Acy led to the loss of one factor, because PMF could not predict the temporal trend for this compound and Q values did not converge when this compound was included. This may be an example of one of the limitations of receptor modelling, which is that minor sources are sometimes ignored,

and thus major sources can be overestimated.

To conclude, extensive interpretation was conducted to assign sources to PMF factor profiles. And the quantitative analysis of PMF was helpful in obtaining physically understandable factor profiles. Daily measurements taken in Jeddah made it possible to compare temporal variations (weekdays/weekend); and UK long-term datasets provided information with an annual and seasonal contribution for individual sources in PMF. In addition, information on local emissions was useful for providing a reasonable explanation when interpreting sources.

CHAPTER 4: COMPARISON WITH SPATIAL ANALYSIS

This chapter discusses a complementary spatial analysis that was performed to extract a local source profile for PAH using paired sites with the aim at comparing this result with PMF source profiles. Particle-bound PAH concentrations sampled by the Digitel sampler were used. Local source signatures of PAH for traffic emissions, urban backgrounds and industrial emissions were extracted using three pairs of locations: (1) an urban traffic site (London Crystal Palace Parade) and an urban background site (London Brent); (2) an urban background site (London Brent) and a rural background site (Harwell); and (3) an industrial urban site (Port Talbot) and a nearby urban background site (Swansea). Finally, comparisons with PMF source profiles are provided.

4.1 Background

The fact that measured concentrations of PAH in the air are the outputs of mixed emissions from complex sources, and the fact that source signatures are sometimes overlapped between sources, has led to the introduction of many source identification methods to separate out individual source fingerprints. PMF is an advanced statistical tool which can extract source profiles and segregate source specific contributions quantitatively, and it is applied to measured concentrations at a receptor site without *a priori* knowledge about physicochemical properties for compounds. Users assign PMF

factor profiles to specific source categories subjectively, based on the information about chemical composition taken from direct source measurements in different studies (Khalili et al., 1995).

As shown in Chapter 3, four factors (unburned petroleum, diesel combustion, coal combustion and wood combustion) and three factors (unburned petroleum, diesel combustion and metallurgical industry) are respectively responsible for the sum of PAH concentrations at the urban and the industrial urban sites in the UK. However, the subjective source apportionment used in the PMF method can cause misunderstanding of the main PAH sources, as variable factors such as different regulations, various fuel types, and variable meteorological conditions may influence composition PAH congeners and this complexity adds to the difficulty of interpreting PMF sources. Thus it is essential to evaluate the adequacy of source assignments for PMF factor profiles using complementary approaches. In this section, local source signatures of PAH are extracted using three paired locations and are compared with the PMF factor profiles for these.

4.2 Results

4.2.1 Source profiles of urban sites

A different concentration, referred to as the 'net concentration', was calculated for individual PAH congeners using measurements taken at two sites. A net traffic concentration was calculated by subtracting the levels at an urban background (UB) site from those at an urban traffic (UT) site. The difference in concentrations between the urban background (UB) site and the rural background (RB) site was considered to be the net urban concentration.

There is general agreement on the seasonal variability of measured atmospheric concentrations of PAH in urban areas. An increase in the concentration of vapour phase PAH in the summer, relating to volatility of that PAH, has been reported (Tuominen et al., 1988, Coleman et al., 1997). The elevated level of particle-associated PAH in the cold season has been commonly explained by a lower mixing height (van Drooge and Ballesta, 2009), less intensive atmospheric reactions, enhanced distribution to particulate phase owing to the lower ambient temperature (Ravindra et al., 2008a) and higher seasonal emissions, such as those caused by domestic heating (Schauer et al., 2003, Tan et al., 2006). However, it appears that using separated net concentration between summer and winter can provide supplementary information on source-specific seasonality. Furthermore, it is likely that this shows the aspect of chemical reactivity of PAH, which are compounds that are sensitive to ambient temperature.

The net concentration was plotted separately for the summer and the winter, as shown in Figures 4.1a and 4.1b. Some compounds showed negative net concentrations; but these values were small and were ignored in producing the contribution source profiles (see Figure 4.1c).

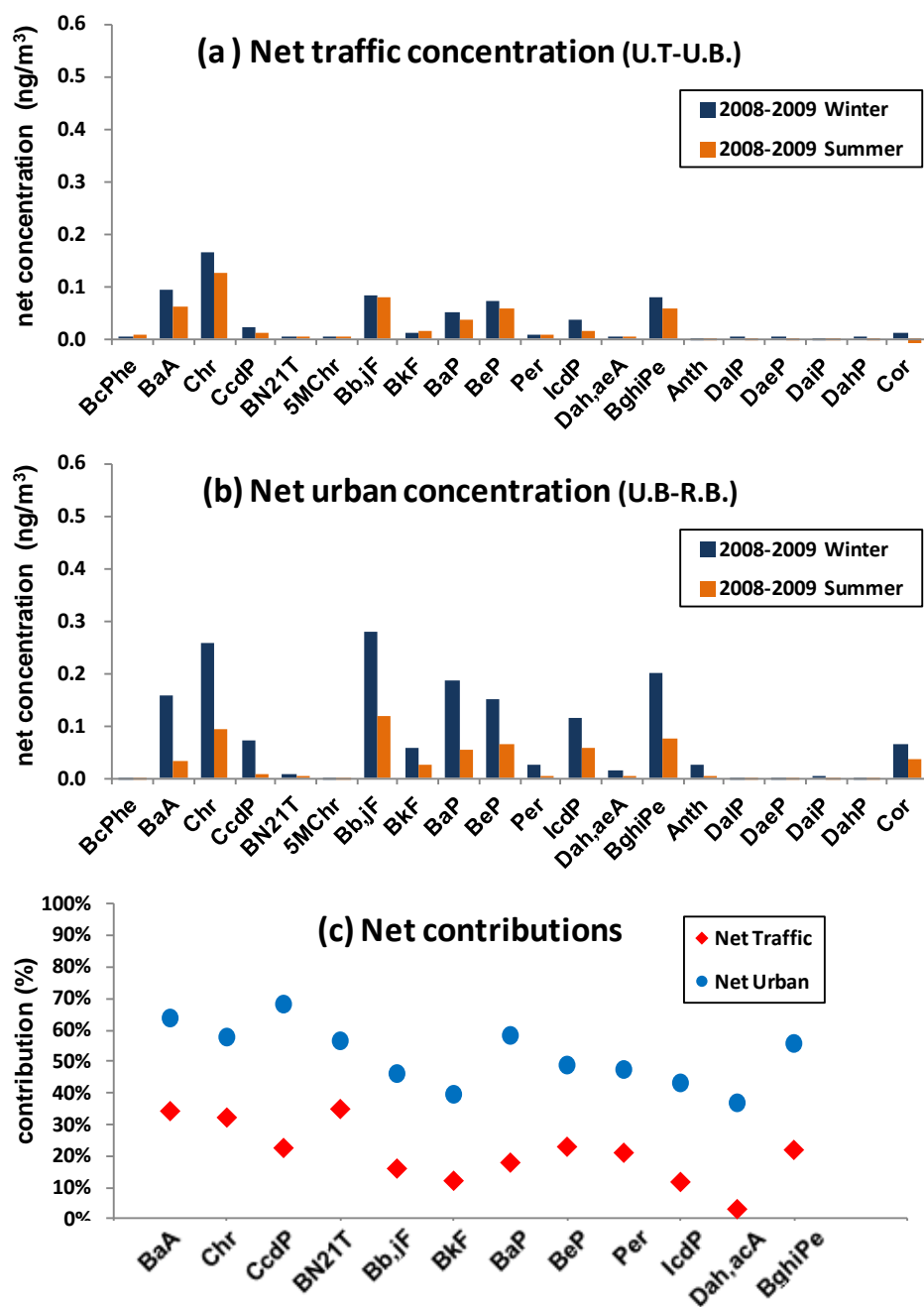


Figure 4.1. Source profile of urban PAH from cross sectional analysis.

There was only a small seasonal difference between summer and winter in the net traffic concentration for PAH congeners (Figure 4.1a). One may conclude from this that the seasonal output of particle-bound PAH from traffic emissions does not significantly vary, thus traffic can be considered as a non-seasonal particulate PAH source, although some authors have reported that low temperatures can increase the emission of airborne particle PAH from vehicles in winter (Nielsen et al., 1995). On the other hand, an apparent seasonal variation was observed in the net urban concentration, as shown in Figure 4.1b, indicating relatively higher levels of particulate PAH in winter than in summer by a factor of over two, which appears to be influenced by domestic heating sources in the cold season. An enhanced chemical reaction of PAH during transport from urban background site to rural background site in the warm season may be an additional explanation for the seasonal difference in the net urban concentration.

Two factor contribution profiles of particle-associated PAH are shown in Figure 4.1c. These were calculated by dividing the net concentration by an absolute concentration at the urban traffic and urban background locations, separately, with reference to the 'net contribution'. Interestingly, a considerable similarity in the composition of PAH congeners between the two net contribution source profiles was shown, although it appeared that the net contribution profiles of particulate PAH for the traffic and urban sites were more affected by the traffic emissions and the domestic combustion sources, respectively. As discussed in the previous chapter, this result reflects the fact that a simple method has limitations in the separation of source-specific profiles of PAH. However, this study provides ancillary source information on PAH congeners. Low emissions of Dah,acA were seen in the net traffic contributions. Slightly enhanced

contributions of CcdP and BaP, observed in the net urban contribution profile, may be related to a local source at the urban background site. The fact that much smaller seasonal ratios (summer/winter) of CcdP and BaP, compared to other PAH congeners, were reported (Nielsen et al., 1999) may explain why these compounds can be source markers for domestic heating in urban areas. This information was consistent with the PMF factor assigned to coal combustion sources in Figure 3.7.

4.2.2 Source profiles of industrial sites

As described in Section 4.2.1, the net concentration of PAH relating to industrial activity was derived by subtracting the level at an urban background (UB), Swansea from that at a nearby industrial site (IU), Port Talbot, which had local PAH emissions from steelworks (see Figure 4.2a). It has been generally reported that the higher concentration of airborne particles associated PAH is seen in the cold season, caused by increased domestic heating emissions, the lower reactivity of PAH congeners with oxidants in cold weather, and the lower mixing height. However, interestingly, the seasonal pattern of the net concentration for industry was apparently different from the net concentrations for traffic and urban backgrounds observed in the previous section. The larger net industrial concentration of particle-bounded PAH was shown in warm season rather than in cold season, which may explained by the significant local emission source at Port Talbot.

The net contribution profile at the Port Talbot site, calculated as $(IU - UB) / IU \times 100$, showed that industrial emissions significantly influence predominantly the HMW PAH, including the highest value of DaiP (Figure 4.2b), and this appeared to be different from the previous two net urban contribution profiles. Again, this study provides indirect information on the possibility of using of DaiP as a source marker for emissions from steel works. The significance of HMW PAH and their relatively enhanced contribution in the warm season were also observed from the industrial factor of PMF (see Figure 3.10).

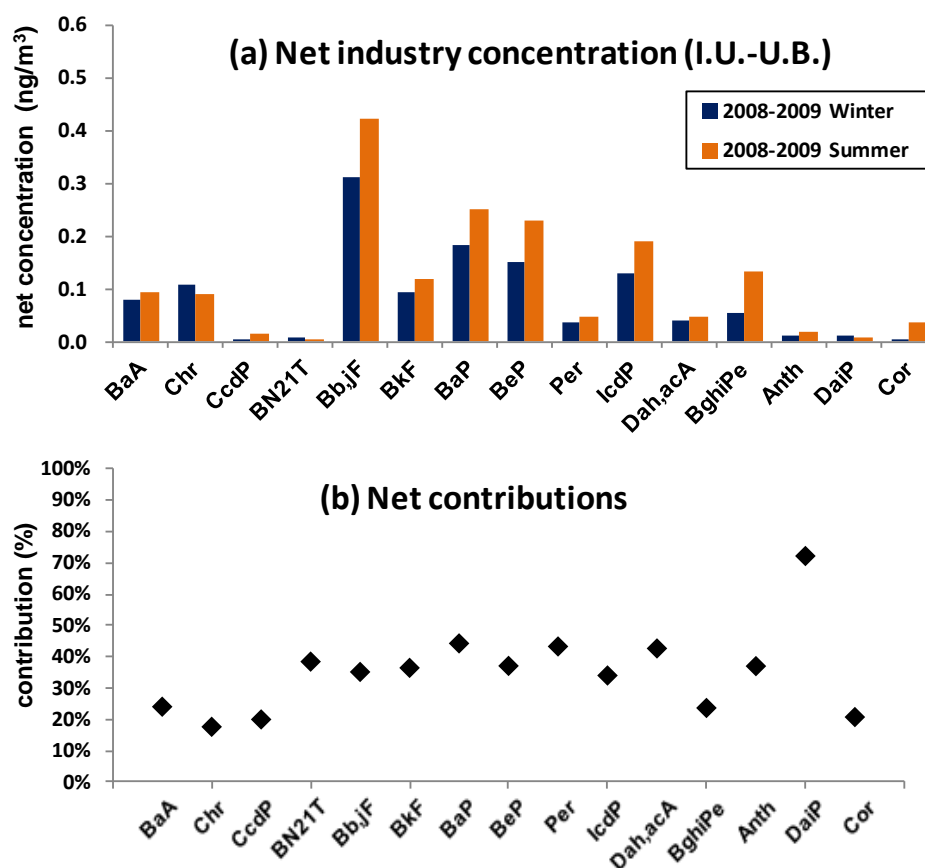


Figure 4.2. Source profiles of industrial urban PAH from cross sectional analysis.

4.2.3 Comparison between PMF source profiles and net concentration profiles

Three net contribution profiles were taken from the spatial analysis of particle-associated PAH and these were expressed as percentages. This simple method is not able to provide detailed information on the source-specific signatures of PAH congeners, as the net concentration of PAH at the receptor site can be a mixed value, influenced by various sources. However, this analysis provided us with some information in the aspect of sources. CcdP and BaP can be potential source markers for domestic heating at an urban background area, and dibenzopyrenes for steel works emissions, mostly produced through the coal combustion activity. In addition, it was seen that seasonal variations in net industrial emissions of airborne particle-associated PAH can be different from the general seasonal trend, having a larger mass in the warm season. In terms of sources, this information derived from spatial analysis should be a good physical match for the results of source apportionment obtained using PMF, which were subjectively decided by users. Thus, in this section, detailed comparison was made between the signatures of PAH congeners from a source specific profile extracted from PMF analysis and a local net contribution profile obtained from spatial analysis.

Figure 4.3 plots the net contribution of PAH congeners expressed as percentages, and using these, source signatures taken from the PMF tool and the spatial analysis were compared with common variables. The sum of the vapour and total suspended particle (TSP)-associated concentrations of PAH was used for PMF analysis; on the other hand,

the spatial analysis included PM₁₀ airborne particle-bound PAH. However the fact that most PAH congeners used in this comparison predominantly exist in the particulate phase, and they are mostly distributed as fine particles, makes it possible to compare the factor-specific contribution pattern of PAH congeners between the two different sampling methodologies.

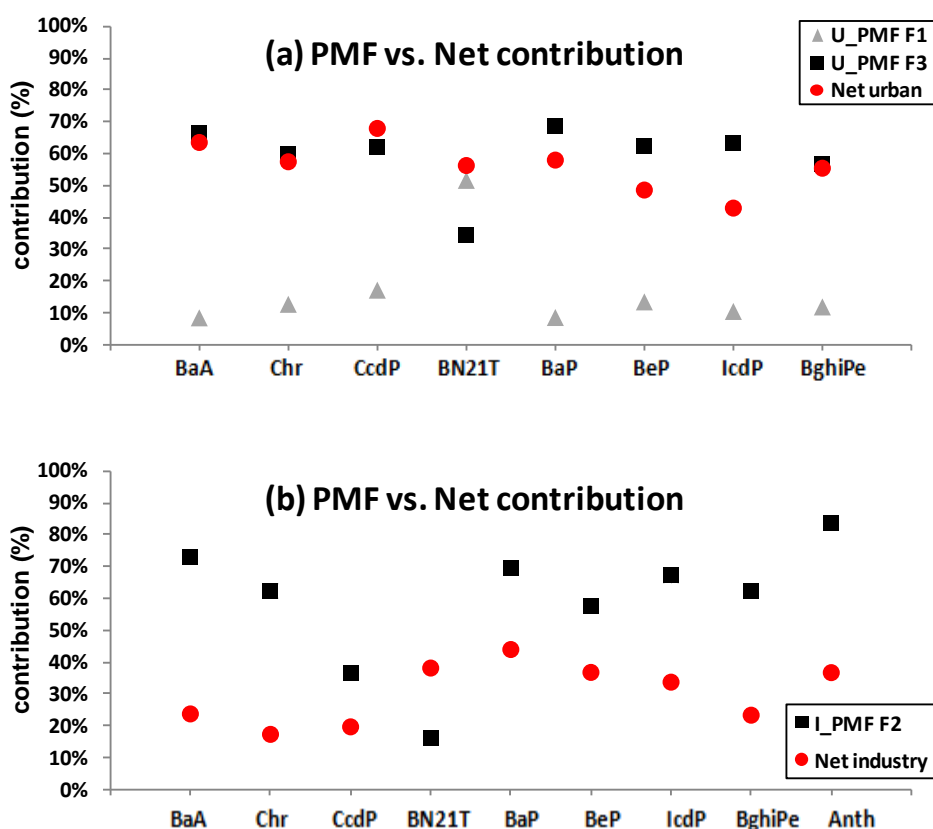


Figure 4.3. Comparison between PMF source profiles and net contribution profiles.

A considerable similarity between the PMF factor contribution profile assigned to ‘coal combustion’ (U_PMF F3) in the urban dataset and the net urban contribution profile, except in relation to BN21T, was observed, and is recorded in Figure 4.3a. PMF extracted another source profile that was distinguished by BN21T and assigned to a

‘diesel emissions’ source (U_PMF F1). It is likely that the combined factor contribution of two PMF results (U_PMF F1 and U_PMF F3) became quite comparable to the one for net urban profile. This may explain the difference between the two methods. To conclude, there is agreement between the two approaches on the broad physical interpretation of the sources of particle-associated PAH; but the PMF tool seems to be better for separating out sources in detail when applied to mixed concentrations at receptor sites.

The two different types of contribution profiles for PAH are compared in Figure 4.3b using common compounds. The net industry contribution profile shows a significant proportion of most of the HMW PAH. When this profile was compared with the PMF profile (I_PMF F2) assigned to metallurgical industry emissions related to coal combustion, the two factor contribution signatures of PAH congeners showed similarities. However, a more enhanced factor contribution was observed for the PMF profile. Although a PAH vapour emitted at a high temperature can quickly be partitioned into particulate phase in the ambient temperature, it appears that PMF result provides information on the significant contribution of vapour phase PAH to steelwork emissions. This is because the concentration for PMF consisted of the sum of gaseous and particulate PAH, sampled by the Andersen high volume sampler, and only particle-bound PAH were included in the net contribution profiles.

4.3 Conclusion

This study calculated the net concentration of particulate PAH and produced net contribution profiles using paired locations. Varied information relating to source markers and the seasonality of sources can be obtained based on this type of simple spatial analysis.

It appears that net traffic emissions are not associated with a seasonal source of PAH. By contrast, net urban background concentrations are significantly influenced by seasonal sources, showing larger mass contributions in the winter, which may be explained by domestic heating sources. The net industry concentration reveals that the concentration of particulate PAH is not always higher in the cold season, if the receptors are significantly influenced by non-seasonal local emissions.

The slightly enhanced significance of the two congeners CcdP and BaP for the net urban contribution profile, compared to the net traffic contribution signature, may support the possibility of using these compounds as source identifiers for domestic heating emissions in urban background areas. And it seems that DaiP can be used as a source marker for emissions for steel works.

Additionally, this result provides supplementary information when compared with source profiles extracted using the PMF tool. Although, owing to the limited field measurements for total (gaseous and particulate) PAH at the rural background site

(Harwell, in this study), PM₁₀-bound PAH sampled between 2008 and 2009 were used in this study, which represented a different sampling period for the data of PMF. There was general agreement between local source contribution profiles and PMF source profiles. However, the much larger mass contributions of some PAH for the PMF industry profile, as compared with those for the net industry contribution profile, reflect the significant emissions of vapour phase PAH from steelworks activity near the receptors.

CHAPTER 5: COMPARISON WITH UK EMISSIONS INVENTORY

In this chapter, major national sources of the total PAH concentration (gaseous and particulate) in the UK are described in detail based on UK emission estimates. This can provide a complementary perspective for the interpretation of the source profiles obtained in Chapters 3 and 4.

5.1 Background

PMF is one of the receptor modelling tools that identifies the major sources statistically using real measurements at the receptors. The advantage of this method is that knowledge, such as the photochemical reactivity of interesting compounds or the meteorological conditions, is not required. However, there have been doubts over the application of PMF to reactive PAH congeners. The subjective interpretation of PMF results by users has been considered another concern, because main sources can be misunderstood. Chapter 4 showed that local source profiles included information that agreed with PMF source profiles, in terms of the source markers and the seasonality of sources. However, it is essential to investigate PMF factor profiles from various angles, whether identifications for sources are physically understandable or not.

Detailed estimations for PAH emissions between 2002 and 2006 in the UK can be obtained from the UK National Atmospheric Emissions Inventory website (<http://naei.defra.gov.uk/>) (see Table B1 in Appendix B). In this study, source-specific profiles of the PAH congeners, expressed as both a concentration (tonne/yr) and a relative source contribution (%), were extracted separately based on the activity code. There may be a discrepancy of source profiles between the two approaches in terms of complex atmospheric reactivity of PAH and heterogeneous targeting regions. The PMF method separates sources statistically using field measurements at the receptor sites, focusing on the urban locations in this study (top-down approach). On the other hand, the emission inventory approach considers all possible sources and estimates total emissions on a national scale (bottom-up approach). However the fact that the dataset for PMF consisted of merged urban sites throughout the UK may make it possible to obtain supportive explanations for the PMF factor profiles by comparing the two approaches.

5.2 Results

5.2.1 Source profiles for industrial activities

A high level of similarity in the chemical composition for PAH congeners was shown between the coke production industry and the iron and steel making industry (see Figures 5.1a and 5.1b).

The contribution to the HMW PAH, such as BbF, BkF, BaP and IcdP, is relatively high, followed by three- and four-ring PAH (Phe, Ant, FluA, Pyr and BaA). It has been reported that PAH from the iron and steel making industry can be released through the coke manufacturing, sintering, iron making, casting and steel making processes (Yang et al., 2002). Coke oven emissions are responsible for the predominant contribution of two- and three-ring PAH such as Na, Acy, Flu and Phe (Khalili et al., 1995). PCA separated two sources from the ambient measurements at a location near steelmaking facilities (Ciaparra et al., 2009): one source of emissions was a coke making activity, which was characterized by LMW PAH (Acy, Flu, Phe, Ant and FluA); the other source was a sintering process operated under a high temperature, which was more associated with the HMW PAH emissions, including pyrene derivatives (BaP and IcdP). The fact that PAH congeners are produced from the coal combustion activities for both coke production and iron and steel making may lead to a high level of similarity between the two source signatures.

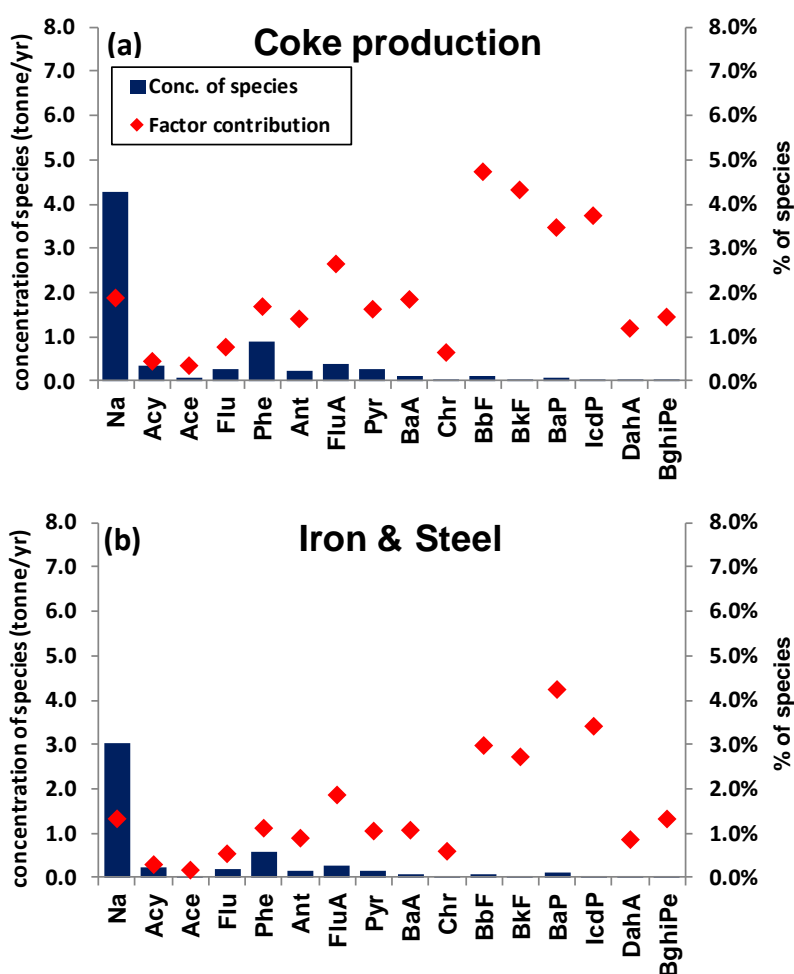


Figure 5.1. PAH source profiles of industry extracted from UK emission estimates.

5.2.2 Source profiles for domestic combustion

Whilst access to natural gas has increased, PAH emissions produced from domestic heating source have decreased. However, there are still significant PAH emissions in the UK, which are released from the combustion of solid fossil fuels, such as wood and coal, for residential heating (Butterfield and Brown, 2012).

In Figure 5.2a, a domestic wood combustion source profile extracted from the UK National Emissions Inventory shows that there is a significant factor contribution of Acy to this source, followed by an appreciable loading of four-ring PAH such as BaA and Chr. Additionally a meaningful contribution of BaP was observed. These results are comparable to those reported by other studies on PAH emissions from wood burning (McDonald et al., 2000). Retene, which is widely used as a source marker for PAH emissions from wood combustion activities (Khalili et al., 1995, Wang et al., 2009, Dvorská et al., 2012), was not included in the UK emission estimates. However this study provides an alternative source marker of Acy for wood combustion emissions.

A source profile for domestic coal combustion was extracted from the UK national emission estimates, accounting for a significant contribution to the relatively HMW PAH such as BaP, IcdP and DahA (see Figure 5.2b). According to the UK energy statistics, coal has been predominantly consumed by the power stations, followed by industrial and domestic uses (see Table C1 in Appendix C). However PAH emissions, especially HMW PAH, from power stations were not significant than other source categories on a national scale. PAH are formed by incomplete combustion, but it appears that operating conditions in power stations cause them to be considered as a less significant source for PAH. On the other hand, a high number of PAH emissions have been reported from domestic heating activity, where incomplete combustion conditions are prevalent.

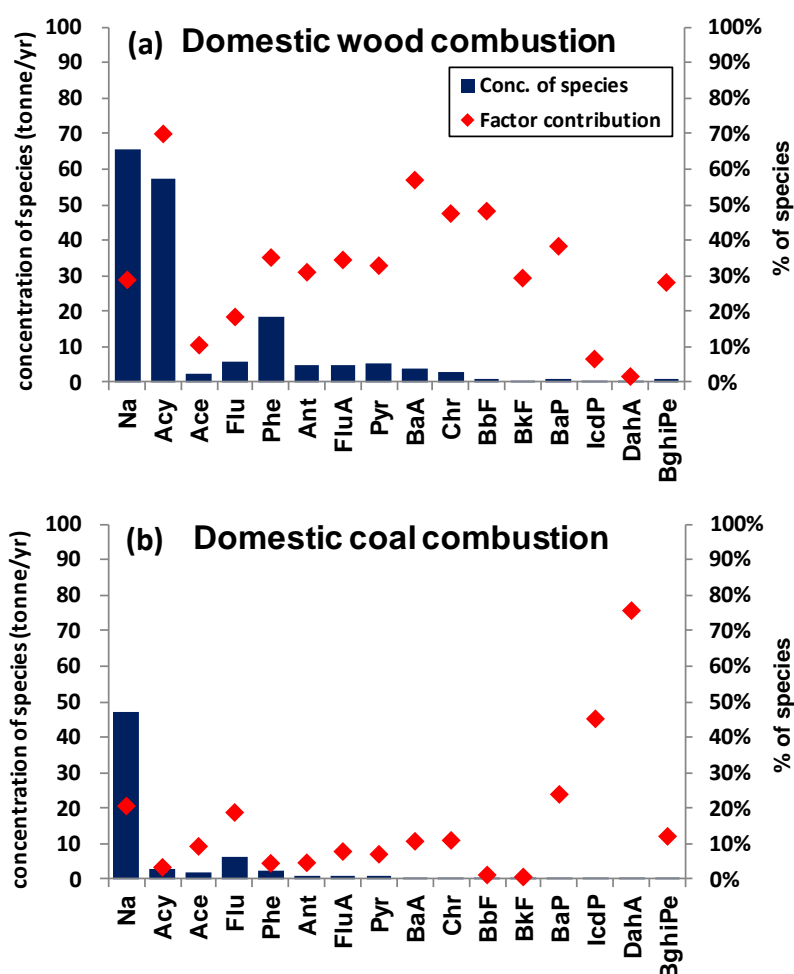


Figure 5.2. PAH source profiles of domestic combustion extracted from UK emission estimates.

5.2.3 Source profiles relating to vehicular emissions

Traffic emissions are known to make a significant contribution to atmospheric PAH levels in urban areas. Various efforts have been made to reduce traffic emissions worldwide (Colville et al., 2001). However, a great many field measurements focused on traffic exhaust emissions are still conducted, because an increased traffic volume in urban areas is related to a high concentration of pollutants including PAH, which is reported as a mutagenic and carcinogenic compound (Farmer et al., 2003, Delgado-

Saborit et al., 2011).

Two kinds of vehicular source profiles were extracted from the UK emission estimates (see Figures 5.3a and 5.3b). One profile was retrieved from the national PAH emissions for diesel combustion activity from road traffic. This was characterised by relatively LMW PAH such as Ace, Phe and FluA (see Figure 5.3a). A significant contribution of volatile PAH to diesel vehicle emissions was reported (Zielinska et al., 2004). The fact that LMW PAH are predominantly distributed to the vapour phase shows an agreement between the two results. The other source signature (see Figure 5.3b), composed of gasoline emissions, was distinguished by relatively HMW PAH such as IcdP and BghiPe. An extensive study has been conducted to distinguish between the PAH source signatures of diesel combustion and those of gasoline combustion. A higher contribution of BbF and BkF to those of diesel-fueled traffic than those of gasoline-powered vehicles was reported (Harrison et al., 1996, Marchand et al., 2004, Rajput and Lakhani, 2010). The larger significance of IcdP, BghiPe and Cor for gasoline vehicle exhaust, compared to the diesel exhaust has been commonly reviewed (Zielinska et al., 2004, Li et al., 2011).

To conclude, traffic related source signatures for PAH congeners obtained from the UK national emissions estimates showed a general agreement with those of other studies that were applied to ambient measurements. In addition, this study showed that the mass contribution for BaP from traffic emissions was relatively less significant than the one from domestic combustion sources, on a UK national scale.

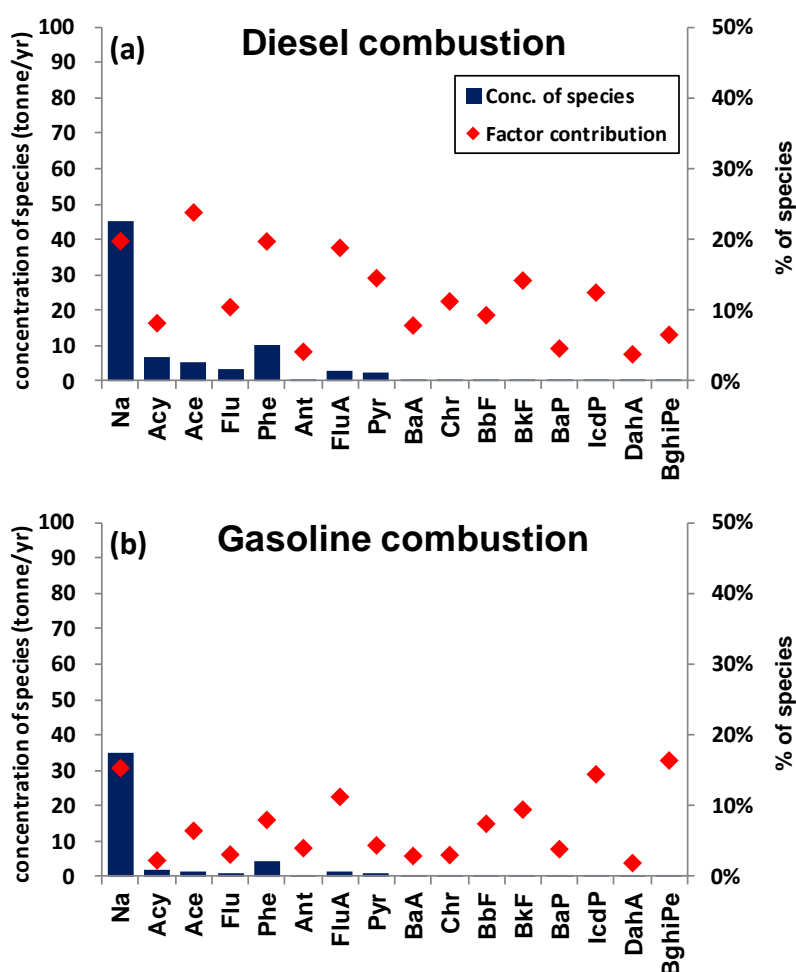


Figure 5.3. PAH source profiles of traffic emissions extracted from UK emission estimates.

5.2.4 Comparison between PMF source profiles and UK emission estimate source profiles

Source-specific mass contributions for 16 USEPA priority PAH were calculated based on the activity for emissions that were taken from the UK NAEI. Source signatures were plotted from data for 2002 - 2006. As a concurrent period for both the UK national emissions and the dataset for PMF, this may provide complementary information on the interpretation of the PMF source profiles. Physically, above two types of source-specific

profiles – one derived from the nationally estimated emissions; the other statistically extracted from PMF receptor modelling – should show general agreement. In this section, the two types of source profiles are compared for eleven common compounds.

A PMF factor profile that was assigned to the diesel combustion source with a marker of BN21T for the urban dataset (see Figure 5.4a), and a source profile for national emissions from diesel combustion activity (see Figure 5.4f) were compared. The source contributions to LMW PAH were relatively large for both profiles. However, a reduced composition for the mass of Acy was apparent in the PMF signature, compared to the national emission estimates. This may be related to the short atmospheric half-lived time that Acy has after being emitted from its sources.

Two PAH source profiles related to traffic emissions were compared, as shown in Figure 5.4b and Figure 5.4g, and little similarity was observed. The highest source contribution to Phe, followed by the LMW PAH such as Flu, FluA and Pyr, was seen in the PMF source profile that was assigned to the unburned petroleum source. On the other hand, little contribution of LMW PAH was observed in the national source profile of gasoline combustion for vehicles. The fact that the former source is related to volatile emissions which that have escaped from the internal combustion engine depending on ambient temperature, and the latter source is associated with gasoline exhaust emissions from road traffic, may lead to the discrepancy between the two signatures. Interestingly, when PMF source profiles were plotted using eleven PAH congeners, a considerable similarity in distribution of factor contribution was observed between the diesel combustion profile and the unburned petroleum profile (see Figure 5.4a and Figure

5.4b). Based on above results, one may conclude that datasets consisting of extensive PAH congeners can make it possible for a PMF tool to separate source types in detail, and to reduce the limitation of the underestimation of minor sources.

The significant contribution to the HMW PAH was comparable between the PMF profile that was assigned to coal combustion sources for urban dataset (see Figure 5.4c) and the estimated signature for domestic coal combustion activity that was derived from the UK National Emissions Inventory (see Figure 5.4h). Two kinds of source profiles related to the coal combustion activity – one for the domestic usage and the other for the iron and steel industry – can be extracted using the UK emissions estimates (see Figure 5.4h and Figure 5.4i). Even though great uncertainty about PAH emissions from industrial processes was reported, owing to the non routine measurements (AEA, 2011), PAH emissions for industrial coal combustion were much less than those for domestic coal usage throughout the UK. This may lead to decision not to separate the two different types of coal combustion source for PMF (Figure 5.4c), where measurements taken from urban areas are used. It has been reported that factor analysis sometimes ignores minor sources.

On the other hand, Figure 5.4d shows the source profile for the coal combustion, which was extracted from the industrial urban dataset using the PMF method. Both the LMW and the HMW PAH contributed significantly to this source. However, this industrial factor extracted through PMF was not consistent with national source profiles for the iron and steel industry. It appeared that national emission source profiles could not reflect local industrial emissions in detail, because emissions for the iron and steel

industry are minor on a national scale.

The data in Figure 5.4e, extracted from the UK urban dataset, was assigned to the domestic wood combustion source based on the reported information (McDonald et al., 2000). The contribution of Acy to this source is significantly high, at around 90%. However, the mass composition of Acy was much weaker than in the national source signature for domestic wood combustion (Figure 5.4j). As mentioned above, this difference may reflect the reactivity of Acy, as the concentration of Acy can diminish significantly between the source region and the receptor site.

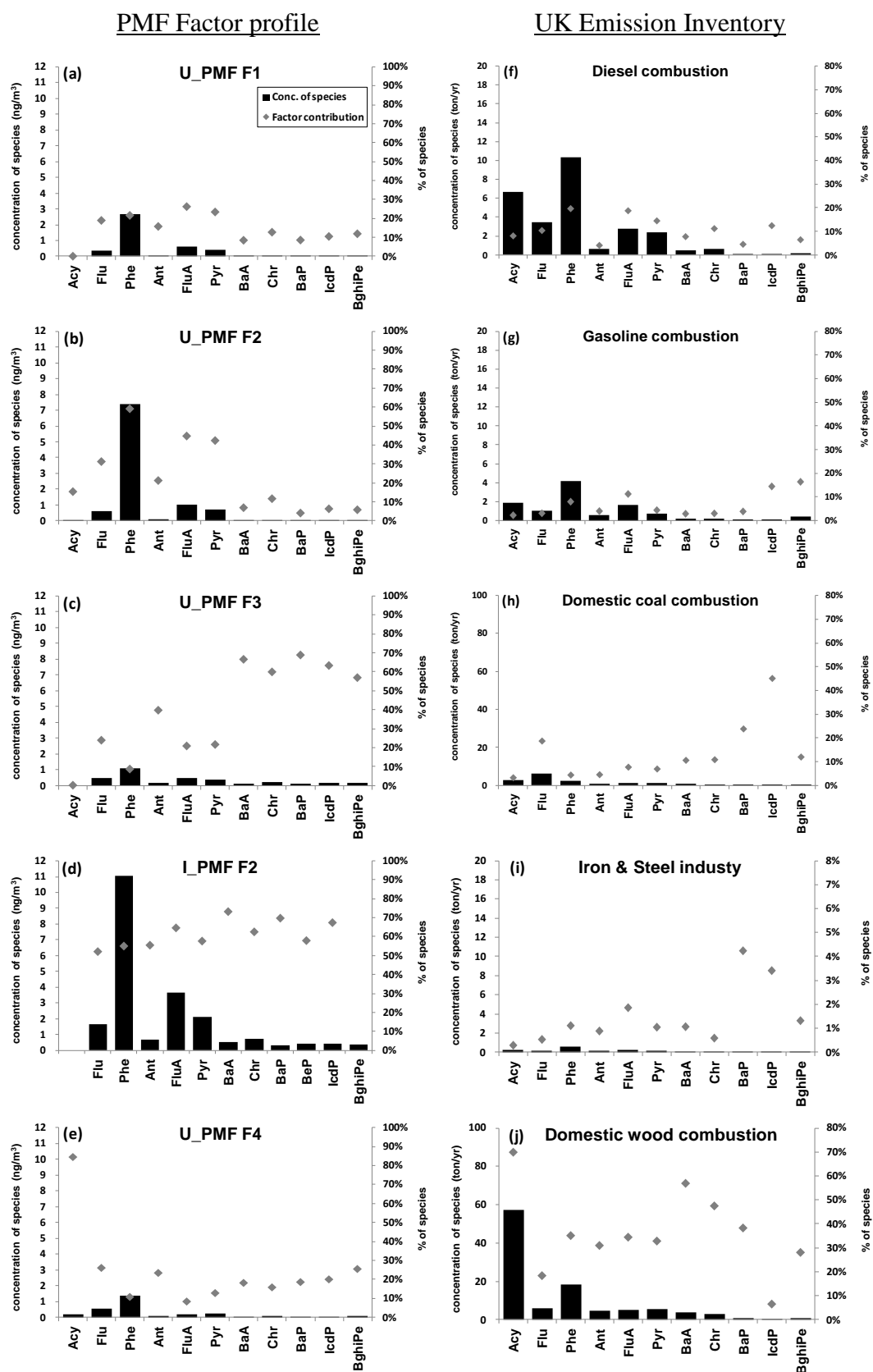


Figure 5.4. Comparison of source profiles obtained with different approaches.

5.3 Conclusion

In this study, source specific signatures for PAH congeners were taken using national emission estimates for the UK. When the source profiles were plotted with a mass concentration only, the compositions of PAH showed a high degree of similarity among source types, with a larger concentration of LMW PAH than that of HMW PAH. Meanwhile, the plots for the relative source-specific contribution values, which are expressed as a percentage (%), were useful to separate sources with source-indicated compounds. In addition, it appeared that a dataset consisting of extensive PAH congeners was helpful for a PMF to split source types in detail.

A comparison between the national emissions source profiles and the PMF source profiles was conducted. Some differences, for example in mass composition and source-specific contribution, were observed between the two types of approach. This may have arisen from the difference in dataset scales: one approach was based on data produced on a UK national scale, and the other used atmospheric measurements at the receptors in the UK. However, there was general agreement on the source identifiers in the source signatures of PAH congeners. In addition, this study provided supplemental information on the source signatures for PAH congeners. The potential for significant reactivity of LMW PAH during transport from the source to the receptors was observed. However, it seemed that the reactivity of compounds had little influence on the technical source separation in the PMF analysis.

CHAPTER 6: OVERVIEW OF POSSIBILITY OF MEANINGFUL SOURCE PROFILES

6.1 Introduction

The PMF method has been widely used in recent studies on quantitative source identification for PAH emissions, because it is an advanced receptor modelling tool with constraints on negative outcomes. However, there have been some doubts over the application of PMF to PAH, due to their high and differing atmospheric reactivity and the partitioning mechanism between the gaseous and particulate phases. As shown in Chapters 4 and 5, source signatures expressed as a mass concentration, for example as ng/m^3 , or as tonne/yr , can provide information on absolute source-specific PAH emissions on both the national and the local scale. The other expression of a relative source-specific contribution (%) can give a supporting explanation when different sources are distinguished. The above two types of expressions were included in source profiles in the previous chapters. Physical comparisons of PAH source profiles derived from PMF in Chapter 3 were in general agreement with those taken from spatial analysis (Chapter 4) and national emissions inventories (Chapter 5).

This chapter offers an attempt to discuss whether PMF can extract meaningful source profiles or not using HMW PAH and focusing on the reactivity of PAH congeners. The G-P phase distribution for three- to four-ring PAH is quite sensitive to ambient

temperature (Yamasaki et al., 1982). Thus some PMF factors involving these compounds may be determined by their volatility, which is not related to the actual source. The use of the sum of vapour and particulate PAH concentrations can minimize the effect of G/P partitioning on statistical factor analysis. However, only particle-bound PAH concentrations, sampled by the Digitel sampler, are included in this chapter because of the availability of these for the preparation of detailed datasets for PMF. The fact that the HMW PAH limited in this study (from BaA to Cor) are predominantly associated with the particulate phase may overcome the problem which arises when applying factor analysis to particle-only PAH datasets.

The work described in Chapter 3 led to the preparation of two datasets with different local emissions relating to coal combustion activity. In Section 6.2, two datasets are described that provided information on PAH with different predominant local emission sources: one is a domestic combustion dataset consisting of measurements at Northern Ireland sites where there is limited access to natural gas; the other is an industrial dataset consisting of measurements taken near a source of coal combustion emissions; both are subjected to PMF. Finally, PMF source profiles for an urban dataset are interpreted based on the PMF results that were obtained from the previous two datasets. Section 6.3 provides a comparison of PMF results, in terms of reactivity of PAH, between two datasets for which the sampling times are obviously different. One dataset consists of a total (vapour + particulate) concentration for HMW PAH that was sampled for 14 days using an Andersen sampler; the other includes daily measurements for particle-associated PAH taken using a Digitel sampler. Lastly, sensitivity results can be seen in Section 6.4. LMW PAH are more volatile and reactive than HMW PAH. This

may lead to greater uncertainty about measurements of LMW PAH. A dataset in which additional uncertainty is applied to the individual PAH congeners corresponding to their rate coefficients with the OH radical is subjected to PMF. This PMF result is compared with a previous one that applied a uniform uncertainty of 10% concentration.

6.2 Source profiles of particle-bound PAH

6.2.1 Domestic combustion sites

Particle-bound PAH were measured from 2008 on at three sites in Northern Ireland of Ballymena Ballykeel, Derry Brandwell and Lisburn Dunmurry using a Digitel sampler, because a relatively high concentration of PAH had been reported at these sites where, due to the limited availability of natural gas, there was a high usage of solid fuels for domestic heating (AEA, 2011). Information on distinctive local emissions is useful to interpret source profiles which are taken by statistical receptor modelling, i.e. PMF in this study.

A number of factors were examined, ranging from three to seven, by varying an additional modelling uncertainty. PMF showed that a three-factor solution was the best model fit. The calculated theoretical Q value was 402; and the robust Q obtained was 455. The correlation coefficient (r^2) for individual PAH ranged from 0.84 for DahA to 0.99 for BN21T. There were no unmapped bootstrap factors to the base factor run. The sum of the squares of the differences in scaled residuals for each base run was under one.

Mass contributions for 14 PAH congeners ($\sum_{\text{par}}\text{PAH}$) were 33.5, 51.1 and 15.4% for Factors 1, 2 and 3, respectively.

A significant contribution of CcdP and Anth was observed (Figure 6.1), which was explained in Chapter 3 as being related to emissions from coal combustion activity, either from an industrial process or from domestic heating. A considerable contribution of Per – over 70% – was observed in this factor. It has been a matter of controversy whether the source for the Per is a product of biosynthesis (Grice et al., 2009, Liu et al., 2012b) or outputs from fossil fuel combustion (Suzuki et al., 2010). Kavouras et al. (2001) extracted one single component (Per) factor using PCA with the measurement of airborne particulate-bound PAH, and assigned it to the fossil fuel emissions source, based on the fact that most particulate PAH congeners are produced through the combustion process. Relatively less significant contributions of BghiPe and Cor, which have been widely used as traffic source markers, may lead one to conclude that this factor is related to a non-traffic source. Significantly smaller summer-to-winter ratios for CcdP and Anth than for other PAH congeners (Nielsen et al., 1999) may support that these compounds are related to a seasonal source. The much smaller mass contributions in the summer than in the winter lead one to assign this factor to a domestic coal combustion source.

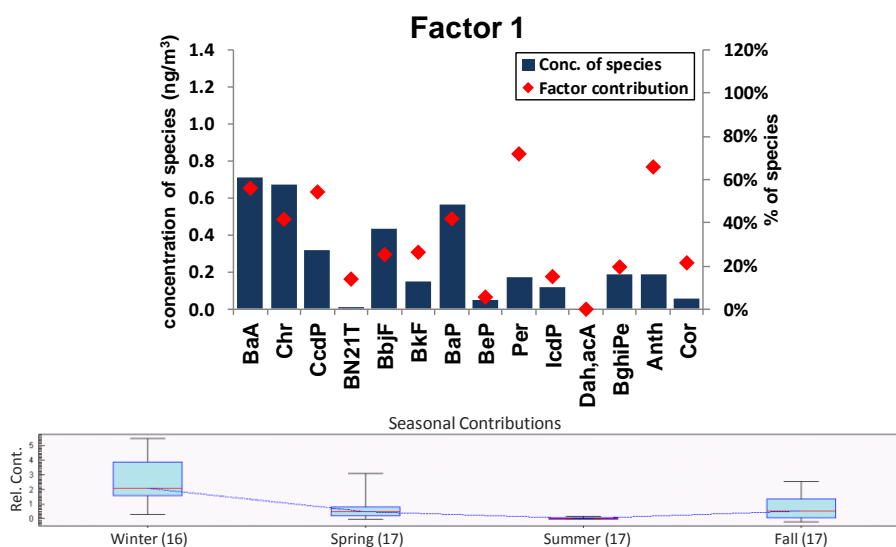


Figure 6.1. PMF factor profile for PM_{10} -bound PAH and source-specific seasonal variation (Northern Ireland – Factor 1).

In Figure 6.2, the PMF factor profile of Factor 2 was characterised by BbjF, BkF, BeP, IcdP, Dah,acA, BghiPe and Cor. These compounds have been commonly reported as source markers for traffic emissions. Fresh airborne particles, collected in a tunnel where vehicles were the main source, were analysed for their PAH composition (Ning et al., 2007, Rajput and Lakhani, 2010). They showed that FluA, Chr and Pyr were more related to the emissions from diesel vehicles, while BghiPe and Cor were distinctive compounds in the emissions from gasoline internal engines.

A seasonal variation, showing a higher mass contribution in the cold season, was observed. This was consistent with the general mass concentration trend for particle-bound PAH, which is related to atmospheric reactivity, G/P distribution, the mixing height, and photochemical reactions depending on seasons. So it was possible to conclude that this factor should be assigned to traffic emissions.

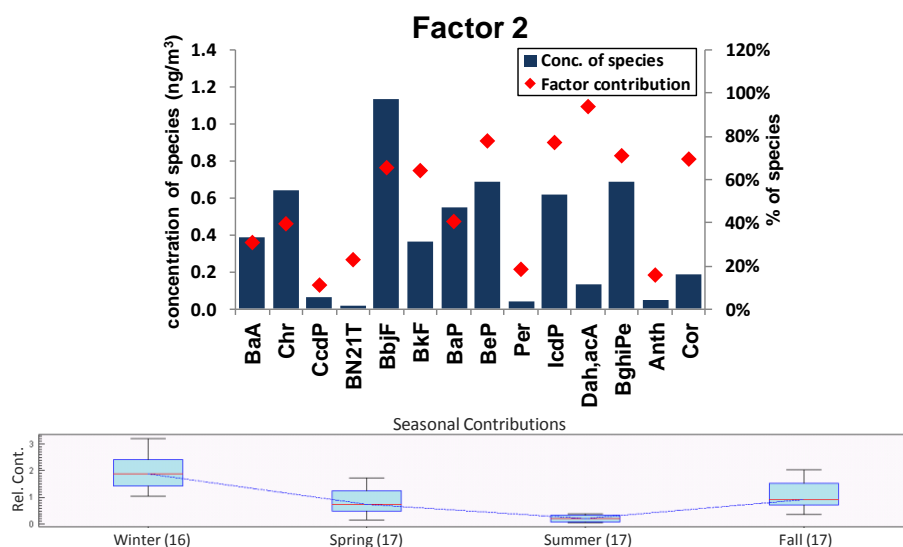


Figure 6.2. PMF factor profile for PM_{10} -bound PAH and source-specific seasonal variation (Northern Ireland – Factor 2).

Factor 3, as shown in Figure 6.3, was identified with BN21T, which as mentioned in Chapter 3 is used as a source indicator for diesel combustion. This factor profile showed a strong seasonality, having little mass contribution in the summer. This seasonal trend was slightly different from that of the diesel combustion factor, which was extracted from the Andersen urban dataset of 2002-2006. Moreover, the fact that a requirement for fuels sold to be sulphur free ($< 10\text{ppm}$) was partially instituted from 4 December 2007, and expanded to all retailers who sold UK highway vehicle fuels from 1 January 2009 (Jones et al., 2012), meant that an alternative explanation for this factor was needed. This dataset, which consisted of measurements taken during the period following sulphur-reduction regulation (2009-2010) at domestic-combustion-prevalent sites, is more likely to be influenced by residential activity. To conclude, this factor is related to domestic emissions being emitted from the combustion of fuel oils (kerosene) (Ward et al., 2012).

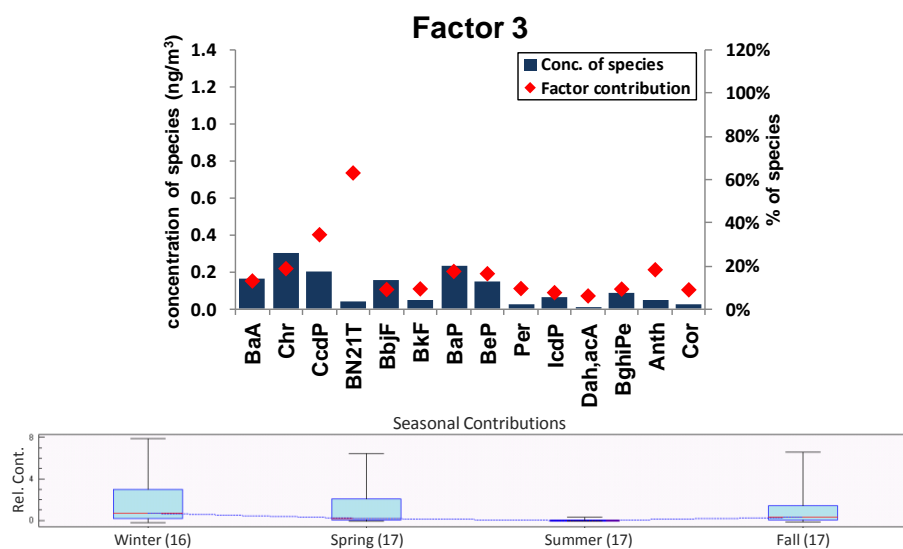


Figure 6.3. PMF factor profile for PM₁₀-bound PAH and source-specific seasonal variation (Northern Ireland – Factor 3).

Figure 6.4 shows the source-specific mass concentrations for the sum of particle-bound PAH congeners ($\sum_{\text{par}}\text{PAH}$) at each site. The combustion activity using fuels (coal and oil) for domestic heating was extensively responsible for contributions both to the $\sum_{\text{par}}\text{PAH}$ and to the BaP at three sites in Northern Ireland. Fuel combustion by vehicles was an additional significant contributor to PAH levels at these sites.

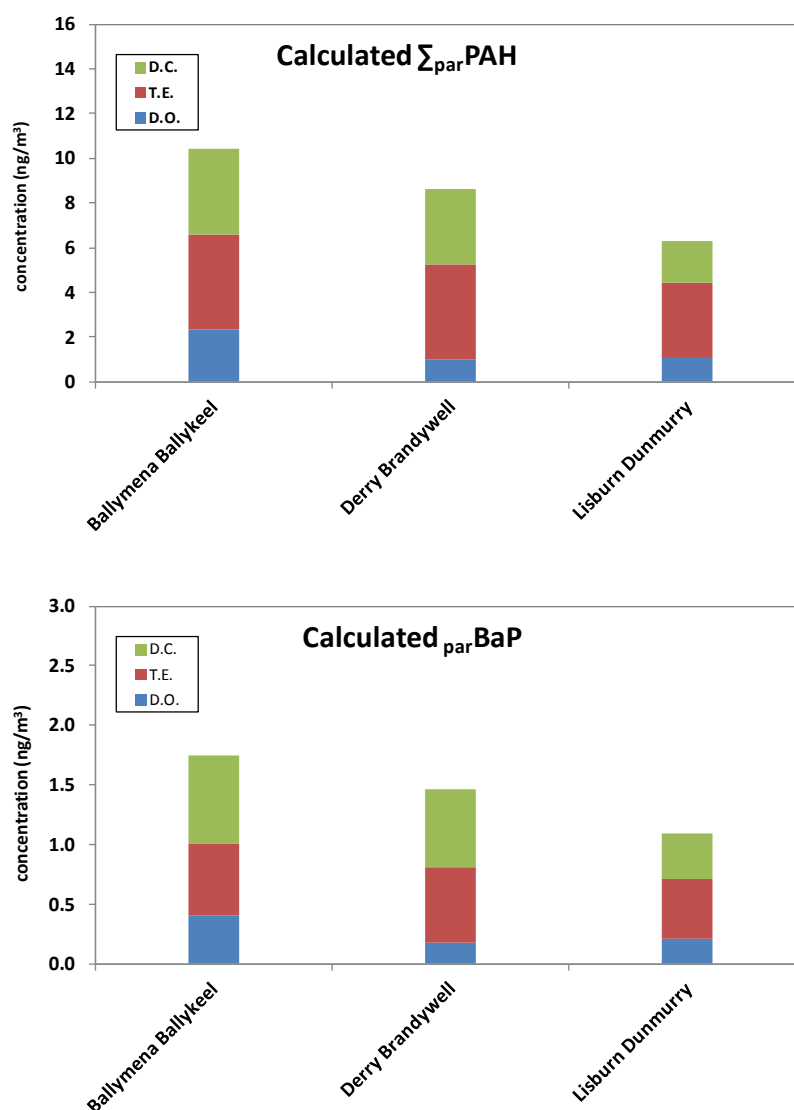


Figure 6.4. Site-specific source contributions (DO: domestic oil combustion; TE: traffic emissions; DC: domestic coal combustion).

6.2.2 Industrial urban sites

In the previous PMF analysis, a coal combustion profile that was extracted from the total PAH measurements at the urban sites could not be separated between domestic usage and industrial activities (see Section 3.2.2), although the PAH levels at the urban

background sites could have been influenced by the nearby industrial activity, as outlined in the Section 4.2.3.

One dataset consisting of data for seven merged industrial urban sites was prepared and subjected to PMF. Atmospheric measurements for particle-associated PAH between 2009 and 2010 were used in this study. The information on local sources for the PAH emissions at each site are shown in Table 6.1 (Brown and Brown, 2012).

Table 6.1. *Details of industrial sites.*

Site name	Local PAH sources
Bolsover	Former coalite works
Middlesbrough	Steel and chemistry works
Port Talbot Margam	Steel works
Royston	Coke works
Scunthorpe Low Santon	Steel works
Scunthorpe Town	Steel works
South Hiendley	Coke works

The optimum number of factors was ascertained by varying this from three to eight. A four-factor solution with modelling uncertainty of 11% showed the best model fit. The $Q(\text{theoretical})$ and $Q(\text{robust})$ values were 1610 and 1386, respectively. A correlation coefficient (r^2) for individual PAH varied from 0.83 for CcdP to 0.99 for BbjF. Unmapped bootstrap factors which did not match with base run factors were not observed. Mass contributions for the 15 PAH congeners ($\sum_{\text{par}} \text{PAH}$) were 20.1, 43.4, 20.6 and 15.9% for the factors 1, 2, 3 and 4, respectively.

Factor 1 was significantly associated with DaiP, followed by Per, BkF, BaP and BaA (see Figure 6.5). A meaningful concentration for Per, DaiP and DahP in coals has been reported (Kashimura et al., 2004, Achten and Hofmann, 2009). This factor signature of PAH congeners was similar to the one for the domestic coal combustion that was extracted from the Northern Ireland sites except for CcdP and Anth (see Figure 6.1). However, this profile showed a different seasonal variation, compared to the general seasonal trend for particulate PAH, in which a higher mass concentration is usually seen in the cold season. This reflected the potential for another type source related to coal combustion activity. Unusual seasonal variations of particulate PAH and a significant mass contribution of DaiP have also been observed in spatial analysis in which a site-pair bringing together an industrial site (Port Talbot) and an urban background (Swansea) were used (see Section 4.2.2). This leads one to assign this factor to the coal combustion source relating to industrial activities.

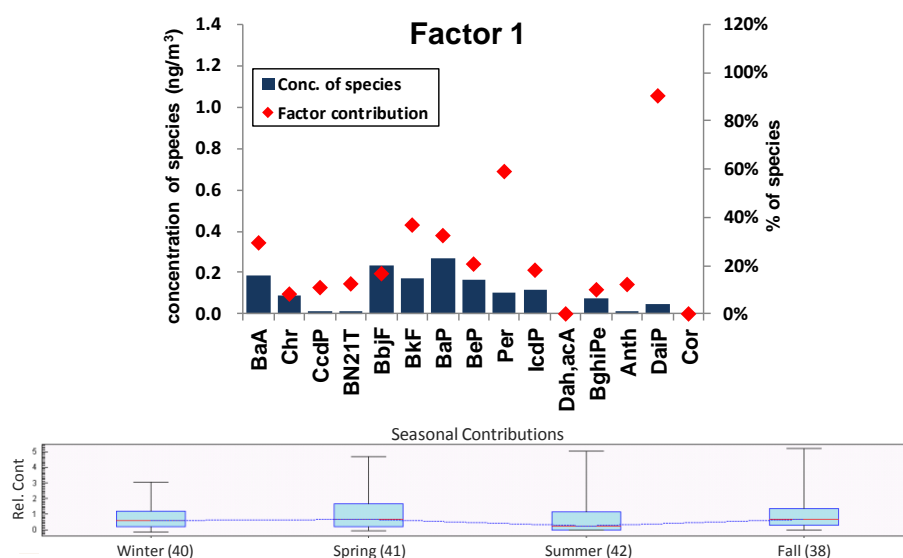


Figure 6.5. PMF factor profile for PM_{10} -bound PAH and source-specific seasonal variation (Industrial urban – Factor 1).

Factor 2 in Figure 6.6 shows that there were significant contributions of BbjF, BkF, IcdP, BghiPe and Cor to this factor. These compounds have commonly been reported as source markers for traffic emissions. A considerable similarity between this signature and the one that was extracted from the Northern Ireland dataset (see Figure 6.2) was observed.

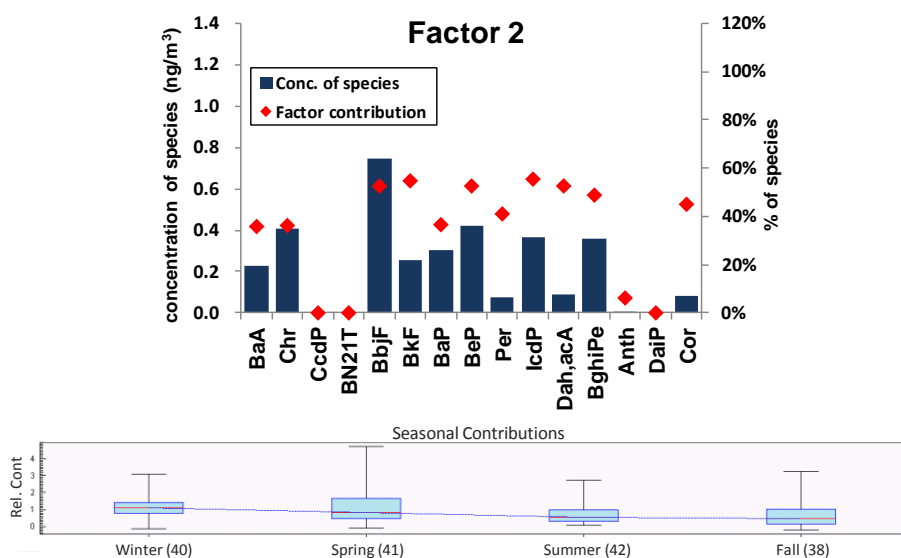


Figure 6.6. PMF factor profile for PM_{10} -bound PAH and source-specific seasonal variation (Industrial urban – Factor 2).

The source signature in Figure 6.7 shows a considerable similarity to the one for domestic coal combustion that was extracted from the Northern Ireland dataset, as described in Section 6.2.1 (see Figure 6.1). This source was distinguished by significant contributions of CcdP and Anth. An obvious seasonal variation showing an increased mass concentration in the winter may explain this factor as coal combustion emissions for domestic heating. As expected, the concentration of individual PAH from domestic sources was much less significant in this industrial dataset, compared to the contribution to the Northern Ireland dataset.

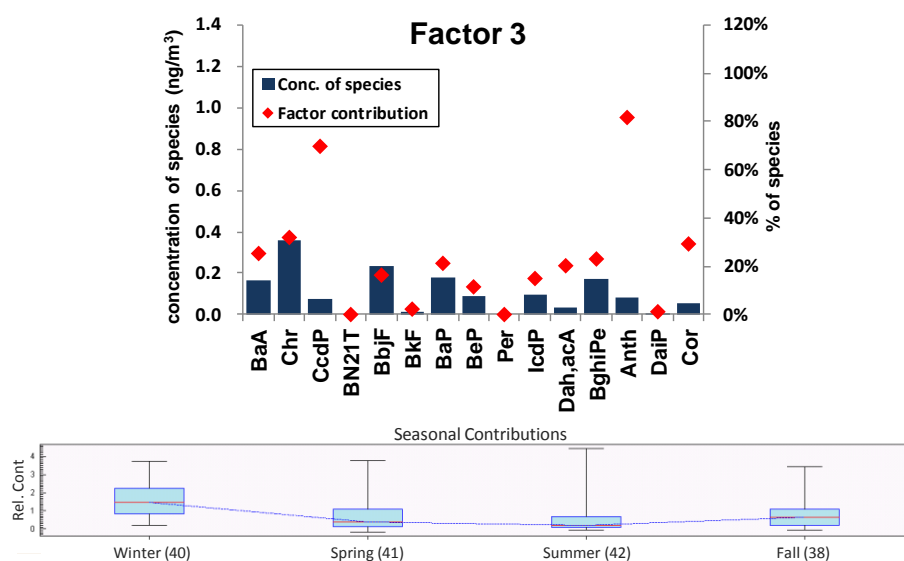


Figure 6.7. PMF factor profile for PM_{10} -bound PAH and source-specific seasonal variation (Industrial urban – Factor 3).

Factor 4 was identified with BN21T, which has been reported as being used as a source marker for emissions from diesel combustion (McCarry et al., 1996). As mentioned in the previous section, the fact that this dataset consisted of measurements taken during the period of post-sulphur reduction and there was a higher mass contribution in the winter leads one to assign this factor to the domestic oil combustion source.

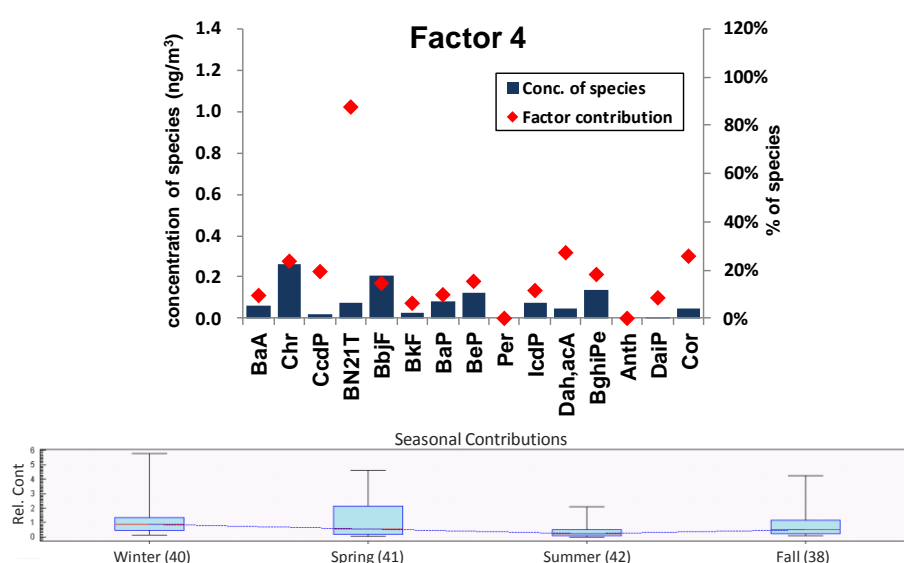


Figure 6.8. PMF factor profile for PM_{10} -bound PAH and source-specific seasonal variation (Industrial urban – Factor 4).

PMF separated four factors for the particle-bounded PAH at the industrial urban sites: domestic oil combustion (DO), traffic emissions (TE), domestic coal combustion (DC) and the metallurgical industry (MI). When the source-specific concentration was calculated separately for the seven industrial urban sites, the largest contribution to $\Sigma_{\text{par}}\text{PAH}$ was caused by coal combustion activity, such as in the metallurgical industry and for domestic heating (see Figure 6.9). Traffic emissions were also significantly responsible for the PAH mass at these sites. With regard to BaP, apparently significant emissions were caused by coal combustion activity by the metallurgical industry.

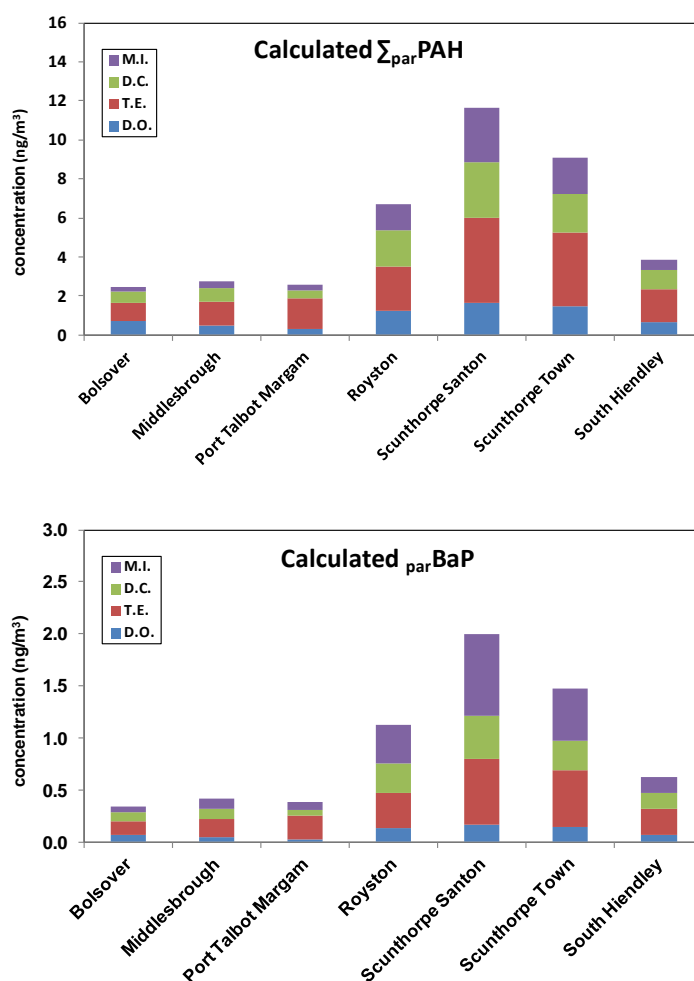


Figure 6.9. Site-specific source contributions (DO: domestic oil combustion; TE: traffic emissions; DC: domestic coal combustion; MI: metallurgical industry).

6.2.3 Urban sites

The two datasets (Northern Ireland sites and industrial urban sites) that included the known information on local sources for PAH emissions provided supporting explanations for the source identification in PMF results. In Section 6.2.1 and Section 6.2.2, the source profile for domestic combustion and that for industrial activity could be distinguished. These results appeared to be helpful in working out source categories for PAH at the urban background sites, where complex sources existed.

The PMF method was applied to the fourteen merged urban sites, which consisted of the twelve urban background sites and the two urban traffic sites. It was assumed that traffic emissions were significant contributors to PAH levels at the urban background sites, thus the fourteen sites had similar source compositions.

The number of factors was changed from three to seven by varying an additional modelling uncertainty (0-25%). A four-factor solution provided the best model fit. An estimated theoretical Q value was 2576; and a Q (robust) value obtained from the PMF tool was 2286. The correlation coefficient (r^2) for each PAH was over 0.8. Unmapped bootstraps were not observed during the bootstrapping analysis. For all variables, the sum of the squares of the differences in scaled residuals for each base run was near zero. Mass contributions for 15 PAH congeners ($\sum_{\text{par}} \text{PAH}$) were 63.0, 11.2, 16.8 and 9.0% for Factors 1, 2, 3 and 4, respectively.

Figure 6.10 shows that Factor 1 was identified with BbjF, BkF, BeP, IcdP, Dah,acA, BghiPe and Cor. These compounds have been widely reported as source markers for traffic emissions. A significantly similar factor signature was also extracted both from the Northern Ireland sites and from the industrial urban dataset.

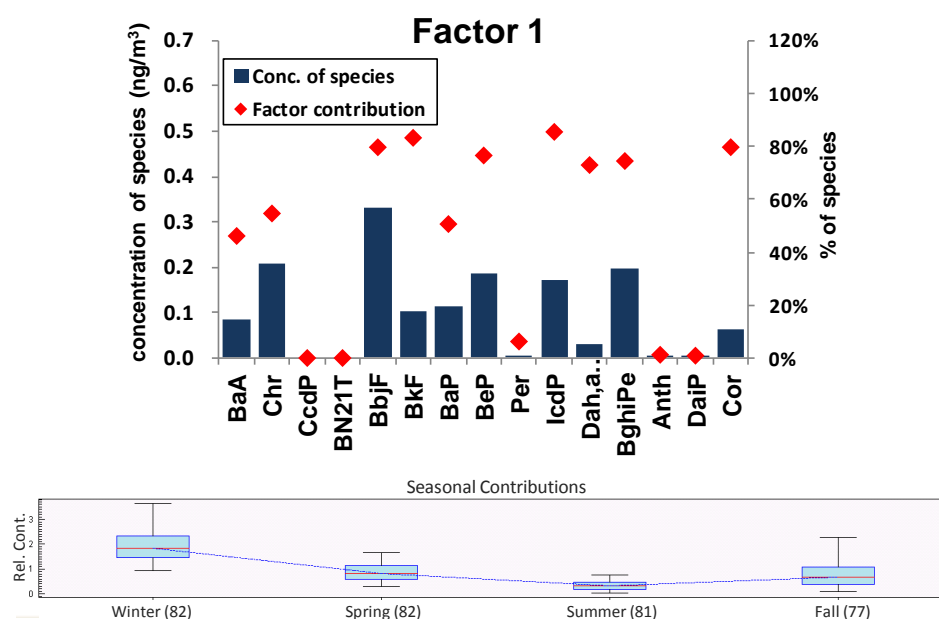


Figure 6.10. PMF factor profile for PM_{10} -bound PAH and source-specific seasonal variation at urban sites (Factor 1).

The signature of PAH congeners in Factor 2 was characterised by a single variable of DaiP, as shown in Figure 6.11. The significance of this compound was also observed both in the spatial analysis (see Section 4.2.2) and in the PMF source apportionment study (see Section 6.2.2.), when PAH measurements were taken at industrial urban sites where high contributions from coal combustion activity could be expected. However, interestingly, this factor showed a different seasonal variation compared to the above two studies. It seems that once PAH have been emitted from industrial sources and transported to the atmosphere in the nearby urban areas, they are more influenced by

urban atmospheric conditions, such as season-dependent mixing heights and meteorological variation. This may lead to this industrial factor having a higher mass concentration in the cold season, which is the commonly reported seasonal trend for particle-associated PAH in urban areas. To conclude, one may assign this source to coal combustion emissions from the metallurgical industry.

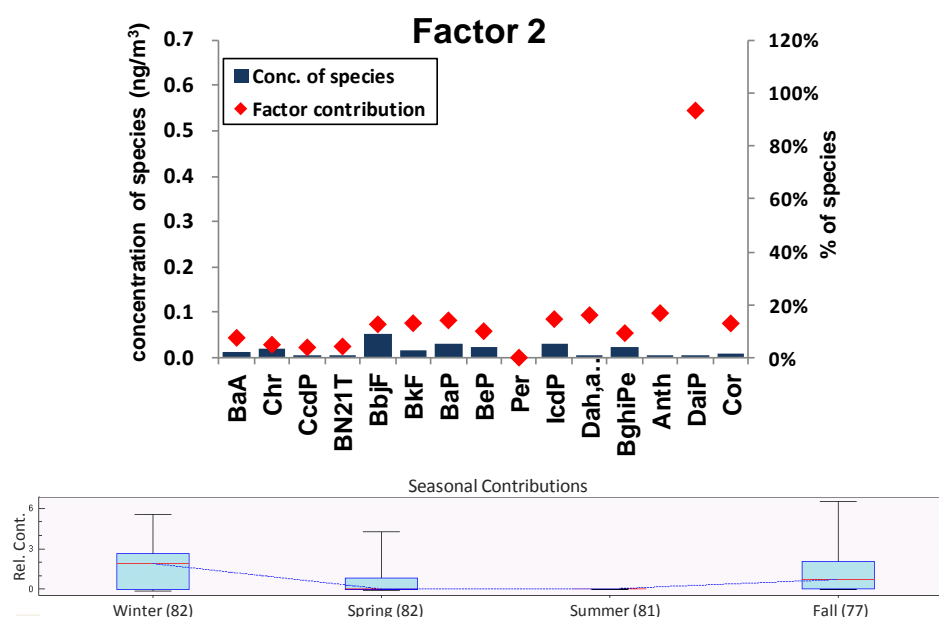


Figure 6.11. PMF factor profile for PM_{10} -bound PAH and source-specific seasonal variation at urban sites (Factor 2).

Figure 6.12 shows that CcdP, Per and Anth are significantly responsible for Factor 3. This signature shows a considerable similarity to the domestic coal combustion source profile that was extracted from the Northern Ireland sites. As expected, much lower mass concentrations for individual PAH were seen for these urban background datasets when these were compared to the Northern Ireland sites, where domestic combustion was the dominant source for PAH. The predominant mass contribution in the winter seems to be related to the influence of the emissions from domestic heating.

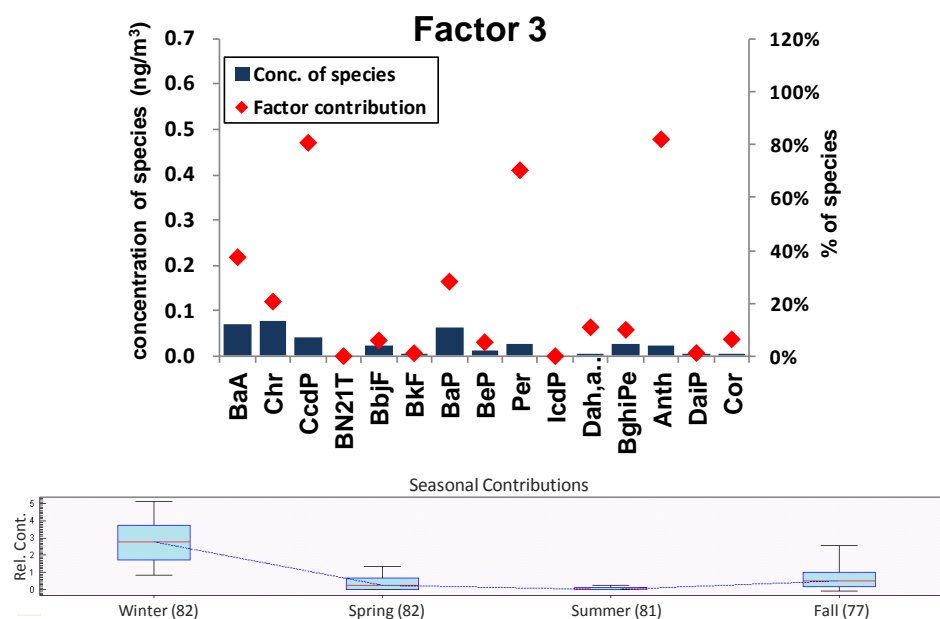


Figure 6.12. PMF factor profile for PM_{10} -bound PAH and source-specific seasonal variation at urban sites (Factor 3).

BN21T was significantly associated with Factor 4 (see Figure 6.13). As mentioned in the previous section (Section 6.2.1), the fact that the measurements for the particulate PAH were conducted during the period following sulphur-reduction legislation (2009-2010) may identify this factor profile with emissions from domestic oil combustion activity, not from the diesel fuel combustion process for vehicles.

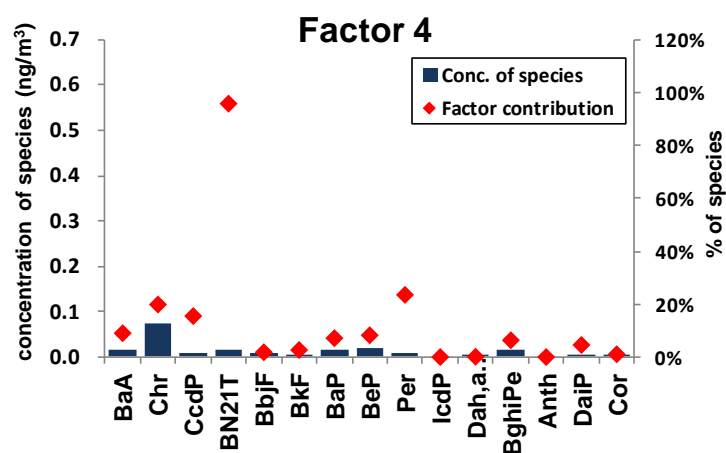


Figure 6.13. PMF factor profile for PM_{10} -bound PAH and source-specific seasonal variation at urban sites (Factor 4).

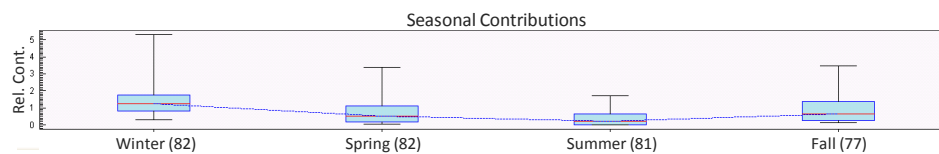


Figure 6.13. (Continued).

In Figures 6.14, source-specific mass contributions to the sum of the particle-associated PAH congeners ($\sum_{\text{par}}\text{PAH}$) and to BaP were calculated at each site for the summer and winter separately.

Traffic emissions (TE) are significantly responsible for $\sum_{\text{par}}\text{PAH}$ at the urban sites all year round. Owing to a reduction in the sulphur content of highway fuels from 2008, a factor profile identified with BN21T was apportioned to the domestic oil combustion source (DO) in this section instead of to the diesel combustion source. However, it appears that this is not an appropriate explanation for the two traffic urban sites at London Crystal Palace and London Marylebone. Small seasonal differences in mass concentration for this factor were observed at these two sites, and this was not consistent with seasonal trends for domestic heating. On the other hand, an obvious seasonality was observed at the other sites. Another seasonal source, coal combustion emissions from domestic heating (DC), showed a distinctive high concentration in the winter. A different type of coal combustion activity, that taking place in the metallurgical industry (MI), also showed a higher concentration in the cold season, although it was reviewed as a non-seasonal source in Section 6.2.2. The elevated PAH concentration at the urban background sites, which was attributed to the transported emissions being emitted from the metallurgical industrial process, was related to the geographical distance from the industrial sites (see Figures 6.14 and 6.15). For example,

the distance from metallurgical sources was around 15, 20, 45 and 55km for Swansea, Leeds Millshaw, Cardiff Lakeside and the Newport St Julians site, respectively.

With regard to BaP, a similar seasonal variation was shown compared to the $\Sigma_{\text{par}}\text{PAH}$. Traffic emissions (TE) are a significant source of BaP from the summer to the winter in urban air. As expected, BaP emissions relating to combustion activities for domestic heating, such as domestic oil combustion (DO) and domestic coal combustion (DC), showed an obvious seasonal variation. Again, the influence of a metallurgical industrial (MI) source on the BaP level near the urban background site was apparent.

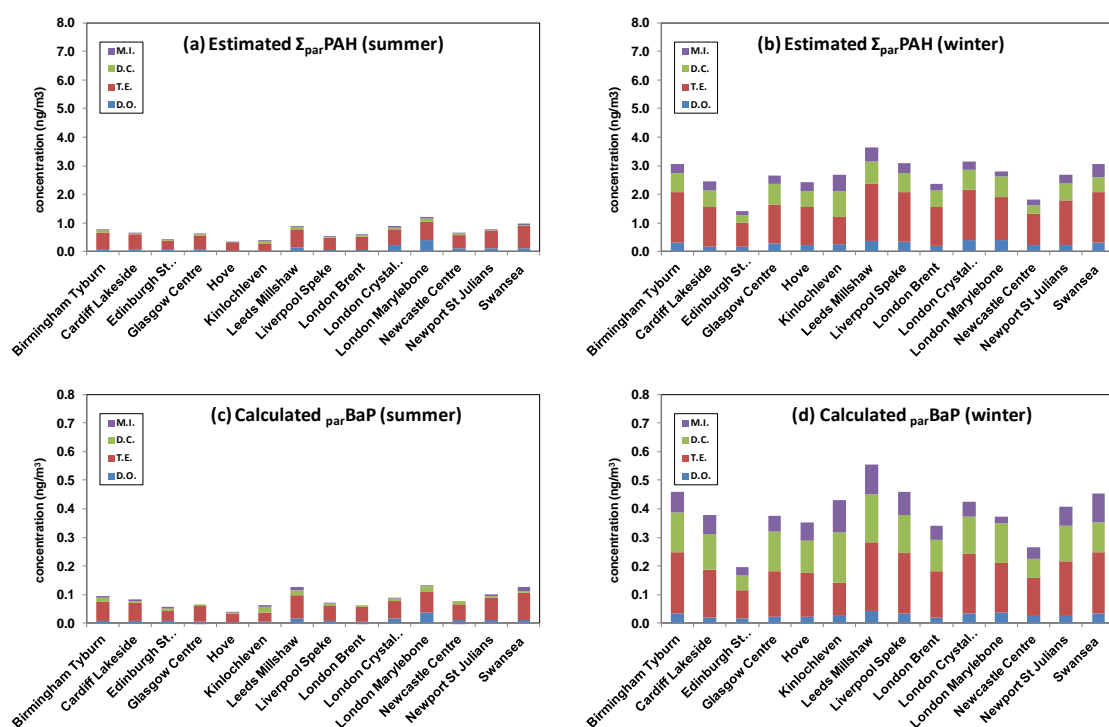


Figure 6.14. Site-specific seasonal source variations for particle-bound PAH, sampled by Digitel sampler (DO: domestic oil combustion; TE: traffic emissions; DC: domestic coal combustion; MI: metallurgical industry).



Figure 6.15. UK PAH monitoring sites (light blue circle: urban background sites; dark blue circle: urban traffic sites; yellow circle: Northern Ireland sites; red circle; industrial urban sites) and the metallurgical industrial sites (black star).

6.3 Source profiles of high molecular weight PAH

6.3.1 Background

PAH is a class of which the individual compounds have varying chemical reactivity. This has caused controversy over an application of a receptor modelling to these compounds in source apportionment. However recent studies have reported that specific PAH factor patterns obtained by PMF analysis are well preserved at the different oxidant levels (Dvorská et al., 2012).

In this section, two data subsets that have distinctively different sampling times are prepared and subjected to PMF separately, to study whether the reactivity of PAH influences source separation in PMF analysis or not. One dataset consists of HMW PAH that were sampled by Andersen sampler (particulate + vapour), with a sampling time of fourteen days, between 2002 and 2006. The other dataset uses daily measurements for particulate PAH that were collected by Digitel sampler from 2009 to 2010. In terms of the phase predominance of PAH, the HMW PAH were predominantly distributed to the particulate phase; thus the big difference between the two data subsets was sampling time, which was related to the exposure time to atmospheric reaction. This analysis may provide a subsidiary explanation in reviewing the degree to which the application of PMF to reactive compounds for a source apportionment is reasonable.

6.3.2 Results

A four-factor solution showed the best model fit when a merged urban dataset that consisted of 13 HMW PAH congeners measured by Andersen sampler, was subjected to PMF. The equation-driven theoretical Q value was 1330, and the robust Q value, taken from the model, was 1032. All the correlation coefficients (r^2) for PAH congeners were over 0.9, except for a 5MChr of 0.85 and a DalP of 0.89. One and two unmapped cases were seen among 100 bootstrappings for Factor 1 and Factor 2, respectively. The mass contributions to the sum of PAH congeners (\sum_{HMWPAH}) for Factors 1, 2, 3 and 4 were 42.3, 26.4, 25.7 and 5.6%, respectively.

In Figure 6.16, source profiles obtained from this analysis are plotted (see Figure 6.16a-d) and compared to those taken from the Digitel particulate PAH dataset mentioned in Section 6.2.3 (see Figure 6.16e-h). The common compounds are coloured black for the bar (concentration, ng/m^3) and red for the diamond (source contribution, %), and different variables are expressed as lighter colours.

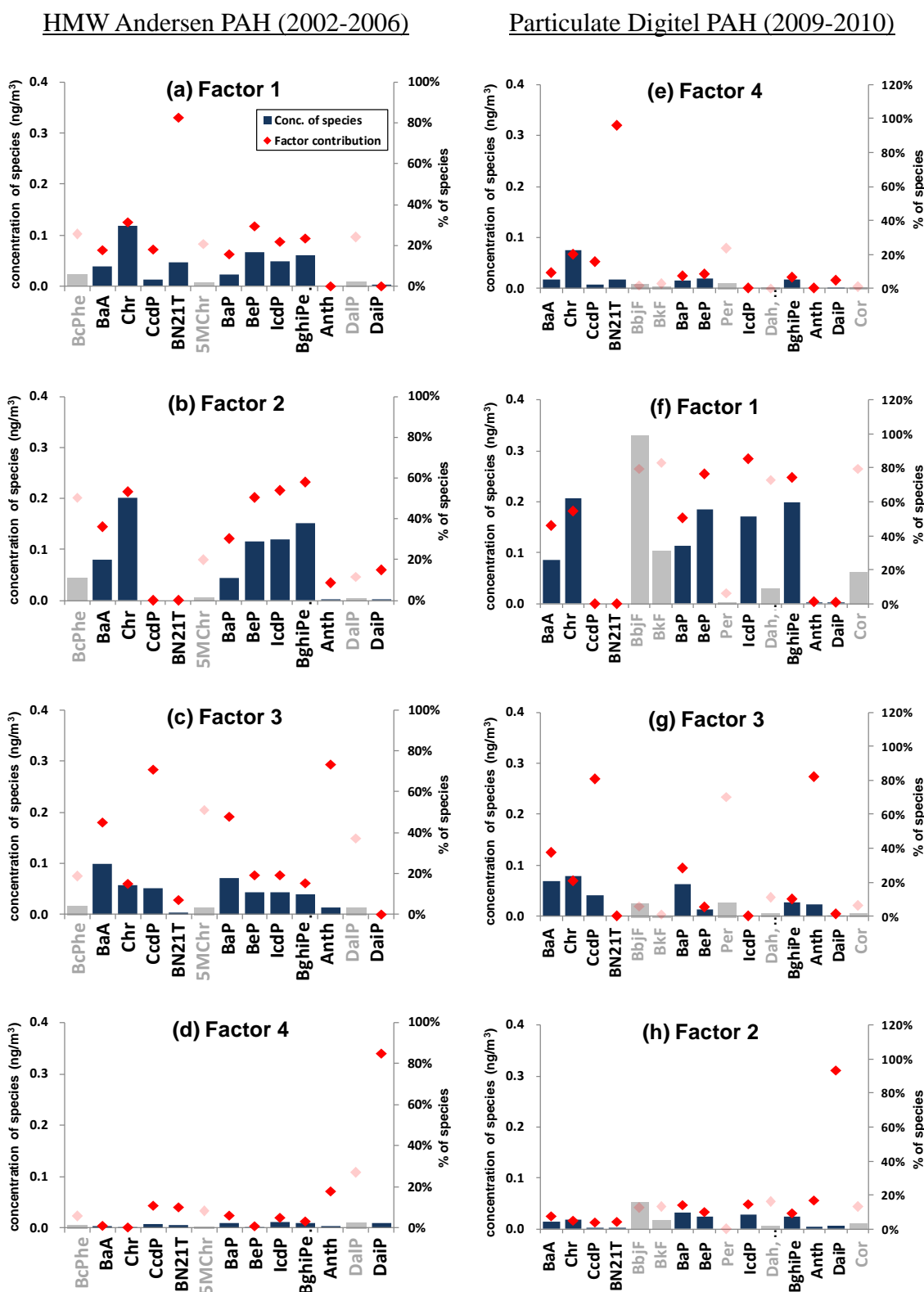


Figure 6.16. Comparison between Andersen high molecular PAH dataset and Digital particulate PAH dataset.

Figure 6.16a indicates that Factor 1 was identified with BN21T. This source signature showed a high similarity to the one obtained from the Digitel dataset (see Figure 6.16e). Although the PAH in the Andersen dataset had a higher potential to undergo reactions, because of the longer sampling time (Brown et al., 2011), this factor showed a larger mass concentration for individual PAH, compared to values in the Digitel dataset. As discussed earlier in Section 6.2.1, this may be explained by two types of activity for oil combustion: oil combustion contribution to the measurements by Andersen sampler with period from 2002 to 2006 is more related to the diesel vehicular exhaust emissions; whereas for the Digitel dataset (2009-2010) it is reasonable to assign oil combustion contribution to domestic oil combustion sources such as kerosene. A 'sulphur free' fuel (< 10ppm) started to be sold on UK highways from 4 December 2007. This may have led to a relatively lowering of PAH emissions from diesel-powered vehicular exhausts.

Factor 2, (Figure 6.16b) obtained from the Andersen dataset for HMW PAH, was characterised by Chr, BeP, IcdP and BghiPe, which have been described as compounds relating to traffic exhaust emissions. A similar source signature was observed in Figure 6.16f, which was extracted from the Digitel particulate PAH dataset. The Digitel dataset provided additional information on the source markers for vehicular emissions of BbjF, BkF and Cor. Slightly increased concentrations of BaP, BeP, IcdP and BghiPe were seen in the Digitel dataset compared to the Andersen dataset. These may be caused either by increased PAH emissions from traffic sources in the period from 2009 to 2010 or by a shorter sampling time with the Digitel sampler. Andersen-Digitel intercomparisons showed that BaP levels measured by Digitel sampler were higher than those measured by Andersen sampler, owing to the shorter degradation time of the Digitel sampler

(Brown et al., 2011).

Both Figure 6.16c and Figure 6.16g were significantly associated with CcdP and Anth. These compounds were related to a domestic coal combustion source (see Section 6.2.1). The mass distributions of individual PAH are very similar between the two figures.

In Figure 6.16d, Factor 4 was identified with dibenzopyrenes such as DaiP and DalP, followed by small Anth. This source signature showed a considerable similarity to the one that was extracted from the Digitel sampler dataset (Figure 6.16h). The significance of DaiP was observed in the source profile for metallurgical industrial emissions discussed in Section 6.2. 2.

Despite doubts over the application of PMF to reactive PAH, this comparison showed that PMF was capable of consistency in extracting meaningful factor profiles for two data subsets, which obviously had different reaction times for PAH, caused by sampling time.

Figure 6.17 shows the source-specific mass contributions to the sum of HMW PAH congeners (\sum_{HMWPAH}) and the BaP at each site for the summer and the winter, separately.

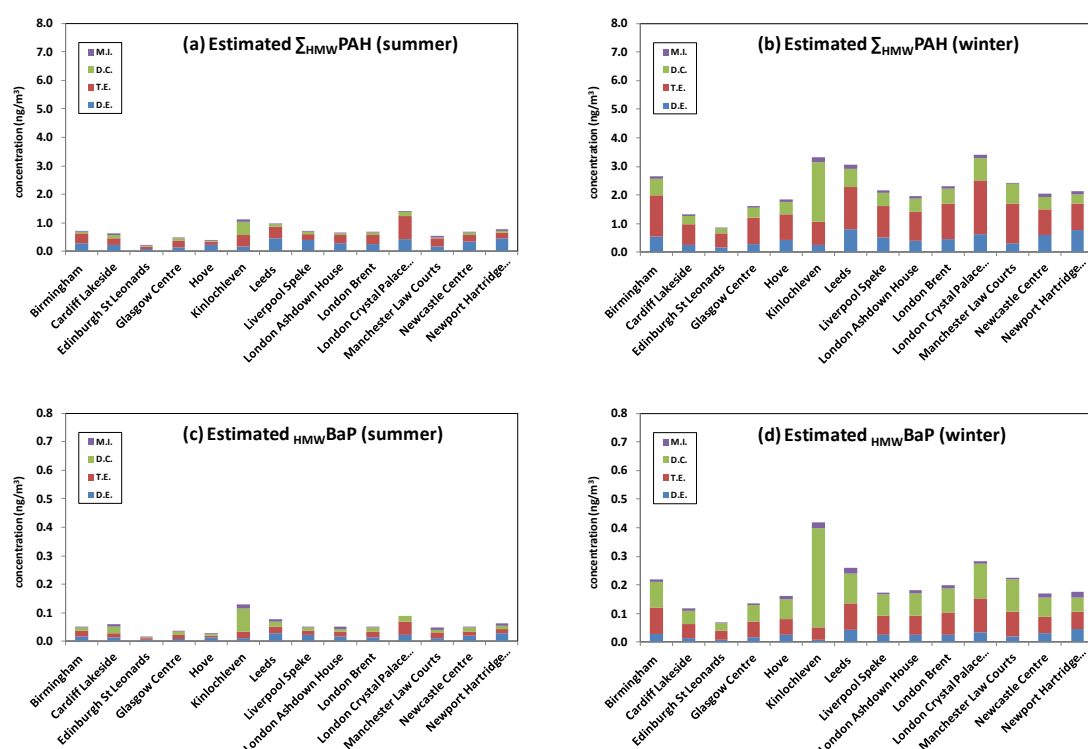


Figure 6.17. Site-specific seasonal source variations based on the PMF results in dataset for HMW compounds, sampled by Andersen sampler (DE: diesel vehicular emissions; TE: traffic emissions; DC: domestic coal combustion; MI: metallurgical industry).

Generally these results were in good agreement with those taken from the Digital dataset discussed in Section 6.2.3 (see Figure 6.14). Traffic related sources such as diesel vehicular emissions (DE) and traffic emissions (TE) contributed significantly to the $\Sigma_{\text{HMW}}\text{PAH}$ and the BaP at the urban sites. The enhancement of the concentration from the traffic sources was apparent in highly populated cities. As expected, the mass contribution from the domestic coal combustion (DC) source showed an obvious seasonality. This was more apparent in the BaP as compared to the $\Sigma_{\text{HMW}}\text{PAH}$. However this was not the case for the site of Kinlochleven. A significant contribution from the domestic coal combustion source was observed during both the summer and the winter at this site in this Andersen dataset (2002-2006), but was not shown in the Digital dataset (2009-2010) (compare Figure 6.14 and Figure 6.17). It seems that local coal

consumption at the Kinlochleven site influenced the PAH levels during both seasons in the period when the Andersen sampler was used, although the aluminium smelter was closed in 2000 (Brown and Brown, 2012).

When PMF analysis was applied to the two data subsets – the Andersen HMW PAH (2002-2006) and the Digitel particle-associated PAH (2009-2010) – which obviously had different sampling times and exposure times for the reactions from PAH, they produced similar results. This shows the ability of PMF to separate sources for the reactive PAH congeners.

6.4 Sensitivity of chemical reactivity

6.4.1 Background

As concluded in Section 6.3, PMF can extract meaningful source profiles when it is applied to reactive compounds. Source separation for the two data subsets, which had different sampling times, was in a good agreement. However, HMW PAH are mostly present in the particulate phase, and they are less reactive compared to the LMW PAH, thus the above comparison between two data subsets, both are consisted of HMW PAH, may have limitations when it comes to reviewing the ability of PMF to extract reasonable sources in the aspect of reactivity issue for PAH.

In this section, LMW PAH, which are more reactive congeners than HMW PAH, were included in the dataset for PMF. An input dataset for uncertainty was synthetically prepared by providing individual PAH with extra uncertainty corresponding to their reactivity with the OH radical, because it was expected that LMW PAH would predominantly be present in the gas phase, and they would have a higher potential for reactive loss than HMW PAH. With regards to three- and four-ring PAH, extra uncertainty was calculated based on their gaseous rate coefficients with the OH radical, obtained from the US EPA's EPI Suite (US EPA, 2012). PAH having over five rings are predominantly distributed in the particulate phase, thus upper limit values from the experimental heterogeneous reaction constants for OH with adsorbed PAH on the solid surface (Keyte et al., 2013) were applied to this calculation (see Table 6.2). Several PAH, having no available information for heterogeneous reaction coefficient were assumed to be $5 \times 10^{-12} \text{ cm}^3 \text{ molecules}^{-1} \text{ s}^{-1}$ in this study. Finally, PMF results for this synthetic input dataset, with its extra uncertainty corresponding to reactivity for individual PAH, were compared with the previous PMF source profiles that applied to a uniform uncertainty of 10% concentration ($U = 0.1C + \text{MDL}/3$).

Table 6.2. A calculated extra uncertainty based on the reactions of PAH with the OH radical.



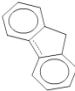
Chemicals	Abbreviation	Structure	MW	Experimental /estimated $k_{\text{OH}} (\times 10^{-12})$ ($\text{cm}^3 \text{ molecules}^{-1} \text{ s}^{-1}$)	Normalized by k_{IcdP}^*	Extra uncertainty (%)
Acenaphthylene	Acy		152	75.5	216	220%
Acenaphthene	Ace		154	66.9	191	190%
Fluorene	Flu		166	8.9	25	30%

Table 6.2. (Continued).

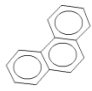
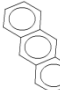
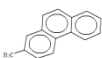
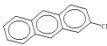
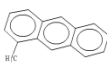

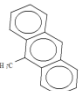

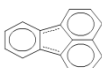

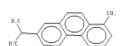

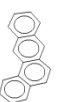
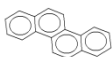
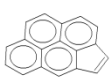
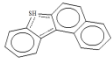
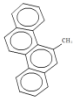




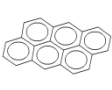



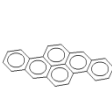
Chemicals	Abbreviation	Structure	MW	Experimental /estimated $k_{OH} (\times 10^{-12})$ ($\text{cm}^3 \text{molecules}^{-1} \text{s}^{-1}$)	Normalized by k_{IcdP}^*	Extra uncertainty (%)
Phenanthrene	Phe		178	13	37	40%
Anthracene	Ant		178	40	114	110%
2-Methyl-phenanthrene	2MPhe		192	34.1	97	100%
2-Methyl-anthracene	2MA		192	104.6	299	300%
1-Methyl-anthracene	1MA		192	104.6	299	300%
1-Methyl-phenanthrene	1MPhe		192	34.1	97	100%
9-Methyl-anthracene	9MA		192	104.6	299	300%
4,5-Methylene-phenanthrene	4,5MPhe		190	40.0	114	110%
Fluoranthene	FluA		202	26.8	77	80%
Pyrene	Pyr		202	50	143	140%
Retene	Ret		234	41.7	119	120%
Benzo[c]-phenanthrene	BcPhe		228	50	143	140%
Benzo[a]-anthracene	BaA		228	126.2	361	360%
Chrysene	Chr		228	50	143	140%
Cyclopenta[c,d]-pyrene	CcdP		226	(5) [†]	14	10%

Table 6.2. (Continued).

Chemicals	Abbreviation	Structure	MW	Experimental /estimated $k_{OH} (\times 10^{-12})$ ($\text{cm}^3 \text{molecules}^{-1} \text{s}^{-1}$)	Normalized by k_{IcdP}^*	Extra uncertainty (%)
Benzo[<i>b</i>]naph- [2,1- <i>d</i>]thiophene	BN21T		234	(5) [†]	14	10%
5-Methyl- chrysene	5MChr		242	(5) [†]	14	10%
Benzo[<i>a</i>]- pyrene	BaP		252	4.1	12	10%
Benzo[<i>e</i>]- pyrene	BeP		252	4.7	13	10%
Indeno[123, <i>cd</i>]- pyrene	IcdP		276	0.35	1	5%
Benzo[<i>ghi</i>]- perylene	BghiPe		276	5.9	17	20%
Anthanthrene	Anth		276	(5) [†]	14	10%
Dibenzo[<i>al</i>]- pyrene	DalP		302	(5) [†]	14	10%
Dibenzo[<i>ae</i>]- pyrene	DaeP		302	(5) [†]	14	10%
Dibenzo[<i>ai</i>]- pyrene	DaiP		302	(5) [†]	14	10%
Dibenzo[<i>ah</i>]- pyrene	DahP		302	(5) [†]	14	10%

[†] Assumed heterogeneous rate coefficient of PAH with OH radical^{*} Upper limit of heterogeneous rate coefficient of IcdP with OH, $k_{IcdP} = 0.35 \times 10^{-12} \text{ cm}^3 \text{ molecules}^{-1} \text{ s}^{-1}$

6.4.2 Results

Numbers of factors from three to seven were explored, and a four-factor solution showed the best model fit. The estimated theoretical Q value was 3774, and the PMF model driven robust Q value was 2610. The correlation coefficients (r^2) for most PAH were over 0.7, except for those of a few compounds – Flu, Phe, Ant, Ret, CcdP and 5MChr –which ranged from 0.57 to 0.65. On average, each factor had one unmapped bootstrap among the 100 bootstrap runs.

Figure 6.18 compares PMF source profiles which were taken from the two different datasets: one assigning a uniform uncertainty of 10% concentration to individual PAH (Uniform U), and the other providing additional uncertainty to PAH corresponding to their reactivity to the OH radical (Weighted U). There was a slight difference in the source-specific mass contributions for individual PAH between the two datasets. However, generally, source signatures that were identified with source markers were consistent between the two datasets. Again, given concerns about the reasonableness of applying PMF to the quite reactive compounds, one can see that source separation of PAH did prove possibility with the PMF method.

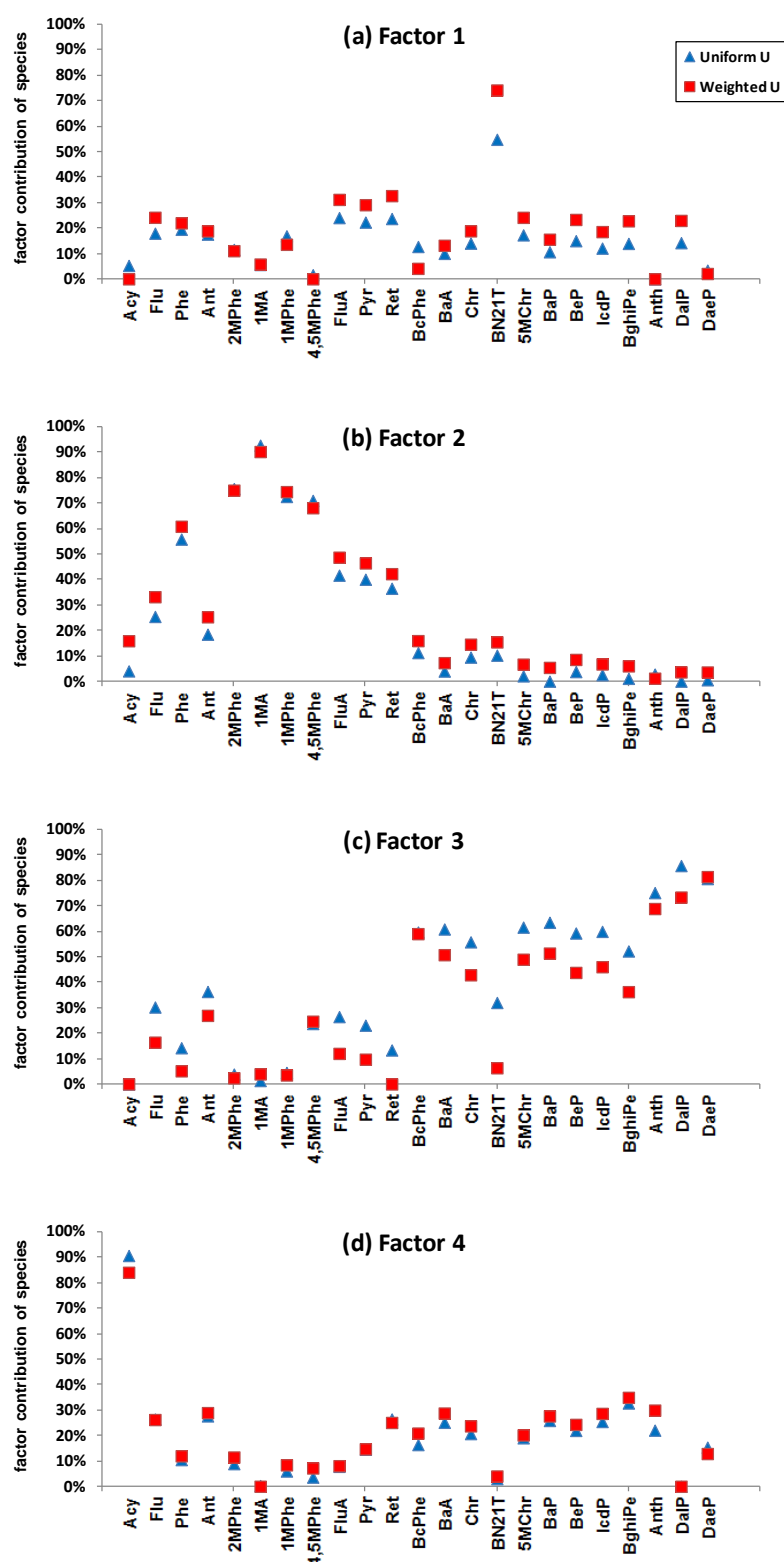


Figure 6.18. PMF sensitivity analysis for uncertainty of variables.

6.5 Summary and discussion

In this chapter, extended studies were conducted to review the ability of PMF to separate sources convincingly in terms of the reactivity of PAH congeners. Two data subsets – one consisting of Northern Ireland sites whose main source for PAH was domestic combustion, and the other consisting of industrial urban sites where metallurgical PAH emissions were significant – were subjected to PMF. The above information for local sources was useful for identifying sources for particulate PAH at the urban background sites in which mixed sources existed. A factor was assigned to domestic coal combustion source for urban dataset owing to the considerable similarity in PMF-derived PAH signature between the Northern Ireland and the urban dataset. However, the factor contribution of coal combustion source might be a combination of space heating sources at the urban background sites, as discussed in Chapter 3. Secondly, PMF results obtained from the Andersen dataset, which had a high potential for reactivity loss, showed themselves to be in good agreement with those taken from the dataset for particle-associated PAH that were sampled by Digitel sampler, having much shorter sampling time. Lastly, the sensitivity study in which extra uncertainty was applied to individual PAH corresponding to their rate coefficients with the OH radical showed that PMF could extract source profiles for the PAH even though there had previously been doubt over the application of the receptor modelling tool to reactive compounds. It appears that the uncertainty arising from reactivity of PAH does not influence the separating of sources in PMF analysis with minor variation of source contributions.

CHAPTER 7: SIMULATION OF PAH REACTIVITY

7.1 Background

The previous chapters recounted how meaningful polycyclic aromatic hydrocarbon (PAH) source profiles, expressed as both concentrations (ng m^{-3}) and relative contributions (%), were obtained by applying PMF to field measurements from combined urban sites, despite concerns over the application of receptor modelling to quite reactive PAH existing both in the vapour phase and the particulate phase in the air. Additionally, an explanation was provided of how PMF was used to quantify source-specific PAH levels at individual sites. However, these source profiles extracted from urban datasets may not be applicable at remote sites, as PAH levels at rural sites are determined by transported air mass and individual PAH with different degrees of reactivity may undergo a change in their source signatures during transport.

UK long-term trends in PAH have shown that urban atmospheric PAH are mostly attributable to local sources, and remote areas are less dependent on source signatures (Meijer et al., 2008). The fact that few studies have applied receptor models to rural datasets may reflect the difficulty of fully understanding the complex chemistry of individual PAH during transport from their source to remote sites, leading to changes in PAH source profiles. The lower molecular weight (LMW) PAH, which are more associated with the gaseous phase, are mainly removed through oxidation by oxidants

such as O₃, NO₃ and OH. On the other hand, the higher molecular weight (HMW) PAH, which are mostly associated with soot-rich particles, are thought to be less accessible to oxidants (Lammel et al., 2009), because they resist oxidation from radicals by adsorbing onto the airborne particles and absorbing into organic matter. Moreover, gases surrounding airborne particles provide a diffusion limitation for radicals to reach the particle-associated PAH. Laboratory studies may have a limitation in simulating real atmospheric reactions perfectly, although many experiments have shown a relatively slow rate of on-particulate oxidation for HMW PAH (Keyte et al., 2013). The low reactivity of HMW PAH can be inferred from the estimated life time, depending on their phase distribution. The calculated half life for BaP vapour is 2.6 hours, having a rate coefficient with OH radicals of 5.0×10^{-11} molecules cm⁻³ s⁻¹ (US EPA, 2012). Lammel et al. (2009) have reported that an unrealistically short lifetime of BaP in the air of 0.17 hours was obtained when a G/P partitioning scenario adopted similar degradability for the gaseous and particulate phase BaP. However, two modelling approaches that excluded radical reactions for particulate BaP led to the estimation of an atmospheric residence time for this compound, ranging from 16 to 48 hours (Lammel et al., 2009). These results suggest that the association of PAH with airborne particles and low reactivity can lead them to have a longer lifetime and potential for long-range transport. Ravindra et al. (2008a) reported that HMW PAH are removed by wet/dry deposition. However, it has been suggested that a predominant association of HMW PAH with a fraction of the size 0.4 to 1.1 µm allows particle-bound PAH to be transported over long distances with a less significant deposition flux (Baek et al., 1991). To conclude, complex atmospheric chemistry accompanied by continuous changes in the phase distribution between gaseous and particulate PAH (G/P partitioning) during transport

from source to remote regions, adds to the difficulty of interpreting source-specific contributions at rural sites.

Diagnostic ratios (DR) have been widely applied to gain qualitative information about sources using two PAH congeners with similar physicochemical characteristics (Rogge et al., 1993, Khalili et al., 1995, Ravindra et al., 2008a, Yang et al., 2010, Brown and Brown, 2012). The application of DR can enable a comparison of source types at urban sites and at remote sites (Ravindra et al., 2008b, Callen et al., 2011). However, the variability of sources, and the complex physicochemical reactivity accompanying a G/P phase re-equilibrium in the atmosphere, has been widely considered as a limitation of using DR in source identification. The change of ratios between PAH congeners was simulated as a function of distance from source to receptor in a recent study (Katsoyiannis and Breivik, 2014), and this showed the possibility of change in PAH ratios depending on the distance from source, and suggested that the application of congener ratios in discerning sources should be undertaken with caution.

In this study, the ratios between two PAH congeners were simulated from a source to a remote site, not for source identification, but to better understand their chemical reactivity, because paired compounds are diluted to a similar extent during transport, and detailed meteorological conditions need not be considered. Radical oxidation and G/P partitioning were included in this simulation, which was based on several assumptions and on information obtained from real measurements in a source region and at a remote site.

7.2 Methodology

7.2.1 Sampling and air mass trajectory analysis

Four daily concentrations of total (gaseous and particulate) PAH were measured at the Bristol Road Observatory Site (BROS; 1.93°W, 52.45°N) in Birmingham during summer campaign, between 3rd August 2009 and 25th August 2009. Daily measurement of total PAH was conducted at the urban background Elms Road Observatory site (EROS; 1.93°W, 52.46°N), located in an open green field within in the University of Birmingham, from 7th January 2010 to 26th January 2010. Information on the sampling site (Alam et al., 2013) and sampler description (Delgado-Saborit et al., 2013) are available elsewhere.

Sampling campaigns at a remote site (Weybourne; 1.14°E, 52.94°N), located on the North Norfolk coast, measured daily PAH congener concentrations both in winter (February 2010) and in summer (August 2010) (Alam et al., 2014). There are no significant local PAH sources at the remote site, thus the atmospheric PAH level at Weybourne may be determined by transported air masses. Consequently, backward trajectory analysis was conducted at 10, 100 and 500 m air mass heights, using the National Oceanographic and Atmospheric Administration's (NOAA's) Hybrid Single Particle Lagrangian Integrated Trajectory model (HYSPLIT4) at the Weybourne site to identify a source region based on the hourly meteorological data obtained from the Global Data Assimilation System (GDAS1) Archive in the Air Resources Laboratory

(ARL). Additionally, cluster analysis for the backward trajectories was implemented using HYSPLIT4 to obtain the dominant daily trajectories transported to the Weybourne site, corresponding to the 24 hours sampling period for PAH.

7.2.2 OH estimation

It has been widely reported that OH radical oxidation is a predominant loss mechanism for gaseous PAH, although other oxidants such as NO₃ and O₃ are involved in the oxidation of PAH (Keyte et al., 2013). During the daytime, PAH are predominantly oxidized by the OH radical; but NO₃ can become a significant oxidant during nighttime owing to the depletion of OH levels. The atmospheric level of OH has been estimated as 2×10^6 molecules cm⁻³ (Robinson et al., 2007) and 1×10^6 , for daytime and a 24-hour average in summer, respectively, with OH reaction being very slow at night (Atkinson and Arey, 1994, Keyte et al., 2013). Many laboratory studies have shown that the heterogeneous reactions of particle-bound PAH with NO₃ and O₃ may be of some importance (Esteve et al., 2004, Perraudin et al., 2005, Esteve et al., 2006, Perraudin et al., 2007, Liu et al., 2012a). However in practice, the degree of heterogeneous reaction of particulate PAH with oxidants can be relatively less significant than one of gaseous reaction due to the limited access of oxidants to the particle-associated PAH (Lammel et al., 2009). It has been reported by Atkinson and Arey (1994) that the estimated rate (s⁻¹) of OH radical reaction with gas-phase PAH is higher than that of NO₃ or O₃ by several orders of magnitude, calculated using a 12-hour daytime average OH concentration of 1.6×10^6 molecules cm⁻³, a 12-hour nighttime average NO₃ oxidant concentration of $5 \times$

10^8 molecules cm^{-3} (approximately 20 ppt_v), and a 24-hour average O_3 concentration of 7×10^{11} molecules cm^{-3} (30 ppb_v).

In this study, there was no concurrent field measurement of OH concentrations with PAH. So an indirect methodology (see Equation 7.1) was applied to estimate the OH level using measurements of PAH predominantly present as vapour, both at a source and at a remote site (Blake et al., 1993). The use of a ratio between two compounds is advantageous as it can normalize the plume dilution effect.

$$\ln([\text{PAH}_i]_t/[\text{PAH}_j]_t) = \ln([\text{PAH}_i]_0/[\text{PAH}_j]_0) + [\text{OH}](k'_{(g)\text{OH}} - k_{(g)\text{OH}})t \quad \text{Equation 7.1.}$$

where $[\text{PAH}_i]_t$ and $[\text{PAH}_j]_t$ are the final concentrations of PAH congeners i and j after reaction time (t), $[\text{PAH}_i]_0$ and $[\text{PAH}_j]_0$ are the initial concentrations of PAH congeners, $[\text{OH}]$ is an expected hydroxyl concentration, and $k_{(g)\text{OH}}$ and $k'_{(g)\text{OH}}$ are the OH reaction rate coefficients for PAH_i and PAH_j , respectively.

In order to estimate the OH concentration, several assumptions were made.

- Oxidation by OH radicals was the predominant gaseous PAH loss mechanism during transport.
- Source ratios ($[\text{PAH}_i]_0/[\text{PAH}_j]_0$) and ageing ratios ($[\text{PAH}_i]_t/[\text{PAH}_j]_t$) were taken from measurements at urban sites (EROS for winter and BROS for summer) and at a remote site (Weybourne), respectively. There was a high degree of similarity in the composition of the PAH sources at the urban background site and at the roadside site, as reported by Jang et al. (2013).

- Experimentally determined rate coefficients were available for the vapour phase reactions of four LMW PAH (phenanthrene, anthracene, fluoranthene and pyrene) from the USEPA EPI Suite and literatures. However two congeners (Phe and Pyr) were used in Equation 7.1, as measurements of anthracene were very variable, and the reported values of the k_{OH} for fluoranthene varied widely ($11\text{-}50\text{ cm}^3\text{ molecules}^{-1}\text{ s}^{-1}$).
- Weybourne measurements were used selectively, based on cluster analysis results for backward trajectories, to identify air masses transported from the UK mainland.
- Reaction time was calculated based on cluster analyzed back trajectories.

7.2.3 Particle fractions

7.2.3.1 Theoretical particle fractions

PAH are semi-volatile compounds (SVCs), mostly produced thorough incomplete combustion processes. They can exist in both a gaseous and a particulate phase. Atmospheric temperatures, the physical properties of aerosol particles, and complex chemical reactivity may influence their G/P phase distributions.

It has been reported that G/P partitioning determines the atmospheric fate of PAH. Several models have been developed to understand the phase distribution of PAH in the air. The Junge-Pankow (J-P) model is based on the concept that G/P partitioning of

SVCs is governed by adsorption onto particles, as controlled by subcooled liquid vapour pressure (P_L^0) (Pankow, 1987).

$$\varphi = \frac{c\theta}{P_L^0 + c\theta} \quad \text{Equation 7.2.}$$

where φ is the sorbed fraction on the aerosol particles of the total concentration (dimensionless), c is a constant of the compound (usually assumed to be 17.2 Pa cm for PAH (Wang et al., 2013)), θ is the aerosol surface area per unit volume of air ($\text{cm}^2 \text{cm}^{-3}$), assumed to be higher in urban (1.1×10^{-5}) and lower in rural air ($4.2 - 35 \times 10^{-7}$) (Harner and Bidleman, 1998b).

Harner and Bidleman (1998) suggest that G/P partitioning is determined by an absorption expressed as the octanol-air partition coefficient (K_{OA}), which can be used instead of vapour pressure (Harner and Bidleman, 1998a).

$$K_p = f_{OM} \frac{MW_{OCT} \gamma_{OCT}}{MW_{OM} \gamma_{OM} \rho_{OCT} 10^{12}} K_{OA} \quad \text{Equation 7.3.}$$

where K_p is the partition coefficient ($\text{m}^3 \mu\text{g}^{-1}$), f_{OM} is the fraction of organic matter in the particles, MW is the molecular weight, γ is the activity coefficient, and ρ is the density of octanol (0.82 kg L^{-1} at 20°C).

The above equation can be simplified under the assumption that $MW_{OCT} / MW_{OM} = 1$, $\gamma_{OCT} / \gamma_{OM} = 1$,

$$\log K_p = \log K_{OA} + \log f_{OM} - 11.91 \quad \text{Equation 7.4.}$$

The strong association of PAH with soot particles in soot-water systems reflects the fact that the adsorption mechanism can be a significant factor for G/P partitioning of atmospheric PAH (Odabasi et al., 2006). The concurrent production of PAH and soot creates the necessity for including an adsorptive term in PAH phase partitioning, even though an initial predominance of adsorption onto the surface of particles can shift to an absorption into the organic material when an available surface is insufficient for the increased concentration or when secondary aerosols are dominant (Dachs and Eisenreich, 2000, Lohmann and Lammel, 2004). The prolonged atmospheric lifetime of particle-bound PAH has been explained by the low accessibility of oxidants to particle-bound PAH (Lammel et al., 2009). These results reflect the fact that the estimated particulate fractions, calculated from the Junge-Pankow and Harner-Bildeman models, may have been underestimated (Friedman et al., 2014). To conclude, it seems that two types of sorption are involved in a G/P partitioning. A nonlinear equation considering both absorption and adsorption can be expressed as,

$$K_p = 10^{-12} \left(f_{OM} \frac{MW_{oct} \gamma_{oct}}{MW_{OM} \gamma_{OM} \rho_{oct}} K_{OA} + f_{BC} \frac{\sigma_{atm-BC}}{\sigma_{soot} \rho_{BC}} K_{soot-air} \right) \quad \text{Equation 7.5.}$$

where ρ_{BC} is the density of BC, $K_{soot-air}$ is the partitioning coefficient between diesel soot and air, and σ_{atm-BC} and σ_{soot} are the available surface areas of the atmospheric BC and diesel soot, respectively.

A particle fraction (P(%)), the percentage of the particulate fraction to the total PAH) can be calculated based on the simplified equations of Dachs and Eisenreich (2000) and Galarneau et al.(2013), which work on the assumption that there is a linear correlation between total suspended particle concentration and aerosol surface area (Sitaras et al.,

2004).

$$K_p = 10^{-12} \left(\frac{1.5f_{oc}}{\rho_{oct}} K_{OA} + f_{EC} K_{SA} \right) = \frac{(\sum C_p / C_{TSP})}{C_g} \quad \text{Equation 7.6.}$$

where $1.5f_{oc}$ is the organic carbon fraction of the particulate matter ($OM = 1.5OC$, dimensionless), ρ_{oct} is the bulk density of octanol (0.82 kg L^{-1}), K_{OA} is the octanol-air partition coefficient (dimensionless), f_{EC} is the elemental carbon fraction of the particulate matter, K_{SA} is the soot-air partition coefficient (L kg^{-1}), C_p is the particulate PAH concentration (ng m^{-3}), C_{TSP} is the total particulate matter concentration ($\mu\text{g m}^{-3}$), and C_g is the gas-phase concentration (ng m^{-3}).

In this study, Equation 7.6 was applied to calculate the theoretical particle fractions of individual PAH.

7.2.3.2 Measured particle fractions

Particle fractions ($P(\%)$) were calculated using the real measurements of total (gaseous and particulate) PAH. Atmospheric reactions occur in both the vapour and the particulate phases, which may change the G/P phase distribution of individual PAH during transport. Thus, $P(\%)$ was separately calculated for an urban source site (EROS for winter and BROS for summer) and a receptor site (Weybourne) segregated by back trajectory analysis. Finally, these results were compared with those obtained theoretically in the previous section.

7.2.4 Simulation description

There are difficulties in predicting the transported concentrations of semi-volatile organic compounds (SVOCs) at a remote site using source measurements. This is because SVOCs undergo physicochemical reactions during transport, including continuous G/P partitioning; and variable meteorological conditions between source and remote sites add complexity. However, the use of the ratio between two compounds is useful in a simulation study, as various factors between two sites affect the concentration of both compounds equally. To conclude, ratio simulations may provide a conceptual approach to PAH chemistry, including to the physicochemical atmospheric fate of PAH.

For the simulation of the ratio between PAH congeners, several assumptions were made.

- A ratio change from a point near a source ($[PAH_i]_0/[PAH_j]_0$) to a remote site ($[PAH_i]_t/[PAH_j]_t$) was simulated.
- Two pairs of ratio were utilised. One was the ratio of Phe to Pyr, two compounds for which measured k_{OH} values for gas phase reaction were available. These two compounds were used to estimate an OH concentration explained in the previous section. The other ratio was that of Phe to BaP. The only information available for the k_{OH} of BaP was an estimated value for the vapour.
- Measurements in Birmingham (both at BROS and at EROS site) and those at Weybourne (remote site) of PAH transported from the UK mainland were

representative of source ($t = 0$) and receptor ($t = t$) concentrations, respectively.

- Transport time (t) was derived from air mass backward trajectory analysis.
- Additional sources of PAH between the two sites were small.
- Only gaseous PAH were subject to OH oxidation during transport, and they were degraded in a pseudo-first-order chemical reaction ($C_t = C_0 e^{-kt}$).
- Heterogeneous reactions were not considered on the assumption that particle-bound PAH reactions were slow, due to the limited access for gaseous oxidants.
- Estimated OH concentration and experimental rate coefficients (k_{OH}) were applied.
- Instantaneous equilibrium partitioning between gaseous PAH and particulate PAH occurred during the oxidation of gas-phase PAH by OH oxidant.
- G/P partitioning of PAH adjusted during atmospheric transport.
- Measured phase distributions from Birmingham and Weybourne were linearly interpolated with time for the ratio simulations.

7.3 Results

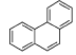
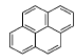
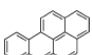
7.3.1 Data selection

With regards to source-receptor pairs for winter, measurements of 14 parent PAH congeners at the EROS and Weybourne sites (Alam et al., 2013, Alam et al., 2014) were reviewed. There was limited information about the physicochemical properties of individual PAH congeners, and only four PAH congeners (phenanthrene, anthracene, fluoranthene and pyrene) had experimentally determined gaseous rate coefficients ($k_{(g)OH}$). However, two LMW PAH (anthracene and fluoranthene) were not included in this study, because concentration levels of anthracene were very variable and it was reported that the measured values of the $k_{(g)OH}$ of fluoranthene ranged from 11 to $50 \times 10^{12} \text{ cm}^3 \text{ molecules}^{-1} \text{ s}^{-1}$. Even though no measurements for gaseous rate coefficients of benzo[*a*]pyrene (BaP), which is predominantly present in the particulate phase, were available, and the atmospheric reactions of particle-associated forms of BaP were not clearly understood, this compound was included in this study owing to its toxicity and its broad use for the regulation of PAH mixtures. In a similar way, the source-receptor pair for summer was reviewed using measurements at the BROS and Weybourne sites (Alam et al., 2013, Delgado-Saborit et al., 2013).

To conclude, the reactivity study selected two LMW PAH (phenanthrene and pyrene) that were predominantly distributed to the vapour phase, with apparently different gaseous rate coefficients, and one HMW PAH (BaP). The physicochemical properties

of the three compounds, such as their structures, octanol-air partition coefficients (K_{OA}), soot-air partition coefficients (K_{SA}), and the OH radical rate coefficients of gaseous PAH ($k_{(g)OH}$), are reviewed in Table 7.1.

Table 7.1. *Physicochemical properties of gaseous PAH congeners.*

	Structure	$\log K_{OA}^a$	$\log K_{SA}^a$	$k_{(g)OH}^b$ ($10^{-12} \text{ cm}^3 \text{ molec}^{-1} \text{ s}^{-1}$)
Phenanthrene (Phe)		7.6	9.4	31
Pyrene (Pyr)		8.7	10.6	50
Benzo[<i>a</i>]pyrene (BaP)		11.1	13.0	(50)

^a Lohmann and Lammel (2004), ^b Keyte et al. (2013)

The average concentrations of the three congeners, the two compound ratios (Phe/Pyr and Phe/BaP), and the standard deviation (SD) between the ratios both at the source (EROS and BROS) and at the receptor (Weybourne) site can be seen in Tables 7.2 and 7.3. With regard to the Weybourne site, the above values were calculated separately depending on the results of cluster analysis, because air masses with three distinct source regions influenced this site during the sampling campaign (Alam et al., 2014).

Table 7.2. Concentrations and ratios at a source site (EROS) and three aged air masses (at Weybourne) during winter campaign.

	Mean concentrations (ng m ⁻³)			Mean ratios \pm S.D.			
	Total (vapour)			between total concentrations		between vapour concentrations	
	Phe	Pyr	BaP	Phe/Pyr	Phe/BaP	Phe/Pyr	Phe/BaP
EROS							
n=16	20.633 (20.152)	10.120 (9.855)	0.144 (0.025)	2.4 \pm 1.3	184.8 \pm 126.7	2.4 \pm 1.3	1484.6 \pm 1566.7
Weybourne (segregated as a function of backward trajectory analysis)							
from UK mainland, London							
n = 6	1.528 (0.992)	0.228 (0.124)	0.047 (0.006)	7.0 \pm 1.6	35.1 \pm 13.9	8.8 \pm 1.4	222.7 \pm 171.5
from EU mainland							
n = 5	1.398 (1.071)	0.198 (0.117)	0.033 (0.004)	7.2 \pm 1.6	53.4 \pm 29.8	11.1 \pm 5.4	303.2 \pm 186.8
from North Sea							
n = 2	0.502 (0.349)	0.109 (0.061)	0.015 (0.002)	4.2 \pm 4.2	29.8 \pm 28.9	5.2 \pm 5.0	223.0 \pm 253.8

Table 7.3. Concentrations and ratios at a source site (BROS) and three aged air masses (at Weybourne) during summer campaign.

	Mean concentrations (ng m ⁻³)			Mean ratios \pm S.D.			
	Total (vapour)			between total concentrations		between vapour concentrations	
	Phe	Pyr	BaP	Phe/Pyr	Phe/BaP	Phe/Pyr	Phe/BaP
BROS							
n=4	12.718 (11.972)	4.375 (4.025)	0.115 (0.000)	5.2 \pm 2.8	155.4 \pm 101.5	6.1 \pm 3.6	-
Weybourne (segregated as a function of backward trajectory analysis)							
from South England							
n = 8	1.045 (0.795)	0.145 (0.091)	0.025 (0.000)	7.2 \pm 0.7	41.4 \pm 4.9	8.8 \pm 1.0	-
from UK midland, Ireland and Atlantic Ocean							
n = 7	0.875 (0.673)	0.128 (0.080)	0.023 (0.000)	6.8 \pm 0.5	38.1 \pm 4.1	8.4 \pm 0.6	-
from North Sea							
n = 9	0.580 (0.479)	0.110 (0.072)	0.016 (0.000)	5.3 \pm 1.1	37.0 \pm 10.3	6.7 \pm 1.3	-

As expected, the concentration of LMW PAH (Phe and Pyr) was predominantly present in the vapour phase and BaP was largely associated with the particulate phase (Tables 7.2 and 7.3). Interestingly, it seemed that the phase re-distribution of PAH occurred during transport. Higher particle fractions were apparent in the transported air masses at Weybourne than in the air near the source. There has been little study of changes in the partitioning of PAH from source to remote areas, using field measurements, even though many authors agree that G/P partitioning determines the fate of PAH during long range transport (Lohmann and Lammel, 2004, Galarneau et al., 2013, Wang et al., 2013). However, field work on particle fractions of polychlorinated dibenzo-*p*-dioxins and furans (PCDD/Fs) as a function of transport distance (Chao et al., 2004), and the influence of phase on the reactivity of semi-volatile compounds (SVCs) (Donahue et al., 2013) provides a conceptual framework for the design of a simulation study of the atmospheric reactivity of PAH.

When the mean ratios between PAH congeners that had different OH rate coefficients were considered, one pair consisting of LMW PAH (Phe/Pyr) clearly increased from near the source to the remote site, which might have been explained by a relatively higher $k_{(g)OH}$ of Pyr than of Phe during transport. According to this simple approach, the ratio of gaseous Phe to BaP should also have increased with reaction time, as the estimated value of the $k_{(g)OH}$ of BaP is larger than that of Phe (see Table 7.1). However, in practice the ratio decreased with transport (see Table 7.2). This discrepancy might have been explained by a different phase distribution of Phe and BaP during transport, and the difference in mass transfer limitations of oxidants between the two phases (Donahue et al., 2013).

For the simulation of PAH transport during winter, samples were carefully selected to minimize the influence of the non-concurrent sampling periods at EROS (January, 2010) and Weybourne (February, 2010). Only weekday air samples were included in the simulation to reduce difference in source contribution between weekdays and weekends (Alghamdi et al., 2015). Mean concentrations and mean ratios ($n = 11$) at EROS were used as the source values. Measurements at Weybourne as a function of the clustered backward trajectory were used as the concentration for aged airmass. From six samples transported from the UK mainland, three (5th, 19th and 25th Feb 2010) that had a similar range of ratios (Phe/Pyr and Phe/BaP) and similar dominant trajectories were selected (see Figure 7.1 and Table 7.4). Similar procedures were applied to the simulation of PAH transport for summer. Mean concentrations and mean ratios ($n = 4$) at BROS were used as the source values. Five samples (6th, 10th, 19th, 20th and 23rd Aug 2010) that travelled from Southern England and arrived at the Weybourne site during weekdays, were selected for aged airmasses (see Table 7.5).

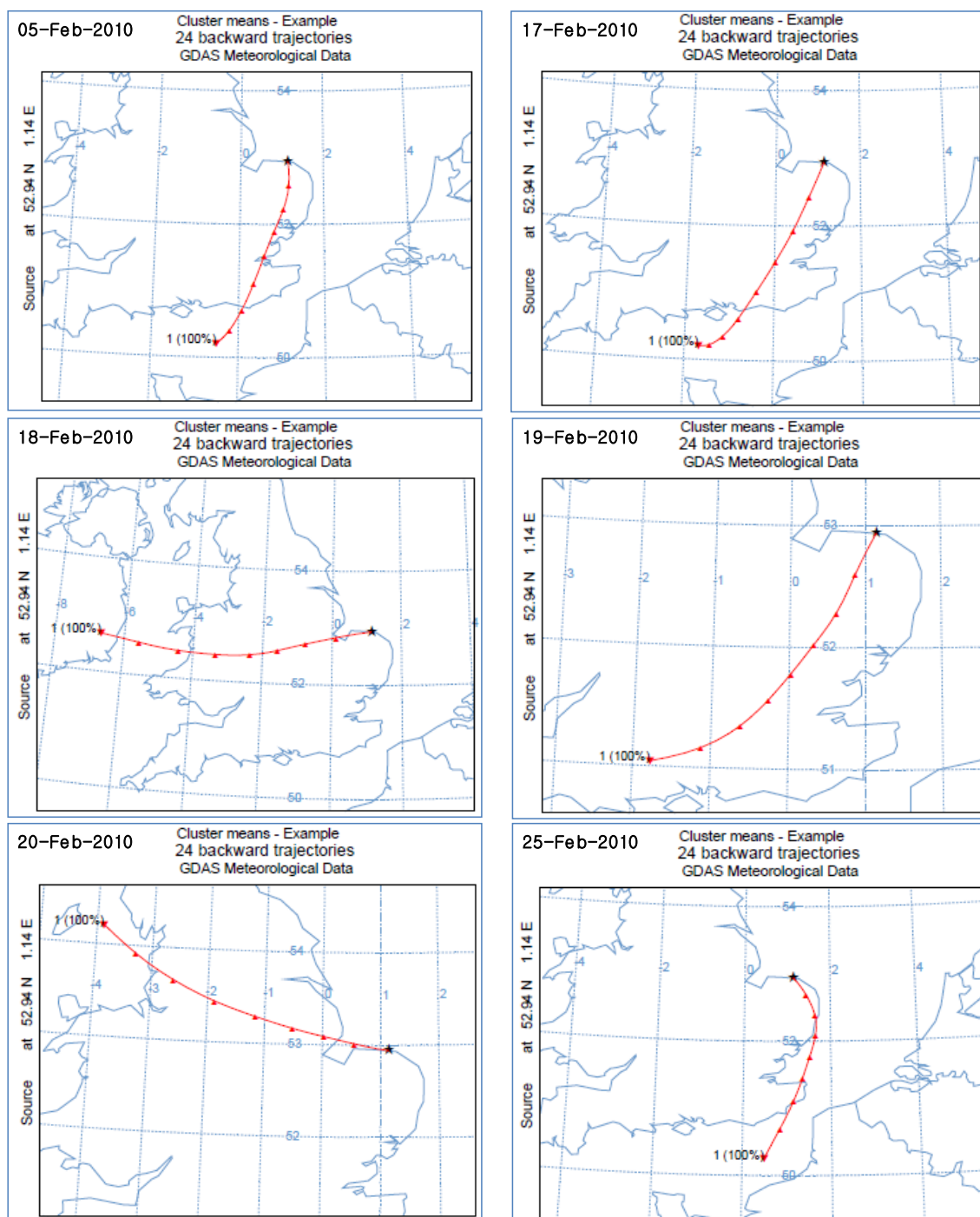


Figure 7.1. Backward trajectory of clustered air mass, at Weybourne transported from UK mainland during winter campaign (each point; three hours).

Table 7.4. Selected samples for a simulation of PAH transport for winter.

	Concentrations			Ratios		Meteorological data	
	Total (gaseous)			Between total (between gaseous)		Temp.	Wind speed
	Phe (ng m ⁻³)	Pyr (ng m ⁻³)	BaP (ng m ⁻³)	Phe/Pyr (-)	Phe/BaP (-)		
Source (at EROS)							
Jan, 2010 (n =11)	24.782 (24.322)	10.244 (9.993)	0.144 (0.025)	2.4 (2.4)	163.9 (1484.6)	1.2	1.2
Transported from South England (at Weybourne)							
05-Feb, 2010	1.818 (1.450)	0.270 (0.183)	0.049 (0.008)	6.7 (7.9)	37.2 (192.4)	4.9	2.7
17-Feb, 2010	0.940 (0.295)	0.187 (0.031)	0.079 (0.007)	5.0 (9.6)	11.9(44.0)	1.3	2.5
18-Feb, 2010	0.989 (0.466)	0.101 (0.048)	0.030 (0.008)	9.8 (9.8)	33.0(59.7)	2.2	5.6
19-Feb, 2010	2.509 (1.638)	0.388 (0.228)	0.057 (0.004)	6.5 (7.2)	44.2 (407.7)	1.2	5.4
20-Feb, 2010	1.093 (0.669)	0.140 (0.063)	0.035 (0.001)	7.8 (10.6)	31.4 (450.1)	0.8	3.6
25-Feb, 2010	1.817 (1.434)	0.284 (0.190)	0.034 (0.008)	6.4 (7.5)	53.1 (182.1)	7.1	4.7
Mean of selected	2.048 (1.507)	0.314 (0.200)	0.047 (0.006)	6.5 (7.6)	44.8 (260.7)	2.9	4.3

Table 7.5. Selected samples for a simulation of PAH transport for summer.

	Concentrations			Ratios		Meteorological data
	Total (gaseous)			Between total (between gaseous)		Temp. (°C)
	Phe (ng m ⁻³)	Pyr (ng m ⁻³)	BaP (ng m ⁻³)	Phe/Pyr (-)	Phe/BaP (-)	
Source (at BROS)						
Aug, 2009 (n =4)	12.718 (11.972)	4.375 (4.025)	0.115 (0.000)	5.2 (6.1)	155.4 (-)	16.9
Transported from UK mainland (at Weybourne)						
06-Aug, 2010	0.934 (0.710)	0.137 (0.087)	0.024 (0.000)	6.8 (8.1)	38.2 (-)	16.0
07-Aug, 2010	1.065 (0.809)	0.155 (0.098)	0.025 (0.000)	6.9 (8.3)	43.2(-)	18.5
10-Aug, 2010	1.027 (0.781)	0.141 (0.089)	0.023 (0.000)	7.3 (8.8)	43.7(-)	19.3
19-Aug, 2010	1.013 (0.780)	0.130 (0.081)	0.026 (0.000)	7.8 (9.7)	39.1 (-)	16.5
20-Aug, 2010	1.114 (0.869)	0.155 (0.096)	0.027 (0.000)	7.2 (9.0)	40.6 (-)	20.5
21-Aug, 2010	0.964 (0.723)	0.160 (0.099)	0.027 (0.000)	6.0 (7.3)	36.3 (-)	23.0
22-Aug, 2010	1.070 (0.8130)	0.146 (0.091)	0.028 (0.000)	7.3 (9.0)	38.4 (-)	17.5
23-Aug, 2010	1.171 (0.878)	0.137 (0.085)	0.023 (0.000)	8.6 (10.4)	51.8 (-)	17.5
Mean of selected	1.052 (0.803)	0.140 (0.088)	0.025 (0.000)	7.5 (9.2)	42.7 (-)	18.0

7.3.2 OH estimation

The mean ratio between the vapour phase measurements of the two PAH congeners at the Birmingham sites (EROS and BROS) was used in Equation 7.1 as a source ratio ($t = 0$), instead of the value at the London site, because of the high level of similarity in source composition at the urban sites (Birmingham and London) (Jang et al., 2013). Three selected ratios and five at the Weybourne site present in air masses transported from the UK mainland, were used as a transported air ratio ($t = t$) for winter and summer respectively. A transport time of 12 to 15 hours was estimated, based on the function of 24-hour clustered backward trajectories (Figure 7.1), in which each point accounted for three hours.

Estimated OH levels, derived from Equation 7.1 using a transport time of 15 hours (54000s), can be seen in Tables 7.6 and 7.7. They varied ($1.15 - 1.25 \times 10^6$ molecules cm^{-3}) when the gaseous ratio of Phe to Pyr for winter was applied to the transported air plume equation. With regards to summer data, estimated OH concentrations ranged 1.16 to 1.29×10^6 molecules cm^{-3} . The estimations were comparable to the winter range at the highest (solar noon) OH of $(0.5 - 4) \times 10^6$ molecules cm^{-3} and the summer range at solar noon of $(2 - 9) \times 10^6$ molecules cm^{-3} , measured in Birmingham (Emmerson et al., 2005). Calculated values were also near to the estimated global concentrations, as the winter OH concentration was reported to be lower than the typical daily summer concentration of 1.0×10^6 molecules cm^{-3} (Keyte et al., 2013).

Table 7.6. Estimated concentrations of hydroxyl radicals (OH) for winter (2.9 °C).

	Estimated OH (molecules cm ⁻³)
Case 1 (5 th Feb 2010)	
$\ln \left[\frac{1.450}{0.183} \right] = \ln [2.400] + [\text{OH}] ((4.65 - 2.88) \text{ E-11}) * (54000)$	1.25E+06
Case 2 (19 th Feb 2010)	
$\ln \left[\frac{1.638}{0.228} \right] = \ln [2.400] + [\text{OH}] ((4.65 - 2.88) \text{ E-11}) * (54000)$	1.15E+06
Case 3 (25 th Feb 2010)	
$\ln \left[\frac{1.434}{0.190} \right] = \ln [2.400] + [\text{OH}] ((4.65 - 2.88) \text{ E-11}) * (54000)$	1.20E+06
Mean : 1.20E+06	

Table 7.7. Estimated concentrations of hydroxyl radicals (OH) for summer (18.0 °C).

	Estimated OH (molecules cm ⁻³)
Case 1 (6 th Aug 2010)	
$\ln \left[\frac{0.710}{0.087} \right] = \ln [6.084] + [\text{OH}] ((4.88 - 3.03) \text{ E-11}) * (54000)$	1.16E+06
Case 2 (10 th Aug 2010)	
$\ln \left[\frac{0.781}{0.089} \right] = \ln [6.084] + [\text{OH}] ((4.88 - 3.03) \text{ E-11}) * (54000)$	1.20E+06
Case 3 (19 th Aug 2010)	
$\ln \left[\frac{0.780}{0.081} \right] = \ln [6.084] + [\text{OH}] ((4.88 - 3.03) \text{ E-11}) * (54000)$	1.25E+06
Case 4 (20 th Aug 2010)	
$\ln \left[\frac{0.869}{0.096} \right] = \ln [6.084] + [\text{OH}] ((4.88 - 3.03) \text{ E-11}) * (54000)$	1.22E+06
Case 5 (23 th Aug 2010)	
$\ln \left[\frac{0.878}{0.085} \right] = \ln [6.084] + [\text{OH}] ((4.88 - 3.03) \text{ E-11}) * (54000)$	1.29E+06
Mean : 1.22E+06	

7.3.3 Phase distribution of PAH between gaseous and particulate phases

7.3.3.1 Theoretical particle fractions

As mentioned in Section 7.2.3.1, both sorption processes (ab/adsorption) have an influence on the G/P partitioning for PAH. If the two values ($1.5f_{OC}/p_{oct}$ and f_{EC}) are ranged similarly in the simplified partitioning equation (Equation 7.6), the adsorption term has a greater impact on the theoretical P(%), as the soot-air partition coefficient (K_{SA}) is larger than the octanol-air partition coefficient (K_{OA}) by a factor of two (Dachs and Eisenreich, 2000). However, in practice there are many variables that influence the phase distribution of PAH in the atmosphere. The values of K_{SA} can vary by over an order of magnitude, depending on the types of adsorptive substrate (Jonker and Koelmans, 2002). The G/P partitioning can be predominantly driven by an absorption mechanism when the organic matter fraction (f_{OM}), expressed as $1.5 \times f_{OC}$ in Equation 7.6, becomes much more significant than the elemental carbon fraction (f_{EC}), for example, in secondary or vegetation-derived aerosols (Dachs and Eisenreich, 2000). High seasonality of the ratio of f_{OM} to f_{OC} (hereafter referred to as OM/OC) in fine particulate matter was observed at the rural sites, having a greater OM/OC value in the warm season owing to the greater formation of secondary organic aerosols; but this was not the case at the urban background sites (Bae et al., 2006). Results obtained from other studies show the variability of OM/OC depending on the sampling areas (Table 7.8). The difference in the ratio of f_{OC} to f_{EC} (hereafter referred to as OC/EC) depending

on the aerosol particle size was also reported both at the urban background site and at the rural site (Table 7.9).

Table 7.8. Variation of OM/OC ratios depending on sources and seasons.

OM/OC	Sources and seasons
1.2 ^a	Diesel engines
1.3 ^a	Catalyzed gasoline engines
1.3 ^b	Roadside
1.4^b	Urban background
1.6^c	Rural, cold season
2.2 ^c	Rural, warm season

^a Russell (2003), ^b Harrison et al. (2003), ^c Bae et al. (2006)

Table 7.9. Different ratio of OC/EC depending on airborne particle size fraction and location (Laongsri, 2012).

OC/EC	Urban background (Birmingham, UK)	Rural background (Harwell, UK)
PM₁₀	1.2	2.2
PM _{2.5}	0.75	1.8

In this study, a simplified G/P partitioning equation including both sorption mechanisms (ab/adsorption) for the association of PAH to particulate matter (see Equation 7.6) was applied to the source site (EROS) and the remote site (Weybourne) respectively for the cold season data. The particle fraction (P(%)) of individual PAH was then calculated. Because of the lack of concurrent measurements for carbon fractions (f_{OC} and f_{EC}), the reported information for f_{EC} in PM₁₀, 0.05 and 0.02 respectively for the urban background and rural sites (Harrison et al., 2004, Lohmann and Lammel, 2004) was used. The values for f_{OC} and f_{OM} were calculated using the detailed information highlighted in Tables 7.8 and 7.9. The estimated carbon fractions in PM₁₀ for winter

both at the urban background site (EROS) and at the rural background site (Weybourne) can be seen in Table 7.10.

Table 7.10. Carbon fractions in PM_{10} used in this study both at the EROS site and at the Weybourne site.

	Urban background (EROS)	Rural background (Weybourne)
f_{EC}^a	0.050	0.020
f_{OC}^b	0.060	0.044
OM/OC	1.4 ^c	1.6 ^d

^a Harrison et al. (2004), Lohmann and Lammel (2004), ^b Produced the estimation for this study using reported ratios for OC/EC in Table 7.9, ^c Harrison et al. (2003), ^d Bae et al. (2006).

The properties of PAH are sensitive to atmospheric temperature. Thus, the sorption coefficients in Equation 7.6 (both K_{OA} and K_{SA}) needed to be adjusted to the temperature of each air mass to estimate the theoretical particle fractions reasonably. With regard to the absorption term, the K_{OA} can be calculated based on Equation 7.7 using the temperature-dependent regression parameters listed in Table 7.11 (Harner and Bidleman, 1998a, Odabasi et al., 2006).

$$\log K_{OA} = A + B/T$$

Equation 7.7.

where K_{OA} is the octanol-air partition coefficient (dimensionless), A and B are temperature-dependent parameters, and T is the temperature (K).

Table 7.11. Regression parameters for Equation 7.7 and calculated K_{OA} .

	A	B	K_{OA} (Calculated)	
			EROS (274.2K)	Weybourne (275.9K)
Phe ^a	-5.62	3942	5.71E+08	4.65E+08
Pyr ^a	-5.94	4417	1.47E+10	1.17E+10
BaP ^b	-6.50	5382	1.34E+13	1.02E+13

^a Harner and Bidleman (1998a), ^b Odabasi et al. (2006)

The K_{SA} was estimated as a function of temperature based on Equations 7.8 and 7.9 (Dachs et al., 2004) using an extrapolated equation for Henry's law constants obtained from the experimentally derived regressions (Bamford et al., 1999) (see Table 7.12). The equation for Chr was alternatively used in calculating H' for BaP, owing to their similar vapour pressures (Bojes and Pope, 2007). In this study, the values for K_{SW} obtained from diesel soot were used (Lohmann and Lammel, 2004).

$$\log K_{SA} = \log (K_{SW}/H') \quad \text{Equation 7.8.}$$

where K_{SA} is the estimated partition constant between soot and air ($L\ kg^{-1}$), K_{SW} is the measured soot-water partition constant ($L\ kg^{-1}$), and H' is the Henry's law constant (dimensionless).

$$H' = H/RT \quad \text{Equation 7.9.}$$

where H is the Henry's law constant with dimension, $Pa\ m^3\ mol^{-1}$, R is the ideal gas constant ($8.314\ Pa\ m^3\ mol^{-1}\ K^{-1}$).

Table 7.12. Regression equations for Henry's law constant and calculated K_{SA}

	Equation for H' ^a	K_{SA} (Calculated)	
		EROS (274.2K)	Weybourne (275.9K)
Phe	$H' = 3E-12 * e^{0.0676T}$	1.18E+10	1.05E+10
Pyr	$H' = 8E-12 * e^{0.0613T}$	1.25E+11	1.13E+11
BaP	$H' = 2E-23 * e^{0.1473T}$	3.61E+13	2.81E+13

^a Bamford et al. (1999)

Total particle matter concentration (C_{TSP}) was not measured during the campaigns, but was estimated using UK PM_{10} monitoring measurements both at the London Kensington site (urban background) and at the Harwell site (rural) during February 2010, by applying the winter ratio of C_{TSP} to PM_{10} (Gomišček et al., 2004). Finally, the estimated C_{TSP} and the theoretically calculated particle fractions (P(%)) were produced using estimated parameters as a function of temperature (Tables 7.10, 7.11 and 7.12), and these are shown in Table 7.13.

Table 7.13. Estimated C_{TSP} and theoretical particle fractions for PAH (P(%)) at an urban site (EROS, 274.2K) and at a rural site (Webbourne, 275.9K).

	PM_{10} ^a ($\mu g m^{-3}$)	C_{TSP} ^b ($\mu g m^{-3}$)	Particle coefficient (K_p) ($m^3 \mu g^{-1}$)			Particle fraction ($C_p / (C_p + C_g)$) P(%)		
			Phe	Pyr	BaP	Phe	Pyr	BaP
urban	20.8	27.9	$6.48 * 10^{-4}$	$7.76 * 10^{-3}$	$3.18 * 10^0$	1.77	17.77	98.88
rural	16.9	18.1	$2.50 * 10^{-4}$	$3.26 * 10^{-3}$	$1.44 * 10^0$	0.45	5.58	96.30

^a Measurements on February, 2010, ^b Estimated concentration

Theoretical P(%) showed that LMW PAH (Phe and Pyr) were mostly attributed to the gaseous phase, and HMW PAH (BaP) were more associated with the particle phase, which is consistent with atmospheric measurements from other studies. At a remote site, a decreased particle fraction as compared to that near the source site was estimated

In the real atmosphere, there are no significant local PAH sources at the rural site, and atmospheric PAH concentrations were determined by the air masses transported from source regions. It appeared that complex physicochemical reactivity might be involved in the changes to the P(%) of PAH during transport from a near source to a remote site. The next section reports how measured particle fractions at both an urban and a rural site, were reviewed so that they could be compared with the above theoretical results.

7.3.3.2 Field measurements of particle fractions

Particle fractions (P(%)) at an urban background site (EROS) and a remote site (Weybourne) for the cold season were calculated separately. The PAH levels at the remote site are assumed to be determined by a flux transported from sources and by various atmospheric chemical reactions during transport. Thus the P(%) at Weybourne was calculated as a function of the daily cluster of backward trajectories that segregated air masses into different source regions, with mean temperature (see Figure 7.2).

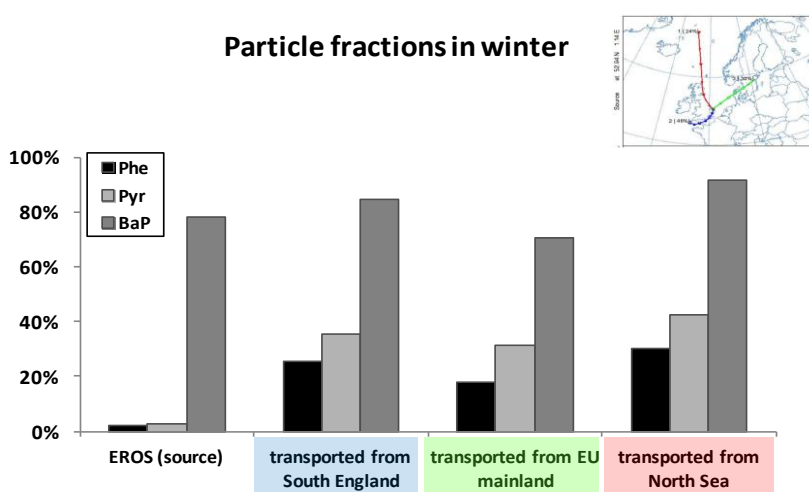


Figure 7.2. Measured particle fractions (P(%)) at EROS (1.2 °C) and at Weybourne transported from the UK mainland (2.9 °C), EU mainland (2.6 °C) and North Sea (2.0 °C).

If EROS and Weybourne are considered as a source site and a receptor air mass site, respectively, it seems that the P(%) of LMW PAH (Phe and Pyr) is increased significantly during transport (Figure 7.2), although there were no field measurements of the source for either the EU and or the North Sea. The higher increment of P(%) at the Weybourne site was apparently seen for Pyr which had a larger rate coefficient ($k_{(g)OH}$) than Phe, in the order: transported from EU < transported from UK mainland < transported from the North Sea. The values of the P(%) for Phe showed the same order.

The change of P(%) for the HMW PAH (BaP) from source to remote site was relatively small, although the gaseous rate coefficient ($k_{(g)OH}$) of BaP is similar to that of Pyr. This may be explained by a dominant attribution to the particle phase for BaP, which allows only a small amount of BaP vapour to be involved in oxidation reactions and leads to little change in the P(%). Interestingly, the long-range transported air mass from the North Sea showed the highest P(%) for all three PAH congeners. An enhanced particle fraction of PCDD/Fs congeners as a function of distance from source during atmospheric transport has also been reported by Chao et al. (2004).

7.3.3.3 Comparison of phase distribution for three PAH congeners between theoretical estimation and empirical measurement

The trend in the above empirically-based particle fractions was not consistent with the theoretically estimated values. In the thermodynamic calculations, a lower P(%) was predicted for the rural site compared to the value at the urban site in Section 7.3.3.1 (see

Table 7.13), where the trend does not agreed with that in measured values (Section 7.3.3.2). The experimental study by Galarneau et al. (2006) showed that there was a good agreement between the experimental and the estimated particle coefficients ($\log K_p$) for FluA at the urban site. On the other hand, the value of $\log K_p$ for FluA was underestimated at the rural site by one order of magnitude. This may be due to various assumptions applied in the theoretical estimation and reflects the complex atmospheric chemistry of PAH during transport. It has been suggested that the difference in partitioning mechanisms between an urban and a remote site may be due to different particle properties and a coating effect on aged particles which prevents G/P equilibrium (Lohmann and Lammel, 2004). An increase in the non-exchangeable fractions of PAH from urban to rural sites may account for the higher P(%) of aged aerosols at a rural site (Terzi and Samara, 2004). In practice, the composition of airborne particles in urban and rural areas is variable, which can influence the dominant G/P partitioning mechanism. The carbon fractions can vary depending on the aging of airborne particles (Aiken et al., 2008). A diesel soot was assumed for the adsorption of PAH in the G/P partitioning calculation in this study. However, the study by Jonker and Koelmans (2002) showed that the adsorptive parameter of the sorbent-water distribution coefficient (K_{SW}) can vary depending on soot types. Moreover, it would be more appropriate to normalize by particle surface than by total suspended particle mass (C_{TSP}) for Equation 7.6 when organic matter including PAH is predominantly adsorbed. On the other hand, it is better to replace C_{TSP} by organic mass when PAH are absorbed into particle-phase organic matter predominantly (Turpin et al., 2000). A secondary organic aerosol (SOA) can interfere with the evaporation of PAH trapped in the SOA, especially in remote areas, causing a higher measured P(%) value of PAH than the one theoretically expected

(Friedman et al., 2014). Additionally, the viscosity of a SOA can influence the G/P phase partitioning of trapped PAH (Zelenyuk et al., 2012). Theoretical partitioning equations are based on bulk particles. However, the fact that the BeP in the rural samples was more associated with the coarser particle fraction than that in the urban samples (Allen et al., 1996), and the size distribution shows variation for individual particle-associated PAH (Yu and Yu, 2012), reflects the significance of airborne particle size in G/P partitioning of PAH. In this study, the mean temperature was used to estimate both the OH concentration and the theoretical values for P(%) at each site, with the assumption of advected emissions from source region to remote site. However, PAH could experience a lower temperature during long-range transport when the vertical mixing processes within a boundary layer are included (Tao et al., 2007). In a sensitivity study, when a decreased temperature from 2.9 °C to 0 °C was applied to Equation 7.6, a slightly higher P(%) was predicted at the Weybourne site, 0.56% for Phe, 7.06% for Pyr and 97.62% for BaP. However, these values were still lower than those predicted at the EROS site.

To conclude, one may suggest that the P(%) of PAH is changed during transport, which may be explained either by a degradation rate for PAH vapours that is relatively faster than the re-equilibration rate between the two phases (G/P re-partitioning) or by a shielding effect in which radicals are unable to access to the inner particle-associated PAH because of the less reactive surface layer surrounding airborne particles.

This enhancement of the particle fraction with reaction time may influence the global long-range transport of semi-volatile compounds to remote areas where there are no

local emission sources, such as in the Arctic and Antarctic. In the following section, the reactivity of PAH is simulated based on the empirical P(%) reported in this section and the estimated OH concentrations from Section 7.3.2.

7.3.4 Simulations

From the work discussed in the previous sections, it is clear that phase distributions can change during atmospheric transport. In the work reported on in this section, the change of concentrations with transport time was simulated based on results derived from empirical measurements taken in Sections 7.3.1, 7.3.2 and 7.3.3.2 and several assumptions (see below).

- The dominant removal mechanism of gaseous PAH is OH radical oxidation.
- Only PAH vapour is involved in oxidation with a pseudo-first order chemical reaction.

$$C_t = C_0 * e^{-k_{(g)OH}[OH]*t} \quad \text{Equation 7.8.}$$

where C_t is the final [PAH] over a reaction time of t , C_0 is an initial [PAH], $k_{(g)OH}$ is the rate coefficient of gaseous PAH with OH, [OH] is the atmospheric concentration, and t is the reaction time.

- Estimated OH concentrations are 1.20×10^6 molecules cm^{-3} and 1.22×10^6 molecules cm^{-3} for winter and summer, respectively (see Tables 7.6 and 7.7).
- The particle fraction (P(%)) of PAH is changed linearly during transport from source to remote site, and it is interpolated based on real measurements which

are mean values obtained from the selected samples at the Birmingham site and at the Weybourne site in Tables 7.4 and 7.5. With regards to P(%) for winter, values change for Phe (1.8% to 25.3%), Pyr (2.7% to 35.5%) and BaP (78.3% to 84.8%). For summer, they change for Phe (6.5% to 23.6%), Pyr (15.3% to 37.4%) but not BaP (100% to 100%). The latter must be a measurement artefact.

The above information was applied in the simulation study. Generalised equations which calculate both gaseous and particulate PAH concentrations, experiencing a consecutive degradation of gas fraction and a phase re-distribution every second, can be seen in Table 7.14. After reaction time t , the final total PAH concentrations ($C((1-a)K + a)^n$) consist of gaseous ($((1-a)C((1-a)K + a))^n$) and particulate ($(aC((1-a)K + a))^n$) phases.

Table 7.14. Generalised concentrations over reaction time ($e^{-k(g)OH^*[OH]^*t}$, denotes K).

		t	Gaseous con.	Particulate con.	Total con.	p-fraction
		(s)	(ng m ⁻³)	(ng m ⁻³)	(ng m ⁻³)	-
	C ₀	0	(1-a)C	aC	C	a
Reaction	C ₁	1	(1-a)C K	aC	C ((1-a)K + a))	
Re-partitioning	C ₁ '		(1-a)C ((1-a)K + a))	aC ((1-a)K + a))	C ((1-a)K + a))	a
Reaction	C ₂	2	(1-a)C ((1-a)K + a)) K	aC ((1-a)K + a))	C ((1-a)K + a)) ²	
Re-partitioning	C ₂ '		(1-a)C ((1-a)K + a)) ²	aC ((1-a)K + a)) ²	C ((1-a)K + a)) ²	a
	
	
Reaction	C _n	t	(1-a)C ((1-a)K + a)) ⁿ⁻¹ K	aC ((1-a)K + a)) ⁿ⁻¹	C ((1-a)K + a)) ⁿ	
Re-partitioning	C _n '		(1-a)C ((1-a)K + a)) ⁿ	aC ((1-a)K + a)) ⁿ	C ((1-a)K + a)) ⁿ	a

Based on the generalised equation, the change in the initial concentration (C_0) at source sites (Birmingham) over a total reaction time of 15 hours was simulated both in winter and in summer. The normalized concentrations as a function of reaction time can be seen in Figure 7.3.

As expected, Pyr, having a higher $k_{(g)OH}$ than Phe, degraded faster than Phe (see Figures 7.3a and 7.3b). However, this concept could not be applied to the BaP concentration. Although the estimated $k_{(g)OH}$ of BaP is similar to that of Pyr, the loss rate of BaP was the slowest, which may be explained by a minor partition of BaP to the gaseous fraction (see Figure 7.3a). The plots for BaP for summer was not included in the graph (see Figure 7.3b), because the fact that above simulation only includes oxidation loss of PAH vapour by OH radicals but there was no gaseous concentration available in the summer measurements, leading to no loss in BaP concentrations during summer.

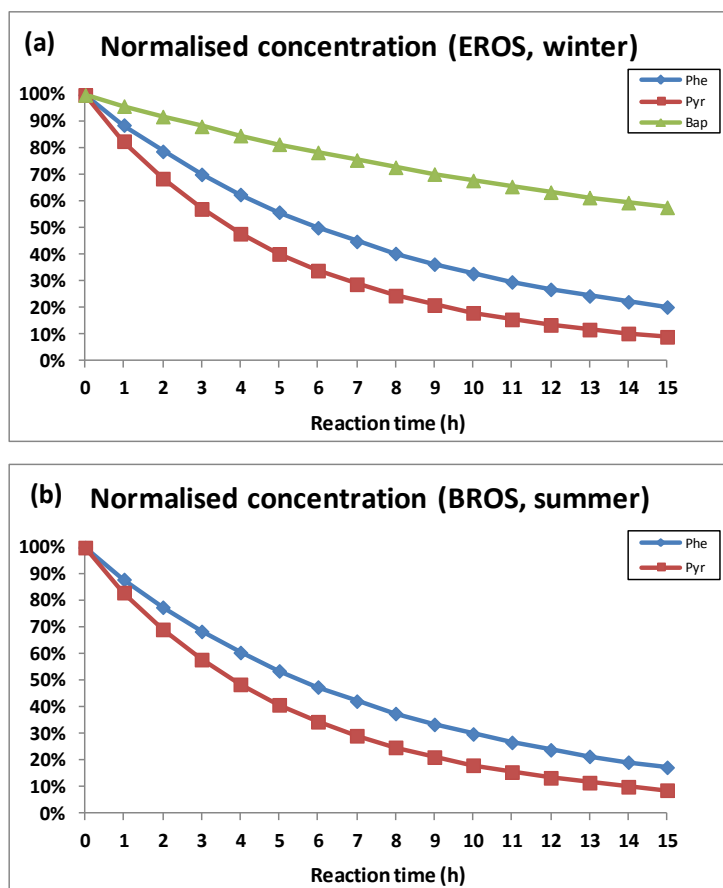


Figure 7.3. Normalised concentrations over reaction time.

In an ideal case the simulated concentration at $t = t$ would have been similar to the level at Weybourne. However, the different sampling periods for the source and receptor within a pair for winter (source: Jan 2010 and receptor: Feb 2010) and for summer (source: Aug 2009 and receptor: Aug 2010) might have led to a discrepancy between the measured and the simulated concentrations. Moreover, differences between the meteorological conditions near the source and those in the remote area might have caused difficulty in the exact estimation of the PAH level at the remote site. In this study, the use of ratios between two congeners overcame such concerns. In Figure 7.4 the simulated ratios of PAH pairs are plotted. As mentioned above, the gaseous ratios for Phe/BaP were not included in simulated plot for summer, owing to the lack of gas fraction data for BaP in the summer measurements.

The trend of Phe/Pyr ratios can be explained by the magnitude of the OH rate coefficient ($k_{(g)OH}$), which showed little difference between total-total (see Figures 7.4a) and gas-gas ratios (see Figures 7.4b). However, the difference in the phase distribution between Phe and BaP leads to a huge difference in the ratio of total-total from that of gas-gas. These simulated graphs may reflect the fact that there is a limitation in the G/P re-equilibrium of BaP, while BaP vapour is oxidized. Otherwise, the hourly plotted ratios between gaseous phases (Phe/BaP) should have increased, owing to the higher value of the $k_{(g)OH}$ for BaP than that for Phe. With regards to the simulation for summer, a similar trend was observed (Figures 7.4c and 7.4d). However the ratio between total concentrations for Phe/BaP may not be meaningful because there was no loss in concentration for BaP vapour in the simulation.

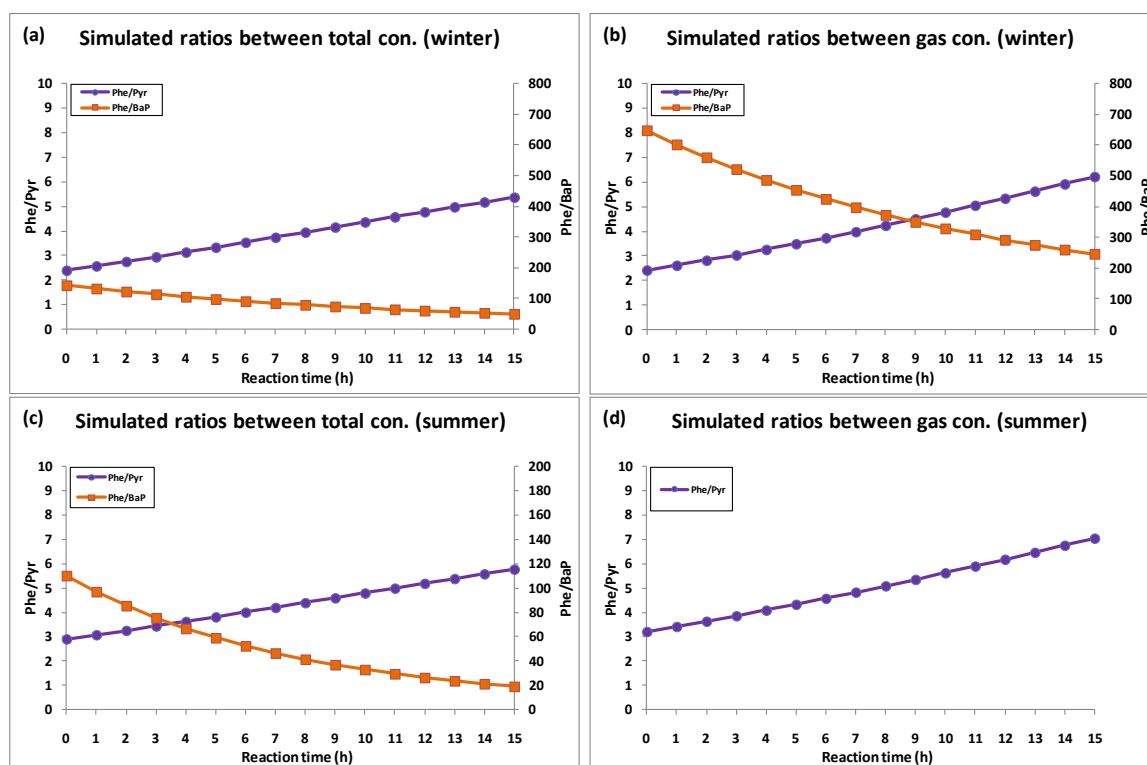


Figure 7.4. Simulated ratios during transport.

When the above simulated ratios and real measured ratios from Weybourne were compared (see Table 7.15), a consistent trend was seen. The Phe/Pyr ratio was increased, and Phe/BaP ratio was decreased during transport from the source to the receptor site.

Table 7.15. Comparison of ratios between simulation and real measurement for winter.

	Source (EROS)	Rural (Weybourne)	Simulated rural ratios	EU background ^a (Košetice)	Rural ^b (Gosan)	Remote ^c (Arctic ocean)
phase	T-T (G-G)	T-T (G-G)	T-T (G-G)	T-T	T-T	T-T
Phe/Pyr	2.4 (2.4)	6.5 (7.6)	5.4 (6.2)	3.9	2.3	7.0
Phe/BaP	185 (1485)	45 (261)	50 (247)	15	68	37

^a Dvorská et al. (2012), ^b Kim et al. (2012), ^c Wang et al. (2013)

To conclude, it seems that the phase distribution of PAH is changed during transport, especially for LMW PAH, which may be driven by the difference between the degradation rate of vapour fractions and the re-equilibration rate between gaseous and particulate fractions. Concurrently, the ratios between PAH congeners may be changed over transport time, due to the different chemical reactivity of individual PAH. From this simulation, one may conclude that not only source types but also degrees of aging of air masses can influence and vary the ratio between PAH congeners, which makes it difficult to identify sources from ratios between PAH congeners. In addition, the HMW PAH showed a greater potential for long-range transport.

7.3.5 Sensitivity

7.3.5.1 Sensitivity of simulated ratios to variations in parameters

Several assumptions have been made for this simulation study of the chemical reactivity of PAH; therefore various uncertainties should be considered. Averaged ratios between gaseous PAH congeners in Birmingham, used as a source ratio for the UK mainland, are subject to sampling uncertainty. OH radical reaction was assumed to be the dominant loss mechanism of gaseous PAH in the simulation. However, other oxidants such as NO_3 and O_3 could also react with PAH. The experimental rate coefficients ($k_{(g)\text{OH}}$) may imply uncertainties about the chemical reactivity of PAH congeners. Thus as part of the work reported on in this chapter, a sensitivity study was designed to quantify the influence of uncertainties on the previously simulated ratios.

The uncertainty of the source ratios was varied by -10% and 10% in scenarios S1 and S2, respectively. In S3, the transport time was changed from 15 hours to 12 hours, based on the backward trajectory results. The estimated value of the $k_{(g)OH}$ for BaP was used in the previous analyses, but was varied by -10% and 10% in S4 and S5, respectively. It was assumed that OH oxidation was the dominant loss mechanism of gaseous PAH, as the $k_{(g)OH}$ was larger than the $k_{(g)NO_3}$ by one to three orders of magnitude, followed by the $k_{(g)O_3}$ (Keyte et al., 2013). In S6, oxidation by NO_3 was added, but the O_3 reaction was not included because of the paucity of information on the value of the $k_{(g)O_3}$ and its small likely magnitude. The sensitivity results can be seen in Table 7.16 and Figure 7.5.

Table 7.16. Simulated ratios at $t = t$ (at Weybourne).

	S0	S1	S2	S3	S4	S5	S6	Measurements
Reaction time (h)	15	15	15	12	15	15	15	at Weybourne
Source ratio (G-G)	2.40	2.16	2.64	2.40	2.40	2.40	2.40	
Estimated OH*E+6	1.20	1.31	1.10	1.50	1.20	1.20	1.20	
T-T (Phe/Pyr)	5.37	5.21	5.53	5.35	5.37	5.37	5.37	6.54
G-G (Phe/Pyr)	6.22	6.03	6.40	6.19	6.22	6.22	6.22	7.56
T-T (Phe/BaP)	50	46	55	50	47	53	50	44.8
G-G (Phe/BaP)	247	224	269	247	233	260	247	260.7

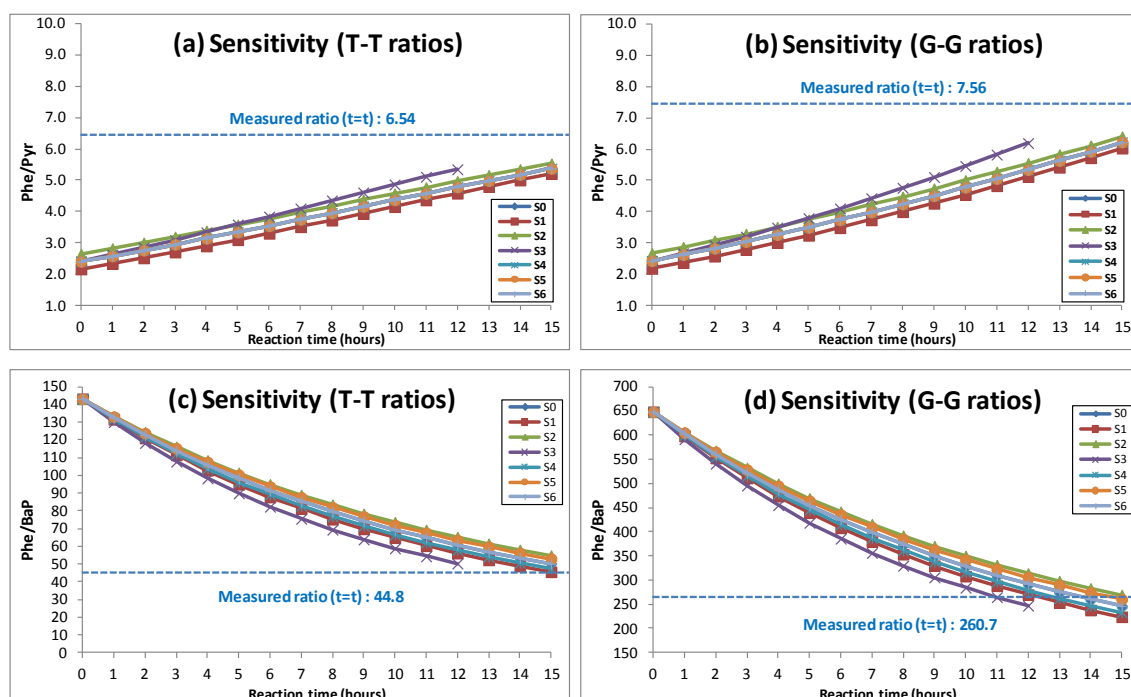


Figure 7.5. Sensitivity of PAH-PAH ratios to variations in parameters.

A change of source ratio, expressed as gaseous concentrations of Phe to Pyr can vary the estimated OH value, as shown in Equation 7.1, which can influence concentration distribution between gaseous and particulate PAH, as described in the generalised equation (see Table 7.14). $\pm 10\%$ of uncertainty in the source ratio leads to $\pm 3\%$, and $\pm 10\%$ changes in the Phe/Pyr and Phe/BaP respectively (S1, S2). A change of transport time also influences the estimated OH value from $1.2\text{E} + 6 \text{ molecules cm}^{-3}$ for a 15-hour reaction time to $1.5\text{E} + 6 \text{ molecules cm}^{-3}$ for a 12-hour reaction time. However, the influence of this uncertainty on the ratio in simulations is insignificant (S3). The result can be anticipated on a theoretical basis. The reduced reaction time leads to an increment in the OH concentration, shown in Equation 7.1, which allows PAH to be oxidized for a shorter time with the higher OH concentration. On the other hand, the increased transport time causes a decrement in the OH estimation which makes it possible for PAH to react with the lower OH concentration for a longer time. The

inverse relationship between reaction time and OH concentration leads to little change in the ratios simulated in S3. The variation of the $k_{(g)OH}$ of BaP by -10% and 10%, only affects the ratio of Phe/BaP by $\pm 5\%$ (S4, S5). Finally, the involvement of NO_3 oxidation in the fate of PAH showed little influence on the ratio simulations (S6).

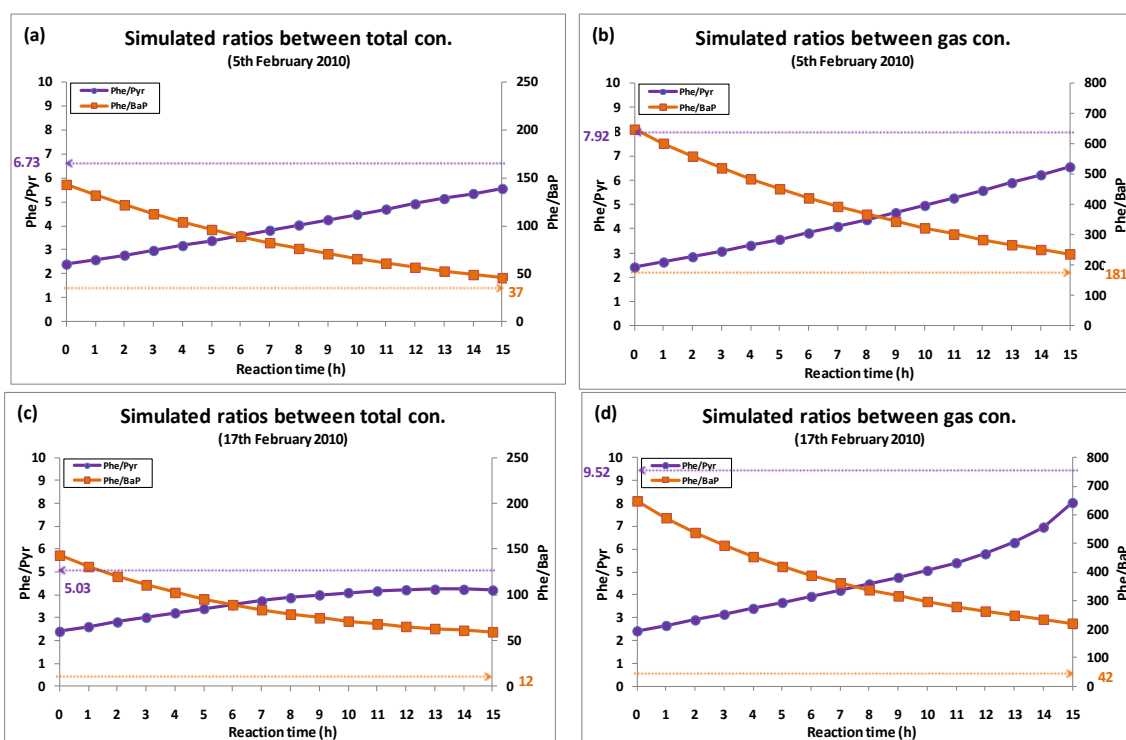
The above sensitivity results showed that the simulated ratios were comparable to the field measurements.

7.3.5.2 Simulations for individual air masses for winter

The simulation study conducted in the previous section used mean values of source ratios and an OH estimation that were derived from three selected samples (5th, 19th and 25th February, 2010), having a similar range of ratios (Phe/Pyr and Phe/BaP) and similar trajectories; and they showed comparable ratios to those obtained from field measurements (see Table 7.15). In this study, simulations were applied to each sample as a function of air mass backward-trajectory with a consistent travelling time of 15 hours, because the sensitivity study described in the previous section showed that the travelling time had little influence on the ratios simulated at $t = t$. The OH estimations and the simulated ratios for individual air masses can be seen in Table 7.17 and Figure 7.6.

Table 7.17. Estimated OH concentrations using individual samples at Weybourne site.

	(molecules cm ⁻³)
Case 1 (05/02/2010)	
$\ln \left[\frac{1.450}{0.183} \right] = \ln [2.400] + [\text{OH}] ((4.65 - 2.88) \text{ E-11}) * (54000)$	1.25E+06
Case 2 (17/02/2010)	
$\ln \left[\frac{0.295}{0.031} \right] = \ln [2.400] + [\text{OH}] ((4.65 - 2.88) \text{ E-11}) * (54000)$	1.45E+06
Case 3 (18/02/2010)	
$\ln \left[\frac{0.466}{0.048} \right] = \ln [2.400] + [\text{OH}] ((4.65 - 2.88) \text{ E-11}) * (54000)$	1.47E+06
Case 4 (19/02/2010)	
$\ln \left[\frac{1.638}{0.228} \right] = \ln [2.400] + [\text{OH}] ((4.65 - 2.88) \text{ E-11}) * (54000)$	1.15E+06
Case 5 (25/02/2010)	
$\ln \left[\frac{1.434}{0.190} \right] = \ln [2.400] + [\text{OH}] ((4.65 - 2.88) \text{ E-11}) * (54000)$	1.20E+06

**Figure 7.6.** Comparison between simulated ratios and measured ratios as a function of back trajectory.

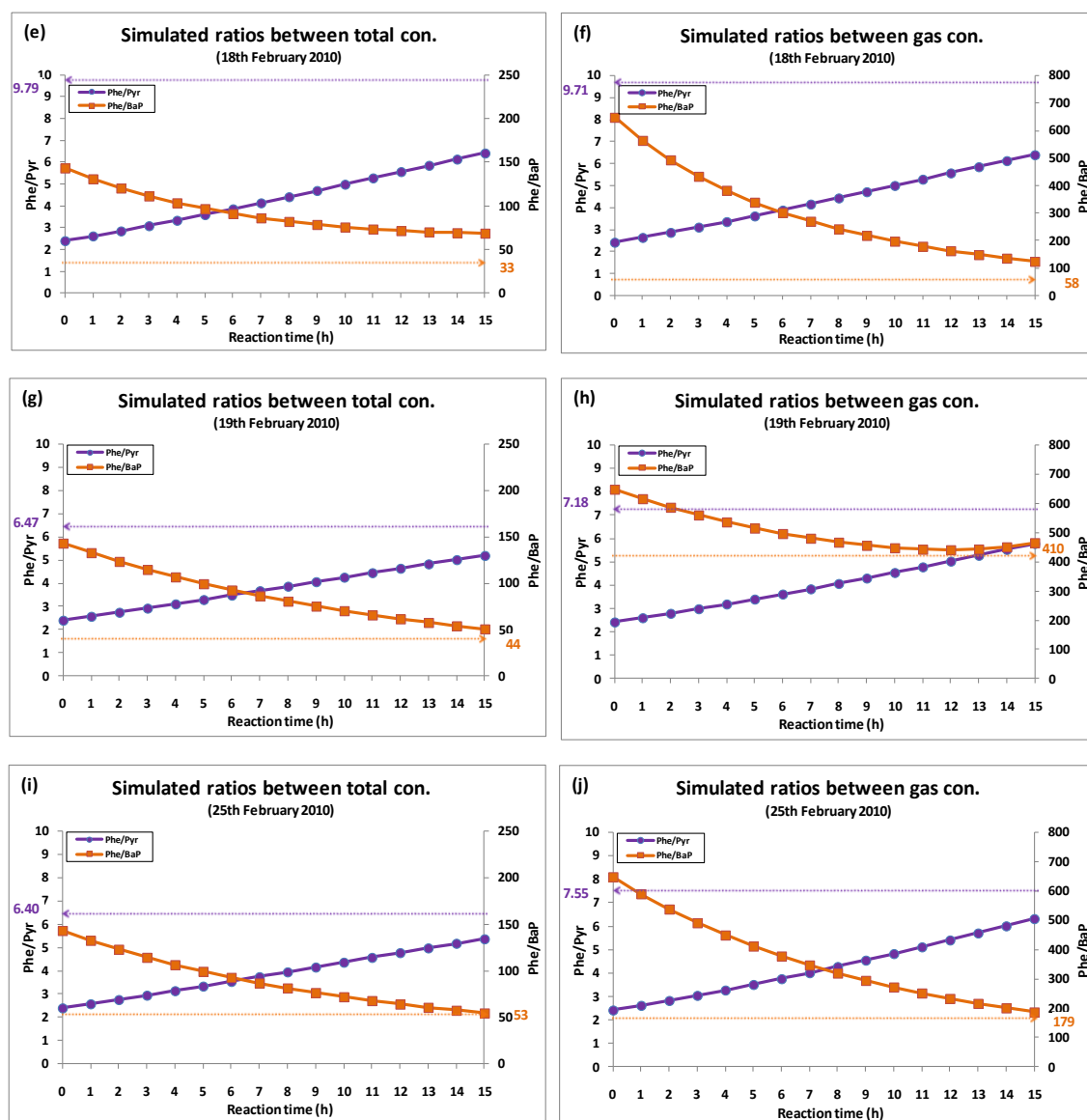


Figure 7.6. (Continued).

As expected, the three samples (5th, 19th and 25th February) that were mentioned in the previous section showed comparable values between the simulated ratios (at $t = t$) and the measured ones at Weybourne (see Figures 7.6a-b and 7.6g-j). However, two other samples did not show good simulation results: one was the air mass that passed over London on 17th February, showing a similar trajectory to the previous three samples; and the other was the air mass that passed over the UK Midlands on 18th February (see Figure 7.1). The unsuccessful simulated ratios for these two samples may be explained

by an inappropriate pairing of the travelling time taken from the back trajectory and the OH concentration based on this travelling time (see Equation 7.1). The sampling periods were different between the source area (EROS, January 2010) and the rural site (Weybourne, February 2010). Thus the estimated OH concentration derived from the two values - one was travelling time as a function of trajectory at Weybourne and the other source ratios at EROS - may not have been consistent with the actual oxidation conditions. For example, the two samples transported to Weybourne could have undergone more oxidation than expected owing to a higher OH concentration; or the PAH could have been oxidized for longer than the expected transport time derived from back trajectory.

The above two potential cases were simulated. The ratios between the PAH congeners were plotted hourly over the reaction time of the PAH with the OH radicals by optimizing the OH concentration and the transport time until they provided a good fit to the actual ratios at the Weybourne site. There was an improvement in the simulation fit (at $t = t$) for two samples (17th and 18th August 2010) compared to the previous simulation results shown in Figures 7.6c-f, when an increased OH concentration of 2.0×10^6 molecules cm^{-3} with no change in the transport time of 15 hours (see Figure 7.7), or an increased reaction time of 20 hours with OH concentrations of 1.45 and 1.47×10^6 molecules cm^{-3} for 17th and 18th January 2010 respectively (see Figure 7.8) was applied to the simulation.

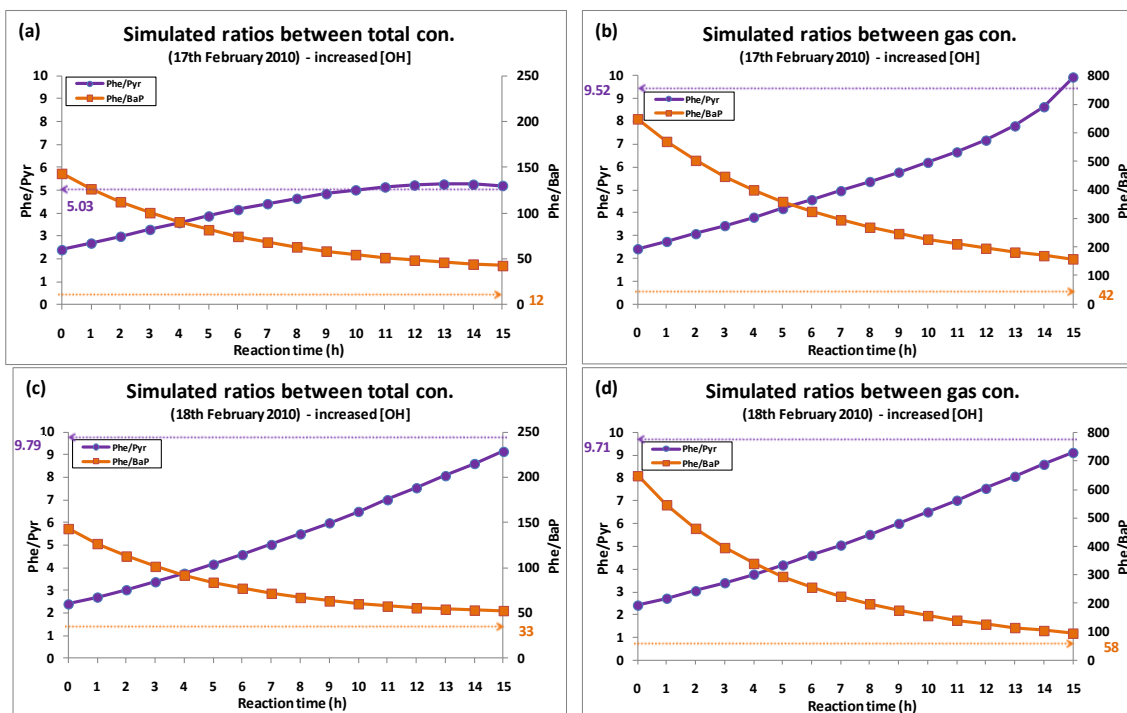


Figure 7.7. Simulated ratios with increased OH radical concentration of 2.0×10^6 molecules cm^{-3} with transport time of 15 hours.

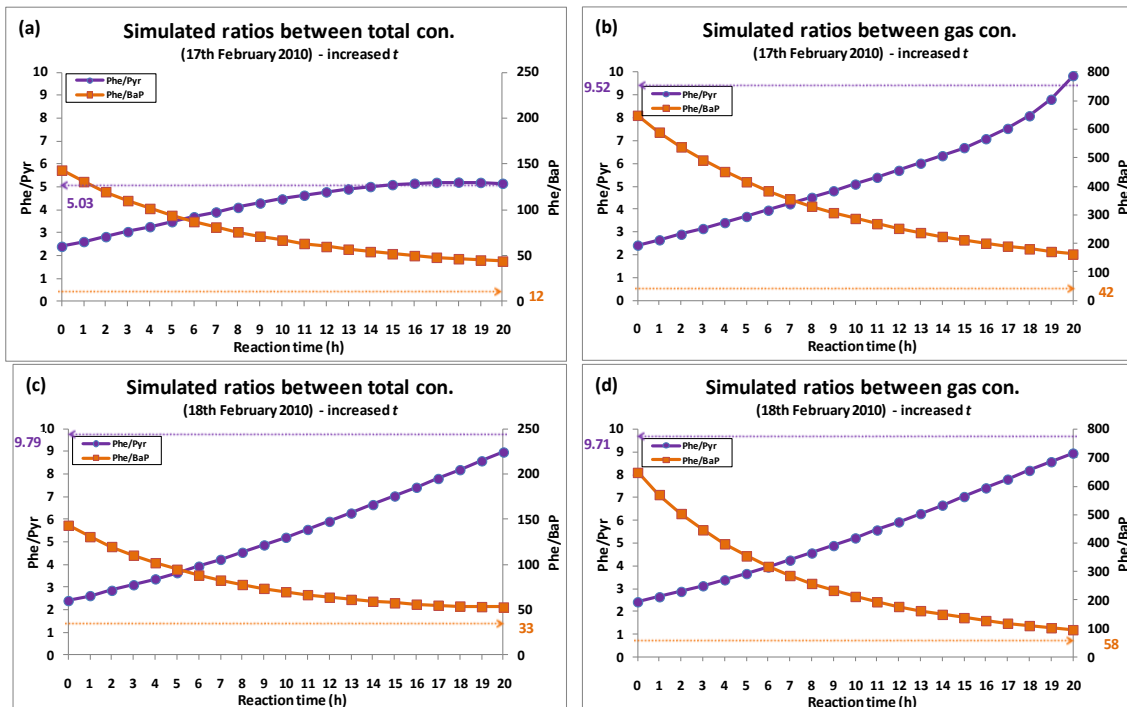


Figure 7.8. Simulated ratios with increased transport time of 20 hours at the estimated OH concentrations of 1.45 and 1.47×10^6 molecules cm^{-3} sampled on 17th and 18th February 2010, respectively.

7.4 Discussion

Experimental data showed that enhanced particle fractions (P(%)) of three PAH (Phe, Pyr and BaP) were seen in the transported airborne particles. The P(%) near the source area (EROS) was much less than that of the three aged air masses at the remote site (Weybourne), which was the largest in the air mass transported from the North Sea. This practical trend was different from the P(%) obtained from the theoretical equation considering both sorptions (ab/adsorption). This discrepancy may reflect the complex reactivity of PAH influenced by the heterogeneous physico-chemical composition of aerosol as a function of transport time and a continuous phase re-distribution between gaseous and particulate phases.

Interpolated values of P(%) based on the winter field measurements taken between EROS ($t = 0$) and Weybourne for an air mass transported from the UK mainland ($t = t$) over a 15-hour transport time, and an estimated OH concentration (1.20×10^6 molecules cm^{-3}) were applied to the ratio simulations. Comparable values (Phe/Pyr, Phe/BaP) could be obtained for simulated and measured ratios. These simulated ratios were not significantly affected by uncertainties caused by making several assumptions for source measurements, transport time, dominant mechanism, and rate coefficient. Simulation of the ratios for individual air masses reflected the fact that some samples could have been measured either under more atmospherically reactive conditions with higher OH concentrations than expected or for a longer oxidation time than the transport time taken from back trajectory.

The estimated daily average OH concentration applied to the air mass transport equation using the winter ratio between PAH congeners at the source and at the remote site (see Equation 7.1) was around 1.20×10^6 molecules cm^{-3} . This value was within the probable range in the boundary layer (Keyte et al., 2013) and similar to the estimated concentration for summer (1.22×10^6 molecules cm^{-3}), but it seems to be higher than reported winter concentrations. Field measurements conducted at the urban background site in Birmingham showed that the OH concentration at solar noon ranged $(2-9) \times 10^6$ molecules cm^{-3} and $(0.5-4) \times 10^6$ molecules cm^{-3} in summer and winter, respectively (Emmerson et al., 2005). Daily average concentrations in Tokyo were 2×10^6 molecules cm^{-3} and 5×10^5 molecules cm^{-3} in summer and winter, respectively (Kanaya et al., 2007).

There is a complex chemistry determining the OH concentration in the ambient air. During summer time, OH production is mainly related to ozone photolysis followed by the reaction of electronically excited oxygen atoms ($\text{O}(^1\text{D})$) with water vapour, although the contribution from alkene + O_3 reactions to the OH concentration can be increased during heatwaves (Emmerson et al., 2007). In polluted atmospheres, other photolytic processes become significant contributors to OH production, while the contribution from the reaction $\text{O}(^1\text{D}) + \text{H}_2\text{O}$ is decreased. For example, the contribution from photolysis of nitrous acid (HONO) and alkene + O_3 was increased both in summer (46% and 29%), and in winter (62% and 36%) during pollution episodes (Heard et al., 2004). Additionally, there is a contribution from photolysis of formaldehyde (HCHO) to OH production (Emmerson et al., 2007). However, the above air pollutants can also concurrently be a sink for OH because the OH radical reacts as a powerful oxidant.

The empirical study reported that the summer/winter ratio of daytime peak OH concentrations was about 2, despite of a high value of $j(\text{O}^1\text{D})_{\text{summer}} / j(\text{O}^1\text{D})_{\text{winter}}$ of around 15 (Harrison et al., 2006). The high peak-concentration of OH, 1.20×10^7 molecules cm^{-3} during a pollution episode was observed with the daily averaged OH concentration for a clean day in summer, $(3 - 4) \times 10^6$ molecules cm^{-3} . Emissions may be attributable to the enhancement of the OH concentration (Mount and Williams, 1997).

The above experimental results may reflect that there is a source which has enhanced OH formation in winter under the low solar UV density. The short life of OH ($<1\text{s}$) implies that OH concentration is more influenced by local concentrations of O_3 , VOCs, CO and NO_x than transported contributions (Emmerson et al., 2007).

There were no daily air pollution measurements except O_3 at the Weybourne site, thus 24-h mean concentrations for NO_x and benzene representative of the VOCs were reviewed at the Harwell site (rural background, UK Midlands), and these were available from the DEFRA (Table 7.18). Data showed that two samples collected on 17th and 18th February 2010 at the Weybourne site could be influenced by more polluted air masses having a potential for larger OH concentrations.

Table 7.18. Daily air pollution concentrations at rural background site (Harwell).

			$\mu\text{g m}^{-3}$
	Oxides of nitrogen	Benzene	Ozone
05/02/2010	14.3	0.49	57
17/02/2010	24.9	0.79	42
18/02/2010	49.8	1.23	28
19/02/2010	13.6	0.69	51
25/02/2010	15.5	0.56	50

Alternatively, there may be an additional PAH input to the transported air mass between EROS and Weybourne, such as vehicle emissions or volatilisation from soil. Wild and Jones (1995) have suggested that the re-emission of LMW PAH to the ambient air from a terrestrial environment where atmospheric deposition of PAH has accumulated (i.e., re-volatilisation) can significantly contribute to the atmospheric load of PAH. If this is the case, the simulated gaseous ratios of Phe/Pyr at the Weybourne site for the two samples (17th and 18th February, 2010) could be increased by the addition of a large load of re-volatilised Phe during transport, caused by larger vapour pressure and the lower k_{ab} /adsorption coefficients of Phe than Pyr. The other ratio of Phe/BaP is also expected to be increased during transport. However in practice, the simulated values for Phe/BaP at $t = t$ were overestimated (see Figure 7.6). It has been reported that deposition is a significant loss mechanism for HMW PAH in the air (Kaupp and Michael, 1998, Ravindra et al., 2008a). If this was an important process during PAH transport, the total (gaseous and particulate) ratio of Phe/BaP could be expected to be larger in the simulation, leading to a larger gap in ratios between the simulated results and the measured ones, provided that there was a kinetic limitation to re-equilibration.

To conclude, there was a good agreement in the ratio trend over reaction time between field measurements and simulated values. However, some samples could either have been measured under more atmospherically reactive conditions than expected with enhanced OH concentrations caused by local air pollution or have experienced longer transport time than estimated.

CHAPTER 8: CONCLUSIONS

8.1 Summary

Polycyclic aromatic hydrocarbons (PAH) are a group that causes concern as air pollutants, as some of them have been reported as carcinogenic compounds. The major objectives of this research were to identify the source category of PAH using pooled atmospheric measurements at urban sites and to quantify the source-specific contributions at individual sites through positive matrix factorization (PMF) analysis. PMF source profiles were extensively compared with emission information on a local and national scale. The possibility of extracting source profiles using PMF was evaluated with particular focus on the reactivity of PAH. Additionally, conceptual reactivity was designed to better understand the atmospheric fate of PAH.

When total PAH measurements (vapour + particulate phases) at the UK urban sites were subjected to the PMF tool, four major sources were found to be responsible for the atmospheric PAH levels. The largest contribution to the sum of PAH mass (Σ PAH) was observed from traffic-related sources such as unburned petroleum and diesel exhaust emissions, followed by coal combustion and wood combustion sources. However, emissions of BaP were substantially determined by solid fossil fuel combustion sources, such as coal combustion and wood combustion for residential heating. With regard to

the industrial sites, the most significant contribution both to Σ PAH and to BaP was seen from the coal combustion source. A considerable similarity was observed in PMF-derived PAH signatures for coal combustion sources between the urban and the industrial dataset, except for low molecular weight (LMW) PAH. On the other hand seasonal variation was evidently different between the two datasets. The results may suggest that there are different types of coal combustion activities.

Three local source profiles for particulate PAH emissions were obtained from the net concentration of paired locations and these showed a high similarity to the specific source signatures found through PMF. This analysis was limited in its ability to separate detailed source categories compared to the PMF analysis. However, it provided supplementary information in terms of source markers, for which PMF could not discriminate between the different types of coal combustion activities. The slightly enhanced significance of the two congeners CcdP and BaP for the net urban contribution profile supported the possibility of using these compounds as source markers for emissions from domestic coal combustion sources. It could suggest that DaiP is a source identifier for coal combustion emissions relating to steel works. Additionally, a comparison between PMF results and the source-specific signatures taken from the UK national emissions estimates showed general agreement on the source identifiers. The results obtained from the local and national emissions provided supporting information in identifying source types for PMF analysis.

The use of high quality datasets combined with informed knowledge of local emissions, for example at the Northern Ireland sites and the industrial urban sites, made possible

reasonable identification of source types of particle-associated PAH at the urban sites through PMF analysis. The results of sensitivity analysis demonstrate that the PMF tool could extract source-specific profiles for PAH, even though there was some uncertainty arising from the reactivity of the PAH.

It was evident that PMF analysis allowed quantitative comparison of source-specific contributions, depending on the season and the sampling region, at urban sites. However, this may not be the case for rural sites, where the atmospheric PAH level is determined by transported air masses, and individual PAH exhibit differing reactivity and G/P partitioning during transport. The conceptual scenario for the transport of PAH has been developed based on what the literature reports for the rate coefficient of PAH with oxidants and the field measurements for both gaseous and particulate PAH concentrations. The simulated ratios between PAH congeners (Phe/Pyr, Phe/BaP) in the backward-trajectory-derived transport time were in strong agreement with the ratios obtained from field measurements at the rural sites under the following assumptions: PAH vapour is predominantly oxidised by OH radicals; and the G/P phase distribution changes during transport from source to remote area. The results may suggest that high molecular weight (HMW) PAH including BaP, have the potential to have a longer atmospheric life than might be expected. Limited access of oxidants to the particle-associated PAH caused by shielding gases may be a potential explanation for the long-range transport of HMW PAH. Slow G/P phase re-equilibrium between the rates for oxidation of PAH vapour and the rates for the re-partitioning of the two phases may be an additional possible explanation.

8.2 Implications

The work conducted in this thesis made an extensive study of PAH congeners by subjecting them to positive matrix factorization (PMF). Most source apportionment (SA) studies have focused on the USEPA's 16 congeners and there are limited SA results using various atmospheric PAH, thus it was difficult to assign sources to PMF factor profiles. However, a comparison between PMF results and source-specific signatures taken from local and national emissions provided information that supported the identification of source types for PMF analysis. The use of high quality datasets combined with informed knowledge of local emissions made possible reasonable identification of source types through PMF analysis.

The results showed that the atmospheric levels of carcinogenic BaP were substantially determined by solid fossil fuel combustion sources and traffic related sources at the UK urban sites. Two kinds of PAH source profiles for coal combustion were separated out: one a domestic coal combustion profile and the other an industrial coal combustion profile. In addition, PMF analysis provided seasonal and regional comparisons for source-specific contributions in urban areas. These have significant implication in terms of the development of effective pollution control strategy on a local and national scale. For example, increasing the availability of natural gas may be helpful to reduce PAH emissions in Northern Ireland sites. Improvements in fuel quality and efficiency of internal combustion engines may lead to a reduction in traffic-related PAH levels on a national scale.

Both a sudden decline in the relative contribution of the diesel combustion source and an increased relative contribution for unburned petroleum was observed from 2005 in the source apportionment results. This is consistent with the large reduction of sulphur content in fuels sold in the UK and EU countries between 2001 and 2007 (Table 3.1). The attribution to individual sources in receptor modelling is basically determined by users based on chemical profiles derived from the literature. However this study clearly illustrates that regulations cause alteration of profiles and that PAH source profiles are not invariant with time.

The PMF source profiles taken from two geographically different locations: one in Saudi Arabia and one in the UK, shows that other factors, such as fuel types used, meteorology and regulations can produce slightly different interpretation of specific-source types in different locations. This implies that source attribution should be conducted cautiously when source types are determined based on the published literature.

The best interpretation of source profiles is obtained when analysing long-term datasets in receptor modelling. Although it was not explicitly discussed in the result chapters, the importance of quality of datasets should be considered in receptor modelling. The UK PAH National Network operated with Andersen samplers between 1991 and 2008 which were replaced with Digitel samplers from 2009. Consistent methodology in the national monitoring programme would have generated a larger dataset and improved the accuracy of source profiles when the long-term data was subjected to receptor modelling. Improvement of accuracy in the measured data from UK monitoring stations

might allow identification of emissions from none of the sources in the UK national inventory. As a result, source profiles or source-specific contributions obtained from receptor modelling using national network measurements might be more comparable to the UK emissions inventory.

The heterogeneous source-specific contributions from individual sites in the PMF analysis imply that site classifications should reflect the local emission characteristics representatively. A pooled dataset with different emission characteristics may not produce accurate source profiles from receptor modelling. For example three sites in Northern Ireland are categorised as ‘urban background’ sites in the UK PAH national network, but actually show a much larger contribution from a domestic heating source to PAH levels compared to other urban sites. In addition, the source composition at the Kinlochleven site was slightly different from that at other urban background sites.

The complex and differing atmospheric chemistry of individual PAH reflects the limitations to an application of receptor modelling to measurements at the remote sites where air pollution levels are determined by transported air masses from source regions, because fresh source profiles can change during transport. The fact that enhanced particle fractions (P(%)) for three PAH (Phe, Pyr and Bap) were observed at the remote site compared to the values at the source region, although this trend was not consistent with the theoretically estimated results derived from the G/P partitioning equation that included both sorptions, suggested that PAH are influenced by complex atmospheric chemistry during transport. Many factors, such as ambient temperatures, physicochemical particle properties, accessibility of oxidants to aerosol particles and the

degree of G/P phase re-equilibrium, may lead to different partitioning mechanisms between an urban and a remote site.

The results obtained from the conceptual simulation of PAH ratios as a function of backward trajectory in this thesis, were in good agreement with empirically obtained values. This provided a better understanding of PAH reactivity during transport, indicating the potential for long-range transport of HMW PAH. In addition, this study implies that extensive monitoring both for total (vapour and particulate) PAH and for at rural sites is significant to understand the atmospheric fate for PAH comprehensively.

8.3 Future work

In this study, daily measurements were subjected to PMF to identify major sources for airborne particle-associated PAH, under the assumption that the PAH level at the receptor (urban site, in this thesis) is predominantly determined by mixed sources. However, it is likely that the subsection of backward-trajectory-dependent PAH data at the rural site to PMF and a comparison of factor profiles between urban and rural datasets would extend our understanding of the reactivity of PAH during transport. And this result might provide further insights into the fate of PAH in parallel with reactivity simulation results obtained in this study.

The application of PMF to long-term PAH measurements with consistent sampling methodology could provide a better understanding of change in source-specific contributions, which would have relevance for the enactment of legislation for air

pollution control.

Most of the thermodynamic parameters needed for the estimation of PAH particle fractions ($P(\%)$) were estimated based on the literature. The theoretically calculated $P(\%)$ at the remote site were different from empirically obtained values. This discrepancy might decrease if boundary layer temperatures and vertical distributions of PAH, as a function of backward trajectory, were applied to the G/P partitioning equation. Extensive rural measurements of these parameters related to aerosol properties might provide an insight into PAH phase distribution, significantly determining the fate of atmospheric PAH.

Within this thesis the concept has been tested that oxidation by the OH radical is the predominant loss mechanism for PAH in the vapour phase. However, the comprehensiveness of the research could be improved by adding other loss processes, such as wet/dry deposition, and including a multi-compartment model in the simulation study.

Appendix A: Source emission contributions of air pollutants ranked by sector

Table A.1. Source contribution of air quality pollutant (<http://naei.defra.gov.uk/>).

England, 2012							[unit : %]
Overall Rank	Sector	CO	NOx	SO ₂	PM ₁₀	NMVOC	
1	Transport sources	38.9	43.2	2.4	25.0	7.5	
2	Industrial processes	11.1	0.7	3.8	15.5	6.4	
3	Commercial, domestic and agricultural combustion	19.7	7.8	7.2	20.9	4.2	
4	Industrial combustion	23.3	16.1	15.5	9.2	2.8	
5	Energy industries	4.9	29.3	67.8	9.3	0.0	
6	Agriculture	0.0	0.0	0.0	10.3	8.1	
7	Other	1.8	2.7	1.7	5.2	0.9	
8	Fugitive	0.3	0.0	1.7	0.4	13.8	
9	Solvent processes	0.0	0.0	0.0	4.2	50.6	
10	Waste	0.0	0.0	0.0	0.0	5.6	
Total		100	100	100	100	100	
(ktonnes)		(1,508)	(796)	(314)	(86)	(573)	

Scotland, 2012							[unit : %]
Overall Rank	Sector	CO	NOx	SO ₂	PM ₁₀	NMVOC	
2	Transport sources	30.1	37.8	2.2	19.6	2.5	
4	Industrial processes	2.8	0.0	1.2	9.7	44.4	
1	Commercial, domestic and agricultural combustion	39.0	11.8	13.6	36.9	3.8	
5	Industrial combustion	20.2	14.5	7.4	6.9	1.1	
3	Energy industries	5.7	33.3	74.7	9.2	0.0	
6	Agriculture	0.0	0.0	0.0	10.8	7.1	
7	Other	1.8	2.7	0.7	4.0	0.5	
8	Fugitive	0.4	0.0	0.2	1.0	16.7	
9	Solvent processes	0.0	0.0	0.0	2.0	19.8	
10	Waste	0.0	0.0	0.0	0.0	4.0	
Total		100	100	100	100	100	
(ktonnes)		(165)	(98)	(65)	(12)	(141)	

Table A.1. (Continued).

Wales, 2012		[unit : %]				
Overall Rank	Sector	CO	NO _x	SO ₂	PM ₁₀	NMVOC
3	Transport sources	17.1	25.8	3.3	16.0	5.3
2	Industrial processes	38.8	2.2	12.8	19.2	4.3
1	Commercial, domestic and agricultural combustion	22.6	7.6	12.3	35.3	8.0
4	Industrial combustion	13.8	13.2	15.2	5.8	3.1
5	Energy industries	4.3	50.3	52.8	10.2	0.0
6	Agriculture	0.0	0.0	0.0	8.6	15.9
7	Other	2.9	0.0	2.9	0.5	21.7
8	Fugitive	0.6	1.0	0.7	2.5	1.3
9	Solvent processes	0.0	0.0	0.0	1.9	35.9
10	Waste	0.0	0.0	0.0	0.0	4.6
Total		100	100	100	100	100
(ktonnes)		(205)	(88)	(29)	(47)	(47)

Northern Ireland, 2012		[unit : %]				
Overall Rank	Sector	CO	NO _x	SO ₂	PM ₁₀	NMVOC
2	Transport sources	27.6	42.5	2.8	16.9	4.1
6	Industrial processes	0.0	0.0	0.1	5.9	7.7
1	Commercial, domestic and agricultural combustion	44.2	19.7	52.7	35.3	8.2
3	Industrial combustion	24.6	17.6	25.4	8.9	2.0
5	Energy industries	2.4	18.4	18.2	1.9	0.0
4	Agriculture	0.0	0.0	0.0	26.7	39.3
7	Other	1.1	1.9	0.8	2.7	0.6
8	Fugitive	0.0	0.0	0.0	1.6	31.6
9	Solvent processes	0.0	0.0	0.0	0.0	3.7
10	Waste	0.0	0.0	0.0	0.0	2.8
Total		100	100	100	100	100
(ktonnes)		(75)	(32)	(16)	(5)	(30)

Table A.2. *Source contribution of USEPA's 16 priority PAH including BaP, UK 2012*
(<http://naei.defra.gov.uk/>).

Activity	Source	16PAH (%)	BaP (%)
Coal/Charcoal	Power station	5.0	0.2
	Domestic combustion	12.7	12.9
Coke	Coke production	1.1	1.6
Wood	Domestic combustion	42.0	28.0
	Others	0.4	0.2
Diesel engine road vehicles (DERV)	Road transport	9.0	1.1
Petrol	Road transport	3.2	1.0
Forest and moorland	Natural fires	12.2	45.1
Others	Others	10.0	9.9
Total		100%	100%
(tonnes)		(780.9)	(6.4)

Appendix B: PAH emissions in the UK, 2002 – 2006

Table B.1. USEPA's priority 16 PAH emissions for major sources in the UK (<http://naei.defra.gov.uk/>).

Coke production	[kg]				
	2002	2003	2004	2005	2006
Naphthalene	4082.9	4112.9	3825.2	3776.8	5584.5
Acenaphthylene	347.5	350.0	325.6	321.4	475.3
Acenaphthene	71.5	72.1	67.0	66.2	97.9
Fluorene	240.2	241.9	225.0	222.2	328.5
Phenanthrene	-	839.0	780.4	770.5	1139.3
Anthracene	204.4	205.9	191.5	189.1	279.6
Fluoranthene	367.9	370.6	344.7	340.3	503.2
Pyrene	250.4	252.2	234.6	231.6	342.5
Benzo[a]anthracene	112.4	113.3	105.3	104.0	153.8
Chrysene	35.8	36.0	33.5	33.1	48.9
Benzo[b]fluoranthene	102.2	103.0	95.8	94.5	139.8
Benzo[k]fluoranthene	51.1	51.5	47.9	47.3	69.9
Benzo[a]pyrene	81.8	82.4	76.6	75.6	111.8
Indeno[1,2,3-cd]pyrene	35.8	36.0	33.5	33.1	48.9
Dibenzo[ah]anthracene	10.2	10.3	9.6	9.5	14.0
Benzo[ghi]perylene	35.8	36.0	33.5	33.1	48.9

Aluminum production	[kg]				
	2002	2003	2004	2005	2006
Naphthalene	9274.9	3082.2	2775.1	281.6	549.2
Acenaphthylene	1065.0	374.5	341.7	64.7	93.7
Acenaphthene	3597.3	1195.4	1076.3	109.2	213.0
Fluorene	5789.8	1928.6	1737.4	183.0	349.6
Phenanthrene	-	1394.3	1003.5	277.9	1893.5
Anthracene	329.1	89.0	200.2	45.9	45.7
Fluoranthene	1075.1	732.9	740.7	413.0	855.9
Pyrene	9044.9	3325.4	3065.5	777.6	1011.5
Benzo[a]anthracene	254.4	128.0	121.1	80.3	133.5
Chrysene	404.0	216.6	242.9	130.6	231.9
Benzo[b]fluoranthene	663.8	236.8	212.6	23.1	96.4
Benzo[k]fluoranthene	653.7	216.3	188.2	19.2	47.8
Benzo[a]pyrene	672.2	246.2	226.8	56.3	73.8
Indeno[1,2,3-cd]pyrene	99.9	53.1	41.8	50.5	77.7
Dibenzo[ah]anthracene	60.8	25.8	25.0	20.3	27.9
Benzo[ghi]perylene	119.4	40.6	36.6	50.3	58.9

Iron and Steel making					[kg]
	2002	2003	2004	2005	2006
Naphthalene	2746.9	3251.2	3417.0	3139.0	2529.9
Acenaphthylene	224.3	266.2	264.8	244.6	195.0
Acenaphthene	34.6	40.1	39.8	36.9	30.2
Fluorene	166.7	195.3	194.1	179.6	145.1
Phenanthrene	-	641.4	638.2	589.0	467.9
Anthracene	126.8	151.1	150.4	138.8	110.3
Fluoranthene	254.3	302.3	300.9	277.6	220.5
Pyrene	158.8	189.1	188.1	173.6	138.0
Benzo[<i>a</i>]anthracene	64.0	76.0	75.6	69.8	55.6
Chrysene	32.5	38.2	38.1	35.2	28.2
Benzo[<i>b</i>]fluoranthene	63.0	75.2	74.8	69.0	54.7
Benzo[<i>k</i>]fluoranthene	31.6	37.6	37.5	34.5	27.4
Benzo[<i>a</i>]pyrene	98.8	107.7	117.4	105.5	93.7
Indeno[1,2,3- <i>cd</i>]pyrene	32.2	38.1	37.9	35.0	27.9
Dibenzo[<i>ah</i>]anthracene	7.4	8.4	8.4	7.8	6.5
Benzo[<i>ghi</i>]perylene	32.1	38.1	37.9	35.0	27.9

Domestic wood combustion					[kg]
	2002	2003	2004	2005	2006
Naphthalene	55544.2	55986.0	63210.0	72240.0	81270.0
Acenaphthylene	48347.5	48732.0	55020.0	62880.0	70740.0
Acenaphthene	1906.8	1922.0	2170.0	2480.0	2790.0
Fluorene	5105.4	5146.0	5810.0	6640.0	7470.0
Phenanthrene	-	15128.0	17080.0	19520.0	21960.0
Anthracene	3998.2	4030.0	4550.0	5200.0	5850.0
Fluoranthene	4244.2	4278.0	4830.0	5520.0	6210.0
Pyrene	4490.3	4526.0	5110.0	5840.0	6570.0
Benzo[<i>a</i>]anthracene	3075.5	3100.0	3500.0	4000.0	4500.0
Chrysene	2337.4	2356.0	2660.0	3040.0	3420.0
Benzo[<i>b</i>]fluoranthene	922.7	930.0	1050.0	1200.0	1350.0
Benzo[<i>k</i>]fluoranthene	307.6	310.0	350.0	400.0	450.0
Benzo[<i>a</i>]pyrene	799.6	806.0	910.0	1040.0	1170.0
Indeno[1,2,3- <i>cd</i>]pyrene	55.4	55.8	63.0	72.0	81.0
Dibenzo[<i>ah</i>]anthracene	12.3	12.4	14.0	16.0	18.0
Benzo[<i>ghi</i>]perylene	615.1	620.0	700.0	800.0	900.0

Domestic coal combustion	[kg]				
	2002	2003	2004	2005	2006
Naphthalene	58582.0	51945.2	45655.8	36198.4	42325.0
Acenaphthylene	3396.0	3011.3	2646.7	2098.4	2453.6
Acenaphthene	2488.8	2206.9	1939.7	1537.9	1798.1
Fluorene	7699.2	6826.9	6000.3	4757.4	5562.6
Phenanthrene	-	2762.8	2428.3	1925.3	2251.1
Anthracene	878.7	779.1	684.8	543.0	634.8
Fluoranthene	1415.4	1255.0	1103.1	874.6	1022.6
Pyrene	1415.4	1255.0	1103.1	874.6	1022.6
Benzo[<i>a</i>]anthracene	850.2	753.9	662.6	525.3	614.3
Chrysene	793.2	703.3	618.2	490.1	573.1
Benzo[<i>b</i>]fluoranthene	33.3	29.5	25.9	20.5	24.0
Benzo[<i>k</i>]fluoranthene	9.5	8.4	7.4	5.9	6.9
Benzo[<i>a</i>]pyrene	736.2	652.8	573.8	454.9	531.9
Indeno[1,2,3- <i>cd</i>]pyrene	565.2	501.2	440.5	349.3	408.4
Dibenzo[<i>ah</i>]anthracene	850.2	753.9	662.6	525.3	614.3
Benzo[<i>ghi</i>]perylene	389.5	345.4	303.5	240.7	281.4

Diesel exhaust emissions	[kg]				
	2002	2003	2004	2005	2006
Naphthalene	45146.6	44853.2	45097.6	45076.2	44810.4
Acenaphthylene	6566.2	6609.6	6709.0	6732.4	6749.6
Acenaphthene	5152.1	5126.9	5152.1	5129.2	5112.7
Fluorene	3447.2	3429.9	3441.7	3420.3	3384.5
Phenanthrene	-	10121.0	10380.7	10513.1	10358.5
Anthracene	626.4	627.6	633.5	632.1	628.1
Fluoranthene	2952.6	2833.7	2744.3	2647.0	2520.6
Pyrene	2632.4	2470.9	2342.3	2213.8	2086.9
Benzo[<i>a</i>]anthracene	534.2	516.9	503.3	486.4	461.8
Chrysene	745.8	693.7	651.1	608.0	571.5
Benzo[<i>b</i>]fluoranthene	246.0	225.5	208.6	192.1	179.6
Benzo[<i>k</i>]fluoranthene	213.2	191.7	173.6	156.3	144.8
Benzo[<i>a</i>]pyrene	130.9	120.7	112.5	104.9	97.4
Indeno[1,2,3- <i>cd</i>]pyrene	143.1	133.0	124.7	116.8	108.7
Dibenzo[<i>ah</i>]anthracene	38.7	36.2	34.0	31.9	29.2
Benzo[<i>ghi</i>]perylene	206.7	184.9	166.7	150.6	135.1

Gasoline exhaust emissions	[kg]				
	2002	2003	2004	2005	2006
Naphthalene	39492.8	37401.4	35239.5	32416.0	29995.8
Acenaphthylene	2217.8	2031.3	1832.6	1671.1	1526.1
Acenaphthene	1671.0	1529.0	1377.0	1254.2	1143.2
Fluorene	1192.2	1102.4	1008.3	929.3	860.6
Phenanthrene	-	5219.1	4313.8	3850.5	3393.6
Anthracene	799.9	695.9	582.0	521.3	462.7
Fluoranthene	2086.0	1840.3	1569.4	1420.9	1278.1
Pyrene	862.6	781.0	692.4	637.1	586.6
Benzo[<i>a</i>]anthracene	205.0	194.1	183.6	175.0	168.7
Chrysene	189.1	182.3	176.7	169.2	164.8
Benzo[<i>b</i>]fluoranthene	191.2	178.6	166.2	157.1	149.9
Benzo[<i>k</i>]fluoranthene	125.3	120.6	117.0	112.6	110.1
Benzo[<i>a</i>]pyrene	109.7	102.3	94.3	88.3	83.0
Indeno[1,2,3- <i>cd</i>]pyrene	171.5	157.2	141.5	131.4	122.2
Dibenzo[<i>ah</i>]anthracene	16.9	17.0	17.4	17.2	17.4
Benzo[<i>ghi</i>]perylene	489.6	452.0	415.6	391.3	373.1

Appendix C: UK energy consumption

Table C.1. *UK coal consumption, 1980 to 2011* (<https://www.gov.uk/government/statistics/uk-energy-in-brief-2012>).

	[Million tonnes]					
	1980	1990	2000	2009	2010	2011
Power stations	89.6	84.0	46.9	39.7	41.5	41.9
Domestic	8.9	4.2	1.9	0.7	0.7	0.7
Industry	7.9	6.3	1.9	1.7	1.7	1.7
Services	1.8	1.2	0.08	0.09	0.06	0.05
Other energy industries	15.3	12.5	9.2	6.6	7.5	7.2
Total consumption	123.5	108.3	59.9	48.8	51.5	51.5

References

- Achten, C., Hofmann, T. (2009). Native polycyclic aromatic hydrocarbons (PAH) in coals – A hardly recognized source of environmental contamination. *Science of The Total Environment* **407**, 2461-2473.
- AEA (2009). EU Fuel Quality Monitoring – 2007 Summary Report. *United Kingdom Atomic Energy Authority Group*.
- AEA (2011). Final Contract Report for the UK PAH monitoring and Analysis Network (2004-2010). *United Kingdom Atomic Energy Authority Group*.
- Aekplakorn, W. (2003). Acute effect of sulphur dioxide from a power plant on pulmonary function of children, Thailand. *International Journal of Epidemiology* **32**, 854-861.
- Aiken, A. C., Decarlo, P. F., Kroll, J. H., Worsnop, D. R., Huffman, J. A., Docherty, K. S., Ulbrich, I. M., Mohr, C., Kimmel, J. R. and Sueper, D. (2008). O/C and OM/OC ratios of primary, secondary, and ambient organic aerosols with high-resolution time-of-flight aerosol mass spectrometry. *Environmental Science and Technology*, **42**, 4478-4485.
- Alam, M. S., Delgado-Saborit, J. M., Stark, C. and Harrison, R. M. (2013). Using atmospheric measurements of PAH and quinone compounds at roadside and urban background sites to assess sources and reactivity. *Atmospheric Environment*, **77**, 24-35.
- Alam, M. S., Delgado-Saborit, J. M., Stark, C. and Harrison, R. M. (2014). Investigating PAH relative reactivity using congener profiles, quinone measurements and back trajectories. *Atmospheric Chemistry and Physics*, **14**, 2467-2477.
- Allen, J. O., Dookeran, N. M., Smith, K. A., Sarofim, A. F., Taghizadeh, K. and Lafleur, A. L. (1996). Measurement of Polycyclic Aromatic Hydrocarbons Associated with Size-Segregated Atmospheric Aerosols in Massachusetts. *Environmental Science and Technology*, **30**, 1023-1031.

- Alsberg, T., H Kansson, S., Strndell, M. and Westerholm, R. (1989). Profile analysis of urban air pollution. *Chemometrics and Intelligent Laboratory Systems*, **7**, 143-152.
- Atkinson, R. and Arey, J. (1994). Atmospheric chemistry of gas-phase polycyclic aromatic hydrocarbons: formation of atmospheric mutagens. *Environmental Health Perspectives*, **102**, 117-126.
- Atkinson, R. and Arey, J. (2007). Mechanisms of the gas-phase reactions of aromatic hydrocarbons and PAH with OH and NO₃ radicals. *Polycyclic Aromatic Compounds*, **27**, 15-40.
- Atkinson, R. and Aschmann, S. M. (1988). Kinetics of the reactions of acenaphthene and acenaphthylene and structurally-related aromatic compounds with OH and NO₃ radicals, N₂O₅ and O₃ at 296±2 K. *International Journal of Chemical Kinetics*, **20**, 513-539.
- Ayi-Fanou, L., Avogbe, P. H., Fayomi, B., Keith, G., Hountondji, C., Creppy, E. E., Autrup, H., Rihn, B. H. and Sanni, A. (2011). DNA-adducts in subjects exposed to urban air pollution by benzene and polycyclic aromatic hydrocarbons (PAH) in Cotonou, Benin. *Environmental Toxicology*, **26**, 93-102.
- Bae, M. S., Demerjian, K. L. and Schwab, J. J. (2006). Seasonal estimation of organic mass to organic carbon in PM_{2.5} at rural and urban locations in New York state. *Atmospheric Environment*, **40**, 7467-7479.
- Baek, S. O., Goldstone, M. E., Kirk, P. W. W., Lester, J. N. and Perry, R. (1991). Phase distribution and particle size dependency of polycyclic aromatic hydrocarbons in the urban atmosphere. *Chemosphere*, **22**, 503-520.
- Bamford, H. A., Poster, D. L. and Baker, J. E. (1999). Temperature dependence of Henry's law constants of thirteen polycyclic aromatic hydrocarbons between 4°C and 31°C. *Environmental Toxicology and Chemistry*, **18**, 1905-1912.
- Baraniecka, J., Pyrzyńska, K., Szewczyńska, M., Pośniak, M. and Dobrzyńska, E. (2010). Emission of polycyclic aromatic hydrocarbons from selected processes in steelworks. *Journal of Hazardous Materials*, **183**, 111-115.

- Belis, C. A., Larsen, B. R., Amato, F., Haddad, I. E., Favez, O., Harrison, R. M., Hopke, P. K., Nava, S., Paatero, P., Prévôt, A., Quass, U., Vecchi, R. and Viana, M. (2014). European Guide on Air Pollution Source Apportionment with Receptor Models.
- Benner, B. A. (1995). Distinguishing the Contributions of Residential Wood Combustion and Mobile Source Emissions Using Relative Concentrations of Dimethylphenanthrene Isomers. *Environmental science*, **29**, 2382-2389.
- Benner, B. A., Gordon, G. E. and Wise, S. A. (1989). Mobile sources of atmospheric polycyclic aromatic hydrocarbons: a roadway tunnel study. *Environmental Science and Technology*, **23**, 1269-1278.
- Black, D. and Black, J. (2009). A Review of the Urban Development and Transport Impacts on Public Health with Particular Reference to Australia: Trans-Disciplinary Research Teams and Some Research Gaps. *International Journal of Environmental Research and Public Health*, **6**, 1557-1596.
- Blake, N., Penkett, S., Clemitshaw, K., Anwyl, P., Lightman, P., Marsh, A. and Butcher, G. (1993). Estimates of atmospheric hydroxyl radical concentrations from the observed decay of many reactive hydrocarbons in well-defined urban plumes. *Journal of Geophysical Research: Atmospheres (1984–2012)*, **98**, 2851-2864.
- Bojes, H. K. and Pope, P. G. (2007). Characterization of EPA's 16 priority pollutant polycyclic aromatic hydrocarbons (PAH) in tank bottom solids and associated contaminated soils at oil exploration and production sites in Texas. *Regulatory Toxicology and Pharmacology*, **47**, 288-295.
- Brown, A. S. and Brown, R. J. C. (2012). Correlations in polycyclic aromatic hydrocarbon (PAH) concentrations in UK ambient air and implications for source apportionment. *Journal of Environmental Monitoring*, **14**, 2072-2082.
- Brown, A. S., Butterfield, D. M., Brown, R. J., Hughey, P., Whiteside, K. J., Goddard, S. L. and Williams, M. (2011). Annual Report for 2010 on the UK PAH Monitoring and Analysis Network. *NPL Report AS*, **62**, 1-54.

- Brubaker, W. W. and Hites, R. A. (1998). OH reaction kinetics of polycyclic aromatic hydrocarbons and polychlorinated dibenzo-p-dioxins and dibenzofurans. *The Journal of Physical Chemistry A*, **102**, 915-921.
- Butterfield, D. and Brown, R. (2012). Polycyclic Aromatic Hydrocarbons in Northern Ireland. *NPL Report AS*, **66**, 1-94.
- Cabrerizo, A., Dachs, J., Moeckel, C., Ojeda, M.-J., Caballero, G., Barcel, D. and Jones, K. C. (2011). Ubiquitous Net Volatilization of Polycyclic Aromatic Hydrocarbons from Soils and Parameters Influencing Their Soil–Air Partitioning. *Environmental Science and Technology*, **45**, 4740-4747.
- Callen, M. S., Lopez, J. M. and Mastral, A. M. (2011). Characterization of PM₁₀-bound polycyclic aromatic hydrocarbons in the ambient air of Spanish urban and rural areas. *Journal of Environmental Monitoring*, **13**, 319-327.
- Cao, Q., Wang, H. and Chen, G. (2011). Source apportionment of PAHs Using Two Mathematical Models for Mangrove Sediments in Shantou Coastal Zone, China. *Estuaries and Coasts*, **34**, 950-960.
- Chao, M. R., Hu, C. W., Chen, Y. L., Chang-Chien, G. P., Lee, W. J., Chang, L. W., Lee, W. S. and Wu, K. Y. (2004). Approaching gas–particle partitioning equilibrium of atmospheric PCDD/Fs with increasing distance from an incinerator: measurements and observations on modelling. *Atmospheric Environment*, **38**, 1501-1510.
- Chen, Y. J., Sheng, G. Y., Bi, X. H., Feng, Y. L., Mai, B. X. and Fu, J. M. (2005). Emission factors for carbonaceous particles and polycyclic aromatic hydrocarbons from residential coal combustion in China. *Environmental Science and Technology*, **39**, 1861-1867.
- Christensen, E. R. and Arora, S. (2007). Source apportionment of PAH in sediments using factor analysis by time records: Application to Lake Michigan, USA. *Water Research*, **41**, 168-176.

- Ciaparra, D., Aries, E., Booth, M.-J., Anderson, D. R., Almeida, S. M. and Harrad, S. (2009). Characterisation of volatile organic compounds and polycyclic aromatic hydrocarbons in the ambient air of steelworks. *Atmospheric Environment*, **43**, 2070-2079.
- Cincinelli, A., Bubba, M. D., Martellini, T., Gambaro, A. and Lepri, L. (2007). Gas-particle concentration and distribution of n-alkanes and polycyclic aromatic hydrocarbons in the atmosphere of Prato (Italy). *Chemosphere*, **68**, 472-478.
- Cohen, A. J., Ross A. H., Ostro, B., Pandey, K. D., Krzyzanowski, M., Künzli, N., Gutschmidt, K., Pope, A., Romieu, I. and Samet, J. M. (2005). The global burden of disease due to outdoor air pollution. *Journal of Toxicology and Environmental Health, Part A*, **68**, 1301-1307.
- Coleman, P. J., Lee, R. G. M., Alcock, R. E. and Jones, K. C. (1997). Observations on PAH, PCB, and PCDD/F Trends in U.K. Urban Air, 1991–1995. *Environmental Science and Technology*, **31**, 2120-2124.
- Collins, J. F., Brown, J. P., Alexeeff, G. V. and Salmon, A. G. (1998). Potency Equivalency Factors for Some Polycyclic Aromatic Hydrocarbons and Polycyclic Aromatic Hydrocarbon Derivatives. *Regulatory Toxicology and Pharmacology*, **28**, 45-54.
- Colvile, R., Hutchinson, E., Mindell, J. and Warren, R. (2001). The transport sector as a source of air pollution. *Atmospheric Environment*, **35**, 1537-1565.
- Comandini, A., Malewicki, T. and Brezinsky, K. (2012). Chemistry of Polycyclic Aromatic Hydrocarbons Formation from Phenyl Radical Pyrolysis and Reaction of Phenyl and Acetylene. *The Journal of Physical Chemistry A*, **116**, 2409-2434.
- Corval N, A. P.-Ü. A. C. (2006). Preventing disease through healthy environments. *WHO Library Cataloguing-in-Publication Data*.
- Curtis, L., Rea, W., Smith-Willis, P., Fenyves, E. and Pan, Y. (2006). Adverse health effects of outdoor air pollutants. *Environment International*, **32**, 815-830.

- Dachs, J. and Eisenreich, S. J. (2000). Adsorption onto Aerosol Soot Carbon Dominates Gas-Particle Partitioning of Polycyclic Aromatic Hydrocarbons. *Environmental Science and Technology*, **34**, 3690-3697.
- Daisey, J. M., Cheney, J. L. and Lioy, P. J. (1986). Profiles of organic particulate emissions from air pollution sources: status and needs for receptor source apportionment modelling. *Journal of Air Pollution Control Association*, **36**, 17-33.
- Dachs, J., Ribes, S., Van Drooge, B., Grimalt, J., Eisenreich, S. J. and Gustafsson, Ø. (2004). Response to the comment on “Influence of soot carbon on the soil-air partitioning of polycyclic aromatic hydrocarbons”. *Environmental Science and Technology*, **38**, 1624-1625.
- Dall’osto, M., Booth, M. J., Smith, W., Fisher, R. and Harrison, R. M. (2008). A Study of the Size Distributions and the Chemical Characterization of Airborne Particles in the Vicinity of a Large Integrated Steelworks. *Aerosol Science and Technology*, **42**, 981-991.
- Dall’osto, M., Drewnick, F., Fisher, R. and Harrison, R. M. (2012). Real-Time Measurements of Nonmetallic Fine Particulate Matter Adjacent to a Major Integrated Steelworks. *Aerosol Science and Technology*, **46**, 639-653.
- Delgado-Saborit, J. M., Stark, C. and Harrison, R. M. (2011). Carcinogenic potential, levels and sources of polycyclic aromatic hydrocarbon mixtures in indoor and outdoor environments and their implications for air quality standards. *Environment International*, **37**, 383-392.
- Delgado-Saborit, J. M., Stark, C. and Harrison, R. M. (2013). Use of a Versatile High Efficiency Multiparallel Denuder for the Sampling of PAH in Ambient Air: Gas and Particle Phase Concentrations, Particle Size Distribution and Artifact Formation. *Environmental Science and Technology*, **48**, 499-507.
- Delhomme, O. and Millet, M. (2012). Characterization of particulate polycyclic aromatic hydrocarbons in the east of France urban areas. *Environmental Science and Pollution Research*, **19**, 1791-1799.

- Dennis, R., Fox, T., Fuentes, M., Gilliland, A., Hanna, S., Hogrefe, C., Irwin, J., Rao, S. T., Scheffe, R., Schere, K., Steyn, D. and Venkatram, A. (2010). A framework for evaluating regional-scale numerical photochemical modelling systems. *Environmental Fluid Mechanics*, **10**, 471-489.
- Dillon, M., Lamanna, M., Schade, G., Goldstein, A. and Cohen, R. (2002). Chemical evolution of the Sacramento urban plume: Transport and oxidation. *Journal of Geophysical Research: Atmospheres (1984–2012)*, **107**, ACH 3_1-ACH 3_15.
- Donahue, N., Chuang, W., Epstein, S., Kroll, J., Worsnop, D., Robinson, A., Adams, P. and Pandis, S. (2013). Why do organic aerosols exist? Understanding aerosol lifetimes using the two-dimensional volatility basis set. *Environmental Chemistry*, **10**, 151-157.
- Duan, J., Bi, X., Tan, J., Sheng, G. and Fu, J. (2007). Seasonal variation on size distribution and concentration of PAH in Guangzhou city, China. *Chemosphere*, **67**, 614-622.
- Dutton, S. J., Vedal, S., Piedrahita, R., Milford, J. B., Miller, S. L. and Hannigan, M. P. (2010). Source apportionment using positive matrix factorization on daily measurements of inorganic and organic speciated PM_{2.5}. *Atmospheric Environment*, **44**, 2731-2741.
- Dvorská, A., Komprdová, K., Lammel, G., Klánová, J., and Plachá, H. (2012). Polycyclic aromatic hydrocarbons in background air in central Europe – Seasonal levels and limitations for source apportionment. *Atmospheric Environment*, **46**, 147-154.
- Dvorská, A., Lammel, G. and Klánová, J. (2011). Use of diagnostic ratios for studying source apportionment and reactivity of ambient polycyclic aromatic hydrocarbons over Central Europe. *Atmospheric Environment*, **45**, 420-427.
- Ebi, K. L. and McGregor, G. (2008). Climate Change, Tropospheric Ozone and Particulate Matter, and Health Impacts. *Environmental Health Perspectives*, **116**, 1449-1455.

- Emmerson, K. M., Carslaw, N., Carpenter, L. J., Heard, D. E., Lee, J. D. and Pilling, M. J. (2005). Urban Atmospheric Chemistry During the PUMA Campaign 1: Comparison of Modelled OH and HO₂ Concentrations with Measurements. *Journal of Atmospheric Chemistry*, **52**, 143-164.
- Emmerson, K. M., Carslaw, N., Carslaw, D. C., Lee, J. D. Mcfiggans, G., Bloss, W. J., Gravestock, T., Heard, D. E., Hopkins, J., Ingham, T., Pilling, M. J., Smith, S. C., Jacob, M. and Monks, P. S. (2007). Free radical modelling studies during the UK TORCH Campaign in Summer 2003. *Atmospheric Chemistry and Physics*, **7**, 167-181.
- Esteve, W., Budzinski, H. and Villenave, E. (2004). Relative rate constants for the heterogeneous reactions of OH, NO₂ and NO radicals with polycyclic aromatic hydrocarbons adsorbed on carbonaceous particles. Part 1: PAH adsorbed on 1–2 µm calibrated graphite particles. *Atmospheric Environment*, **38**, 6063-6072.
- Esteve, W., Budzinski, H. and Villenave, E. (2006). Relative rate constants for the heterogeneous reactions of NO₂ and OH radicals with polycyclic aromatic hydrocarbons adsorbed on carbonaceous particles. Part 2: PAH adsorbed on diesel particulate exhaust SRM 1650a. *Atmospheric Environment*, **40**, 201-211.
- Farmer, P. B., Singh, R., Kaur, B., Sram, R. J., Binkova, B., Kalina, I., Popov, T. A., Garte, S., Taioli, E. and Gabelova, A. (2003). Molecular epidemiology studies of carcinogenic environmental pollutants: effects of polycyclic aromatic hydrocarbons (PAH) in environmental pollution on exogenous and oxidative DNA damage. *Mutation Research/Reviews in Mutation Research*, **544**, 397-402.
- Fattore, E., Paiano, V., Borgini, A., Tittarelli, A., Bertoldi, M., Crosignani, P. and Fanelli, R. (2011). Human health risk in relation to air quality in two municipalities in an industrialized area of Northern Italy. *Environmental Research*, **111**, 1321-1327.
- Friedman, C. L., Pierce, J. R. and Selin, N. E. (2014). Assessing the Influence of Secondary Organic versus Primary Carbonaceous Aerosols on Long-Range Atmospheric Polycyclic Aromatic Hydrocarbon Transport. *Environmental Science and Technology*, **48**, 3293-3302.

- Fu, F., Tian, B., Lin, G., Chen, Y. and Zhang, J. (2010). Chemical Characterization and Source Identification of Polycyclic Aromatic Hydrocarbons in Aerosols Originating from Different Sources. *Journal of the Air and Waste Management Association*, **60**, 1309-1314.
- Gaffney, J. S. and Marley, N. A. (2009). The impacts of combustion emissions on air quality and climate – From coal to biofuels and beyond. *Atmospheric Environment*, **43**, 23-36.
- Galarneau, E. (2008). Source specificity and atmospheric processing of airborne PAH: Implications for source apportionment. *Atmospheric Environment*, **42**, 8139-8149.
- Galarneau, E., Bidleman, T. F. and Blanchard, P. (2006). Seasonality and interspecies differences in particle/gas partitioning of PAH observed by the Integrated Atmospheric Deposition Network (IADN). *Atmospheric Environment*, **40**, 182-197.
- Galarneau, E., Makar, P., Zheng, Q., Narayan, J., Zhang, J., Moran, M., Bari, M., Pathela, S., Chen, A. and Chlumsky, R. (2013). PAH concentrations simulated with the AURAMS-PAH chemical transport model over Canada and the USA. *Atmospheric Chemistry and Physics Discussions*, **13**, 18417-18449.
- Gillespie-Bennett, J., Pierse, N., Wickens, K., Crane, J., Howden-Chapman, P. and Housing Heating and Health Study Research Team. (2011). The respiratory health effects of nitrogen dioxide in children with asthma. *European Respiratory Journal*, **38**, 303-309.
- Gogou, A., Stratigakis, N., Kanakidou, M. and Stephanou, E. G. (1996). Organic aerosols in Eastern Mediterranean: components source reconciliation by using molecular markers and atmospheric back trajectories. *Organic Geochemistry*, **25**, 79-96.
- Gomišček, B., Hauck, H., Stopper, S. and Preining, O. (2004). Spatial and temporal variations of PM₁, PM_{2.5}, PM₁₀ and particle number concentration during the AUPHEP—project. *Atmospheric Environment*, **38**, 3917-3934.

- Grice, K., Lu, H., Atahan, P., Asif, M., Hallmann, C., Greenwood, P., Maslen, E., Tulipani, S., Williford, K. and Dodson, J. (2009). New insights into the origin of perylene in geological samples. *Geochimica et Cosmochimica Acta*, **73**, 6531-6543.
- Gun L Vblad, L. T., Kjetil T Rseth (2004). Convention on Long-range Transboundary Air Pollution. *EMEP Assessment Report*.
- Guo, H. (2003). Particle-associated polycyclic aromatic hydrocarbons in urban air of Hong Kong. *Atmospheric Environment*, **37**, 5307-5317.
- Gustafson, K. E. and Dickhut, R. M. (1996). Particle/Gas Concentrations and Distributions of PAH in the Atmosphere of Southern Chesapeake Bay†. *Environmental Science and Technology*, **31**, 140-147.
- Halsall, C. J., Sweetman, A. J., Barrie, L. A. and Jones, K. C. (2001). Modelling the behaviour of PAH during atmospheric transport from the UK to the Arctic. *Atmospheric Environment*, **35**, 255-267.
- Harkov, R., Greenberg, A., Darack, F., Daisey, J. M. and Lioy, P. J. (1984). Summertime variations in polycyclic aromatic hydrocarbons at four sites in New Jersey. *Environmental Science and Technology*, **18**, 287-291.
- Harner, T. and Bidleman, T. F. (1998a). Measurement of Octanol–Air Partition Coefficients for Polycyclic Aromatic Hydrocarbons and Polychlorinated Naphthalenes. *Journal of Chemical and Engineering Data*, **43**, 40-46.
- Harner, T. and Bidleman, T. F. (1998b). Octanol–Air Partition Coefficient for Describing Particle/Gas Partitioning of Aromatic Compounds in Urban Air. *Environmental Science and Technology*, **32**, 1494-1502.
- Harrison, R. M. and Jones, A. M. (2005). Multisite Study of Particle Number Concentrations in Urban Air. *Environmental Science and Technology*, **39**, 6063-6070.

- Harrison, R. M., Jones, A. M. and Lawrence, R. G. (2003). A pragmatic mass closure model for airborne particulate matter at urban background and roadside sites. *Atmospheric Environment*, **37**, 4927-4933.
- Harrison, R. M., Jones, A. M. and Lawrence, R. G. (2004). Major component composition of PM₁₀ and PM_{2.5} from roadside and urban background sites. *Atmospheric Environment*, **38**, 4531-4538.
- Harrison, R. M., Smith, D. J. T. and Luhana, L. (1996). Source Apportionment of Atmospheric Polycyclic Aromatic Hydrocarbons Collected from an Urban Location in Birmingham, U.K. *Environmental Science and Technology*, **30**, 825-832.
- Harrison, R. M., Yin, J., Tilling, R. M., Cai, X., Seakins, P. W., Hopkins, J. R., Lansley, D. L., Lewis, A. C., Hunter, M. C., Heard, D. E., Carpenter, L. J., Creasey, D. J., Lee, J. D., Pilling, M. J., Carslaw, N., Emmerson, K. M., Redington, A., Derwent, R. G., Ryall, D., Mills, G. and Penkett, S. A. (2006). Measurement and modelling of air pollution and atmospheric chemistry in the U.K. West Midlands conurbation: Overview of the PUMA Consortium project. *Science of The Total Environment*, **360**, 5-25.
- Hays, M. D. and Vander Wal, R. L. (2007). Heterogeneous Soot Nanostructure in Atmospheric and Combustion Source Aerosols. *Energy and Fuels*, **21**, 801-811.
- Heard, D., Carpenter, L., Creasey, D., Hopkins, J., Lee, J., Lewis, A., Pilling, M., Seakins, P., Carslaw, N. and Emmerson, K. (2004). High levels of the hydroxyl radical in the winter urban troposphere. *Geophysical research letters*, **31**, L18112.
- Heeb, N. V., Schmid, P., Kohler, M., Gujer, E., Zennegg, M., Wenger, D., Wichser, A., Ulrich, A., Gfeller, U., Honegger, P., Zeyer, K., Emmenegger, L., Petermann, J.-L., Czerwinski, J., Mosimann, T., Kasper, M. and Mayer, A. (2008). Secondary Effects of Catalytic Diesel Particulate Filters: Conversion of PAH versus Formation of Nitro-PAH. *Environmental Science and Technology*, **42**, 3773-3779.

- Hemann, J., Brinkman, G., Dutton, S., Hannigan, M., Milford, J. and Miller, S. (2008). Assessing positive matrix factorization model fit: a new method to estimate uncertainty and bias in factor contributions at the daily time scale. *Atmospheric Chemistry and Physics Discussions*, **8**, 2977-3026.
- Homann, K. H. and Wagner, H. G. (1967). Some new aspects of the mechanism of carbon formation in premixed flames. *Symposium (International) on Combustion*, **11**, 371-379.
- Hopke, P. K. (2000). A guide to positive matrix factorization. *In: Workshop on UNMIX and PMF as Applied to PM₂*.
- Hopke, P. K., Ito, K., Mar, T., Christensen, W. F., Eatough, D. J., Henry, R. C., Kim, E., Laden, F., Lall, R., Larson, T. V., Liu, H., Neas, L., Pinto, J., Stolzel, M., Suh, H., Paatero, P. and Thurston, G. D. (2005). PM source apportionment and health effects: 1. Intercomparison of source apportionment results. *J Expos Sci Environ Epidemiol*, **16**, 275-286.
- Ito, K., Christensen, W. F., Eatough, D. J., Henry, R. C., Kim, E., Laden, F., Lall, R., Larson, T. V., Neas, L., Hopke, P. K. and Thurston, G. D. (2005). PM source apportionment and health effects: 2. An investigation of intermethod variability in associations between source-apportioned fine particle mass and daily mortality in Washington, DC. *J Expos Sci Environ Epidemiol*, **16**, 300-310.
- Jang, E., Alam, M. S. and Harrison, R. M. (2013). Source Apportionment of Polycyclic Aromatic Hydrocarbons in Urban Air Using Positive Matrix Factorization and Spatial Distribution Analysis. *Atmospheric Environment*, **79**, 271-285.
- Jones, A. M. and Harrison, R. M. (2011). Temporal trends in sulphate concentrations at European sites and relationships to sulphur dioxide. *Atmospheric Environment*, **45**, 873-882.

- Jones, A. M., Harrison, R. M., Barratt, B. and Fuller, G. (2012). A large reduction in airborne particle number concentrations at the time of the introduction of “sulphur free” diesel and the London Low Emission Zone. *Atmospheric Environment*, **50**, 129-138.
- Kameda, Y., Shirai, J., Komai, T., Nakanishi, J. and Masunaga, S. (2005). Atmospheric polycyclic aromatic hydrocarbons: size distribution, estimation of their risk and their depositions to the human respiratory tract. *Science of The Total Environment*, **340**, 71-80.
- Kashimura, N., Hayashi, J.-I., LI, C.-Z., Sathe, C. and Chiba, T. (2004). Evidence of poly-condensed aromatic rings in a Victorian brown coal. *Fuel*, **83**, 97-107.
- Kanaya, Y., Cao, R., Akimoto, H., Fukuda, M., Komazaki, Y., Yokouchi, Y., Koike, M., Tanimoto, H., Takegawa, N. and Kondo, Y. (2007). Urban photochemistry in central Tokyo: 1. Observed and modeled OH and HO₂ radical concentrations during the winter and summer of 2004. *Journal of Geophysical Research: Atmospheres*, **112**, D21312.
- Katsoyiannis, A. and Breivik, K. (2014). Model-based evaluation of the use of polycyclic aromatic hydrocarbons molecular diagnostic ratios as a source identification tool. *Environmental Pollution*, **184**, 488-494.
- Katsoyiannis, A., Sweetman, A. J. and Jones, K. C. (2011). PAH Molecular Diagnostic Ratios Applied to Atmospheric Sources: A Critical Evaluation Using Two Decades of Source Inventory and Air Concentration Data from the UK. *Environmental Science and Technology*, **45**, 8897-8906.
- Kaupp, H. and Michael, S. (1998). Atmospheric particle size distributions of polychlorinated dibenzo-p-dioxins and dibenzofurans (PCDD/Fs) and polycyclic aromatic hydrocarbons (PAH) and their implications for wet and dry deposition. *Atmospheric Environment*, **33**, 85-95.
- Kavouras, I. G., Koutrakis, P., Tsapakis, M., Lagoudaki, E., Stephanou, E. G., Von Baer, D. and Oyola, P. (2001). Source Apportionment of Urban Particulate Aliphatic and Polynuclear Aromatic Hydrocarbons (PAH) Using Multivariate Methods. *Environmental Science and Technology*, **35**, 2288-2294.

- Kavouras, I. G. and Stephanou, E. G. (2002). Particle size distribution of organic primary and secondary aerosol constituents in urban, background marine, and forest atmosphere. *Journal of Geophysical Research: Atmospheres (1984–2012)*, **107**, AAC 7-1-AAC 7-12.
- Kelishadi, R. and Poursafa, P. (2010). Air pollution and non-respiratory health hazards for children. *Archives of Medical Science*, **6**, 483-495.
- Keyte, I. J., Harrison, R. M. and Lammel, G. (2013). Chemical reactivity and long-range transport potential of polycyclic aromatic hydrocarbons—a review. *Chemical Society Reviews*, **42**, 9333-9391.
- Khalili, N. R., Scheff, P. A. and Holsen, T. M. (1995). PAH source fingerprints for coke ovens, diesel and, gasoline engines, highway tunnels, and wood combustion emissions. *Atmospheric Environment*, **29**, 533-542.
- Kim, D., Kumfer, B. M., Anastasio, C., Kennedy, I. M. and Young, T. M. (2009). Environmental aging of polycyclic aromatic hydrocarbons on soot and its effect on source identification. *Chemosphere*, **76**, 1075-1081.
- Kim, E. and Hopke, P. K. (2007). Comparison between sample-species specific uncertainties and estimated uncertainties for the source apportionment of the speciation trends network data. *Atmospheric Environment*, **41**, 567-575.
- Kuhn, T., Biswas, S., Fine, P. M., Geller, M. and Sioutas, C. (2005). Physical and chemical characteristics and volatility of PM in the proximity of a light-duty vehicle freeway. *Aerosol Science and Technology*, **39**, 347-357.
- Kulkarni, P. and Venkataraman, C. (2000). Atmospheric polycyclic aromatic hydrocarbons in Mumbai, India. *Atmospheric Environment*, **34**, 2785-2790.
- Lammel, G., Sehili, A. M., Bond, T. C., Feichter, J. and Grassl, H. (2009). Gas/particle partitioning and global distribution of polycyclic aromatic hydrocarbons – A modelling approach. *Chemosphere*, **76**, 98-106.

- Laongsri, B. (2012). Study of the properties of particulate matter in the UK atmosphere. Thesis. *University of Birmingham*.
- Larsen, R. K. and Baker, J. E. (2003). Source Apportionment of Polycyclic Aromatic Hydrocarbons in the Urban Atmosphere: A Comparison of Three Methods. *Environmental Science and Technology*, **37**, 1873-1881.
- Lee, J., Gigliotti, C., Offenberg, J., Eisenreich, S. and Turpin, B. (2004). Sources of polycyclic aromatic hydrocarbons to the Hudson River Airshed. *Atmospheric Environment*, **38**, 5971-5981.
- Lee, S., Liu, W., Wange, Y. H., Russell, A. G. and Edgerton, E. S. (2008). Source apportionment of PM_{2.5}: Comparing PMF and CMB results for four ambient monitoring sites in the southeastern United States. *Atmospheric Environment*, **42**, 4126-4137.
- Li, J., Zhang, G., Li, X. D., Qi, S. H., Liu, G. Q. and Peng, X. Z. (2006). Source seasonality of polycyclic aromatic hydrocarbons (PAH) in a subtropical city, Guangzhou, South China. *Science of The Total Environment*, **355**, 145-155.
- Li, W., Peng, Y., Shi, J., Qiu, W., Wang, J. and Bai, Z. (2011). Particulate polycyclic aromatic hydrocarbons in the urban Northeast Region of China: Profiles, distributions and sources. *Atmospheric Environment*, **45**, 7664-7671.
- Lim, L. H., Harrison, R. M. and Harrad, S. (1999). The contribution of Traffic to Atmospheric Concentrations of Polycyclic Aromatic Hydrocarbons. *Environmental Science and Technology*, **33**, 3538-3542.
- Lim, M. C. H., Ayoko, G. A., Morawska, L., Ristovski, Z. D. and Rohan Jayaratne, E. (2005). Effect of fuel composition and engine operating conditions on polycyclic aromatic hydrocarbon emissions from a fleet of heavy-duty diesel buses. *Atmospheric Environment*, **39**, 7836-7848.
- Lima, A. L. C., Eglinton, T. I. and Reddy, C. M. (2002). High-Resolution Record of Pyrogenic Polycyclic Aromatic Hydrocarbon Deposition during the 20th Century. *Environmental Science and Technology*, **37**, 53-61.

- Ling, Z. H., Guo, H., Cheng, H. R. and Yu, Y. F. (2011). Sources of ambient volatile organic compounds and their contributions to photochemical ozone formation at a site in the Pearl River Delta, southern China. *Environmental Pollution*, **159**, 2310-2319.
- Liu, C., Zhang, P., Yang, B., Wang, Y. and Shu, J. (2012a). Kinetic Studies of Heterogeneous Reactions of Polycyclic Aromatic Hydrocarbon Aerosols with NO₃ Radicals. *Environmental Science and Technology*, **46**, 7575-7580.
- Liu, L. Y., Wang, J. Z., Wei, G. L., Guan, Y. F. and Zeng, E. Y. (2012b). Polycyclic aromatic hydrocarbons (PAH) in continental shelf sediment of China: Implications for anthropogenic influences on coastal marine environment. *Environmental Pollution*, **167**, 155-162.
- Lohmann, R. and Lammel, G. (2004). Adsorptive and Absorptive Contributions to the Gas-Particle Partitioning of Polycyclic Aromatic Hydrocarbons: State of Knowledge and Recommended Parametrization for Modelling. *Environmental Science and Technology*, **38**, 3793-3803.
- Lu S Ferreira Braga, A., Zanobetti, A. and Schwartz, J. (2001). The Lag Structure Between Particulate Air Pollution and Respiratory and Cardiovascular Deaths in 10 US Cities. *Journal of Occupational and Environmental Medicine*, **43**, 927-933.
- Ma, W. L., Li, Y. F., Qi, H., Sun, D. Z., Liu, L. Y. and Wang, D. G. (2010). Seasonal variations of sources of polycyclic aromatic hydrocarbons (PAH) to a northeastern urban city, China. *Chemosphere*, **79**, 441-447.
- Manoli, E., Kouras, A. and Samara, C. (2004). Profile analysis of ambient and source emitted particle-bound polycyclic aromatic hydrocarbons from three sites in northern Greece. *Chemosphere*, **56**, 867-878.
- Marchand, N., Besombes, J. L., Chevron, N., Masclet, P., Aymoz, G. and Jaffrezo, J. L. (2004). Polycyclic aromatic hydrocarbons (PAH) in the atmospheres of two French alpine valleys: sources and temporal patterns. *Atmospheric Chemistry and Physics*, **4**, 1167-1181.

- Mari, M., Harrison, R. M., Schuhmacher, M., Domingo, J. L. and Pongpiachan, S. (2010). Inferences over the sources and processes affecting polycyclic aromatic hydrocarbons in the atmosphere derived from measured data. *Science of The Total Environment*, **408**, 2387-2393.
- Marr, L. C., Dzepina, K., Jimenez, J. L., Reisen, F., Bethel, H. L., Arey, J., Gaffney, J. S., Marley, N. A., Molina, L. T. and Molina, M. J. (2006). Sources and transformations of particle-bound polycyclic aromatic hydrocarbons in Mexico City. *Atmospheric Chemistry and Physics*, **6**, 1733-1745.
- Marr, L. C., Grogan, L. A., W Hrnshimmel, H., Molina, L. T., Molina, M. J., Smith, T. J. and Garshick, E. (2004). Vehicle Traffic as a Source of Particulate Polycyclic Aromatic Hydrocarbon Exposure in the Mexico City Metropolitan Area. *Environmental Science and Technology*, **38**, 2584-2592.
- Marr, L. C., Kirchstetter, T. W., Harley, R. A., Miguel, A. H., Hering, S. V. and Hammond, S. K. (1999). Characterization of Polycyclic Aromatic Hydrocarbons in Motor Vehicle Fuels and Exhaust Emissions. *Environmental Science and Technology*, **33**, 3091-3099.
- Mastral, A. M., L Pez, J. M., Call N, M. A. S., GarcíA, T., Murillo, R. and Navarro, M. A. V. (2003). Spatial and temporal PAH concentrations in Zaragoza, Spain. *Science of The Total Environment*, **307**, 111-124.
- Mccarry, B. E., Allan, L. M., Legzdins, A. E., Lundrigan, J. A., Marvin, C. H. and Bryant, D. W. (1996). Thia-Arenes as Pollution Source Tracers in Urban Air Particulate. *Polycyclic Aromatic Compounds*, **11**, 75-82.
- Mcdonald, J. D., zielinska, B., fujita, E. M., sagebiel, J. C., chow, J. C. and watson, J. G. (2000). Fine Particle and Gaseous Emission Rates from Residential Wood Combustion. *Environmental Science and Technology*, **34**, 2080-2091.

- Meijer, S. N., Sweetman, A. J., Halsall, C. J. and Jones, K. C. (2008). Temporal Trends of Polycyclic Aromatic Hydrocarbons in the U.K. Atmosphere: 1991–2005. *Environmental Science and Technology*, **42**, 3213-3218.
- Menezes, H. C. and Cardeal, Z. L. (2012). Study of polycyclic aromatic hydrocarbons in atmospheric particulate matter of an urban area with iron and steel mills. *Environmental Toxicology and Chemistry*, **31**, 1470-1477.
- Mi, H. H., Lee, W. J., Chen, C. B., Yang, H. H. and Wu, S. J. (2000). Effect of fuel aromatic content on PAH emission from a heavy-duty diesel engine. *Chemosphere*, **41**, 1783-1790.
- Miller, L., Lemke, L. D., Xu, X., Molaroni, S. M., You, H., Wheeler, A. J., Booza, J., Grgicak-Mannion, A., Krajenta, R. and Graniero, P. (2010). Intra-urban correlation and spatial variability of air toxics across an international airshed in Detroit, Michigan (USA) and Windsor, Ontario (Canada). *Atmospheric Environment*, **44**, 1162-1174.
- Mooibroek, D., Schaap, M., Weijers, E. P. and Hoogerbrugge, R. (2011). Source apportionment and spatial variability of PM_{2.5} using measurements at five sites in the Netherlands. *Atmospheric Environment*, **45**, 4180-4191.
- Monks, P. S., Granier, C., Fuzzi, S., Stohl, A., Williams, M. L., Akimoto, H., Amann, M., Baklanov, A., Baltensperger, U., Bey, I., Blake, N., Blake, R. S., Carslaw, K., Cooper, O. R., Dentener, F., Fowler, D., Fragkou, E., Frost, G. J., Generoso, S., Ginoux, P., Grewe, V., Guenther, A., Hansson, H. C., Henne, S., Hjorth, J., Hofzumahaus, A., Huntrieser, H., Isaksen, I. S. A., Jenkin, M. E., Kaiser, J., Kanakidou, M., Klimont, Z., Kulmala, M., Laj, P., Lawrence, M. G., Lee, J. D., Liousse, C., Maione, M., Mcfiggans, G., Metzger, A., Mieville, A., Moussiopoulos, N., Orlando, J. J., O'dowd, C. D., Palmer, P. I., Parrish, D. D., Petzold, A., Platt, U., P Schl, U., Pr V T, A. S. H., Reeves, C. E., Reimann, S., Rudich, Y., Sellegri, K., Steinbrecher, R., Simpson, D., Ten Brink, H., Theloke, J., Van Der Werf, G. R., Vautard, R., Vestreng, V., Vlachokostas, C. and Von Glasow, R. (2009). Atmospheric composition change – global and regional air quality. *Atmospheric Environment*, **43**, 5268-5350.

- Motelay-Massei, A., Ollivon, D., Garban, B., Tiphagne-Larcher, K., Zimmerlin, I. and Chevreuil, M. (2007). PAH in the bulk atmospheric deposition of the Seine river basin: Source identification and apportionment by ratios, multivariate statistical techniques and scanning electron microscopy. *Chemosphere*, **67**, 312-321.
- Mount, G. H. and Williams, E. J. (1997). An overview of the Tropospheric OH Photochemistry Experiment, Fritz Peak/Idaho Hill, Colorado, fall 1993. *Journal of Geophysical Research: Atmospheres*, **102**, 6171-6186.
- NAEI (2012). Air quality pollutants inventories for England, Scotland, Wales and Northern Ireland: 1990-2012. *National Atmospheric Emissions Inventory*.
- Neuberger, M., Rabczenko, D. and Moshhammer, H. (2007). Extended effects of air pollution on cardiopulmonary mortality in Vienna. *Atmospheric Environment*, **41**, 8549-8556.
- Nielsen, T. (1996). Traffic contribution of polycyclic aromatic hydrocarbons in the center of a large city. *Atmospheric Environment*, **30**, 3481-3490.
- Nielsen, T., Feilberg, A. and Binderup, M. L. (1999). The variation of street air levels of PAH and other mutagenic PAC in relation to regulations of traffic emissions and the impact of atmospheric processes. *Environmental Science and Pollution Research*, **6**, 133-137.
- Nielsen, T., J Rgensen, H., Poulsen, M., Palmgren Jensen, F., Larsen, J., Bang Jensen, A., Schramm, J. and T Nnesen, J. (1995). Traffic PAH and other mutagens in air in Denmark. *Ministry of the Environment and Eneergy, Denmark*, **285**, 1-148.
- Ning, Z., Geller, M. D., Moore, K. F., Sheesley, R., Schauer, J. J. and Sioutas, C. (2007). Daily variation in chemical characteristics of urban ultrafine aerosols and inference of their sources. *Environmental Science and Technology*, **41**, 6000-6006.
- Norris, G., Vedantham, R., Wade, K., Brown, S., Prouty, J. and Foley, C. (2008). EPA positive matrix factorization (PMF) 3.0 fundamentals and user guide. *Prepared for the US Environmental Protection Agency, Washington, DC, by the National Exposure Research Laboratory, Research Triangle Park*.

- Odabasi, M., Cetin, E. and Sofuoglu, A. (2006). Determination of octanol–air partition coefficients and supercooled liquid vapor pressures of PAH as a function of temperature: application to gas–particle partitioning in an urban atmosphere. *Atmospheric Environment*, **40**, 6615-6625.
- Ooi, T. C. and Lu, L. M. (2011). Formation and mitigation of PCDD/Fs in iron ore sintering. *Chemosphere*, **85**, 291-299.
- Orjuela, M. A., Liu, X., Warburton, D., Siebert, A. L., Cujar, C., Tang, D., Jobanputra, V. and Perera, F. P. (2010). Prenatal PAH exposure is associated with chromosome-specific aberrations in cord blood. *Mutation Research/Genetic Toxicology and Environmental Mutagenesis*, **703**, 108-114.
- Paatero, P. and U. Tapper (1994). Positive matrix factorization: A non-negative factor model with optimal utilization of error estimates of data values. *Environmetrics*, **5**, 111-126.
- Paatero, P., Hopke, P. K., Begum, B. A. and Biswas, S. K. (2005). A graphical diagnostic method for assessing the rotation in factor analytical models of atmospheric pollution. *Atmospheric Environment*, **39**, 193-201.
- Pankow, J. F. (1987). Review and comparative analysis of the theories on partitioning between the gas and aerosol particulate phases in the atmosphere. *Atmospheric Environment (1967)*, **21**, 2275-2283.
- Parenteau, M. P. and Sawada, M. C. (2011). The modifiable areal unit problem (MAUP) in the relationship between exposure to NO₂ and respiratory health. *International Journal of Health Geographics*, **10**, 1-15.
- Park, S. U., Kim, J. G., Jeong, M. J. and Song, B. J. (2011). Source Identification of Atmospheric Polycyclic Aromatic Hydrocarbons in Industrial Complex Using Diagnostic Ratios and Multivariate Factor Analysis. *Archives of Environmental Contamination and Toxicology*, **60**, 576-589.

- Pekkanen, J., Brunner, E. J., Anderson, H. R., Tiittanen, P. and Atkinson, R. W. (2000). Daily concentrations of air pollution and plasma fibrinogen in London. *Occupational and Environmental Medicine*, **57**, 818-822.
- Perraudin, E., Budzinski, H. and Villenave, E. (2005). Kinetic study of the reactions of NO₂ with polycyclic aromatic hydrocarbons adsorbed on silica particles. *Atmospheric Environment*, **39**, 6557-6567.
- Perraudin, E., Budzinski, H. and Villenave, E. (2007). Kinetic study of the reactions of ozone with polycyclic aromatic hydrocarbons adsorbed on atmospheric model particles. *Journal of Atmospheric Chemistry*, **56**, 57-82.
- Peters, A., Dockery, D. W., Heinrich, J. and Wichmann, H. E. (1997). Short-term effects of particulate air pollution on respiratory morbidity in asthmatic children. *European Respiratory Journal*, **10**, 872-879.
- Prevedouros, K. (2004). Modelling the atmospheric fate and seasonality of polycyclic aromatic hydrocarbons in the UK. *Chemosphere*, **56**, 195-208.
- Pufulete, M., Battershill, J., Boobis, A. and Fielder, R. (2004). Approaches to carcinogenic risk assessment for polycyclic aromatic hydrocarbons: a UK perspective. *Regulatory Toxicology and Pharmacology*, **40**, 54-66.
- Rajput, N. and Lakhani, A. (2010). Measurements of polycyclic aromatic hydrocarbons in an urban atmosphere of Agra, India. *Atmosfera*, **23**, 165-183.
- Ramdahl, T. (1983). Retene-a molecular marker of wood combustion in ambient air. *Nature*, **306**, 580-582.
- Ravindra, K., Bencs, L., Wauters, E., De Hoog, J., Deutsch, F., Roekens, E., Bleux, N., Berghmans, P. and Van Grieken, R. (2006). Seasonal and site-specific variation in vapour and aerosol phase PAH over Flanders (Belgium) and their relation with anthropogenic activities. *Atmospheric Environment*, **40**, 771-785.

- Ravindra, K., Sokhi, R. and Van Grieken, R. (2008a). Atmospheric polycyclic aromatic hydrocarbons: Source attribution, emission factors and regulation. *Atmospheric Environment*, **42**, 2895-2921.
- Ravindra, K., Wauters, E. and Van Grieken, R. (2008b). Variation in particulate PAH levels and their relation with the transboundary movement of the air masses. *Science of The Total Environment*, **396**, 100-110.
- Read, K. A., Lewis, A. C., Salmon, R. A., Jones, A. E. and Bauguitte, S. (2007). OH and halogen atom influence on the variability of non-methane hydrocarbons in the Antarctic Boundary Layer. *Tellus B*, **59**, 22-38.
- Reff, A., Eberly, S. I. and Bhawe, P. V. (2007). Receptor modelling of ambient particulate matter data using positive matrix factorization: review of existing methods. *Journal of the Air and Waste Management Association*, **57**, 146-154.
- Reisen, F. and Arey, J. (2002). Reactions of hydroxyl radicals and ozone with acenaphthene and acenaphthylene. *Environmental Science and Technology*, **36**, 4302-4311.
- Riddle, S. G., Robert, M. A., Jakober, C. A., Hannigan, M. P. and Kleeman, M. J. (2008). Size-resolved source apportionment of airborne particle mass in a roadside environment. *Environmental Science and Technology*, **42**, 6580-6586.
- Robinson, A. L., Donahue, N. M., Shrivastava, M. K., Weitkamp, E. A., Sage, A. M., Grieshop, A. P., Lane, T. E., Pierce, J. R. and Pandis, S. N. (2007). Rethinking organic aerosols: Semivolatile emissions and photochemical aging. *Science*, **315**, 1259-1262.
- Rogge, W. F., Hildemann, L. M., Mazurek, M. A., Cass, G. R. and Simoneit, B. R. T. (1993). Sources of fine organic aerosol. 2. Noncatalyst and catalyst-equipped automobiles and heavy-duty diesel trucks. *Environmental Science and Technology*, **27**, 636-651.
- Russell, L. M. (2003). Aerosol Organic-Mass-to-Organic-Carbon Ratio Measurements. *Environmental Science and Technology*, **37**, 2982-2987.

- Sander, L. C. and Wise, S. A. (1997). *Polycyclic aromatic hydrocarbon structure index*, US Department of Commerce, Technology Administration, National Institute of Standards and Technology.
- Schauer, C., Niessner, R. and Poschl, U. (2003). Polycyclic aromatic hydrocarbons in urban air particulate matter: Decadal and seasonal trends, chemical degradation, and sampling artifacts. *Environmental Science and Technology*, **37**, 2861-2868.
- Schouten, J. P., Vonk, J. M. and Degraaf, A. (1996). Short term effects of air pollution on emergency hospital admissions for respiratory disease: Results of the APHEA project in two major cities in The Netherlands, (1977-89). *Journal of Epidemiology and Community Health*, **50**, S22-S29.
- Sharma, H., Jain, V. K. and Khan, Z. H. (2007). Characterization and source identification of polycyclic aromatic hydrocarbons (PAH) in the urban environment of Delhi. *Chemosphere*, **66**, 302-310.
- Shen, G., Tao, S., Wei, S., Zhang, Y., Wang, R., Wang, B., Li, W., Shen, H., Huang, Y., Yang, Y., Wang, W., Wang, X. and Simonich, S. L. M. (2012). Retene Emission from Residential Solid Fuels in China and Evaluation of Retene as a Unique Marker for Soft Wood Combustion. *Environmental Science and Technology*, **46**, 4666-4672.
- Shen, G., Wang, W., Yang, Y., Zhu, C., Min, Y., Xue, M., Ding, J., Li, W., Wang, B., Shen, H., Wang, R., Wang, X. and Tao, S. (2010). Emission factors and particulate matter size distribution of polycyclic aromatic hydrocarbons from residential coal combustions in rural Northern China. *Atmospheric Environment*, **44**, 5237-5243.
- Sitaras, I. E., Bakeas, E. B. and Siskos, P. A. (2004). Gas/particle partitioning of seven volatile polycyclic aromatic hydrocarbons in a heavy traffic urban area. *Science of The Total Environment*, **327**, 249-264.
- Sofowote, U. M., Allan, L. M. and Mccarry, B. E. (2010a). A comparative study of two factor analytic models applied to PAH data from inhalable air particulate collected in an urban-industrial environment. *Journal of Environmental Monitoring*, **12**, 425-433.

- Sofowote, U. M., Allan, L. M. and Mccarry, B. E. (2010b). Evaluation of PAH diagnostic ratios as source apportionment tools for air particulates collected in an urban-industrial environment. *Journal of Environmental Monitoring*, **12**, 417-424.
- Sofowote, U. M., Hung, H., Rastogi, A. K., Westgate, J. N., Deluca, P. F., Su, Y. and Mccarry, B. E. (2011). Assessing the long-range transport of PAH to a sub-Arctic site using positive matrix factorization and potential source contribution function. *Atmospheric Environment*, **45**, 967-976.
- Sofowote, U. M., Hung, H., Rastogi, A. K., Westgate, J. N., Su, Y., Sverko, E., D'sa, I., Roach, P., Fellin, P. and Mccarry, B. E. (2010c). The gas/particle partitioning of polycyclic aromatic hydrocarbons collected at a sub-Arctic site in Canada. *Atmospheric Environment*, **44**, 4919-4926.
- Sofowote, U. M., Mccarry, B. E. and Marvin, C. H. (2008). Source Apportionment of PAH in Hamilton Harbour Suspended Sediments: Comparison of Two Factor Analysis Methods. *Environmental Science and Technology*, **42**, 6007-6014.
- Sundqvist, K. (2009). Sources of dioxins and other POPs to the marine environment: Identification and apportionment using pattern analysis and receptor modelling. *Umeå University, Chemistry, Thesis*, 1-69.
- Suzuki, N., Yessalina, S. and Kikuchi, T. (2010). Probable fungal origin of perylene in Late Cretaceous to Paleogene terrestrial sedimentary rocks of northeastern Japan as indicated from stable carbon isotopes. *Organic Geochemistry*, **41**, 234-241.
- Tan, J.-H., Bi, X.-H., Duan, J.-C., Rahn, K. A., Sheng, G.-Y. and Fu, J.-M. (2006). Seasonal variation of particulate polycyclic aromatic hydrocarbons associated with PM₁₀ in Guangzhou, China. *Atmospheric Research*, **80**, 250-262.
- Tao, S., Wang, Y., Wu, S., Liu, S., Dou, H., Liu, Y., Lang, C., Hu, F. and Xing, B. (2007). Vertical distribution of polycyclic aromatic hydrocarbons in atmospheric boundary layer of Beijing in winter. *Atmospheric Environment*, **41**, 9594-9602.

- Tauler, R., Viana, M., Querol, X., Alastuey, A., Flight, R. M., Wentzell, P. D. and Hopke, P. K. (2009). Comparison of the results obtained by four receptor modelling methods in aerosol source apportionment studies. *Atmospheric Environment*, **43**, 3989-3997.
- Terzi, E. and Samara, C. (2004). Gas-Particle Partitioning of Polycyclic Aromatic Hydrocarbons in Urban, Adjacent Coastal, and Continental Background Sites of Western Greece. *Environmental Science and Technology*, **38**, 4973-4978.
- Tian, F., Chen, J., Qiao, X., Wang, Z., Yang, P., Wang, D. and Ge, L. (2009). Sources and seasonal variation of atmospheric polycyclic aromatic hydrocarbons in Dalian, China: Factor analysis with non-negative constraints combined with local source fingerprints. *Atmospheric Environment*, **43**, 2747-2753.
- Tiwari, M., Sahu, S. K., Bhangare, R. C., Ajmal, P. Y. and Pandit, G. G. (2013). Estimation of polycyclic aromatic hydrocarbons associated with size segregated combustion aerosols generated from household fuels. *Microchemical Journal*, **106**, 79-86.
- Tobiszewski, M. and Namieśnik, J. (2012). PAH diagnostic ratios for the identification of pollution emission sources. *Environmental Pollution*, **162**, 110-119.
- Tom Misselbrook, Laura Cardenas, Ulli Dragosits and Sutton, M. (2010). UK Emissions of Air Pollutants 1970 to 2008. *UK Emissions Inventory Team*, 1-221.
- Tsapakis, M. and Stephanou, E. G. (2005). Occurrence of gaseous and particulate polycyclic aromatic hydrocarbons in the urban atmosphere: study of sources and ambient temperature effect on the gas/particle concentration and distribution. *Environmental Pollution*, **133**, 147-156.
- Tuominen, J., Salomaa, S., Pyysalo, H., Skytta, E., Tikkanen, L., Nurmela, T., Sorsa, M., Pohjola, V., Sauri, M. and Himberg, K. (1988). Polynuclear aromatic compounds and genotoxicity in particulate and vapor phases of ambient air: effect of traffic, season, and meteorological conditions. *Environmental Science and Technology*, **22**, 1228-1234.

- Turpin, B. J., Saxena, P. and Andrews, E. (2000). Measuring and simulating particulate organics in the atmosphere: problems and prospects. *Atmospheric Environment*, **34**, 2983-3013.
- US EPA (2012). Estimation program interface (EPI) suite, available at: <http://www.epa.gov/opptintr/exposure/pubs/episuite.htm>. *US Environmental Protection Agency*.
- Van Drooge, B. L. and Ballesta, P. P. R. (2009). Seasonal and Daily Source Apportionment of Polycyclic Aromatic Hydrocarbon Concentrations in PM₁₀ in a Semirural European Area. *Environmental Science and Technology*, **43**, 7310-7316.
- Vardar, N., Tasdemir, Y., Odabasi, M. and Noll, K. E. (2004). Characterization of atmospheric concentrations and partitioning of PAH in the Chicago atmosphere. *Science of The Total Environment*, **327**, 163-174.
- Vardoulakis, S., Chalabi, Z., Fletcher, T., Grundy, C. and Leonardi, G. S. (2008). Impact and uncertainty of a traffic management intervention: Population exposure to polycyclic aromatic hydrocarbons. *Science of The Total Environment*, **394**, 244-251.
- Vestreng, V., Myhre, G., Fagerli, H., Reis, S. and Tarrasón, L. (2007). Twenty-five years of continuous sulphur dioxide emission reduction in Europe. *Atmospheric Chemistry and Physics*, **7**, 3663-3681.
- Viana, M., Kuhlbusch, T. A. J., Querol, X., Alastuey, A., Harrison, R. M., Hopke, P. K., Winiwarter, W., Vallius, M., Szidat, S., Pr V T, A. S. H., Hueglin, C., Bloemen, H., W Hlin, P., Vecchi, R., Miranda, A. I., Kasper-Giebl, A., Maenhaut, W. and Hitzenberger, R. (2008). Source apportionment of particulate matter in Europe: A review of methods and results. *Journal of Aerosol Science*, **39**, 827-849.
- Vinggaard, A. M., Hnida, C. and Larsen, J. C. (2000). Environmental polycyclic aromatic hydrocarbons affect androgen receptor activation in vitro. *Toxicology*, **145**, 173-183.

- Violi, A., D'anna, A. and D'alessio, A. (1999). Modelling of particulate formation in combustion and pyrolysis. *Chemical Engineering Science*, **54**, 3433-3442.
- Virtanen, A., Ronkko, T., Kannosto, J., Ristimäki, J., Mäkelä, J. M., Keskinen, J., Pakkanen, T., Hillamo, R., Pirjola, L. and Hameri, K. (2006). Winter and summer time size distributions and densities of traffic-related aerosol particles at a busy highway in Helsinki. *Atmospheric Chemistry and Physics*, **6**, 2411-2421.
- Wang, D., Tian, F., Yang, M., Liu, C. and Li, Y.-F. (2009). Application of positive matrix factorization to identify potential sources of PAH in soil of Dalian, China. *Environmental Pollution*, **157**, 1559-1564.
- Wang, W., Massey Simonich, S. L., Xue, M., Zhao, J., Zhang, N., Wang, R., Cao, J. and Tao, S. (2010). Concentrations, sources and spatial distribution of polycyclic aromatic hydrocarbons in soils from Beijing, Tianjin and surrounding areas, North China. *Environmental Pollution*, **158**, 1245-1251.
- Wang, Z., Na, G., Ma, X., Fang, X., Ge, L., Gao, H. and Yao, Z. (2013). Occurrence and gas/particle partitioning of PAH in the atmosphere from the North Pacific to the Arctic Ocean. *Atmospheric Environment*, **77**, 640-646.
- Ward, T., Trost, B., Conner, J., Flanagan, J. and Jayanty, R. (2012). Source Apportionment of PM_{2.5} in a Subarctic Airshed-Fairbanks, Alaska. *Aerosol and Air Quality Research*, **12**, 536-543.
- Weilm Nster, P., Keller, A. and Homann, K. H. (1999). Large molecules, radicals, ions, and small soot particles in fuel-rich hydrocarbon flames: Part I: positive ions of polycyclic aromatic hydrocarbons (PAH) in low-pressure premixed flames of acetylene and oxygen. *Combustion and Flame*, **116**, 62-83.
- Westerholm, R. and Egeback, K. E. (1994). Exhaust emissions from light-duty and heavy-duty vehicles – Chemical composition, impact of exhaust after treatment, and fuel parameters. *Environmental Health Perspectives*, **102**, 13-23.

- Westerholm, R. and Li, H. (1994). A multivariate statistical analysis of fuel-related polycyclic aromatic hydrocarbon emissions from heavy-duty diesel vehicles. *Environmental Science and Technology*, **28**, 965-972.
- WHO (2003). Health Aspects of Air Pollution with Particulate Matter, Ozone and Nitrogen Dioxide. *Report on a WHO Working Group*.
- WHO (2006). WHO Air quality guidelines for particulate matter, ozone, nitrogen and sulphur dioxide. Global update 2005. *World Health Organisation*.
- WHO (2010). Hidden cities: unmasking and overcoming health inequities in urban settings. *WHO Library Cataloguing-in-Publication Data*.
- Wild, S. R. and Jones, K. C. (1995). Polynuclear aromatic hydrocarbons in the United Kingdom environment: A preliminary source inventory and budget. *Environmental Pollution*, **88**, 91-108.
- Yamasaki, H., Kuwata, K. and Miyamoto, H. (1982). Effects of ambient temperature on aspects of airborne polycyclic aromatic hydrocarbons. *Environmental Science and Technology*, **16**, 189-194.
- Yang, F., Zhai, Y. B., Chen, L., Li, C. T., Zeng, G. M., He, Y. D., Fu, Z. M. and Peng, W. F. (2010). The seasonal changes and spatial trends of particle-associated polycyclic aromatic hydrocarbons in the summer and autumn in Changsha city. *Atmospheric Research*, **96**, 122-130.
- Yang, H. H., Lai, S. O., Hsieh, L. T., Hsueh, H. J. and Chi, T. W. (2002). Profiles of PAH emission from steel and iron industries. *Chemosphere*, **48**, 1061-1074.
- Yu, H. and Yu, J. Z. (2012). Polycyclic aromatic hydrocarbons in urban atmosphere of Guangzhou, China: Size distribution characteristics and size-resolved gas-particle partitioning. *Atmospheric Environment*, **54**, 194-200.

- Zelenyuk, A., Imre, D., Ber Nek, J., Abramson, E., Wilson, J. and Shrivastava, M. (2012). Synergy between Secondary Organic Aerosols and Long-Range Transport of Polycyclic Aromatic Hydrocarbons. *Environmental Science and Technology*, **46**, 12459-12466.
- Zhu, Y., Yang, L., Yuan, Q., Yan, C., Dong, C., Meng, C., Sui, X., Yao, L., Yang, F., Lu, Y. and Wang, W. (2014). Airborne particulate polycyclic aromatic hydrocarbon (PAH) pollution in a background site in the North China Plain: Concentration, size distribution, toxicity and sources. *Science of The Total Environment*, **466–467**, 357-368.
- Zielinska, B., Sagebiel, J., Mcdonald, J. D., Whitney, K. and Lawson, D. R. (2004). Emission rates and comparative chemical composition from selected in-use diesel and gasoline-fueled vehicles. *Journal of the Air and Waste Management Association*, **54**, 1138-1150.
- Zuo, Q., Duan, Y. H., Yang, Y., Wang, X. J. and Tao, S. (2007). Source apportionment of polycyclic aromatic hydrocarbons in surface soil in Tianjin, China. *Environmental Pollution*, **147**, 303-310.

Publications arising as a result of this thesis

Jang, E., Alam, M. S. and Harrison, R. M. (2013). Source Apportionment of Polycyclic Aromatic Hydrocarbons in Urban Air Using Positive Matrix Factorization and Spatial Distribution Analysis. *Atmospheric Environment*, 79, 271-285.

Alghamdi, M. A., Alam, M. S., Yin, J., Stark, C., **Jang, E.**, Harrison, R. M., Shamy, M., Khoder, M. I. and Shabbaj, I. I. (2015). Receptor Modelling Study of Polycyclic Aromatic Hydrocarbons in Jeddah, Saudi Arabia. *Science of The Total Environment*, 506-507, 401-408.

Presentations and Awards

Harrison, R. M., **Jang, E.**, and Alam, M. S. (2012). Application of PMF to the Source Apportionment of Polycyclic Aromatic Hydrocarbons (**Oral Presentation**). *European Aerosol Conference (EAC)*. Granada, Spain, 2-7 September, 2012.

Jang, E., Alam, M. S. and Harrison, R. M. (2013). Source apportionment of polycyclic aromatic hydrocarbons across the UK urban (**Poster Presentation**). *Annual UK Review Meeting on Outdoor and Indoor Air Pollution Research*. Cranfield, United Kingdom, 23-24 April, 2013.

Jang, E., Alam, M. S. and Harrison, R. M. (2013). Interpretation of Urban Particle-bound Polycyclic Aromatic Hydrocarbons Source Profiles of PMF with Known Site Specific Emission Characteristics (**Poster Presentation**). *European Aerosol Conference (EAC)*. Prague, Czech Republic, 1-6 September, 2013. (**Best Poster Award**)

Belis, C. A., Karagulian, F., Amato, F., Almeida, M., Argyropoulos, G., Artaxo, P., Bove, M. C., Cesari, D., Contini, D., Diapouli, E., Eleftheriadis, K., Haddad, I. E., Harrison, R. M., Hellebust, S., **Jang, E.**, Jorquera, H., Mooibroek, D., Nava, S., Nøjgaard, J. K., Pandolfi, M., Perrone, M. G., Pietrodangelo A., Pirovano, G., Pokorná, P., Prati, P., Samara, C., Saraga, D., Sfetsos, A., Valli, G., Vecchi, R., Vestenius, M., Yubero, E. and Hopke, P. K. European Intercomparison for Receptor Models Using a Synthetic Database (**Oral Presentation**). *European Aerosol Conference (EAC)*. Prague, Czech Republic, 1-6 September, 2013.

Jang, E., Alam, M. S. and Harrison, R. M. (2013). Positive Matrix Factorization (PMF) source profiles of particulate Polycyclic Aromatic Hydrocarbons (**Poster Presentation**). *Atmospheric Chemistry In The Earth System (ACITES) Networking Meeting*. York, United Kingdom, 2-3 December, 2013.

Jang, E., Alam, M. S. and Harrison, R. M. (2014). Identification of seasonal and spatial source heterogeneity of polycyclic aromatic hydrocarbons in the UK using Positive Matrix Factorisation (**Oral Presentation**). *International Aerosol Conference (IAC)*. Busan, Republic of Korea, 28 August-2 September, 2014.